Western Graduate&PostdoctoralStudies

Western University
Scholarship@Western

Electronic Thesis and Dissertation Repository

9-2-2015 12:00 AM

Clinical and Experimental Importance of Circulating Tumor Cells in Prostate Cancer

Lori Lowes
The University of Western Ontario

Supervisor
Dr. Alison Allan
The University of Western Ontario Joint Supervisor
Dr. Tracy Sexton
The University of Western Ontario

Graduate Program in Anatomy and Cell Biology
A thesis submitted in partial fulfillment of the requirements for the degree in Doctor of Philosophy
© Lori Lowes 2015

Follow this and additional works at: https://ir.lib.uwo.ca/etd

 Part of the Cancer Biology Commons

Recommended Citation

Lowes, Lori, "Clinical and Experimental Importance of Circulating Tumor Cells in Prostate Cancer" (2015). *Electronic Thesis and Dissertation Repository*. 3267.
https://ir.lib.uwo.ca/etd/3267

This Dissertation/Thesis is brought to you for free and open access by Scholarship@Western. It has been accepted for inclusion in Electronic Thesis and Dissertation Repository by an authorized administrator of Scholarship@Western. For more information, please contact wlswadmin@uwo.ca.

Clinical and Experimental Importance of Circulating Tumor Cells in Prostate Cancer

(Thesis format: Integrated Article)

by

Lori Elizabeth Lowes

Graduate Program in Anatomy & Cell Biology

A thesis submitted in partial fulfillment
of the requirements for the degree of
Doctorate of Philosophy

The School of Graduate and Postdoctoral Studies
The University of Western Ontario
London, Ontario, Canada

© Lori E. Lowes 2015

Abstract

Prostate cancer (PCa) remains a leading cause of death in men, primarily due to ineffective treatment in the metastatic setting. During this phase of PCa, circulating tumor cells (CTCs) are shed into the bloodstream and their presence and number are important in patient prognosis. The CellSearch® system (CSS) is the only U.S. Food and Drug Administration (FDA) and Health Canada approved instrument for detection of CTCs, making it the current clinical gold standard in CTC technology. Although the CSS provides a minimally invasive means of patient monitoring in the metastatic setting, little is known about the role of CTCs in early-stage PCa. Additionally, examination of the utility of CTC molecular characterization in personalized patient care is an area of great interest. However, the underlying biology of CTCs remains poorly understood. In the present study, we demonstrated that CTCs are detectable in early-stage, post-surgical PCa patients undergoing adjuvant and salvage radiotherapy, and that in combination with other clinicopathological risk factors, CTCs may be useful in predicting treatment failure earlier then currently utilized clinical techniques. Additionally, we provide 2 technical resources outlining the FDA and Health Canada approved process of CTC identification and enumeration using the CSS, the detailed experimental process of user-defined protein molecular characterization using the CSS, and a comparable CTC assay for use in *in vivo* pre-clinical mouse models of metastasis. Finally, a comprehensive biological examination of the role of the epithelial-to-mesenchymal transition (EMT) in CTC kinetics and metastatic dissemination in PCa is presented, demonstrating that highly mesenchymal PCa cells shed CTCs earlier and in greater numbers during the metastatic cascade and have a greater metastatic capacity then PCa cells with an epithelial phenotype. Collectively these data improve our understanding biology of CTCs in PCa, including CTC kinetics, their relationship with EMT, and metastasis. These results will

guide future research and technology development in the identification and capture of CTCs with the greatest metastatic potential, and may ultimately lead to changes in patient treatment guidelines.

Keywords

Prostate Cancer, Metastasis, Circulating Tumor Cells, Radiation Therapy, Salvage, Adjuvant, Molecular Characterization, Epithelial-to-Mesenchymal Transition

Co-Authorship Statement

The work presented in this thesis would not have been possible without the help and support of a number of individuals. For the studies presented in **Chapters 5**, David Goodale performed all the surgical procedures necessary for the mouse injections and participated in all necropsies; Matt Piaseczny was responsible for the intracardiac collection of many of the blood samples used for the EMT-dependent and -semi-independent assay development and was also involved in many of the necropsies; Ying Xia aided in the processing of many of the experimental mouse CTC samples and along with Freeman Paczkowski performed the western blot analysis of the CTC derived cell lines; and Carl Postenka sectioned and stained all of the collected mouse tissue for histological assessment. In addition, Ben Hedley, Ying Xia, and Ben Chin-Yee were involved in the processing of occasional patient blood samples for studies presented in **Chapters 1, 2, and 4**.

Acknowledgments

Firstly I would like to thank my supervisor Dr. Alison Allan for her continued guidance and support throughout the course of this degree. The lessons that I have learned working under such an inspiring individual stretch far beyond the lab bench and will continue to serve me in my everyday life. I would like to thank her for her continued friendship, for allowing me the freedom to explore new ideas, no matter what the cost, for keeping me calm in my moments of anxiety and doubt, and for gently guiding me back in the right direction when I strayed a little off course. I consider myself extremely fortunate to have ended up under her supervision, as she has been essential in shaping my future goals and aspirations and in making me a stronger and more confident individual overall. Finally, I would like to thank her for essentially bribing me into staying for my PhD. It has been an amazing experience, with many highs and lows, and one that I will always look back on fondly.

Secondly I would like to thank my co-supervisor Dr. Tracy Sexton for always finding the time in her busy schedule to meet with me individually and answer all of my naive questions. Thank you for the excitement you have shown for all of my ideas, no matter how strange, and for always reminding me of the potential clinical value of this research. Knowing that my work may someday have an impact on patients is the greatest motivation I could ask for.

Special thanks are due to all the members of the Allan lab, David Goodale, Dr. Ying Xia, Mauricio Rodriguez, Matt Piaseczny, Gracie Pio, and Maria Vieito. Your support and friendship has made going to work every day a very enjoyable experience. The many hours of conversation and laughter may have given us a bit of a reputation, but I've enjoyed every minute of it.

I would also like to thank my thesis advisory committee members, Dr. Ann Chambers, and Dr. Paul Walton, for their continued advice. The ideas generated during our meetings have been fundamental in shaping this thesis.

Finally, I would like to thank my friends and family for their love and support throughout the last 6 years. Jenna Paolini, Alysha Croker, Irene Ma, and Jenny Chu, you are truly some of the greatest people I know. I am so grateful that I get to call you my friends. Thanks for the many laughs and for providing me with ample opportunities to relieve my stress! To my family, Mom, Dad, and Stephen, thank you for your positivity, for always believing in me, and for reminding me that family comes first. Last but especially not least, I would like to thank Craig Schroeder. Thank you for loving and supporting me through all my crazy and irrational moments, for always calming me down and being there whenever I needed you. I could not have accomplished any of this without you in my life.

Table of Contents

List of Tables

List of Figures

List of Appendices

Abbreviations

aCGH	Comparative genomic hybridization array
ALDH1	Aldehyde dehydrogenase 1
ALK	Anaplastic lymphoma kinase
APC	Allophycocyanin
AR	Androgen receptor
BCF	Biochemical failure
BSA	Bovine serum albumin
cDNA	Complementary DNA
CK	Cytokeratin
CRF	Clinicopathologic risk factors
CSC	Cancer stem cell
CSS	CellSearch® system
CTC	Circulating tumor cell
DAPI	4', 6-diamidino-2-phenylindole
DHT	Dihydrotestosterone
DRE	Digital rectal examination
ECE	Extracapsular extension
EDTA	Ethylenediaminetetraacetic acid
EGF	Epidermal growth factor
EGFR	Epidermal growth factor receptor
EMT	Epithelial-to-mesenchymal transition
EpCAM	Epithelial cell adhesion molecule
ER	Estrogen receptor
FACS	Fluorescence activated cell sorting
FBS	Fetal bovine serum
FCM	Flow cytometry
FDA	Food and Drug Administration
FGF	Fibroblast growth factor
FISH	Fluorescence *in situ* hybridization
FITC	Fluorescein isothiocyanate

H&E	Hematoxylin and eosin
HER2	Human epidermal growth growth factor receptor 2
HGF	Hepatocyte growth factor
HLA	Human leukocyte antigen
HPSE	Heparanase
IGF-1	Insulin-like growth factor 1
IGF-1R	Insulin-like growth factor 1 receptor
IMRT	Intensity modulated radiation therapy
ISET	Isolation by size of epithelial tumor cells
LH	Luteinizing hormone
LHRH	Luteinizing hormone-releasing hormone
MET	Mesenchymal-to-epithelial transition
MFI	Mean fluorescence intensity
miRNA	MicroRNA
MUC-1	Mucin-1
PCa	Prostate cancer
PCR	Polymerase chain reaction
PDGF	Platelet-derived growth factor
PE	Phycoerythrin
PI3K	Phosphatidyl inositol 3-kinase
PI3KCA	Phosphatidylinositol-3-kinase, catalytic subunit α
PIA	Proliferative inflammatory atrophy
PIN	Prostatic intraepithelial neoplasia
PR	Progesterone receptor
PSA	Prostate specific antigen
PSADT	Prostate specific antigen doubling time
PSMA	Prostate-specific membrane antigen
pT	Pathologic T
PTEN	Phosphatase and tensin homolog
PVDF	Polyvinylidene difluoride
RBC	Red blood cell
RP	Radical prostatectomy

RT	Radiation therapy
RTOG	Radiation Therapy Oncology Group
RT-PCR	Reverse-transcription polymerase chain reaction
RT-qPCR	Quantitative reverse-transcription polymerase chain reaction
RUO	Research use only
SDS-PAGE	Sodium dodecyl sulfate polyacrylamide gel electrophoresis
SVI	Seminal vesicle invasion
TGF-β	Transforming growth factor β
TMPRSS2:ERG	Transmembrane protease serine 2:ETS-related gene
TTF1	Thyroid transcription factor 1
UICC	Union for International Cancer Control
VEGFR2	Vascular endothelial growth factor receptor 2
WBC	White blood cell

Chapter 1
Introduction

A version of this chapter has been published as a review paper:
Lowes LE and Allan, AL. Recent advances in the molecular characterization of circulating tumor cells. *Cancers (Basel).* 2014; 6(1):595-624.

1.1 Prostate cancer

Prostate cancer (PCa) is the second leading cause of cancer diagnosis and the third leading cause of cancer-related mortalities in men in North America[1]. The prostate is located just below the bladder in the male reproductive system and is responsible for the production of seminal fluid which will eventually mix with sperm from the testicles to produce semen[2]. There are several pre-cancerous conditions associated with the development of prostate cancer including prostatic intraepithelial neoplasia (PIN) and proliferative inflammatory atrophy (PIA)[3]. Although there are several different types of PCa, 95% are classified as adenocarcinomas and develop from the mucus-secreting gland cells of the prostate[4]. There are currently two tests which are commonly utilized when screening for PCa, the digital rectal examination (DRE) and the prostate specific antigen (PSA) test[5]. DRE involves inspection of the prostate for abnormal regions using manual palpation of the prostate via the rectum[6]. The PSA test involves the collection of a blood sample and subsequent testing for elevated levels of the PSA protein. This protein is typically secreted by the prostate, however, elevated levels may indicate changes in prostate physiology[7,8]. If abnormal results are obtained during the screening process, a prostate biopsy may be ordered and multiple biopsy specimens will be collected for

pathological assessment. Following biopsy, Gleason scoring is performed by a trained pathologist on each biopsy specimen. The Gleason score ranks each specimen on a scale from 2-10 based on the sum of primary and secondary patterns (1-5) of differentiation when compared to normal prostate tissue, with a low number indicating more differentiated tissue (less aggressive disease) and a high number indicating more undifferentiated tissue (more aggressive disease)[9].

1.1.1 Disease staging and prognosis

PCa is staged based on categorization of patients using the TNM classification system, which relies on the size and extent of the primary tumor (T), the spread of disease to regional lymph nodes (N), and tumor dissemination to other organs (M). The details of this classification system are presented in *Table 1.1*. Along with TNM stage, additional criteria such as PSA levels and Gleason score are important in determining prognosis and in assigning risk. *Table 1.2* outlines the prognostic grouping of patients based on TNM, PSA, and Gleason score as defined by the Union for International Cancer Control (UICC). Based on these criteria, patients in group I have a better prognosis then those in group IV[9]. PCa patients may also be further categorized into low, intermediate, and high risk groups. To be classified as low risk, patients must have a TNM stage of T2a or lower, PSA ≤ 9, and a Gleason score of ≤ 6. Intermediate risk patients are those that present with any of the following; TNM stage of T2b-T2c, PSA of 10-20, and/or a Gleason score of 7. Finally patients are classified as high risk if any of the following are present, TNM stage of T3a or higher, PSA > 20, and/or a Gleason score of 8-10[10,11].

Table 1.1. Clinical classifications of prostate cancer using the TNM system

Primary Tumour (T)	
TX	Primary tumour cannot be assessed
T0	No evidence of primary tumour
T1	Clinically inapparant tumor neither palpable nor visible by imaging
T1a	Tumour incidental histologic finding in 5% or less of tissue resected
T1b	Tumour incidental histologic finding in more than 5% of tissue resected
T1c	Tumour identified by needle biopsy
T2	Tumour confined within prostate[#]
T2a	Tumour involved one-half of one lobe or less
T2b	Tumour involved more than one-half of one lobe but not both lobes
T2c	Tumour involved both lobes
T3	Tumour extends thorough the prostate capsule[##]
T3a	Extracapsular extension (unilateral or bilateral) including microscopic bladder neck involvement
T3b	Tumour invades seminal vesicles
T4	Tumour is fixed or invades adjacent structures other then seminal vesicles: bladder neck, external sphincter, rectum, levator muscles, and/or pelvic wall
Regional Lymph Nodes (N)	
NX	Regional lymph nodes cannot be assessed
N0	No regional lymph node metastasis
N1	Regional lymph node metastasis
Distant metastasis (M)	
M0	No distant metastasis
M1	Distant metastasis

#: Tumour found in one or both lobes by needle biopsy, but not palpable or reliably visible by imaging is classified as T1c.

##: Invasion into the prostatic apex or into (but not beyond) the prostatic capsule is classified not as T3 but as T2.

** *Srigley et al., 2009*[9]

Table 1.2. Clinical stage classification of prostate cancer based on TNM criteria, PSA, and Gleason score as defined by the Union for International Cancer Control (UICC)

Group	T	N	M	PSA	Gleason
I	T1a-c	N0	M0	PSA < 10	Gleason ≤ 6
	T2a	N0	M0	PSA < 10	Gleason ≤ 6
	T1-2a	N0	M0	PSA X	Gleason X
IIA	T1a-c	N0	M0	PSA < 20	Gleason 7
	T1a-c	N0	M0	PSA ≥ 10 < 20	Gleason ≤ 6
	T2a	N0	M0	PSA ≥ 10 < 20	Gleason ≤ 6
	T2a	N0	M0	PSA < 20	Gleason 7
	T2b	N0	M0	PSA < 20	Gleason ≤ 7
	T2b	N0	M0	PSA X	Gleason X
IIB	T2c	N0	M0	Any PSA	Any Gleason
	T1-2	N0	M0	PSA ≥ 20	Any Gleason
	T1-2	N0	M0	Any PSA	Gleason ≥ 8
III	T3a-c	N0	M0	Any PSA	Any Gleason
IV	T4	N0	M0	Any PSA	Any Gleason
	Any T	N1	M0	Any PSA	Any Gleason
	Any T	Any N	M1	Any PSA	Any Gleason

Note: When either prostate specific antigen (PSA) or Gleason is not available, grouping should be determined by T stage and/or whichever of either the PSA or Gleason is available.

***Srigley et al., 2009*[9]

1.1.2 Treatment options for prostate cancer

In most cases, PCa is a slow-growing disease and when caught early it is highly treatable. In fact, PCa patients without distant spread show 5 year relative survival rates of 100%. However, the relative survival rates of patients with distant spread of this disease are significantly reduced, with only 31% surviving more than 5 years[1]. The treatment options available for PCa patients depend on disease stage. The poor outcomes observed for patients with distant disease are as a result of a lack of effective treatment options in this disease setting.

1.1.2.1 Active surveillance

Due to the slow-growing nature of PCa, active surveillance is an option that is often offered to men with low risk disease, older men who have a life-expectancy of less than 10 years, and/or men with other significant health problems[11–14]. During active surveillance, patients are routinely monitored every 3-6 months using PSA testing or/and physical examination, including DRE. Repeat biopsies are usually performed every 1-2 years or as clinically indicated.

1.1.2.2 Surgical intervention: radical prostatectomy

Upon evidence of disease progression, PCa patients may be offered surgical removal of the prostate via radical prostatectomy. This treatment option is most typically offered to men with stage I and II disease, under the age of 75, and in good physical health[11,12]. Although less common, radical prostatectomy may also be offered as a treatment option for stage III patients[15]. Following surgical intervention, assessment of the pathological tissue as well as monitoring via PSA testing can assist clinicians in

determining if patients should be recommended for post-surgical radiation therapy (RT)[16,17].

1.1.2.3 Radiation therapy

Brachytherapy is an internal radiation therapy approach often offered to patients with low or intermediate risk disease. This treatment option, utilized in place of radical prostatectomy, relies on the strategic placement of small radioactive implants, either permanent or temporary, into the prostate, thereby slowing killing the cancer cells over time[11]. Brachytherapy may also be utilized in combination with external beam radiation therapy for patients with intermediate or high risk disease[18].

If surgical intervention is chosen, patients with adverse pathological results (e.g., extracapsular extension [ECE], seminal vesicle invasion [SVI], and/or positive margins) without a detectable PSA or patients with a detectable PSA, with or without adverse pathology, may be recommended to undergo adjuvant or salvage external beam radiotherapy respectively[17]. Additionally, external beam radiation therapy, often given in combination with hormonal therapy, is often utilized for treatment of patients with stage III disease[19]. It can also be used in earlier stage patients who are unfit or do not desire surgery.

1.1.2.4 Hormonal therapy: androgen deprivation

In general, hormonal therapies are reserved for those individuals suffering with stage III and IV disease. These therapies exploit PCa's requirement for androgen (testosterone and dihydrotestosterone [DHT]) stimulation in promoting tumor growth. By depriving tumor cells of these necessary androgens, hormonal therapies are able to slow the growth of residual disease[20,21].

Currently, there are 5 classes of hormonal treatments available; *(1)* luteinizing hormone-releasing hormone (LHRH) agonists, *(2)* LHRH antagonists, *(3)* anti-androgens, *(4)* estrogens, and *(5)* orchiectomy[21]. Luteinizing hormone (LH) is released by the pituitary gland, following stimulation by LHRH. LH then activates the testes to release testosterone into the bloodstream thus enhancing tumor cell growth. LHRH agonists (e.g., Lupron [leuprolide acetate], Zoladex [goserelin], Suprefact [buserelin acetate], and Trelstar [triptorelin pamoate]) result in excessive stimulation of the pituitary gland to release LH. Ultimately, the pituitary will stop responding to LHRH thereby preventing stimulation of the testes and reduced secretion of testosterone[22]. In contrast, LHRH antagonists (e.g., Firmagon [degarelix]) work by blocking the release of LH from the pituitary gland, again resulting in reduced testosterone secretion[23]. Unlike LHRH-based therapies which act at the level of androgen secretion, anti-androgen treatments (e.g., Euflex [flutamide], Casodex [bicalutamide], Anandron [nilutamide], Zytiga [abiraterone acetate], and Xtandi [enzalutamide]) act by blocking androgen receptors expressed by prostate cancer cells, thereby preventing cell stimulation[24]. Estrogen therapy is typically reserved for cases in which patients are no longer responding to androgen deprivation. The use of estrogens in these patients has been demonstrated to reduce androgen levels[25]. Finally, orchiectomy is a surgical procedure in which the testes are removed, thus eliminating the primary source of androgen secretion. However, for many men, chemical castration is preferred over this surgical intervention[21]. Unfortunately, although up to 85% of men initially respond well to hormonal treatments, these therapies are not curative and patients will eventually no longer respond to androgen deprivation. This

lethal stage of disease is commonly referred to as castration resistant or hormone refractory PCa[26].

1.1.2.5 Chemotherapy

Chemotherapy in PCa is typically only utilized during the castration resistant phase of disease and its use is strictly palliative. Commonly utilized chemotherapy regimens include treatment with Taxotere, Novantrone, or Jevtana in combination with Prednisone. Although not curative, these combination treatments can be utilized to prolong survival, reduce pain, and improve the quality of life for terminal patients[21]. More recently chemotherapy has been shown to be beneficial in select patients with metastatic hormone sensitive prostate cancer (NIH Trial #:NCT00309985) and in those with high risk disease (NIH Trial #:NCT00288080).

1.1.3 Prognostic biomarkers in prostate cancer

The advent of PSA screening for PCa in the early 1980s revolutionized the management of this disease, allowing for earlier detection and subsequently earlier treatment initiation for PCa patients. However, observed discrepancies between one's lifetime risk of prostate cancer development (1 in 6, ~16%) and lifetime risk of death due to this disease (~2%) has led to controversy regarding the potential for over detection and over treatment of this slow-growing disease[27,28]. In addition to over detection and over treatment, there is also the potential for false-positive results during the screening process. As recently described in the multi-centre European Randomized Study of Screening for Prostate Cancer trial, the false-positive rate is largely influenced by the PSA threshold utilized, with 4.0 ng/ml resulting in 11.3% false-positives versus 3.0 ng/ml resulting in 19.8%. Unfortunately no PSA value has been described that can conclusively

discriminate patients with and without PCa. Therefore great controversy exists with regards to the widespread utilization of PSA testing, especially when considering low- or average- risk patients under the age of 55 or over the age of 70[29]. Currently, aside from the standard clinicopathologic parameters utilized in assessing patient risk (TNM stage, PSA, and Gleason score) there are very few prognostic biomarkers available that are helpful in differentiating indolent disease from aggressive disease. Oncotype DX®, a biopsy-based genomic test, has received prospective validation as a prognostic marker in low-risk patients[28,30,31]. This test measures the expression levels of 17 genes across four biological pathways to assess the anticipated aggressiveness of a given tumor. The results are then reported as a number between 0 and 100, called the Genomic Prostate Score, in which smaller numbers reflect lower risk. This test along with the results of other clinical parameters aids clinicians in selecting better candidates for active surveillance as an initial management strategy. Although concerns regarding over-treatment have received increasing attention in recent years, under-treatment of men with aggressive disease is also a concern. Prolaris® is a prognostic genomic assay that assesses increases in cell cycle progression gene mutations that has been validated to aid in differentiating low-risk and high-risk patient populations when used in combination with standard clinicopathologic parameters[28,30,32–34]. Finally, Decipher®, a genomic based assay, has been validated for predicting the probability of metastasis following surgical intervention via radical prostatectomy, thus better identifying high-risk patients[28,35,36].

However, in spite of the available clinicopathologic parameters and prognostic biomarkers, PCa is still a highly lethal disease, claiming an estimated 4,100 lives this year alone in Canada[1]. Therefore, there is a necessity for novel prognostic biomarkers

that could better predict aggressive disease. Additionally, minimally invasive prognostic biomarkers that could be repeatedly utilized, serving as "real-time biopsies" of ongoing disease progression, would be especially valuable in the management of PCa.

1.2 Metastasis and circulating tumor cells (CTCs)

The majority of PCa cancer-related deaths occur as a result of metastasis. This lethality is largely attributable to our current lack of effective treatments in the metastatic setting[37,38]. One contributing factor to this is that metastatic lesions are highly heterogeneous when compared to their primary tumor counterparts[39–48]; however, the majority of treatment decision-making is currently based upon characteristics of the primary tumor. Although disease outcome is ultimately determined by metastatic spread, biopsy of metastatic lesions is often difficult to perform and can be a significant source of morbidity for patients. Therefore, it is currently not clinically feasible to subject patients to repetitive metastatic biopsies upon disease recurrence or progression, even if this approach could provide information that might improve treatment of metastatic disease. Unfortunately, this suggests that many patients are receiving sub-optimal treatment and therefore techniques that could better assess the characteristics of metastatic disease might enhance treatment efficacy and ultimately improve patient outcomes.

Metastasis has been demonstrated to correlate with the presence of cancer cells in the peripheral blood circulation, hereafter referred to as circulating tumor cells (CTCs)[49–51]. The existence of CTCs has been known since the mid-1800s, when they were first reported by Thomas Ashworth, a resident physician at Melbourne Hospital. Upon autopsy of a patient with numerous (~30) subcutaneous tumors, Ashworth described

these cells as appearing "exactly in shape, size, and appearance" to those seen in the primary lesions. Ashworth postulated that these tumor-like cells were cancer cells in the blood and that their existence could shed light on the "mode of origin" of numerous tumors in one individual[52]. Since the work of Ashworth in 1869, it has since been confirmed that the blood is a major route of transport for disseminating cancer cells, and it has been postulated that these CTCs might act as surrogate biomarkers of disease spread and patient outcome[49–51]. However, only recently has technological advancement allowed for detailed investigation of these cells and their consideration for use in the clinic.

1.2.1 Clinical applications of CTCs

Thus far, the clinical uses of CTCs have focused mainly on enumeration. Due to the rare nature of CTCs, this process typically requires both enrichment and detection steps (*Figure 1.1*). For enrichment, approaches include size or density-based techniques and/or immunomagnetic separation (i.e., positive selection using epithelial-specific or tumor-associated markers; or negative selection using markers expressed by contaminating cells such as leukocytes). For detection, approaches include nucleic acid-based techniques such as reverse transcription polymerase chain reaction (RT-PCR), reverse transcription quantitative-PCR (RT-qPCR), microarray, or sequencing; and/or protein-based techniques such as immunofluorescence or flow cytometry (FCM) using antibody-mediated detection. The advantages and disadvantages of each of these techniques have been extensively reviewed previously[53–58] and therefore will not be discussed here.

Figure 1.1. An overview of the most commonly utilized techniques for the process of CTC enrichment and detection. In general, four approaches currently exist for CTC enrichment: (1) size-based; (2) density-based; (3) immunomagnetic separation; and (4) microfluidic-based. Using size-based enrichment techniques, diluted whole blood is passed through a filtration device with specific sized pores (typically 8 μm). CTCs are captured based on differences in cell size between CTCs (typically >8 μm) and white blood cells (WBCs; typically <8 μm). Density-based enrichment utilizes Ficoll (or similar density gradient medium) to enrich for mononuclear cells (including CTCs) from other blood components. Immunomagnetic separation involves the use of iron-conjugated antibodies targeted toward CTCs (e.g., EpCAM; positive selection) or contaminating blood cells (e.g., CD45; negative selection) and incubation in a magnetic field. For microfluidic-based techniques, whole blood is slowly passed across a chip-based surface and isolated using either CTC targeted antibody-coated microposts and/or other chip surfaces (CTC Chip, Herringbone CTC Chip, iChip, graphene oxide chip, and the OncoBean Chip[59–63]), or dielectrophoresis (DEPArray[64,65]). Current CTC detection techniques use either a protein-based approach (*i.e.*, immunofluorescence or flow cytometry) expressed by whole cells or secreted proteins (EPISPOT assay[66–68]), or nucleic acid-based approaches such as RT-PCR or RT-qPCR, applied at the level of single genes or using a multiplex approach.

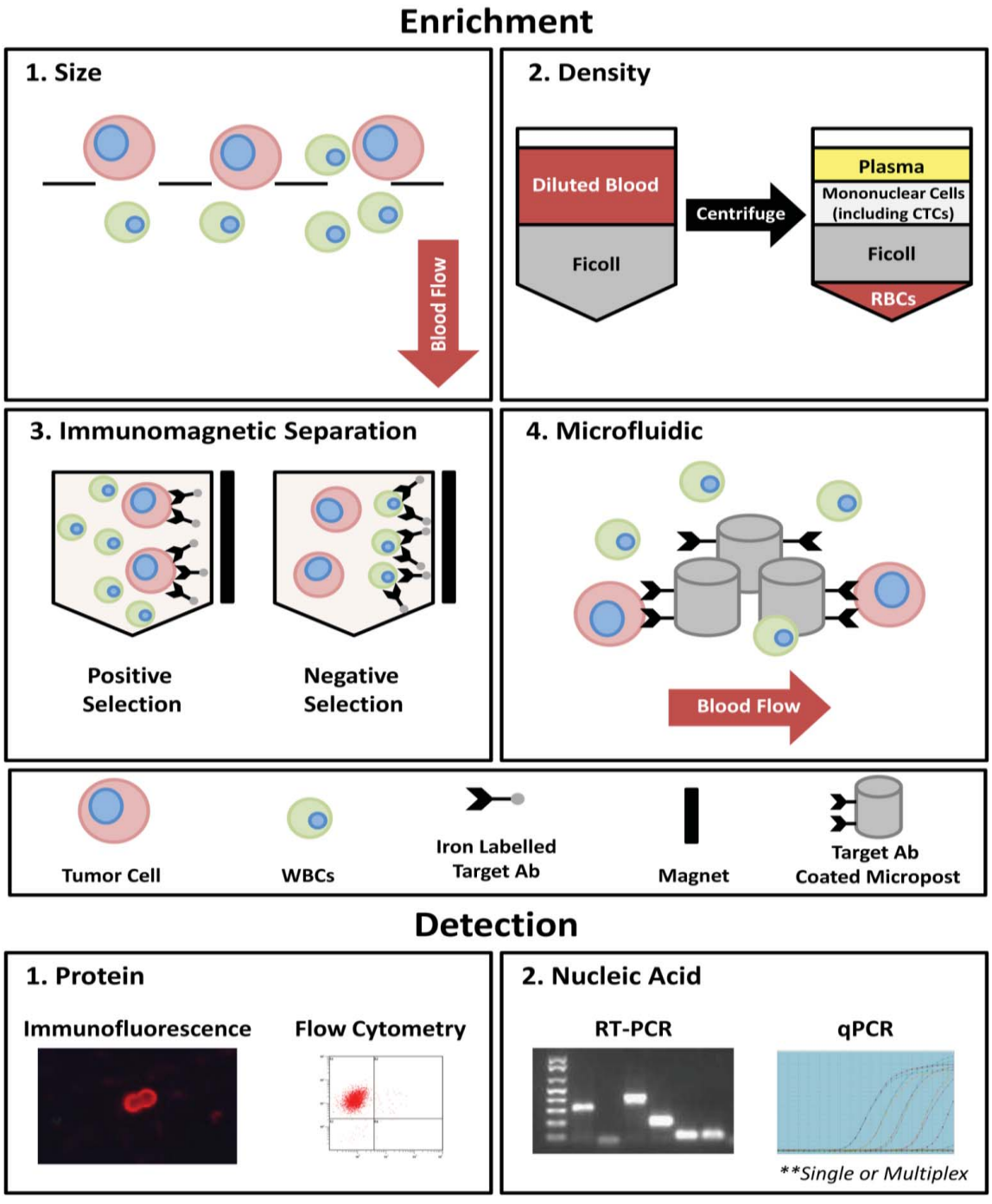
Enrichment
1. Size
Blood Flow
2. Density
Diluted Blood
Ficoll
Centrifuge
Plasma
Mononuclear Cells (including CTCs)
Ficoll
RBCs
3. Immunomagnetic Separation
Positive Selection
Negative Selection
4. Microfluidic
Blood Flow
Tumor Cell
WBCs
Iron Labelled Target Ab
Magnet
Target Ab Coated Micropost
Detection
1. Protein
Immunofluorescence
Flow Cytometry
2. Nucleic Acid
RT-PCR
qPCR
**Single or Multiplex

Despite the development of numerous CTC platforms using various combinations of the above enrichment and detection steps, capture of these cells is still technologically challenging due to their rare nature (~1 CTC per 10^5–10^8 white blood cells[69–71]), the potential presence of contaminating cells that can lead to false positive identification (i.e., non-tumor epithelial cells, circulating endothelial cells), and the lack of a globally accepted marker for capture of all CTCs (e.g., some CTCs may lose EpCAM [epithelial cell adhesion molecule]/CK [cytokeratin] expression as they enter the bloodstream via a process known as epithelial-to-mesenchymal transition [EMT][72]). In fact, currently, the only U.S. Food and Drug Administration (FDA) cleared system for CTC detection and enumeration in the clinic is the CellSearch® system (CSS; Janssen Diagnostics, LLC, Raritan, NJ, USA), developed in the early 2000s. This platform enriches for CTCs using positive immunomagnetic selection based on EpCAM, followed by immunofluorescent staining for CK 8/18/19; CD45; and the DNA dye DAPI (4',6-diamidino-2-phenylindole). Positive CTCs are identified, using semi-automated fluorescence microscopy, as cells with a $CK^+/DAPI^+/CD45^-$ phenotype[73]. The CSS is currently cleared for prognostic use in metastatic breast, prostate, and colorectal cancers, where the presence of ≥5 (breast[73] and prostate[74]) or ≥3 (colorectal[75]) CTCs in 7.5mL of blood is correlated with poorer prognosis compared to patients with fewer CTCs in the same blood volume. Using this platform, CTC enumeration has been utilized not only to assess CTC number at baseline but also throughout the course of treatment and/or following completion of various treatment regimens. It has been demonstrated that CTCs are correlated with patient outcome and that the change in CTC number during treatment is predictive of therapy response, often sooner than currently utilized techniques such as

imaging[74,76–78]. However, as described in the following sections, simple enumeration of CTCs fails to capitalize on their full potential as biomarkers of metastatic disease.

1.2.2 CTCs as surrogate biomarkers of metastatic biopsy

As previously mentioned, although the biopsy and subsequent molecular profiling of metastatic tissue would be ideal for determining appropriate interventional treatments for cancer patients upon disease recurrence or progression, this approach is typically not routinely feasible in the clinic. Therefore, molecular characterization of the cells that seed these metastatic lesions has been proposed as a surrogate for metastatic biopsy. For patients who have been heavily pre-treated with numerous lines of therapy, it is highly likely that the cancer cells that persist in the body are significantly different from those that originally existed in their primary tumor counterpart[39–48]. In addition, outside of the metastatic setting, CTCs may also demonstrate utility in circumstances where no primary tumor is available for characterization, or where the collected tissue is of poor quality and/or insufficient quantity. The molecular characterization of CTCs therefore holds great promise in terms of assessing disease status and will likely better represent the overall heterogeneity of disease at the time of necessary intervention.

Moving forward, molecular characterization of CTCs could provide an attractive and powerful alternative to metastatic biopsies; acting as a minimally invasive "real-time liquid biopsy" that can be repeatedly performed to allow assessment of genetic drift, investigation of molecular disease evolution, and identification of actionable genomic characteristics.

1.3 Current CTC molecular characterization approaches

1.3.1 Protein-based CTC characterization techniques

1.3.1.1 Immunofluorescence

Immunofluorescence is the primary means by which CTCs have been interrogated at the protein level, using specifically targeted antibodies. A number of CTC enrichment techniques have been employed prior to immunofluorescent staining including immunomagnetic approaches (both positive and negative selection)[79–91], density gradient centrifugation[86], and microfluidic chip-based approaches[59]. Using immunofluorescence, CTCs have been characterized for expression of many markers including HER2[62,79,80,82–93], EGFR (epidermal growth factor receptor)[79,94,95], androgen receptor (AR)[96,97], PSA[59], estrogen receptor (ER)[87,94], and progesterone receptor (PR)[94].

Thus far in the literature, the gold standard CSS is the most highly utilized system for CTC characterization at the protein level, using a single fluorescein isothiocyanate (FITC) fluorescence channel not required for CTC identification. Currently the CSS has three commercially available markers that can be used on-system in combination with this platform to examine HER2, EGFR, or insulin-like growth factor 1 receptor (IGF-1R) expression on CTCs. In addition, the CSS is amenable to the development of user-defined protein marker protocols for CTC characterization. However, the CSS is a "closed" platform, with little flexibility in terms of fluorophore selection and fluorescent channel availability, and on-system characterization is currently limited to one additional marker. While this limitation in fluorophore availability is a hurdle that must be overcome by all protein-based platforms, several groups have

developed systems that are more "open" in nature and therefore more amenable to extensive multi-marker CTC characterization.

A microfluidic chip-based assay known as the CTC Chip platform[59], the next generation CTC Chip platform, the iChip which combines microfluidic and magnetic cell sorting technologies[60], and a portable microfiltration platform[98] developed recently are excellent examples of "research-friendly" immunofluorescent techniques that allow flexibility in CTC characterization. These two platforms utilize different CTC enrichment methodologies to capture these rare cells, with the CTC Chip system relying on positive selection using anti-EpCAM coated microposts as blood is passed over the chip surface, versus the microfiltration system which utilizes size-based capture of CTCs. Thus far in the literature these two platforms have been exploited for CTC characterization, examining a variety of markers including PSA, M-30, thyroid transcription factor 1 (TTF1), Ki-67, and HER2[56,59,61,98].

The advantages of utilizing immunofluorescence for CTC characterization include: *(1)* the ability to examine the presence or absence of expression, as well as protein localization and co-localization with additional proteins; *(2)* the ability to examine many proteins of interest simultaneously, limited only by the filter capacity of the investigators' microscope; *(3)* the ability to visually confirm that expression is in CTCs and not contaminating cells; and *(4)* the ability to visualize variations in protein expression levels (it is important to note that this may also be seen as a disadvantage if not properly standardized). Several disadvantages also exist with regards to immunofluorescence techniques including: *(1)* limitations in assay sensitivity (i.e., enough antigens need to be present to display a visible signal); *(2)* bleed-through from

additional fluorescent channels can make interpretation of results confusing; and *(3)* using this approach, result interpretation can be more difficult to standardize (i.e., what constitutes a true positive or negative signal), although automated CTC analysis approaches are evolving to help address this issue[86,92].

In the clinic, the primary benefit of immunofluorescence-based CTC characterization is the ability to identify the presence or absence of particular therapeutic target molecules, thereby expanding the availability of targeted therapies to patients who would previously be considered ineligible based solely upon the characteristics on their primary tumor. An excellent example of a setting in which CTC characterization could augment patient care is illustrated by the limited availability of HER2 targeted therapies to breast cancer patients with $HER2^-$ primary tumors who may have $HER2^+$ disease in sites distant from the primary tumor (i.e., metastases). In particular, the detection of $HER2^+$ CTCs in a patient with a $HER2^-$ primary tumor could predict response to HER2 targeting agents and increase the availability of these personalized treatment options to patients. In the future, we envision serial CTC assessment at the protein level as a tool for predicting therapy response to specific targeting agents and facilitating evaluation of emerging drug resistance based upon the loss/downregulation of target molecules.

1.3.1.2 Flow cytometry

Although immunofluorescence is a powerful tool for CTC characterization at the protein level, its primary limitation is that the data obtained using this approach is largely qualitative. Due to the highly heterogeneous nature of CTCs, quantitative analysis of these rare cells may be advantageous. Quantifiable flow cytometry assays are therefore an attractive alternative for protein-based characterization. In the clinic, FCM has been

proven to be an extremely powerful technology, with clinical FCM being utilized in a number of disciplines, including hematology and oncology[99,100]. In general, FCM has primarily been utilized for CTC enumeration; however, this technique is also an attractive method for multi-marker, on-system, molecular characterization of CTCs. Thus far in the literature, this technology has been utilized to examine the expression of EGFR and its phosphorylated counterpart, ALDH1 (aldehyde dehydrogenase 1), CD44, CD47, MET, and heparanase (HPSE)[101–104]. Simultaneous to on-system characterization, FCM offers the ability to easily sort and collect characterized CTCs using fluorescence activated cell sorting (FACS) technology[102,103]. Additional advantages offered by flow cytometric methods include: *(1)* the ability to examine not only the presence or absence of marker expression but also to examine the level of expression in a measurable and quantifiable fashion; *(2)* the ability to easily perform multi-marker analysis on a single sample, limited only by laser and fluorescent filter set availability; and *(3)* ease of sorted sample collection and downstream characterization using other approaches. However, disadvantages also exist including: *(1)* limitations with regards to assay sensitivity even when combined with pre-enrichment steps[105,106]; and *(2)* the inability to visually confirm that results are from CTCs and not due to leukocyte contamination.

Moving forward, the use of FCM for CTC characterization in the clinic could provide similar benefits as those recognized for immunofluorescent techniques. In brief, these techniques could provide valuable information regarding the expression of protein markers for targeted therapies and the detection of drug resistant phenotypes, as well as the added potential for performing multi-marker protein analysis with a quantifiable readout. When utilized clinically, this approach would be better equipped (relative to

immunofluorescence) for assessing overall CTC heterogeneity and for identifying distinct CTC subpopulations. An example of this has recently been elegantly demonstrated by Baccelli et al. (2013), who identified a $CD44^{+}CD47^{+}MET^{+/-}$ CTC subpopulation that is enriched for metastasis-initiating cells[102]. In addition, FCM would also allow for these subpopulations to be quantified, potentially providing information regarding patient prognosis[102]. However it is important to highlight that current limitations with regards to assay sensitivity restrict the use of this technique as a clinical assay at present, and advances in technology are needed to address this.

1.3.2 Nucleic acid-based CTC characterization techniques

1.3.2.1 Fluorescence *in situ* hybridization

At the genomic level, fluorescence *in situ* hybridization (FISH) has been utilized to interrogate CTCs for changes in individual genes, including gene copy number, gene rearrangement, and/or gene deletion; as well as chromosomal changes, such as select arm deletion or amplification[79–81,92,93,107–113]. Prior to FISH analysis, CTCs are typically enriched from whole blood, with the exception of one group that demonstrated FISH analysis of CTCs without prior enrichment[114]. In the literature several enrichment techniques have been employed, including the CSS[79–81,93,110,111,113], isolation by size of epithelial tumor cells (ISET)[107,109], density gradient centrifugation[79,108,113,115], OncoQuick[112], and microfluidic chip-based assays[79,108,115]. Following enrichment, isolated CTCs from metastatic breast, prostate, and lung cancers have been examined by FISH (either on-platform or after being cytospun onto charged glass slides) for several common genomic aberrations and amplifications including HER2[79,80,92,93,108,110,115], anaplastic lymphoma kinase (ALK)[107,109], phosphatase and tensin homolog (PTEN)[113],

AR[81,111,113], EGFR[79,81], and TMPRSS2:ERG (transmembrane protease serine 2:ETS-related gene) fusions[112]. FISH has previously been demonstrated to be a powerful tool in assessing genomic aberrations in the clinic in primary and metastatic lesions[116]. Therefore it is not surprising that this technique has several advantages with regards to CTC characterization, including: *(1)* the ability to assess the genomic characteristics of individual CTCs with visual confirmation; *(2)* the ability to assign easily defined cut-off/threshold values based on quantifiable ratios of mutation to parent chromosome; and *(3)* the availability of automated FISH enumeration systems. As with all techniques, FISH does present several limitations as well, including: *(1)* the underlying fact that FISH interrogates CTCs at the genomic level and therefore results may not truly reflect CTC phenotype at the functional protein level; and *(2)* FISH assessment does not provide information regarding markers whose regulation and/or function rely on epigenetic changes, phosphorylation, or appropriate protein localization.

Since the results of FISH analysis are not necessarily representative of cellular phenotype and/or target molecule expression at the protein level, it is likely that FISH technologies will demonstrate their greatest clinical benefit at the level of disease prognosis. An example of this is illustrated by Attard et al. (2009), in their characterization of CTCs for hetero- or homozygous deletion of PTEN[113]. PTEN is involved in the phosphoinositide 3-kinase (PI3K) pathway, and inadequate inhibition of this pathway is associated with high Gleason score and tumor progression in prostate cancer[117,118]. Retrospective analysis has demonstrated that PTEN deletion in primary tumors could stratify patients into different prognostic groups, with hetero- or homozygous PTEN deletion resulting in shorter time to biochemical relapse following

surgery and earlier recurrence of disease when compared to those patients without deletion[119]. Although not investigated by Attard et al., presumably PTEN status on CTCs could be utilized in the future for assessing disease progression throughout the course of disease. By assessing PTEN deletion status in CTCs at baseline or changes in PTEN status with repeated sampling, patients deemed at high risk of progression could be recommended for more aggressive treatment options earlier, thereby sparing patients the morbidity associated with ineffective therapies.

1.3.2.2 Reverse transcription polymerase chain reaction (RT-PCR) and reverse transcription quantitative PCR (RT-qPCR)

With regards to CTC analysis, RT-PCR has been utilized as a means to both detect the presence or absence of CTCs as well as a means for specific molecular characterization. The target transcripts or combinations of transcripts utilized for CTC detection are predominantly of either epithelial- or tissue-specific origin (i.e., EpCAM, prostate specific membrane antigen [PSMA], mucin-1 [MUC-1]), and therefore presumably not transcribed by contaminating leukocytes. However, several groups in the literature have also published the use of RT-PCR for additional molecular characterization of these rare cells following CTC enrichment using the immunomagnetic AdnaTest, including assessment of HER2[120], ER[120,121], and/or PR[120,121], and the CTC chip and herringbone CTC chip platforms for assessment of TMPRSS2:ERG gene fusions[61,122]. One major disadvantage that limits the use of RT-PCR in the characterization of CTCs is that, although assay sensitivity is high, specificity can be reduced as a result of illegitimate transcription and false positives. It is because of this limitation that many have chosen to utilize RT-qPCR in place of traditional RT-PCR for

CTC characterization. The major advantage that RT-qPCR has over RT-PCR is the ability to set defined cut-offs, in the form of C_q values, to reduce false positives based on levels of illegitimate transcription observed in healthy donor blood samples. Utilizing this approach results in an assay that is not only highly sensitive but also highly specific. As with RT-PCR, this technique requires prior enrichment for CTCs, with the majority of studies utilizing the CSS's Profile Kit[123,124] or a similar immunomagnetic approach[125,126] for this task, examining a multitude of prognostic markers including (but not limited to) HER2, TWIST1, CD133, EGFR, MET and VEGFR2 (vascular endothelial growth factor receptor 2)[112,120,121,123–127]. The ability to multiplex this approach and examine multiple genes at once from a very small initial sample volume is a significant advantage that this technique offers. In addition, very recent studies have demonstrated that novel PCR approaches may also be useful in examining microRNA (miRNA) expression, methylation status, and single nucleotide mutations on CTCs[124127,128]. However, RT-PCR and RT-qPCR also have several well recognized disadvantages, including: *(1)* the inability to visually confirm that signals obtained are from CTCs and not due to leukocyte contamination; and *(2)* analysis of single CTCs is still technologically challenging using this approach with few studies having published results from patient samples[125]. Therefore the majority of studies in the literature rely on pooled samples, which limits the ability to examine heterogeneity in marker expression across multiple CTCs in a single sample.

Although both RT-PCR and RT-qPCR have been routinely employed for CTC detection and characterization[112,120,121,123–127], their widespread utility, especially with regards to detailed molecular characterization of heterogeneous CTC populations, is

currently restricted by their limited capacity for single-cell analysis. Based on this current limitation and the availability of a number of other excellent single-cell analysis techniques, at present we do not foresee this technique to be the primary CTC characterization choice for predicting targeted therapy response, drug resistance development, or prognosis in the metastatic setting. However one area in which we anticipate that these approaches will be very advantageous is the clinical setting of primary disease. In this clinical setting, blood analysis can yield very low numbers of CTCs[129], with the only way to combat this issue being the collection of larger blood volumes. Therefore characterization of CTCs in patients with primary disease is extremely challenging and extra care must be taken in obtaining the greatest amount of information from this small sample size. PCR approaches are beneficial in this regard as they allow for the amplification of these small samples and for multi-marker analysis allowing for the assessment of many potential targets at once. For example, using this approach, a pooled sample with isolated CTCs from a primary breast cancer patient could be assessed for expression of HER2, EGFR, ER, PR, and cancer stem cell (CSC) markers simultaneously, thereby increasing the likelihood of obtaining useful CTC characterization information that could help direct patient care. Therefore, in the future we anticipate that RT-PCR and RT-qPCR approaches will demonstrate their greatest clinical benefit in the setting of early-stage/primary disease, with the potential for widespread utilization in the metastatic setting based upon the optimization of single-cell analysis protocols.

1.3.2.3 Microarrays

Both gene expression arrays and comparative genomic hybridization arrays (aCGH) have been used to characterize CTCs. Gene expression arrays provide information about samples at the RNA level, in particular the up/down regulation of suspected and novel transcripts; while aCGH provides information about samples at the DNA level, including copy number variations, specific mutational variants, or global genomic changes. Both techniques require that experimental samples be compared to appropriate control samples. Depending upon the information that one wishes to obtain, these controls will vary. For example, to obtain information regarding differences between CTCs (experimental) and primary/metastatic lesions (control), samples of each must be obtained and analyzed for differences using pre-determined cut-off values (i.e., 1.5 fold change). Immunomagnetic enrichment[130–132] and density gradient centrifugation[133] have been the primary means utilized as upstream CTC enrichment techniques prior to microarray analysis. In the literature, microarrays have been primarily utilized to look for genetic signatures of aggressive disease and/or the identification of prognostic/diagnostic biomarkers of disease[131–133]. In addition, gene or copy number aberrations have been examined in CTCs[130,131,134]. The obvious advantages of array-based analysis include: *(1)* automated analysis; *(2)* the ability to set pre-determined cut-off values, thereby standardizing interpretation; *(3)* direct comparison of a multitude of disease settings (e.g., CTCs to primary/metastatic tumors, CTCs in treatment responders versus non-responders, CTCs at baseline versus following systemic treatment, etc.); and *(4)* the potential for novel biomarker identification and/or CTC gene signatures. In addition to the many advantages that this approach offers, several limitations also exist,

including: *(1)* the necessity for specialized bioinformatics personnel for the analysis and interpretation of the massive amount of data that can be generated using this approach; *(2)* the necessity for validation of individually identified genes (gene expression arrays) using RT-qPCR; *(3)* cost; *(4)* difficulty in assessing sample purity to determine if results are from CTCs or contaminating leukocytes; and *(5)* limitations with regards to sensitivity that can make single cell analysis difficult, with few studies reporting on arrays using individual CTCs[134].

In the future, we anticipate that the most useful application of microarray-based approaches for CTC analysis may be in the area of prognosis and patient treatment stratification using CTC gene signatures. This approach has previously been demonstrated to be feasible when examining primary tumor tissue in breast cancer using the FDA approved MammaPrint® Breast Cancer Test by Agendia (Irvine, CA, USA)[135,136]. Using this assay, primary tumor tissue is collected and subjected to array analysis to stratify patients into poor or good prognosis groups, and recommendations for aggressive (hormone therapy plus chemotherapy with or without trastuzumab) or less aggressive (hormone therapy alone) treatment, respectively, can be made based upon the results. Although this level of personalized care has not yet been met using microarrays on isolated CTCs, moving forward, microarray approaches may hold similar potential in this regard.

1.3.2.4 Sequencing

Until recently, the use of sequencing in clinical cancer genomics has presented significant logistical and economic challenges, due to the slow speed of sample processing and the high cost of sequencing. However the development of novel, next-

generation sequencing technologies has renewed enthusiasm in the field of clinical cancer genomics[137–140]. Sequencing is an umbrella term that encompasses a number of different methodologies including traditional gene sequencing approaches (Sanger sequencing; pyrosequencing; MALDI-TOF sequencing; and targeted sequencing approaches such as allele-specific RT-PCR and RT-qPCR melting curve analysis) and next-generation sequencing platforms (Roche 454™ pyrosequncing, Life Technologies SOLiD™ sequencing and Ion Torrent™ sequencing, the Illumina HiSeq™, the Helicos Heliscope™, Pacific Biosciences PacBioRS™, and Complete Genomics CGA™ platform), all of which have been reviewed previously[138–145]. Each technique has specific advantages and disadvantages, with all resulting in the acquisition of the base-by-base sequence information for a particular genome or target region within that genome. Sequencing technology is a powerful tool for the analysis of specific genomic aberrations, especially in the setting of cancer. It is important to note that this technique can be applied to both genomic DNA and transcribed RNA sequences in the form of cDNA (complementary DNA). With regards to CTC analysis, sequencing tends to be applied more frequently at the level of RNA; however several studies have also interrogated CTCs at the DNA level[128,146–148]. In general, for processing at the RNA level, total RNA or mRNA is extracted from CTCs following enrichment using either immunomagnetic methods[149] including the CSS[128,150], density gradient centrifugation[151], or microfluidic chip-based[152] approaches. Isolated RNA is then reverse transcribed into cDNA and PCR amplified using primers that are specific to the mutant/target region. Amplified mutations can be detected using either gel electrophoresis for known length transcripts, and/or analyzed with one of the several commercially available sequencing

platforms mentioned above. For processing at the DNA level instead, total DNA is extracted from CTCs, whole genome amplified using commercially available kits, and subsequently amplified via PCR using primers that are specific to the mutant/target region. As with RNA, the PCR product is then analyzed using either gel electrophoresis or a sequencing platform. Many studies in the literature have utilized these approaches to interrogate CTCs for a variety of single nucleotide changes in KRAS[128], BRAF[128], p53[149], AR[152], TMPRSS2:ERG[152], PI3KCA (phosphatidylinositol-3-kinase, catalytic subunit α)[148], and EGFR[146,147].

One of the first reported studies examining the utility of CTC sequencing was reported by Maheswaran et al. (2008), in their examination of EGFR activating and drug-resistant mutants in non-small-cell lung cancer patients[153]. Throughout the study this group not only demonstrated the presence of the primary EGFR activating mutation in CTCs but also the presence of a T790M mutation known to confer resistance to EGFR-targeted therapies. Using serial CTC analysis, it was additionally observed that the genotype of captured CTCs evolved throughout treatment and that the prevalence of the T790M resistance genotype increased throughout the course of therapy, suggesting that CTCs may be representative of the current state of disease. In a recent report by Heitzer et al. (2013), single CTCs from metastatic colorectal cancer patients were assessed for a panel of 68 colorectal cancer-associated genes[148]. Using this approach, CTCs were shown to harbor mutations found in both the primary and metastatic lesions, metastatic lesions alone, and novel mutations not previously observed in either the primary or metastatic sites (termed private mutations). Subsequent ultra-deep sequencing of primary and metastatic sites often revealed the presence of these private mutations, previously

missed by sequencing but captured by CTC analysis. In addition, many of the identified mutations were for actionable targets, with FDA-approved drugs currently available or being assessed for targeted treatment in ongoing clinical trials.

The utilization of sequencing for CTC analysis has several advantages over other characterization techniques including: *(1)* the ability to identify single nucleotide alterations, since minor aberrations such as these can result in significant phenotypic changes and may be important for predicting response to select therapies; *(2)* results from sequencing are presented as either positive or negative and do not appear as gradations as with immunofluorescence; and *(3)* analysis can be automated to reduce interpreter bias. Sequencing techniques also have several marked disadvantages including: *(1)* limitations with regards to sensitivity that make single cell analysis difficult, with many groups reporting the need for a minimum of 50 or more CTCs for adequate results[128,149]; and *(2)* leukocyte contamination and the inability to visually confirm the source of amplified transcripts can lead to false positive/negative results. However, several groups have attempted to utilize single cell micromanipulation (selecting for CTCs based on immunofluorescent staining prior to the collection of DNA/RNA)[146] and/or adapted PCR protocols (e.g., nested PCR)[128] to combat these issues with promising results.

When considering clinical cancer genomics moving forward, care must be taken in discriminating driver mutations from so-called passenger mutations. As genomic instability is an underlying characteristic of cancer[154,155] one cannot assume that all mutations in a given sample are of equal importance. This is well exemplified by the great clinical benefit of trastuzumab for HER2-amplication in breast and gastric cancers but the lack of this benefit in ovarian and endometrial cancers[137,156–158]. In addition, the

identification of actionable/druggable targets must be at the forefront of clinical cancer genomics. There is concern in this field that the genotyping of tumor tissue biopsies and/or CTCs may not be capturing functionally relevant information[159,160]. The reason for this concern centers on the fact that the cellular genotype is not necessarily reflective of the cellular phenotype and that sample contamination with normal tissue can lead to false negative results. We anticipate that the molecular characterization of CTCs will help to alleviate some of these concerns. Firstly, Heitzer et al. (2013), have described a CTC sequencing approach for single-cell analysis, suggesting that contamination with normal cells may be reduced. Secondly, although the sequencing of CTCs does not change the fact that the readout is still at the level of the genome, we anticipate that, especially in cases in which metastatic lesions are inaccessible, that CTC sequencing will strengthen conclusions regarding mutations that are drivers versus those that are passengers as they may be present not only in the primary/metastatic lesion but also in the cells that were able to escape into the circulation. The conserved nature of these mutations may suggest an important functional contribution to disease progression. In addition, as demonstrated by Heitzer et al., the sequencing of CTCs may identify relevant private mutations, present but not detected in tumor tissue[148].

In the future we anticipate that the greatest clinical benefit of the genomic sequencing of CTCs will be achieved when this approach is utilized to assess the genomic evolution of disease within a patient over time, and to quickly identify actionable target mutations that would make patients eligible for ongoing clinical trials, as demonstrated by Heitzer et al.[148]. As it is still unclear if genomic sequencing will provide functionally relevant information that can be applied for predicting targeted

treatment response and overall patient outcomes, we foresee that this approach, at least in the near future, will likely not be utilized in isolation and instead used in combination with other phenotyping platforms such that firm conclusions can be drawn regarding clinical treatment decision-making.

1.3.3 General considerations for CTC characterization

Although there are currently a number of exciting methodologies available for CTC characterization and even more in development, careful consideration needs to be placed on which technique will produce optimal results for the molecular characteristic(s) under investigation, as it is likely that different aberrations will require different approaches. For example, the presence or absence of a particular marker may be sufficient for some targets, (e.g., estrogen/progesterone receptors)[161], however others may require the presence of particular single nucleotide substitutions (e.g., BCR-ABL mutations which confer drug resistance)[162], copy-number alterations (e.g., AR amplification)[163], aberrant localization (e.g., BRCA1 absent/reduced nuclear expression and association with aggressive phenotypes)[164], or specific functional activation (AKT phosphorylation)[165,166] in order to draw any conclusions regarding novel treatment options or patient outcomes. As not all approaches can provide this information, care must be taken in choosing the appropriate molecular characterization technique or combinations of techniques for each target. In addition, once chosen, the appropriate technique(s) needs to be validated and standardized before it can be considered for routine use in the clinic. This standardization needs to be implemented at both the level of procedure as well as at the level of interpretation. For example, data must be interpreted to determine if analysis of single cells is necessary or if a pooled result from all CTCs in

an individual will suffice. If a single cell approach is chosen, clear-cut criteria must be set with regards to how many cells should be characterized with appropriate minimum or maximum values set. In addition, what constitutes a positive or negative signal must be appropriately defined; if the system is more graduated in nature (i.e., low, medium, or high expression) these gradations need to be specifically defined, and if necessary automated systems need to be implemented to ensure that results are the same across laboratories. The considerations discussed in this section can all have a dramatic impact on the results obtained from individual studies and clinical trials. Therefore when comparing the current literature one must take into account the variety of approaches utilized and the effect these approaches may have on the reported results. These considerations and others have been extensively reviewed previously[55,167–169].

1.3.4 Current limitations of CTC molecular characterization

The most prominent limitation that currently exists in the molecular characterization of CTCs is the low number of CTCs collected, especially from those patients with early-stage disease. These cells appear to be very delicate in nature and can be easily lost or destroyed during processing[110]. Considering that CTC populations tend to be quite heterogeneous, it is very difficult to draw conclusions about treatment if only a small population of cells are available for analysis. To combat this issue, research has begun to focus on the development of novel technologies for enhanced CTC capture as well as focusing on CTC characterization on-system, thereby reducing CTC loss when switching techniques. However, thus far the CSS continues to be the only platform that is FDA-approved for use in the clinic.

1.3.5 Clinical significance of CTC molecular characterization

Although a number of different molecular characteristics have been investigated on CTCs across numerous epithelial cancers, the aberration that has been most widely examined is HER2, an EGFR, known to be over-expressed in a subset of cancer patients. Currently the expression of HER2 can be investigated on individual CTCs captured by the CSS. Based on the results of such an investigation, it may be possible for patients to get access to HER2 targeting therapies (e.g., Herceptin) that are currently reserved for patients whose primary tumors express this protein[170]. In this way, CTCs could act as a liquid biopsy, informing physicians of disease evolution earlier then currently utilized methods, and thereby ultimately improving patient care (*Figure 1.2*). In addition, the characterization of CTCs could identify new targets for novel therapies and enable a better understanding of the mechanisms that allow these cells to escape into the circulation, extravasate into distant tissue and form clinically relevant secondary metastases.

Although promising from a research perspective, thus far data supporting the clinical significance of the molecular characterization of CTCs is inconclusive. Several retrospective studies examining treatment outcomes in patients with $HER2^-$ primary tumors but with $HER2^+$ CTCs who have received Her2-targeting agents have demonstrated mixed results[82,88,171,172]. Thus far, only one prospective clinical trial examining the utility of treatment stratification based on the HER2 status of CTCs has been completed[89]. This multicentre phase II trial aimed to evaluate the use of single-agent lapatinib (targeting both HER2 and EGFR) in metastatic breast cancer patients with $HER2^-$ primary tumors and $HER2^+$ CTCs. Of the seven patients enrolled, one

experienced an adverse event during the treatment period and discontinued treatment. The other six patients demonstrated signs of progressive disease and therefore also discontinued treatment. Following these results the study was terminated. However, several upcoming trials are set to continue to investigate the HER2 status of CTCs and the use of CTCs as a liquid biopsy, including the TREAT CTC[173], DETECT III[174], CirCé01[175], and the COMETI P2[176] trials[177].

The inconclusive results described here raise questions about our current understanding of the biology of these rare cells. CTC research is unique in that it has largely utilized a bedside-to-benchtop approach. This method, unlike benchtop-to-bedside research, which can often take years to impact patient care, has allowed CTCs quick entry into the clinical setting. However, physicians are hesitant to use results from CTC analysis in patient treatment decision-making due to a lack of understanding of their underlying biology. Therefore appropriate pre-clinical mouse models of metastasis and complementary CTC analysis techniques must be utilized in order to properly identify the current limitations that exist with CTC detection, enumeration, and characterization technologies and to further investigate these outstanding biological questions. In addition, a better understanding of CTC biology may shed light on which CTCs are the most important to study and characterize and therefore guide strategies on how to utilize CTCs most effectively in a clinical setting.

1.4 Epithelial-to-mesenchymal transition (EMT)

It is curious to note that in up to 35% of patients with various metastatic cancers, CTCs are undetectable despite the presence of widespread systemic disease[178].

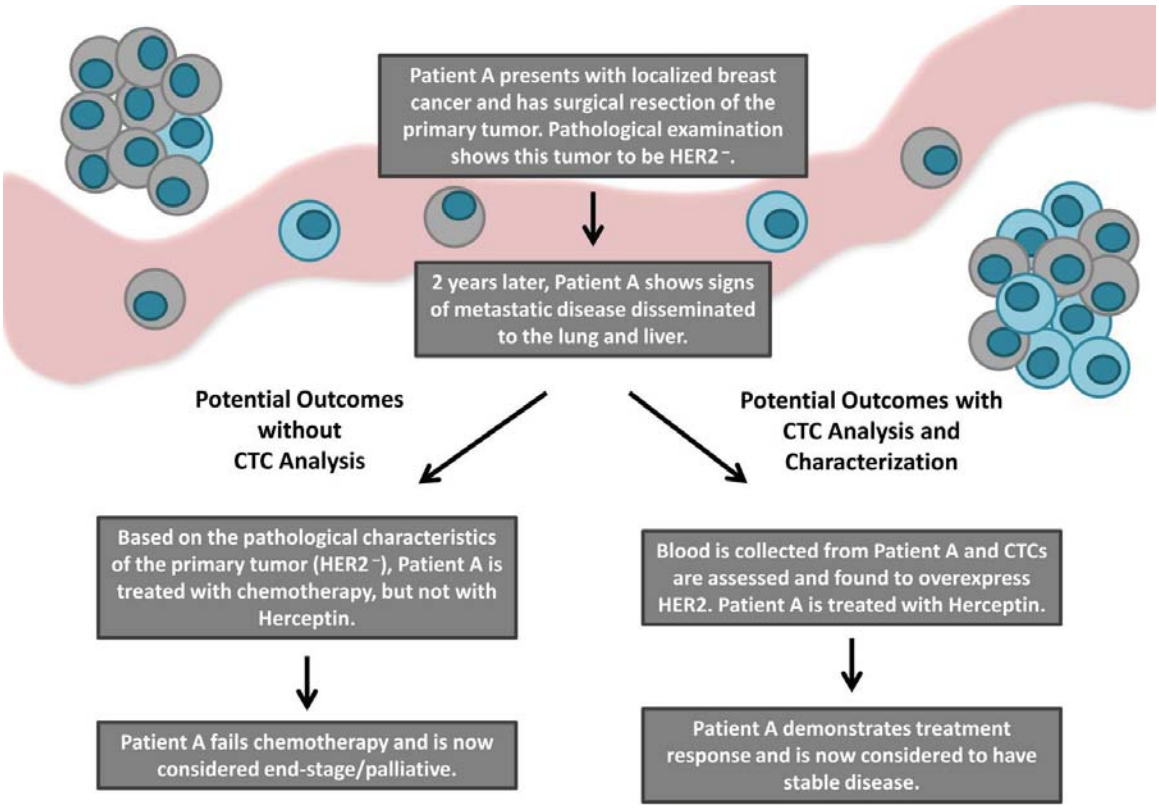

Figure 1.2. An overview of the current and potential patient outcomes following the incorporation of CTC molecular characterization into the clinic. The majority of cancer-related deaths result from the development of metastatic disease. Although metastatic lesions can be highly heterogeneous compared to their primary tumor counterparts, current treatment decision making is typically based on characteristics of the primary tumor, as routine metastatic biopsy is not clinically feasible. CTCs have been suggested as a surrogate to metastatic biopsy. Characterization of therapeutic target molecules such as HER2 on CTCs may increase the availability of targeted therapies (*i.e.*, the HER2 targeting agent Herceptin) to patients previously considered ineligible based upon the characteristics of their primary tumor. Ultimately, utilization of CTC analysis and characterization in the clinic may predict response to targeted therapies and improve patient outcomes.

This lack of detection has been proposed to be a result of the epithelial-to-mesenchymal transition (EMT), a process first described for its essential role in embryo development[179]. The process of EMT involves the conversion of epithelial cells to mesenchymal cells via significant phenotypic changes resulting in the loss of cell-cell adhesion, loss of cell polarity, and the acquisition of a highly invasive and motile phenotype necessary for appropriate embryogenesis[180–182]. The acquisition of this phenotype is only accomplished through significant remodeling of epithelial cells, specifically via reduced expression of various epithelial markers (i.e., E-cadherin and EpCAM) and a corresponding increase in mesenchymal markers (i.e., N-cadherin and vimentin)[72,182–185]. This developmental process is thought to be reactivated in some epithelial cancers, thus allowing for enhanced tumor motility and an increased ability to invade and metastasize to distant organs (*Figure 1.3*)[186,187]. Once reaching a suitable secondary site, it is believed that the reverse process, mesenchymal-to-epithelial transition (MET), may be required to initiate tumor growth. In addition to this enhanced migratory phenotype, EMT has also been associated with increased therapy resistance[188–190].

The mechanisms of EMT in cancer are extremely complex and involve a number of identified and yet unidentified molecular players. In brief, it is believed that the process of EMT can be greatly influenced by EMT-inducers in the tumor microenvironment, including a number of growth factors such as epidermal growth factor (EGF), hepatocyte growth factor (HGF), insulin-like growth factor 1 (IGF-1), platelet-derived growth factor (PDGF), fibroblast growth factor (FGF), and transforming growth factor β (TGF-β)[191–195]. These paracrine (and sometimes autocrine) signals are then

converted into intracellular signals that will eventually result in specific EMT-related phenotypic changes (i.e., enhanced cellular migration, invasion, and cell survival). In general, thus far three intracellular mechanisms have been recognized as controllers that respond to EMT-inductive stimuli. Specifically, *(1)* signal transduction cascades (i.e., Wnt signaling pathway and AR signaling), *(2)* EMT-related transcription factors (i.e., Snail, Twist, and ZEB family members), and *(3)* epigenetic mechanisms (i.e., chromatin remodeling, DNA methylation, and miRNA)[191].

1.4.1 Clinical evidence and implications of EMT in prostate cancer

Although EMT has been extensively recognized in *in vitro* and *in vivo* model systems, due to the plastic nature of this process, it has been difficult to validate in clinical samples. Evidence of EMT in PCa, however, has been demonstrated in a number of studies. The aberrant expression and/or downregulation of the epithelial marker E-cadherin has been the most extensively studied and demonstrated to correlate with advanced Gleason score, tumor grade, disease stage, and N-cadherin overexpression[191,196–200]. In addition, reduction/aberrant expression of this marker is prognostic, predicting for progression following radical prostatectomy, the presence of metastases, and shorter overall survival[199]. Expression changes in various mesenchymal markers and EMT transcription factors, such as N-cadherin, vimentin, Twist, Zeb1, have also been demonstrated in clinical samples. Specifically, overexpression of N-cadherin, Twist, and Zeb1 have been associated with increasing Gleason scores and shown to be absent or reduced in normal and/or benign disease[194,197,201,202]. Additionally, vimentin has been shown to be prognostic in primary PCa, predicting for shorter time to biochemical

Figure 1.3. Contribution of the epithelial-to-mesenchymal transition (EMT) to prostate cancer progression and metastasis. The developmental process of epithelial-to-mesenchymal transition (EMT) has been proposed to be reactivated during cancer progression and required for the intravasation of tumour cells through a basement membrane into the circulation. The enhanced invasive phenotype exhibited by cells that have undergone EMT is due, in part, to significant remodelling of the cytoskeleton, including downregulation of various epithelial proteins (i.e., E-cadherin and EpCAM) and upregulation of various mesenchymal proteins (i.e., N-cadherin and vimentin). This process exists on a continuum from purely epithelial --> hybrid expression --> purely mesenchymal, thereby potentially generating circulating tumour cells (CTCs) with highly heterogeneous EMT phenotypes. Upon reaching an appropriate secondary site, CTCs may extravasate from the bloodstream into the surrounding tissue. However it has been proposed that disseminated tumour cells must undergo the reverse process of mesenchymal-to-epithelial transition (MET) in order to establish micro- and macro-metastases at secondary sites, during which cells downregulate expression of mesenchymal proteins and upregulate expression of epithelial proteins.

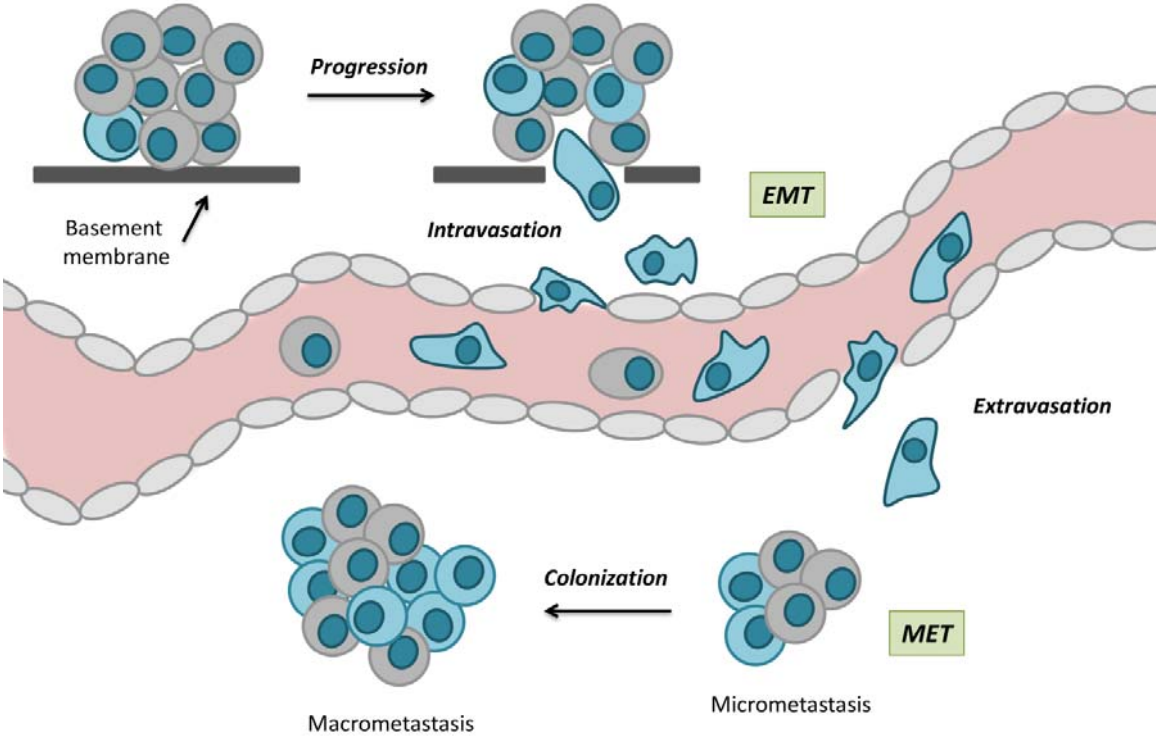
Progression
Basement membrane
Intravasation
EMT
Extravasation
Colonization
MET
Macrometastasis
Micrometastasis

recurrence and has also been associated with the presence of bone metastases and poorly differentiated tumors[203,204].

1.4.2 Clinical evidence and implications of EMT in CTCs

Thus far the majority of EMT characterization in CTCs has been performed in cells that have been enriched for, or detected using, epithelial-based strategies, likely due to a lack of appropriate technologies for selecting highly mesenchymal CTCs. With this in mind, several studies (especially in breast cancer) have detected the expression of various mesenchymal markers in both early-stage (I-III) and metastatic disease. Specifically, the expression (mRNA and/or protein) of vimentin[205–209], fibronectin[205,207], Twist1[206,210–214], AKT2[211,212], PI3K[211,212], Slug[213], FoxC2[213], Snail1[214], Zeb1[62,214], E-cadherin[215], N-cadherin[209], and many others have been assessed in these patient cohorts. A general trend that exists in the current literature is that CTCs with a hybrid EMT phenotype are more likely to be detected in patients with metastatic disease and/or show higher expression of mesenchymal markers compared to those in early-stage disease[205,206,210]. Additionally, it has been demonstrated that in both early-stage and metastatic patients that these hybrid CTCs are not rare, and represent a significant portion of the detectable CTCs within an individual patients[205–207,209–212,214–216]. These hybrid CTCs are also often co-expressed with various stem cell markers including ALDH1[205,210,211,214], CD44[211], and CD133[209,214,215]. A small number of published studies have also attempted to characterize CTCs that are undetectable by current epithelial-based capture techniques, by examining patients with CTC-negative disease[205,207,214]. Although several studies have reported the detection of various mesenchymal markers in

these patients, without reliable mesenchymal CTC markers, these results are difficult to interpret as they may represent false positives.

Of particular interest with regards to EMT characterization of CTCs is the prognostic value of cells with a hybrid epithelial-mesenchymal phenotype. Thus far, only a small number of studies have reported such information. Specifically, Gradilone et al. (2011) noted that metastatic breast cancer patients with CTCs positive for the expression of either vimentin and/or fibronectin (EMT^+) showed worse prognosis compared to those that did not (EMT^-), and compared to patients with CK^+EMT^- disease[207]. Interestingly, this study did not report differences in prognosis between patients with CK^-EMT^+ and CK^+EMT^+ CTCs. In contrast, Pal et al. (2014), have reported that CTC fragments ($CK^+DAPI^{+/-}CD45^-$ events) in a small group of high-risk localized prostate cancer patients (n=35) isolated using the CSS and characterized for E-cadherin and/or CD133 positivity were prognostic of BCF at 1 year following radical prostatectomy[215]. Finally, the relationship of EMT+ CTCs and treatment resistance is a growing area of research, however thus far the results are only correlative in nature, with EMT phenotypes appearing to be associated with disease progression and treatment response[216].

1.5 Overall Rationale

The CSS not only provides a minimally invasive means of patient sample collection and CTC enumeration but also allows for limited molecular characterization of CTCs. Characterization of isolated CTCs could lead to a better understanding of the biological mechanisms that underlie metastasis, aid in the identification of novel targets for new therapies, and ultimately help to direct patient care. In addition to exploring the

molecular characteristics of CTCs, we also aim to investigate several areas of research that have been largely unexplored, including the potential role of CTCs in early-stage disease and therapy response, as well as exploiting an *in vivo* model system to gain a better understanding of the biology of CTCs and their contribution to the metastatic cascade.

1.6 Overall Goal and Objectives

The ***overall goal*** of this thesis is to address the need for improved understanding of the significance of CTCs in early stage prostate cancer, provide novel tools for assessing CTC characteristics in the clinic, and develop a better understanding of CTC biology and its contribution to metastasis.

In order to assess this goal, the ***specific objectives*** of this thesis are:

1. To investigate CTCs in post-surgery prostate cancer patients receiving adjuvant and salvage radiotherapy.
2. To develop and optimize new techniques that would allow for molecular characterization of CTCs on the regulatory-approved CSS.
3. To investigate the effects of epithelial-to-mesenchymal (EMT) on CTC generation and metastasis.

1.7 References

1 Canadian Cancer Statistics, 2015. Toronto: Canadian Cancer Society 2015. Available at: www.cancer.ca. .

2 Prostate Cancer. June 10 2015. Toronto: Canadian Cancer Society 2015. Available at: www.cancer.ca. .

3 Ørsted DD, Bojesen SE. The link between benign prostatic hyperplasia and prostate cancer. *Nat Rev Urol* 2013; **10**: 49–54.

4 Prostate Cancer, Malignant Tumours. June 10 2015. Toronto: Canadian Cancer Society 2015. Available at: www.cancer.ca. .

5 Andriole GL, Crawford ED, Grubb RL, Buys SS, Chia D, Church TR *et al.* Prostate cancer screening in the randomized prostate, lung, colorectal, and ovarian cancer screening trial: Mortality results after 13 years of follow-up. *J Natl Cancer Inst* 2012; **104**: 125–132.

6 Gerber GS, Chodak GW. Digital rectal examination in the early detection of prostate cancer. *Urol Clin North Am* 1990; **17**: 739–744.

7 Lilja H, Ulmert D, Vickers AJ. Prostate-specific antigen and prostate cancer: prediction, detection and monitoring. *Nat Rev Cancer* 2008; **8**: 268–78.

8 Shariat SF, Scardino PT, Lilja H. Screening for prostate cancer: an update. Can. J. Urol. 2008; **15**: 4363–4374.

9 Srigley JR, Humphrey PA, Amin MB, Chang SS, Egevad L, Epstein JI *et al.* Protocol for the examination of specimens from patients with carcinoma of the prostate gland. *Arch Pathol Lab Med* 2009; **133**: 1568–1576.

10 Mohler JL. The 2010 NCCN clinical practice guidelines in oncology on prostate cancer. J. Natl. Compr. Canc. Netw. 2010; **8**: 145.

11 Thompson I, Thrasher JB, Aus G, Burnett AL, Canby-Hagino ED, Cookson MS *et al.* Guideline for the management of clinically localized prostate cancer: 2007 update. *J Urol* 2007; **177**: 2106–31.

12 Scherr D, Swindle PW, Scardino PT. National Comprehensive Cancer Network guidelines for the management of prostate cancer. Urology. 2003; **61**: 14–24.

13 Droz J-P, Aapro M, Balducci L, Boyle H, Van den Broeck T, Cathcart P *et al.* Management of prostate cancer in older patients: updated recommendations of a working group of the International Society of Geriatric Oncology. *Lancet Oncol* 2014; **15**: e404–e414.

14 Klotz L. Active surveillance for prostate cancer: For whom? J. Clin. Oncol. 2005; **23**: 8165–8169.

15 Gakis G, Boorjian SA, Briganti A, Joniau S, Karazanashvili G, Karnes RJ *et al.* The Role of Radical Prostatectomy and Lymph Node Dissection in Lymph Node-Positive Prostate Cancer: A Systematic Review of the Literature. *Eur Urol* 2013; **66**: 191–199.

16 Ohori M, Goad JR, Wheeler TM, Eastham JA, Thompson TC, Scardino PT. Can radical prostatectomy alter the progression of poorly differentiated prostate cancer? *J Urol* 1994; **152**: 1843–9.

17 Pound CR, Partin AW, Epstein JI, Walsh PC. Prostate-specific antigen after anatomic radical retropubic prostatectomy. Patterns of recurrence and cancer control. *Urol Clin North Am* 1997; **24**: 395–406.

18 Koontz BF, Chino J, Lee WR, Hahn CA, Buckley N, Huang S *et al.* Morbidity and prostate-specific antigen control of external beam radiation therapy plus low-dose-rate brachytherapy boost for low, intermediate, and high-risk prostate cancer. *Brachytherapy* 2009; **8**: 191–196.

19 Lawton CA, Winter K, Grignon D, Pilepich M V. Androgen suppression plus radiation versus radiation alone for patients with stage D1/pathologic node-positive adenocarcinoma of the prostate: Updated results based on national prospective randomized trial Radiation Therapy Oncology Group 85-31. *J Clin Oncol* 2005; **23**: 800–807.

20 Ferraldeschi R, Welti J, Luo J, Attard G, de Bono JS. Targeting the androgen receptor pathway in castration-resistant prostate cancer: progresses and prospects. *Oncogene* 2014; : 1–13.

21 Mottet N, Bellmunt J, Bolla M, Joniau S, Mason M, Matveev V *et al.* EAU guidelines on prostate cancer. Part II: Treatment of advanced, relapsing, and castration-resistant prostate cancer. *Eur Urol* 2011; **59**: 572–583.

22 Rick FG, Block NL, Schally A V. Agonists of luteinizing hormone-releasing hormone in prostate cancer. *Expert Opin Pharmacother* 2013; **14**: 2237–47.

23 Shore ND, Abrahamsson P-A, Anderson J, Crawford ED, Lange P. New considerations for ADT in advanced prostate cancer and the emerging role of GnRH antagonists. Prostate Cancer Prostatic Dis. 2012. doi:10.1038/pcan.2012.25.

24 Kaisary A, Iverson P, Tyrrell C, Carroll K, Morris T. Is there a role for antiandrogen monotherapy in patients with metastatic prostate cancer? *Prostate Cancer Prostatic Dis* 2001; **4**: 196–203.

25 Oh WK. The evolving role of estrogen therapy in prostate cancer. *Clin Prostate Cancer* 2002; **1**: 81–89.

26 Strum SB, Scholz MC, McDermed JE. Intermittent androgen deprivation in prostate cancer patients: factors predictive of prolonged time off therapy. 2000 doi:10.1634/theoncologist.5-1-45.

27 Hugosson J, Carlsson S. Overdetection in screening for prostate cancer. *Curr Opin Urol* 2014; **24**: 256–63.

28 Crawford ED, Ventii K, Shore ND. New biomarkers in prostate cancer. *Oncology (Williston Park)* 2014; **28**: 135–42.

29 Care CTF on PH, Bell N, Connor GS, Shane A, Joffres M, Singh H *et al.* Recommendations on screening for prostate cancer with the prostate-specific antigen test. *CMAJ* 2014; **186**: 1225–1234.

30 Sartori DA, Chan DW. Biomarkers in prostate cancer: what's new? *Curr Opin Oncol* 2014; **26**: 259–64.

31 Knezevic D, Goddard AD, Natraj N, Cherbavaz DB, Clark-Langone KM, Snable J *et al.* Analytical validation of the Oncotype DX prostate cancer assay - a clinical RT-PCR assay optimized for prostate needle biopsies. *BMC Genomics* 2013; **14**: 690.

32 Cuzick J, Berney DM, Fisher G, Mesher D, Møller H, Reid JE *et al.* Prognostic value of a cell cycle progression signature for prostate cancer death in a conservatively managed needle biopsy cohort. *Br J Cancer* 2012; **106**: 1095–9.

33 Cooperberg MR, Simko JP, Cowan JE, Reid JE, Djalilvand A, Bhatnagar S *et al.* Validation of a cell-cycle progression gene panel to improve risk stratification in a contemporary prostatectomy cohort. *J Clin Oncol* 2013; **31**: 1428–1434.

34 Freedland SJ, Gerber L, Reid J, Welbourn W, Tikishvili E, Park J *et al.* Prognostic utility of cell cycle progression score in men with prostate cancer after primary external beam radiation therapy. *Int J Radiat Oncol Biol Phys* 2013; **86**: 848–853.

35 Badani K, Thompson DJS, Buerki C, Davicioni E, Garrison J, Ghadessi M *et al.* Impact of a genomic classifier of metastatic risk on postoperative treatment recommendations for prostate cancer patients: a report from the DECIDE study group. *Oncotarget* 2013; **4**: 600–9.

36 Jeffrey Karnes R, Bergstralh EJ, Davicioni E, Ghadessi M, Buerki C, Mitra AP *et al.* Validation of a genomic classifier that predicts metastasis following radical prostatectomy in an at risk Patient population. *J Urol* 2013; **190**: 2047–2053.

37 Chambers AF, Groom AC, MacDonald IC. Dissemination and growth of cancer cells in metastatic sites. *Nat Rev Cancer* 2002; **2**: 563–72.

38 Sethi N, Kang Y. Unravelling the complexity of metastasis - molecular understanding and targeted therapies. *Nat Rev Cancer* 2011; **11**: 735–48.

39 Aitken SJ, Thomas JS, Langdon SP, Harrison DJ, Faratian D. Quantitative analysis of changes in ER, PR and HER2 expression in primary breast cancer and paired nodal metastases. *Ann Oncol* 2010; **21**: 1254–61.

40 Carlsson J, Nordgren H, Sjöström J, Wester K, Villman K, Bengtsson NO *et al.* HER2 expression in breast cancer primary tumours and corresponding metastases. Original data and literature review. *Br J Cancer* 2004; **90**: 2344–8.

41 Regitnig P, Schippinger W, Lindbauer M, Samonigg H, Lax SF. Change of HER-2/neu status in a subset of distant metastases from breast carcinomas. *J Pathol* 2004; **203**: 918–26.

42 Gancberg D, Di Leo a., Cardoso F, Rouas G, Pedrocchi M, Paesmans M *et al.* Comparison of HER-2 status between primary breast cancer and corresponding distant metastatic sites. *Ann Oncol* 2002; **13**: 1036–1043.

43 Vincent-Salomon a, Pierga J-Y, Couturier J, d'Enghien CD, Nos C, Sigal-Zafrani B *et al.* HER2 status of bone marrow micrometastasis and their corresponding primary tumours in a pilot study of 27 cases: a possible tool for anti-HER2 therapy management? *Br J Cancer* 2007; **96**: 654–9.

44 Jensen JD, Knoop A, Ewertz M, Laenkholm A-V. ER, HER2, and TOP2A expression in primary tumor, synchronous axillary nodes, and asynchronous metastases in breast cancer. *Breast Cancer Res Treat* 2012; **132**: 511–21.

45 Jabbour MN, Massad CY, Boulos FI. Variability in hormone and growth factor receptor expression in primary versus recurrent, metastatic, and post-neoadjuvant breast carcinoma. *Breast Cancer Res Treat* 2012; **135**: 29–37.

46 Liu AY, Roudier MP, True LD. Heterogeneity in primary and metastatic prostate cancer as defined by cell surface CD profile. *Am J Pathol* 2004; **165**: 1543–1556.

47 Cheng L, Bostwick DG, Li G, Wang Q, Hu N, Vortmeyer AO *et al.* Allelic imbalance in the clonal evolution of prostate carcinoma. 1999 doi:10.1002/(SICI)1097-0142(19990501)85:9<2017::AID-CNCR20>3.0.CO;2-V.

48 Sakr WA, Macoska JA, Benson P, Grignon DJ, Wolman SR, Pontes JE *et al.* Allelic loss in locally metastatic, multisampled prostate cancer. *Cancer Res* 1994; **54**: 3273–3277.
49 Pantel K, Brakenhoff RH, Brandt B. Detection, clinical relevance and specific biological properties of disseminating tumour cells. *Nat Rev Cancer* 2008; **8**: 329–40.
50 Pantel K, Brakenhoff RH. Dissecting the metastatic cascade. *Nat Rev Cancer* 2004; **4**: 448–56.
51 Valastyan S, Weinberg RA. Tumor metastasis: Molecular insights and evolving paradigms. Cell. 2011; **147**: 275–292.
52 Ashworth TR. A case of cancer in which cells similar to those in the tumors were seen in the blood after death. *Aust Med J* 1869; **14**: 146–147.
53 Lowes LE, Goodale D, Keeney M, Allan AL. Image cytometry analysis of circulating tumor cells. *Methods Cell Biol* 2011; **102**: 261–90.
54 Alix-Panabières C, Pantel K. Circulating tumor cells: liquid biopsy of cancer. *Clin Chem* 2013; **59**: 110–8.
55 Lianidou ES, Markou A. Circulating tumor cells in breast cancer: detection systems, molecular characterization, and future challenges. *Clin Chem* 2011; **57**: 1242–55.
56 Yu M, Stott S, Toner M, Maheswaran S, Haber D a. Circulating tumor cells: approaches to isolation and characterization. *J Cell Biol* 2011; **192**: 373–382.
57 Mostert B, Sleijfer S, Foekens JA, Gratama JW. Circulating tumor cells (CTCs): detection methods and their clinical relevance in breast cancer. *Cancer Treat Rev* 2009; **35**: 463–74.
58 Alunni-Fabbroni M, Sandri MT. Circulating tumour cells in clinical practice: Methods of detection and possible characterization. *Methods* 2010; **50**: 289–97.
59 Nagrath S, Sequist L V, Maheswaran S, Bell DW, Irimia D, Ulkus L *et al.* Isolation of rare circulating tumour cells in cancer patients by microchip technology. *Nature* 2007; **450**: 1235–9.
60 Ozkumur E, Shah AM, Ciciliano JC, Emmink BL, Miyamoto DT, Brachtel E *et al.* Inertial focusing for tumor antigen-dependent and -independent sorting of rare circulating tumor cells. *Sci Transl Med* 2013; **5**: 179ra47.
61 Stott SL, Hsu C, Tsukrov DI, Yu M, Miyamoto DT, Waltman BA *et al.* Isolation of circulating tumor cells using a microvortex-generating herringbone-chip. *Proc Natl Acad Sci U S A* 2010; **107**: 18392–7.
62 Yoon HJ, Kim TH, Zhang Z, Azizi E, Pham TM, Paoletti C *et al.* Sensitive capture of circulating tumour cells by functionalized graphene oxide nanosheets. *Nat Nanotechnol* 2013; **8**: 735–41.
63 Murlidhar V, Zeinali M, Grabauskiene S, Ghannad-Rezaie M, Wicha MS, Simeone DM *et al.* A radial flow microfluidic device for ultra-high-throughput affinity-based isolation of circulating tumor cells. *Small* 2014; **10**: 4895–4904.
64 Fabbri F, Carloni S, Zoli W, Ulivi P, Gallerani G, Fici P *et al.* Detection and recovery of circulating colon cancer cells using a dielectrophoresis-based device: KRAS mutation status in pure CTCs. *Cancer Lett* 2013; **335**: 225–231.
65 Peeters DJE, De Laere B, Van den Eynden GG, Van Laere SJ, Rothé F, Ignatiadis M *et al.* Semiautomated isolation and molecular characterisation of single or

highly purified tumour cells from CellSearch enriched blood samples using dielectrophoretic cell sorting. *Br J Cancer* 2013; **108**: 1358–67.

66 Alix-Panabières C, Vendrell J-P, Slijper M, Pellé O, Barbotte E, Mercier G *et al.* Full-length cytokeratin-19 is released by human tumor cells: a potential role in metastatic progression of breast cancer. *Breast Cancer Res* 2009; **11**: R39.

67 Alix-Panabières C. EPISPOT assay: Detection of viable DTCs/CTCs in solid tumor patients. *Recent Results Cancer Res* 2012; **195**: 69–76.

68 Denève E, Riethdorf S, Ramos J, Nocca D, Coffy A, Daurès JP *et al.* Capture of viable circulating tumor cells in the liver of colorectal cancer patients. *Clin Chem* 2013; **59**: 1384–1392.

69 Tibbe AGJ, Miller MC, Terstappen LWMM. Statistical Considerations for Enumeration of Circulating Tumor Cells. *Cytometry* 2007; **162**: 154–162.

70 Ross AA, Cooper BW, Lazarus HM, Mackay W, Moss TJ, Ciobanu N *et al.* Detection and viability of tumor cells in peripheral blood stem cell collections from breast cancer patients using immunocytochemical and clonogenic assay techniques. *Blood* 1993; **82**: 2605–10.

71 Sleijfer S, Gratama J-W, Sieuwerts AM, Kraan J, Martens JWM, Foekens J a. Circulating tumour cell detection on its way to routine diagnostic implementation? *Eur J Cancer* 2007; **43**: 2645–50.

72 Yang J, Weinberg R a. Epithelial-mesenchymal transition: at the crossroads of development and tumor metastasis. *Dev Cell* 2008; **14**: 818–29.

73 Cristofanilli M, Budd GT, Ellis MJ, Stopeck A, Matera J, Miller MC *et al.* Circulating tumor cells, disease progression, and survival in metastatic breast cancer. *N Engl J Med* 2004; **351**: 781–91.

74 De Bono JS, Scher HI, Montgomery RB, Parker C, Miller MC, Tissing H *et al.* Circulating tumor cells predict survival benefit from treatment in metastatic castration-resistant prostate cancer. *Clin Cancer Res* 2008; **14**: 6302–9.

75 Cohen SJ, Punt CJ a, Iannotti N, Saidman BH, Sabbath KD, Gabrail NY *et al.* Relationship of circulating tumor cells to tumor response, progression-free survival, and overall survival in patients with metastatic colorectal cancer. *J Clin Oncol* 2008; **26**: 3213–21.

76 Hayes DF, Cristofanilli M, Budd GT, Ellis MJ, Stopeck A, Miller MC *et al.* Circulating tumor cells at each follow-up time point during therapy of metastatic breast cancer patients predict progression-free and overall survival. *Clin Cancer Res* 2006; **12**: 4218–24.

77 Budd GT, Cristofanilli M, Ellis MJ, Stopeck A, Borden E, Miller MC *et al.* Circulating tumor cells versus imaging--predicting overall survival in metastatic breast cancer. *Clin Cancer Res* 2006; **12**: 6403–9.

78 Olmos D, Arkenau H-T, Ang JE, Ledaki I, Attard G, Carden CP *et al.* Circulating tumour cell (CTC) counts as intermediate end points in castration-resistant prostate cancer (CRPC): a single-centre experience. *Ann Oncol* 2009; **20**: 27–33.

79 Punnoose E a, Atwal SK, Spoerke JM, Savage H, Pandita A, Yeh R-F *et al.* Molecular biomarker analyses using circulating tumor cells. *PLoS One* 2010; **5**: e12517.

80 Pestrin M, Bessi S, Galardi F, Truglia M, Biggeri A, Biagioni C *et al.* Correlation of HER2 status between primary tumors and corresponding circulating tumor cells in advanced breast cancer patients. *Breast Cancer Res Treat* 2009; **118**: 523–30.
81 Shaffer DR, Leversha MA, Danila DC, Lin O, Gonzalez-Espinoza R, Gu B *et al.* Circulating tumor cell analysis in patients with progressive castration-resistant prostate cancer. *Clin Cancer Res* 2007; **13**: 2023–9.
82 Meng S, Tripathy D, Shete S, Ashfaq R, Haley B, Perkins S *et al.* HER-2 gene amplification can be acquired as breast cancer progresses. *Proc Natl Acad Sci U S A* 2004; **101**: 9393–8.
83 Meng S, Tripathy D, Shete S, Ashfaq R, Saboorian H, Haley B *et al.* uPAR and HER-2 gene status in individual breast cancer cells from blood and tissues. *Proc Natl Acad Sci U S A* 2006; **103**: 17361–5.
84 Fehm T, Müller V, Aktas B, Janni W, Schneeweiss A, Stickeler E *et al.* HER2 status of circulating tumor cells in patients with metastatic breast cancer: a prospective, multicenter trial. *Breast Cancer Res Treat* 2010; **124**: 403–12.
85 Munzone E, Nolé F, Goldhirsch A, Botteri E, Esposito A, Zorzino L *et al.* Changes of HER2 status in circulating tumor cells compared with the primary tumor during treatment for advanced breast cancer. *Clin Breast Cancer* 2010; **10**: 392–7.
86 Ignatiadis M, Rothé F, Chaboteaux C, Durbecq V, Rouas G, Criscitiello C *et al.* HER2-positive circulating tumor cells in breast cancer. *PLoS One* 2011; **6**: e15624.
87 Somlo G, Lau SK, Frankel P, Hsieh H Ben, Liu X, Yang L *et al.* Multiple biomarker expression on circulating tumor cells in comparison to tumor tissues from primary and metastatic sites in patients with locally advanced/inflammatory, and stage IV breast cancer, using a novel detection technology. *Breast Cancer Res Treat* 2011; **128**: 155–63.
88 Hayashi N, Nakamura S, Tokuda Y, Shimoda Y, Yagata H, Yoshida A *et al.* Prognostic value of HER2-positive circulating tumor cells in patients with metastatic breast cancer. *Int J Clin Oncol* 2012; **17**: 96–104.
89 Pestrin M, Bessi S, Puglisi F, Minisini AM, Masci G, Battelli N *et al.* Final results of a multicenter phase II clinical trial evaluating the activity of single-agent lapatinib in patients with HER2-negative metastatic breast cancer and HER2-positive circulating tumor cells. A proof-of-concept study. *Breast Cancer Res Treat* 2012; **134**: 283–9.
90 Hayes DF, Walker TM, Singh B, Vitetta ES, Uhr JW, Gross S *et al.* Monitoring expression of HER-2 on circulating epithelial cells in patients with advanced breast cancer. *Int J Oncol* 2002; **21**: 1111–7.
91 Riethdorf S, Fritsche H, Müller V, Rau T, Schindlbeck C, Rack B *et al.* Detection of circulating tumor cells in peripheral blood of patients with metastatic breast cancer: a validation study of the CellSearch system. *Clin Cancer Res* 2007; **13**: 920–8.
92 Cao S, Li Y, Li J, Li C, Zhang W, Yang Z-Q *et al.* Quantitative determination of HER2 expression by confocal microscopy assay in CTCs of breast cancer. *Oncol Rep* 2010; **23**: 423–8.
93 Fehm T, Becker S, Duerr-Stoerzer S, Sotlar K, Mueller V, Wallwiener D *et al.* Determination of HER2 status using both serum HER2 levels and circulating

tumor cells in patients with recurrent breast cancer whose primary tumor was HER2 negative or of unknown HER2 status. *Breast Cancer Res* 2007; **9**: R74.

94 Nadal R, Fernandez A, Sanchez-Rovira P, Salido M, Rodríguez M, García-Puche JL *et al.* Biomarkers characterization of circulating tumour cells in breast cancer patients. *Breast Cancer Res* 2012; **14**: R71.

95 Stebbing J, Payne R, Reise J, Frampton AE, Avery M, Woodley L *et al.* The efficacy of lapatinib in metastatic breast cancer with HER2 non-amplified primary tumors and EGFR positive circulating tumor cells: a proof-of-concept study. *PLoS One* 2013; **8**: e62543.

96 Miyamoto DT, Lee RJ, Stott SL, Ting DT, Wittner BS, Ulman M *et al.* Androgen receptor signaling in circulating tumor cells as a marker of hormonally responsive prostate cancer. *Cancer Discov* 2012; **2**: 995–1003.

97 Lazar DC, Cho EH, Luttgen MS, Metzner TJ, Uson ML, Torrey M *et al.* Cytometric comparisons between circulating tumor cells from prostate cancer patients and the prostate-tumor-derived LNCaP cell line. *Phys Biol* 2012; **9**: 016002.

98 Lin HK, Zheng S, Williams AJ, Balic M, Groshen S, Scher HI *et al.* Portable filter-based microdevice for detection and characterization of circulating tumor cells. *Clin Cancer Res* 2010; **16**: 5011–8.

99 Mittag A, Tarnok A. Recent advances in cytometry applications: preclinical, clinical, and cell biology. *Methods Cell Biol* 2011; **103**: 1–20.

100 Jaye DL, Bray R a, Gebel HM, Harris W a C, Waller EK. Translational applications of flow cytometry in clinical practice. *J Immunol* 2012; **188**: 4715–9.

101 Tinhofer I, Hristozova T, Stromberger C, Keilhoiz U, Budach V. Monitoring of circulating tumor cells and their expression of EGFR/phospho-EGFR during combined radiotherapy regimens in locally advanced squamous cell carcinoma of the head and neck. *Int J Radiat Oncol Biol Phys* 2012; **83**: e685–90.

102 Baccelli I, Schneeweiss A, Riethdorf S, Stenzinger A, Schillert A, Vogel V *et al.* Identification of a population of blood circulating tumor cells from breast cancer patients that initiates metastasis in a xenograft assay. *Nat Biotechnol* 2013; **31**: 539–44.

103 Zhang L, Ridgway LD, Wetzel MD, Ngo J, Yin W, Kumar D *et al.* The identification and characterization of breast cancer CTCs competent for brain metastasis. *Sci Transl Med* 2013; **5**: 180ra48.

104 Hristozova T, Konschak R, Budach V, Tinhofer I. A simple multicolor flow cytometry protocol for detection and molecular characterization of circulating tumor cells in epithelial cancers. *Cytometry A* 2012; **81**: 489–95.

105 Wang L, Wang Y, Liu Y, Cheng M, Wu X, Wei H. Flow cytometric analysis of CK19 expression in the peripheral blood of breast carcinoma patients: relevance for circulating tumor cell detection. *J Exp Clin Cancer Res* 2009; **28**: 57.

106 Hu Y, Fan L, Zheng J, Cui R, Liu W, He Y *et al.* Detection of circulating tumor cells in breast cancer patients utilizing multiparameter flow cytometry and assessment of the prognosis of patients in different CTCs levels. *Cytometry A* 2010; **77**: 213–9.

107 Pailler E, Adam J, Barthélémy A, Oulhen M, Auger N, Valent A *et al.* Detection of Circulating Tumor Cells Harboring a Unique ALK Rearrangement in ALK-Positive Non-Small-Cell Lung Cancer. *J Clin Oncol* 2013; **31**: 2273–81.
108 Krishnamurthy S, Bischoff F, Ann Mayer J, Wong K, Pham T, Kuerer H *et al.* Discordance in HER2 gene amplification in circulating and disseminated tumor cells in patients with operable breast cancer. *Cancer Med* 2013; **2**: 226–33.
109 Ilie M, Long E, Butori C, Hofman V, Coelle C, Mauro V *et al.* ALK-gene rearrangement: a comparative analysis on circulating tumour cells and tumour tissue from patients with lung adenocarcinoma. *Ann Oncol* 2012; **23**: 2907–13.
110 Flores LM, Kindelberger DW, Ligon a H, Capelletti M, Fiorentino M, Loda M *et al.* Improving the yield of circulating tumour cells facilitates molecular characterisation and recognition of discordant HER2 amplification in breast cancer. *Br J Cancer* 2010; **102**: 1495–502.
111 Leversha MA, Han J, Asgari Z, Danila DC, Lin O, Anand A *et al.* Fluorescence in situ Hybridization Analysis of Circulating Tumor Cells in Metastatic Prostate Cancer. *Clin Cancer Res* 2009; **15**: 2091–2097.
112 Mao X, Shaw G, James SY, Purkis P, Kudahetti SC, Tsigani T *et al.* Detection of TMPRSS2:ERG fusion gene in circulating prostate cancer cells. *Asian J Androl* 2008; **10**: 467–73.
113 Attard G, Swennenhuis JF, Olmos D, Reid AHM, Vickers E, A'Hern R *et al.* Characterization of ERG, AR and PTEN gene status in circulating tumor cells from patients with castration-resistant prostate cancer. *Cancer Res* 2009; **69**: 2912–8.
114 Punnoose E, Tucker E, Marrinucci D, Amler LC, Koeppen H, Patel PH *et al.* Evaluation of PTEN status in circulating tumor cells (CTCs) and matched tumor tissue from patients with castrate-resistant prostate cancer (CRPC). In: *2013 Genitourinary Cancers Symposium*. Orlando, USA, Feb 14-16, 2013.
115 Mayer JA, Pham T, Wong KL, Scoggin J, Sales E V, Clarin T *et al.* FISH-based determination of HER2 status in circulating tumor cells isolated with the microfluidic CEE^{TM} platform. *Cancer Genet* 2011; **204**: 589–95.
116 Wolff AC, Hammond MEH, Schwartz JN, Hagerty KL, Allred DC, Cote RJ *et al.* American Society of Clinical Oncology/College of American Pathologists guideline recommendations for human epidermal growth factor receptor 2 testing in breast cancer. *Arch Pathol Lab Med* 2007; **131**: 18–43.
117 Koksal IT, Dirice E, Yasar D, Sanlioglu AD, Ciftcioglu A, Gulkesen KH *et al.* The assessment of PTEN tumor suppressor gene in combination with Gleason scoring and serum PSA to evaluate progression of prostate carcinoma. *Urol Oncol* 2004; **22**: 307–12.
118 Besson A, Robbins SM, Yong VW. PTEN/MMAC1/TEP1 in signal transduction and tumorigenesis. *Eur J Biochem* 1999; **263**: 605–11.
119 Yoshimoto M, Cunha IW, Coudry R a, Fonseca FP, Torres CH, Soares F a *et al.* FISH analysis of 107 prostate cancers shows that PTEN genomic deletion is associated with poor clinical outcome. *Br J Cancer* 2007; **97**: 678–85.
120 Fehm T, Hoffmann O, Aktas B, Becker S, Solomayer EF, Wallwiener D *et al.* Detection and characterization of circulating tumor cells in blood of primary breast

cancer patients by RT-PCR and comparison to status of bone marrow disseminated cells. *Breast Cancer Res* 2009; **11**: R59.

121 Aktas B, Müller V, Tewes M, Zeitz J, Kasimir-Bauer S, Loehberg CR *et al.* Comparison of estrogen and progesterone receptor status of circulating tumor cells and the primary tumor in metastatic breast cancer patients. *Gynecol Oncol* 2011; **122**: 356–60.

122 Stott SL, Lee RJ, Nagrath S, Yu M, Miyamoto DT, Ulkus L *et al.* Isolation and characterization of circulating tumor cells from patients with localized and metastatic prostate cancer. *Sci Transl Med* 2010; **2**: 25ra23.

123 Sieuwerts AM, Kraan J, Bolt-de Vries J, van der Spoel P, Mostert B, Martens JWM *et al.* Molecular characterization of circulating tumor cells in large quantities of contaminating leukocytes by a multiplex real-time PCR. *Breast Cancer Res Treat* 2009; **118**: 455–68.

124 Sieuwerts AM, Mostert B, Bolt-de Vries J, Peeters D, de Jongh FE, Stouthard JML *et al.* mRNA and microRNA expression profiles in circulating tumor cells and primary tumors of metastatic breast cancer patients. *Clin Cancer Res* 2011; **17**: 3600–18.

125 Markou A, Strati A, Malamos N, Georgoulias V, Lianidou ES. Molecular characterization of circulating tumor cells in breast cancer by a liquid bead array hybridization assay. *Clin Chem* 2011; **57**: 421–30.

126 De Albuquerque A, Kaul S, Breier G, Krabisch P, Fersis N. Multimarker Analysis of Circulating Tumor Cells in Peripheral Blood of Metastatic Breast Cancer Patients: A Step Forward in Personalized Medicine. *Breast Care (Basel)* 2012; **7**: 7–12.

127 Chimonidou M, Strati A, Tzitzira A, Sotiropoulou G, Malamos N, Georgoulias V *et al.* DNA methylation of tumor suppressor and metastasis suppressor genes in circulating tumor cells. *Clin Chem* 2011; **57**: 1169–77.

128 Mostert B, Jiang Y, Sieuwerts AM, Wang H, Bolt-de Vries J, Biermann K *et al.* KRAS and BRAF mutation status in circulating colorectal tumor cells and their correlation with primary and metastatic tumor tissue. *Int J Cancer* 2013; **133**: 130–41.

129 Lowes LE, Lock M, Rodrigues G, D'Souza D, Bauman G, Ahmad B *et al.* Circulating tumour cells in prostate cancer patients receiving salvage radiotherapy. *Clin Transl Oncol* 2012; **14**: 150–6.

130 Magbanua MJM, Sosa E V, Roy R, Eisenbud LE, Scott JH, Olshen A *et al.* Genomic profiling of isolated circulating tumor cells from metastatic breast cancer patients. *Cancer Res* 2013; **73**: 30–40.

131 Magbanua MJM, Sosa E V, Scott JH, Simko J, Collins C, Pinkel D *et al.* Isolation and genomic analysis of circulating tumor cells from castration resistant metastatic prostate cancer. *BMC Cancer* 2012; **12**: 78.

132 Barbazán J, Alonso-Alconada L, Muinelo-Romay L, Vieito M, Abalo A, Alonso-Nocelo M *et al.* Molecular characterization of circulating tumor cells in human metastatic colorectal cancer. *PLoS One* 2012; **7**: e40476.

133 Sergeant G, van Eijsden R, Roskams T, Van Duppen V, Topal B. Pancreatic cancer circulating tumour cells express a cell motility gene signature that predicts survival after surgery. *BMC Cancer* 2012; **12**: 527.

134 Paris PL, Kobayashi Y, Zhao Q, Zeng W, Sridharan S, Fan T *et al.* Functional phenotyping and genotyping of circulating tumor cells from patients with castration resistant prostate cancer. *Cancer Lett* 2009; **277**: 164–73.
135 Buyse M, Loi S, van't Veer L, Viale G, Delorenzi M, Glas AM *et al.* Validation and clinical utility of a 70-gene prognostic signature for women with node-negative breast cancer. *J Natl Cancer Inst* 2006; **98**: 1183–92.
136 Li X, Quigg RJ, Zhou J, Gu W, Nagesh Rao P, Reed EF. Clinical utility of microarrays: current status, existing challenges and future outlook. *Curr Genomics* 2008; **9**: 466–74.
137 Dancey JE, Bedard PL, Onetto N, Hudson TJ. The genetic basis for cancer treatment decisions. *Cell* 2012; **148**: 409–20.
138 Metzker ML. Sequencing technologies - the next generation. *Nat Rev Genet* 2010; **11**: 31–46.
139 Ross JS, Cronin M. Whole cancer genome sequencing by next-generation methods. *Am J Clin Pathol* 2011; **136**: 527–39.
140 Cronin M, Ross JS. Comprehensive next-generation cancer genome sequencing in the era of targeted therapy and personalized oncology. *Biomark Med* 2011; **5**: 293–305.
141 Shendure J, Lieberman Aiden E. The expanding scope of DNA sequencing. *Nat Biotechnol* 2012; **30**: 1084–94.
142 Shendure J a, Porreca GJ, Church GM. Overview of DNA sequencing strategies. *Curr Protoc Mol Biol* 2008; **Chapter 7**: Unit 7.1.
143 Shendure J, Ji H. Next-generation DNA sequencing. *Nat Biotechnol* 2008; **26**: 1135–45.
144 Liu L, Li Y, Li S, Hu N, He Y, Pong R *et al.* Comparison of next-generation sequencing systems. *J Biomed Biotechnol* 2012; **2012**: 251364.
145 Voelkerding K V, Dames S a, Durtschi JD. Next-generation sequencing: from basic research to diagnostics. *Clin Chem* 2009; **55**: 641–58.
146 Ran R, Li L, Wang M, Wang S, Zheng Z, Lin PP. Determination of EGFR mutations in single cells microdissected from enriched lung tumor cells in peripheral blood. *Anal Bioanal Chem* 2013. doi:10.1007/s00216-013-7156-y.
147 Gasch C, Bauernhofer T, Pichler M, Langer-Freitag S, Reeh M, Seifert AM *et al.* Heterogeneity of epidermal growth factor receptor status and mutations of KRAS/PIK3CA in circulating tumor cells of patients with colorectal cancer. *Clin Chem* 2013; **59**: 252–60.
148 Heitzer E, Auer M, Gasch C, Pichler M, Ulz P, Hoffmann EM *et al.* Complex Tumor Genomes Inferred from Single Circulating Tumor Cells by Array-CGH and Next-Generation Sequencing. *Cancer Res* 2013; **73**: 2965–75.
149 Khan ZA, Jonas SK, Le-Marer N, Patel H, Wharton RQ, Tarragona A *et al.* P53 mutations in primary and metastatic tumors and circulating tumor cells from colorectal carcinoma patients. *Clin Cancer Res* 2000; **6**: 3499–504.
150 Jiang Y, Palma JF, Agus DB, Wang Y, Gross ME. Detection of androgen receptor mutations in circulating tumor cells in castration-resistant prostate cancer. *Clin Chem* 2010; **56**: 1492–5.
151 Ashida S, Okuda H, Chikazawa M, Tanimura M, Sugita O, Yamamoto Y *et al.* Detection of circulating cancer cells with von hippel-lindau gene mutation in

peripheral blood of patients with renal cell carcinoma. *Clin Cancer Res* 2000; **6**: 3817–22.

152 Kirby BJ, Jodari M, Loftus MS, Gakhar G, Pratt ED, Chanel-Vos C *et al.* Functional characterization of circulating tumor cells with a prostate-cancer-specific microfluidic device. *PLoS One* 2012; **7**: e35976.

153 Maheswaran S, Sequist L V, Nagrath S, Ulkus L, Brannigan B, Collura C V *et al.* Detection of mutations in EGFR in circulating lung-cancer cells. *N Engl J Med* 2008; **359**: 366–77.

154 Hanahan D, Weinberg RA. The hallmarks of cancer. *Cell* 2000; **100**: 57–70.

155 Hanahan D, Weinberg R a. Hallmarks of cancer: the next generation. *Cell* 2011; **144**: 646–74.

156 Bang Y-J, Van Cutsem E, Feyereislova A, Chung HC, Shen L, Sawaki A *et al.* Trastuzumab in combination with chemotherapy versus chemotherapy alone for treatment of HER2-positive advanced gastric or gastro-oesophageal junction cancer (ToGA): a phase 3, open-label, randomised controlled trial. *Lancet* 2010; **376**: 687–97.

157 Bookman M a. Evaluation of Monoclonal Humanized Anti-HER2 Antibody, Trastuzumab, in Patients With Recurrent or Refractory Ovarian or Primary Peritoneal Carcinoma With Overexpression of HER2: A Phase II Trial of the Gynecologic Oncology Group. *J Clin Oncol* 2003; **21**: 283–290.

158 Fleming GF, Sill MW, Darcy KM, McMeekin DS, Thigpen JT, Adler LM *et al.* Phase II trial of trastuzumab in women with advanced or recurrent, HER2-positive endometrial carcinoma: a Gynecologic Oncology Group study. *Gynecol Oncol* 2010; **116**: 15–20.

159 Roukos DH. Next-generation, genome sequencing-based biomarkers: concerns and challenges for medical practice. *Biomark Med* 2010; **4**: 583–6.

160 Schrijver I, Aziz N, Farkas DH, Furtado M, Gonzalez AF, Greiner TC *et al.* Opportunities and challenges associated with clinical diagnostic genome sequencing: a report of the Association for Molecular Pathology. *J Mol Diagn* 2012; **14**: 525–40.

161 Hammond MEH, Hayes DF, Dowsett M, Allred DC, Hagerty KL, Badve S *et al.* American Society of Clinical Oncology/College of American Pathologists guideline recommendations for immunohistochemical testing of estrogen and progesterone receptors in breast cancer (unabridged version). *Arch Pathol Lab Med* 2010; **134**: e48–72.

162 Gorre ME, Mohammed M, Ellwood K, Hsu N, Paquette R, Rao PN *et al.* Clinical resistance to STI-571 cancer therapy caused by BCR-ABL gene mutation or amplification. *Science* 2001; **293**: 876–80.

163 Koivisto P, Kononen J, Palmberg C, Tammela T, Hyytinen E, Isola J *et al.* Androgen receptor gene amplification: a possible molecular mechanism for androgen deprivation therapy failure in prostate cancer. *Cancer Res* 1997; **57**: 314–9.

164 Rakha E a, El-Sheikh SE, Kandil M a, El-Sayed ME, Green AR, Ellis IO. Expression of BRCA1 protein in breast cancer and its prognostic significance. *Hum Pathol* 2008; **39**: 857–65.

165 Cicenas J. The potential role of Akt phosphorylation in human cancers. *Int J Biol Markers* 2008; **23**: 1–9.
166 Kallergi G, Agelaki S, Kalykaki A, Stournaras C, Mavroudis D, Georgoulias V. Phosphorylated EGFR and PI3K/Akt signaling kinases are expressed in circulating tumor cells of breast cancer patients. *Breast Cancer Res* 2008; **10**: R80.
167 Parkinson DR, Dracopoli N, Petty BG, Compton C, Cristofanilli M, Deisseroth A *et al.* Considerations in the development of circulating tumor cell technology for clinical use. *J Transl Med* 2012; **10**: 138.
168 Danila DC, Pantel K, Fleisher M, Scher HI. Circulating Tumors Cells as Biomarkers. Cancer J. 2011; **17**: 438–450.
169 Devriese LA, Voest EE, Beijnen JH, Schellens JHM. Circulating tumor cells as pharmacodynamic biomarker in early clinical oncological trials. Cancer Treat. Rev. 2011; **37**: 579–589.
170 Hudis CA. Trastuzumab--mechanism of action and use in clinical practice. *N Engl J Med* 2007; **357**: 39–51.
171 Riethdorf S, Müller V, Zhang L, Rau T, Loibl S, Komor M *et al.* Detection and HER2 expression of circulating tumor cells: prospective monitoring in breast cancer patients treated in the neoadjuvant GeparQuattro trial. *Clin Cancer Res* 2010; **16**: 2634–45.
172 Georgoulias V, Bozionelou V, Agelaki S, Perraki M, Apostolaki S, Kallergi G *et al.* Trastuzumab decreases the incidence of clinical relapses in patients with early breast cancer presenting chemotherapy-resistant CK-19mRNA-positive circulating tumor cells: Results of a randomized phase II study. *Ann Oncol* 2012; **23**: 1744–1750.
173 Available online: http://clinicaltrials.gov/ct2/show/NCT01548677?term=CTC+Treat&rank=1 (accessed on 10-Jun-2015). .
174 Available online: http://clinicaltrials.gov/ct2/show/NCT01619111?term=DETECT+III&rank=1 (accessed on 10-Jun-2015). .
175 Available online: http://clinicaltrials.gov/ct2/show/NCT01349842?term=Circe&rank=2 (accessed on 10-Jun-2015). .
176 Available online: http://clinicaltrials.gov/ct2/show/NCT01701050?term=COMETI+P2&rank=1 (accessed on 11-Jun-2015). .
177 Bidard F-C, Fehm T, Ignatiadis M, Smerage JB, Alix-Panabières C, Janni W *et al.* Clinical application of circulating tumor cells in breast cancer: overview of the current interventional trials. *Cancer Metastasis Rev* 2013; **32**: 179–88.
178 Allard WJ, Matera J, Miller MC, Repollet M, Connelly MC, Rao C *et al.* Tumor cells circulate in the peripheral blood of all major carcinomas but not in healthy subjects or patients with nonmalignant diseases. *Clin Cancer Res* 2004; **10**: 6897–904.
179 Hay ED. The mesenchymal cell, its role in the embryo, and the remarkable signaling mechanisms that create it. Dev. Dyn. 2005; **233**: 706–720.

180 Greenburg G, Hay ED. Epithelia suspended in collagen gels can lose polarity and express characteristics of migrating mesenchymal cells. *J Cell Biol* 1982; **95**: 333–339.
181 Locascio A, Nieto MA. Cell movements during vertebrate development: Integrated tissue behaviour versus individual cell migration. Curr. Opin. Genet. Dev. 2001; **11**: 464–469.
182 Hay ED. An overview of epithelio-mesenchymal transformation. *Acta Anat (Basel)* 1995; **154**: 8–20.
183 Gires O, Stoecklein NH. Dynamic EpCAM expression on circulating and disseminating tumor cells: causes and consequences. *Cell Mol Life Sci* 2014; **71**: 4393–402.
184 Rao CG, Chianese D, Doyle G V., Miller MC, Russell T, Sanders RA *et al.* Expression of epithelial cell adhesion molecule in carcinoma cells present in blood and primary and metastatic tumors. *Int J Oncol* 2005; **27**: 49–57.
185 Baum B, Settleman J, Quinlan MP. Transitions between epithelial and mesenchymal states in development and disease. Semin. Cell Dev. Biol. 2008; **19**: 294–308.
186 Thiery JP, Acloque H, Huang RYJ, Nieto MA. Epithelial-mesenchymal transitions in development and disease. *Cell* 2009; **139**: 871–90.
187 Tomaskovic-Crook E, Thompson EW, Thiery JP. Epithelial to mesenchymal transition and breast cancer. *Breast Cancer Res* 2009; **11**: 213.
188 Bitting RL, Schaeffer D, Somarelli J a., Garcia-Blanco M a., Armstrong AJ. The role of epithelial plasticity in prostate cancer dissemination and treatment resistance. *Cancer Metastasis Rev* 2014; **33**: 441–468.
189 Mallini P, Lennard T, Kirby J, Meeson A. Epithelial-to-mesenchymal transition: What is the impact on breast cancer stem cells and drug resistance. Cancer Treat. Rev. 2014; **40**: 341–348.
190 Pinto CA, Widodo E, Waltham M, Thompson EW. Breast cancer stem cells and epithelial mesenchymal plasticity - Implications for chemoresistance. Cancer Lett. 2013; **341**: 56–62.
191 Nauseef JT, Henry MD. Epithelial-to-mesenchymal transition in prostate cancer: paradigm or puzzle? *Nat Rev Urol* 2011; **8**: 428–439.
192 Gan Y, Shi C, Inge L, Hibner M, Balducci J, Huang Y. Differential roles of ERK and Akt pathways in regulation of EGFR-mediated signaling and motility in prostate cancer cells. *Oncogene* 2010; **29**: 4947–4958.
193 Wells CM, Ahmed T, Masters JRW, Jones GE. Rho family GTPases are activated during HGF-stimulated prostate cancer-cell scattering. *Cell Motil Cytoskeleton* 2005; **62**: 180–194.
194 Graham TR, Zhau HE, Odero-Marah VA, Osunkoya AO, Kimbro KS, Tighiouart M *et al.* Insulin-like growth factor-I-dependent up-regulation of ZEB1 drives epithelial-to-mesenchymal transition in human prostate cancer cells. *Cancer Res* 2008; **68**: 2479–2488.
195 Kong D, Wang Z, Sarkar SH, Li Y, Banerjee S, Saliganan A *et al.* Platelet-derived growth factor-D overexpression contributes to epithelial-mesenchymal transition of PC3 prostate cancer cells. *Stem Cells* 2008; **26**: 1425–1435.

196 Rubin MA, Mucci NR, Figurski J, Fecko A, Pienta KJ, Day ML. E-cadherin expression in prostate cancer: a broad survey using high-density tissue microarray technology. *Hum Pathol* 2001; **32**: 690–697.
197 Tomita K, van Bokhoven a, van Leenders GJ, Ruijter ET, Jansen CF, Bussemakers MJ *et al.* Cadherin switching in human prostate cancer progression. *Cancer Res* 2000; **60**: 3650–3654.
198 De Marzo AM, Knudsen B, Chan-Tack K, Epstein JI. E-cadherin expression as a marker of tumor aggressiveness in routinely processed radical prostatectomy specimens. *Urology* 1999; **53**: 707–713.
199 Umbas R, Isaacs WB, Bringuier PP, Schaafsma HE, Karthaus HFM, Oosterhof GON *et al.* Decreased E-cadherin expression is associated with poor prognosis in patients with prostate cancer. *Cancer Res* 1994; **54**: 3929–3933.
200 Umbas R, Schalken JA, Aalders TW, Carter BS, Karthaus HFM, Schaafsma HE *et al.* Expression of the cellular adhesion molecule E-cadherin is reduced or absent in high-grade prostate cancer. *Cancer Res* 1992; **52**: 5104–5109.
201 Kwok WK, Ling MT, Lee TW, Lau TCM, Zhou C, Zhang X *et al.* Up-regulation of TWIST in prostate cancer and its implication as a therapeutic target. *Cancer Res* 2005; **65**: 5153–5162.
202 Jaggi M, Nazemi T, Abrahams NA, Baker JJ, Galich A, Smith LM *et al.* N-cadherin switching occurs in high Gleason grade prostate cancer. *Prostate* 2006; **66**: 193–199.
203 Lang SH, Hyde C, Reid IN, Hitchcock IS, Hart CA, Bryden AAG *et al.* Enhanced expression of vimentin in motile prostate cell lines and in poorly differentiated and metastatic prostate carcinoma. *Prostate* 2002; **52**: 253–263.
204 Zhang Q, Helfand BT, Jang TL, Zhu LJ, Chen L, Yang XJ *et al.* Nuclear factor-kappaB-mediated transforming growth factor-beta-induced expression of vimentin is an independent predictor of biochemical recurrence after radical prostatectomy. *Clin Cancer Res* 2009; **15**: 3557–3567.
205 Raimondi C, Gradilone A, Naso G, Vincenzi B, Petracca A, Nicolazzo C *et al.* Epithelial-mesenchymal transition and stemness features in circulating tumor cells from breast cancer patients. *Breast Cancer Res Treat* 2011.
206 Kallergi G, Papadaki MA, Politaki E, Mavroudis D, Georgoulias V, Agelaki S. Epithelial to mesenchymal transition markers expressed in circulating tumour cells of early and metastatic breast cancer patients. Breast Cancer Res. 2011; **13**: R59.
207 Gradilone A, Raimondi C, Nicolazzo C, Petracca A, Gandini O, Vincenzi B *et al.* Circulating tumour cells lacking cytokeratin in breast cancer: the importance of being mesenchymal. *J Cell Mol Med* 2011; **15**: 1066–70.
208 Lecharpentier A, Vielh P, Perez-Moreno P, Planchard D, Soria JC, Farace F. Detection of circulating tumour cells with a hybrid (epithelial/mesenchymal) phenotype in patients with metastatic non-small cell lung cancer. *Br J Cancer* 2011; **105**: 1338–41.
209 Armstrong AJ, Marengo MS, Oltean S, Kemeny G, Bitting RL, Turnbull JD *et al.* Circulating tumor cells from patients with advanced prostate and breast cancer display both epithelial and mesenchymal markers. *Mol Cancer Res* 2011; **9**: 997–1007.

210 Papadaki MA, Kallergi G, Zafeiriou Z, Manouras L, Theodoropoulos PA, Mavroudis D *et al.* Co-expression of putative stemness and epithelial-to-mesenchymal transition markers on single circulating tumour cells from patients with early and metastatic breast cancer. *BMC Cancer* 2014; **14**: 1–10.
211 Barriere G, Riouallon A, Renaudie J, Tartary M, Michel P rigaud. Mesenchymal and stemness circulating tumor cells in early breast cancer diagnosis. BMC Cancer. 2012; **12**: 114.
212 Kasimir-Bauer S, Hoffmann O, Wallwiener D, Kimmig R, Fehm T. Expression of stem cell and epithelial-mesenchymal transition markers in primary breast cancer patients with circulating tumor cells. *Breast Cancer Res* 2012; **14**: R15.
213 Mego M, Mani S a, Lee B-N, Li C, Evans KW, Cohen EN *et al.* Expression of epithelial-mesenchymal transition-inducing transcription factors in primary breast cancer: The effect of neoadjuvant therapy. *Int J Cancer* 2012; **130**: 808–16.
214 Giordano A, Gao H, Anfossi S, Cohen E, Mego M, Lee B-N *et al.* Epithelial-mesenchymal transition and stem cell markers in patients with HER2-positive metastatic breast cancer. *Mol Cancer Ther* 2012; **11**: 2526–34.
215 Pal SK, He M, Wilson T, Liu X, Zhang K, Carmichael C *et al.* Detection and Phenotyping of Circulating Tumor Cells in High-Risk Localized Prostate Cancer. *Clin Genitourin Cancer* 2014; : 1–7.
216 Yu M, Bardia A, Wittner BS, Stott SL, Smas ME, Ting DT *et al.* Circulating breast tumor cells exhibit dynamic changes in epithelial and mesenchymal composition. *Science* 2013; **339**: 580–4.

Chapter 2

Circulating tumor cells in prostate cancer patients receiving salvage radiotherapy

A version of this chapter has been published:
Lowes LE, Lock M, Rodrigues G, D'Souza D, Bauman G, Ahmad B, Venkatesan V, Allan AL, and Sexton T. *Clin Transl Oncol.* 2012;14(2):150-6.1111

Abstract

Within 10 years of radical prostatectomy (RP), up to 30% of prostate cancer (PCa) patients will have a rise in prostate-specific antigen (PSA), requiring radiation therapy (RT). However, with current technology, distinction between local and distant recurrent PCa is not possible. This lack of an accurate test constrains the decision whether to offer systemic versus local treatment. We hypothesize tests for detecting circulating tumor cells (CTCs) within the blood may assist with clinical decision-making and in this pilot study we investigated whether CTCs could be detected in this patient population using the CellSearch® system (CSS). Blood samples were collected from PCa patients (n=26) prior to RT and 3 months following completion of RT. Samples were analyzed for PSA level via immunoassay and CTC number using the CSS. CTCs could be detected in this patient population and following RT CTCs appeared to decrease. However, no association was observed between a higher PSA and an increased number of CTCs pre- or post-RT. Interestingly, patients who failed RT trended toward an increased/unchanged number of CTCs following RT versus a decreased number in patients with RT response. Our results demonstrate that CTCs can be detected in early-stage PCa, and suggest the possibility that post-treatment reduction in CTC levels may be indicative of RT response . Future studies are aimed at evaluating CTCs in a larger cohort of patients to validate our preliminary findings and further investigate the prognostic value of CTCs in this patient population.

2.1 Introduction

Prostate cancer (PCa) is the second most commonly diagnosed cancer and the third leading cause of cancer-related death in men in Canada[1]. Upon diagnosis, one common treatment option for men under the age of 70 with early-stage, localized disease is surgical removal of the prostate via radical prostatectomy (RP)[2]. Following this surgical intervention, prostate-specific antigen (PSA) testing is utilized to monitor patients for signs of recurrence. Up to 30% of these early-stage patients will have a rise in PSA within 10 years of surgery and require treatment for residual disease[3,4]. Based on patient factors and tumor characteristics such as Gleason score, PSA doubling time (PSADT), and time to biochemical recurrence following RP, patients are recommended for surveillance, potentially curative radiation therapy (RT), or palliative hormonal therapy[5]. Patients who experience a PSA recurrence following RP present a unique problem to physicians, as current imaging technologies are unable to determine precisely where recurrent PCa is located. If the recurrent disease is localized to the prostate bed, salvage RT could potentially cure these patients. However, if the disease has spread beyond the prostate bed and become systemic, local prostate bed radiation may not be sufficient and systemic therapy, such as hormonal treatment may be warranted[5]. Therefore the ability to discriminate between these 2 patient cohorts is essential in order to aid physicians in the effective treatment of patients who will benefit from RT, and avoid unnecessary RT-associated morbidities in those patients for which treatment would likely not provide benefit[6].

Systemic metastatic disease has been shown to correlate with the presence of circulating tumor cells (CTCs) in the blood[7]. In metastatic PCa, de Bono et al. (2008)

have shown that the presence of five or more CTCs in 7.5mL of blood correlates with a significantly lower rate of overall survival, compared to those individuals who have less than five CTCs in the same blood volume[8]. Several methods have been utilized to detect CTCs, including polymerase chain reaction (PCR)-based assays, density-gradient centrifugation, flow cytometry (FCM), and microchip techniques[9]. All of these techniques have unique advantages and disadvantages, however one commonality they all share is a lack of standardization; a necessity for use in the clinical setting. The development of the the CellSearch® system (CSS; Janssen Diagnostics, Raritan, NJ) provides a standardized method for the sensitive detection and quantification of these rare CTCs in human blood using fluorescence microscopy and immunology based techniques[8,10,11].

The CSS has been approved by the U.S. Food and Drug Administration (FDA) and Health Canada for diagnostic and/or prognostic use in metastatic breast, prostate, and colorectal cancer. However, the role of CTCs and the use of the CSS in non-metastatic PCa remains unclear. A study by Tombal et al. (2003) using a reverse transcription-polymerase chain reaction (RT-PCR) approach suggests that the presence of CTCs in the blood of patients following RP is an indication of micrometastatic disease and may predict a less favourable response to salvage RT[12]. We hypothesize the use of the clinically approved, standardized CSS to detect CTCs within the blood may act as a clinically meaningful endpoint and be helpful for assisting with clinical decision-making in this patient population. In the current pilot study, we utilized the CSS to determine if CTCs are detectable in PCa patients with rising PSA levels post-prostatectomy, who have consented to salvage RT.

2.2 Materials and methods

2.2.1 Patient and control population

Studies were carried out under protocol # 15569E approved by the University of Western Ontario's Health Sciences Research Ethics Board (*Appendix 1*). Twenty-six PCa patients with a rising PSA following RP who consented to salvage RT were enrolled in this study following informed consent. To be included in this study, patients were required to have a PSA value > 0.1 ng/mL and a minimum of three PSA values taken one month apart, in order to calculate doubling time. Pre-RT bone scan and CT scan were performed at the treating physicians' discretion. Blood was drawn before radiation and baseline PSA and CTC levels were determined using standard clinical immunoassay for PSA and the CSS for CTC analysis as described below. Baseline characteristics of each patient were noted, including pre-radiation PSA, Gleason score, pathologic T (pT) stage, presence of extracapsular extension (ECE), presence of seminal vesicle invasion (SVI), margin status, lymph node status, months free from relapse, and PSADT. All patients were treated with radiation to the prostate bed as per Radiation Therapy Oncology Group (RTOG) guidelines with 6600 cGy in 33 fractions using a 5 field intensity modulated radiation therapy (IMRT) technique. Three months following the completion of RT, a second set of blood samples were drawn and follow-up PSA and CTC levels were determined.

Blood from 7 healthy individuals was also collected following informed consent and analyzed for CTCs as a negative control. In addition, blood from 4 biochemically controlled patients with undetectable PSA for a minimum of 3 years was collected following informed consent and assessed for PSA and CTC levels. This cohort

consisted of two post-RP patients and two post-salvage RT patients. Blood was collected at enrolment and at a 3 month follow-up visit for PSA and CTC analysis.

2.2.2 PSA determination

Blood samples were collected into a 6mL red topped Vacutainer® venous blood collection tube and analyzed for total PSA concentration by the London Health Sciences Centre Endocrinology Laboratory on the AutoDelfia using a time resolved fluorimmunoassay from Perkin Elmer.

2.2.3 Circulating tumor cell enumeration

Blood samples were collected into CellSave Preservative tubes (Janssen Diagnostics) and CTCs were enumerated using the CSS as per the manufacturer's directions within 96 hours of sample collection[13]. The CSS consists of two components, *(1)* the CellTracks™ AutoPrep system, which automates the blood sample preparation, and *(2)* the CellTracks™ Analyzer II, which scans the prepared samples. The AutoPrep system uses an antibody mediated, ferrofluid-based magnetic separation technique and differential staining with fluorescent particles to distinguish CTCs from contaminating leukocytes in blood samples (*Figure 2.1*). Initially, an EpCAM (epithelial cell adhesion molecule) selection is performed using anti-EpCAM antibodies conjugated to iron nanoparticles incubated in a magnet. The only $EpCAM^+$ cells in the blood should be the tumor cells. The remainder of the fluid is then aspirated from the sample, selected tumor cells are resuspended, and differential staining antibodies are added to the samples. Samples are then incubated in a magnetic cartridge called a MagNest™ and scanned using the CellTracks™ Analyzer II. Samples are scanned using three different filters, each with the exposure time optimized to the appropriate fluorescent particle. CTCs are

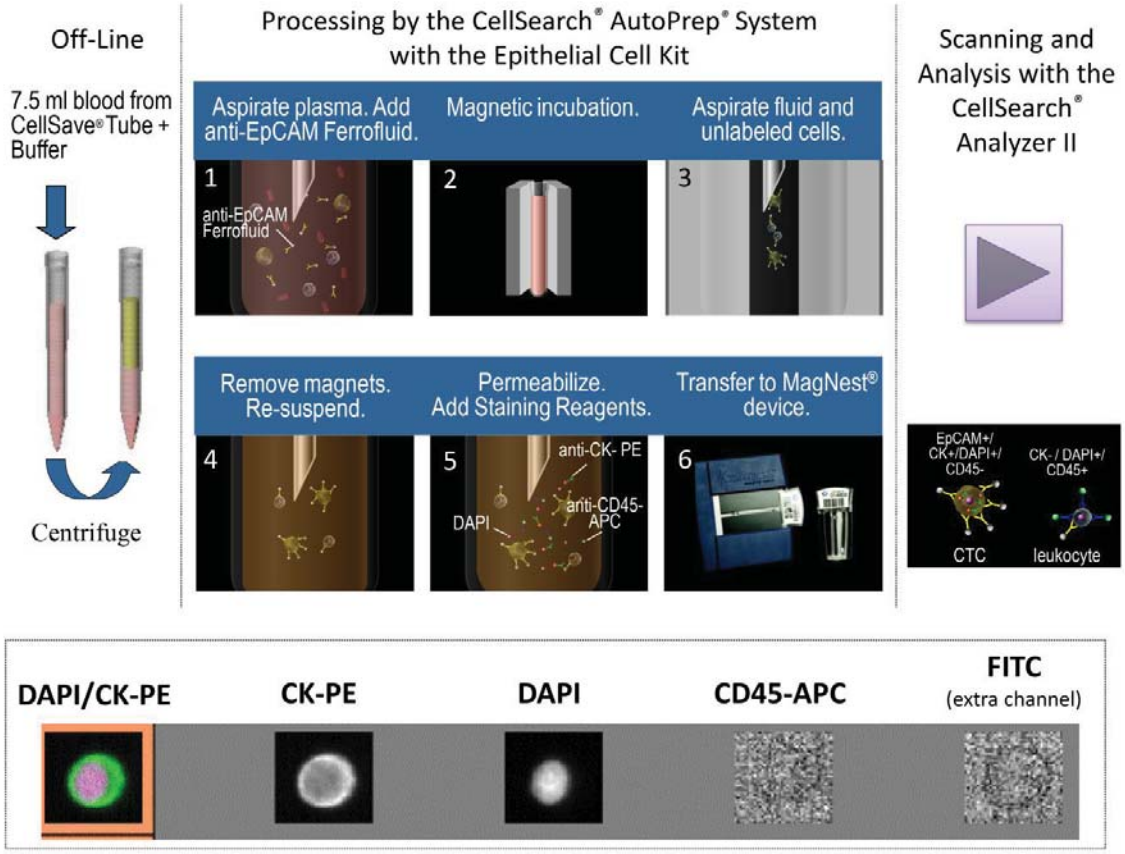

Figure 2.1. Schematic overview of the step-by-step processing of CTC blood samples using the CellSearch® system (Source: Immunicon [adapted]). Following sample collection into a CellSave tube, 7.5ml of blood is mixed with dilution buffer and centrifuged (800g x 10 min) to collect blood and tumour cells. The centrifuged sample is then loaded onto the CellSearch® AutoPrep, the plasma is aspirated, and anti-EpCAM ferrofluid is added. Following a magnetic incubation, unlabelled cells are aspirated and the remaining sample is permeabilized and incubated with the appropriate staining reagents (CK/CD45/DAPI). The completed sample is then transferred to a MagNest® and incubated for a minimum of 20 min (up to 24 hours). The MagNest device is then loaded onto the CellSearch Analyzer for sample scanning and subsequent qualitative examination by a trained operator (bottom panel).

identified as events bound by anti-EpCAM and stained with anti-pan-cytokeratin (CK)-phycoerythrin (PE) (CK 8, 18 and 19 are characteristic of epithelial cells), and the DNA stain 4', 6-diamidino-2-phenylindole (DAPI). Leukocytes are identified as events bound by anti-CD45-allophycocyanin (APC) and DAPI. After the scan is complete, a gallery of computer-defined, potential tumor cells is presented. These galleries were reviewed by 3 independent and blinded observers, and CTCs were confirmed via qualitative analysis based on the differential staining criteria discussed above. If any discrepancies in the number of selected events were noted between observers, these events were discussed until a consensus was reached.

2.2.4 Statistical analysis

Mean and standard deviations were calculated for the following variables: age, PSA, PSADT and Gleason score. The mean and standard deviations were compared with CTC count (0 vs >0 and <2 vs ≥2) using the Independent-Samples t-test procedure. Fisher's Exact test was used to compare CTC count (0 vs >0 and <2 vs ≥2) with pT stage, presence of ECE, SVI and margin status. In addition, the Pearson Correlation Coefficient and the Spearman Correlation Coefficient were used to look for associations between age, PSADT, Gleason score, change in PSA (pre-RT vs post-RT) and change in CTC number (pre-RT vs post-RT). CTC cut-off values were chosen based on results suggesting that CTC levels in early-stage PCa patients appear to be lower than those observed in metastatic populations[14].

2.3 Results

Blood samples from 7 healthy control donors and 4 biochemically controlled patients were processed for CTCs using the CSS. These biochemically controlled patients all underwent a RP, 2 received RT a minimum of 3 years prior to study entry, and all had undetectable PSA values for at least 3 years. Characteristics of these patients are summarized in *Table 2.1*. All biochemically controlled patients had pT2 disease and the two patients who received RT had positive margins. Blood sample analysis showed that CTCs were not present in the circulation of healthy control donors. However, interestingly, CTCs were detected in PCa patients with undetectable PSA, and CTC levels appeared to fluctuate over time (*Figure 2.2A*).

Twenty-six PCa patients were enrolled in this pilot study with characteristics as shown in *Table 2.2*. Sample analysis showed that CTCs could be detected in 73% of patients in this population pre-RT (*Figure 2.2B*). pT stage, Gleason grade, ECE, SVI, margin status, and PSADT did not appear to be statistically different between pre-RT patients with negative (0 CTC) versus positive (≥1 CTC) CTC status (*Table 2.3*; p values = 0.56, 0.51, 0.67, 0.63, 0.41, and 0.79 respectively).

Following RT there appeared to be a trend toward decreased CTCs, although the difference from baseline was not statistically significant (*Figure 2.2B*). As seen with pre-RT characteristics, pT stage, Gleason grade, ECE, SVI, margin status, and PSADT were not statistically different between patients with negative versus positive CTC status post-RT (*Table 2.4*; p values = 0.15, 1.0, 1.0, 0.08, 0.71, and 0.78 respectively).

Patients were subsequently divided into two groups, those who demonstrated biochemical response to therapy (i.e. a decreasing or unchanged PSA value post-RT) and

Table 2.1. Biochemically controlled population characteristics.

	N (%)
pT Stage:	
T2	4 (100)
T3a	0 (0)
T3b	0 (0)
Gleason Score:	
6 (3+3)	2 (50)
7 (3+4)	1 (25)
7 (4+3)	0 (0)
8 (4+4)	0 (0)
8 (5+3)	1 (25)
9 (4+5)	0 (0)
Extracapsular Extension:	
Negative	4 (100)
Positive	0 (0)
Seminal Vesicle Invasion:	
Negative	4 (100)
Positive	0 (0)
Margins:	
Negative (RP only)	2 (50)
Positive (RP and RT)	2 (50)
PSA Doubling Time[1]:	
≤ 10 Months	0 (0)
> 10 Months	1 (100)
CTC Detection Rate:	
Day 0	4 (100)
Day 90	4 (100)

1: Only one patient's PSADT was measured as the rest of the patients were either in the adjuvant setting or did not receive RT.

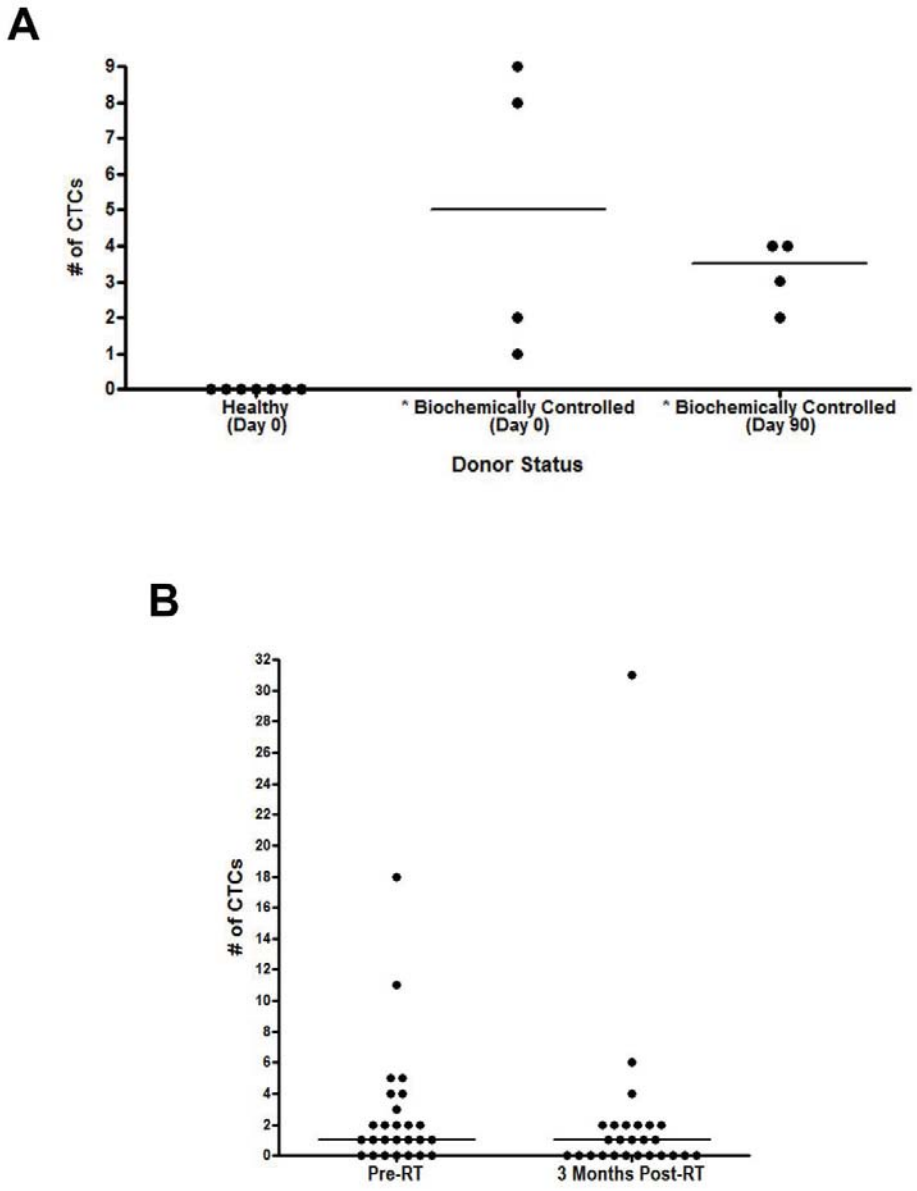

Figure 2.2. CTC distribution in control donors and patient blood samples. ***(A)*** CTC distribution of healthy donors at day 0 (n=7) and biochemically controlled donors (n=4), at day 0 and 90. ***(B)*** CTC distribution of patients pre- and post-RT. Circles and horizontal lines represent individual donors and medians respectively.

Table 2.2. Study population characteristics.

	N (%)
pT Stage:	
T2	11 (42)
T3a	8 (31)
T3b	7 (27)
Gleason Score[1]:	
6 (3+3)	4 (16)
7 (3+4)	10 (40)
7 (4+3)	8 (32)
8 (4+4)	1 (4)
8 (5+3)	1 (4)
9 (4+5)	1 (4)
Extracapsular Extension:	
Negative	14 (54)
Positive	12 (46)
Seminal Vesicle Invasion:	
Negative	20 (77)
Positive	6 (23)
Margins:	
Negative	14 (54)
Positive	12 (46)
PSA Doubling Time:	
≤ 10 Months	13 (50)
> 10 Months	13 (50)
CTC Detection Rate:	
Pre-RT[2]	19 (73)
Post-RT[3]	14 (54)

1: One patient had a Gleason score of 7 with unknown primary and secondary scores and therefore was not included in Gleason score percentage calculation.

2 :Due to poor blood draw 1 patient had 6.7 mL of blood for CTC analysis.

3: Due to poor blood draw 2 patients had 4.6 mL or 7.1 mL of blood for CTC analysis.

Table 2.3. Patient characteristics pre-radiation therapy.

	Pre-RT CTC Status		
	Negative (0 CTC) N (%)	**Positive (≥1 CTC) N (%)**	***p value***
pT Stage:			
T2	2 (29)	9 (47)	0.56
T3a	2 (29)	6 (32)	
T3b	3 (43)	4 (21)	
Gleason Score[1]:			
6 (3+3)	0 (0)	4 (22)	
7 (3+4)	3 (43)	7 (39)	
7 (4+3)	3 (43)	5 (28)	0.51[2]
8 (4+4)	1 (14)	0 (0)	
8 (5+3)	0 (0)	1 (6)	
9 (4+5)	0 (0)	1 (6)	
Extracapsular Extension:			
Negative	4 (57)	10 (53)	0.67
Positive	3 (43)	9 (47)	
Seminal Vesicle Invasion:			
Negative	5 (71)	15 (79)	0.63
Positive	2 (29)	4 (21)	
Margins:			
Negative (RP only)	2 (29)	12 (63)	0.41
Positive (RP and RT)	5 (71)	7 (37)	
PSA Doubling Time:			
≤ 10 Months	5 (71)	8 (42)	0.79
> 10 Months	2 (29)	11 (58)	

Statistical analysis were performed using a t test (Gleason score and PSADT) or Fisher's exact test (pT stage, ECE, SVI, Margins, CTC detection rate).

1: One patient (positive for CTCs pre-RT) had a Gleason score of 7 with unknown primary and secondary scores and therefore was not included in Gleason score percentage calculation.

2 :Analyzed as continuous variable.

Table 2.4. Patient characteristics post-radiation therapy.

	Post-RT CTC Status		
	Negative (0 CTC) N (%)	**Positive (≥1 CTC) N (%)**	***p value***
pT Stage:			
T2	6 (59)	5 (36)	0.15
T3a	5 (42)	3 (21)	
T3b	1 (8)	6 (43)	
Gleason Score[1]:			
6 (3+3)	2 (18)	2 (14)	
7 (3+4)	4 (36)	6 (43)	
7 (4+3)	4 (36)	4 (29)	1.0[2]
8 (4+4)	0 (0)	1 (7)	
8 (5+3)	0 (0)	1 (7)	
9 (4+5)	1 (9)	0 (0)	
Extracapsular Extension:			
Negative	6 (50)	8 (57)	1.0
Positive	6 (50)	6 (43)	
Seminal Vesicle Invasion:			
Negative	11 (92)	9 (64)	0.08
Positive	1 (8)	5 (36)	
Margins:			
Negative	7 (58)	7 (50)	0.71
Positive	5 (42)	7 (50)	
PSA Doubling Time:			
≤ 10 Months	5 (42)	8 (57)	0.78
> 10 Months	7 (58)	6 (43)	

Statistical analysis were performed using a t test (Gleason score and PSADT) or Fisher's exact test (pT stage, ECE, SVI, Margins, CTC detection rate).

1: One patient (negative for CTCs post-RT) had a Gleason score of 7 with unknown primary and secondary scores and therefore was not included in Gleason score percentage calculation.

2: Analyzed as continuous variable.

those who demonstrated biochemical failure (BCF) to therapy (i.e. an increasing PSA post-RT). Patients with biochemical response to therapy (n=21) were more likely to have a decrease in CTC number following RT versus patients with BCF (n=5) who were more likely to have an increase or no change in CTC number following RT (*Figure 2.3*), although the differences did not reach statistical significance. Interestingly, of the patients that demonstrated BCF following RT, 80% had a short PSADT (≤ 10 months) and/or negative surgical margins, both of which are well established risk factors for systemic failure and predict for failure post-RT. Furthermore, the pre-RT PSA did not appear to predict for failure as the mean PSA value (0.43 ng/mL) was similar to that of the patients who responded to radiation (0.53 ng/mL; *Table 2.5*)[15].

2.4 Discussion

Current imaging technologies are unable to differentiate local from systemic failure following RP. Regardless, these patients often receive RT because we currently lack technology that can distinguish those who will benefit from this therapy versus those who will not. However, in up to 30% of these patients the cancer will have spread beyond the prostate bed and RT will not be beneficial. Therefore the ability to distinguish these patient groups before the initiation of RT is essential. In this pilot study we sought to investigate whether CTCs could be detected in this patient population prior to the initiation of RT using the CSS.

Although this patient population had low pre-RT PSA values, we were successful in detecting CTCs in over 70% of patients sampled and in all of our control patients with undetectable PSA values. This indicated that the CSS is sensitive enough to

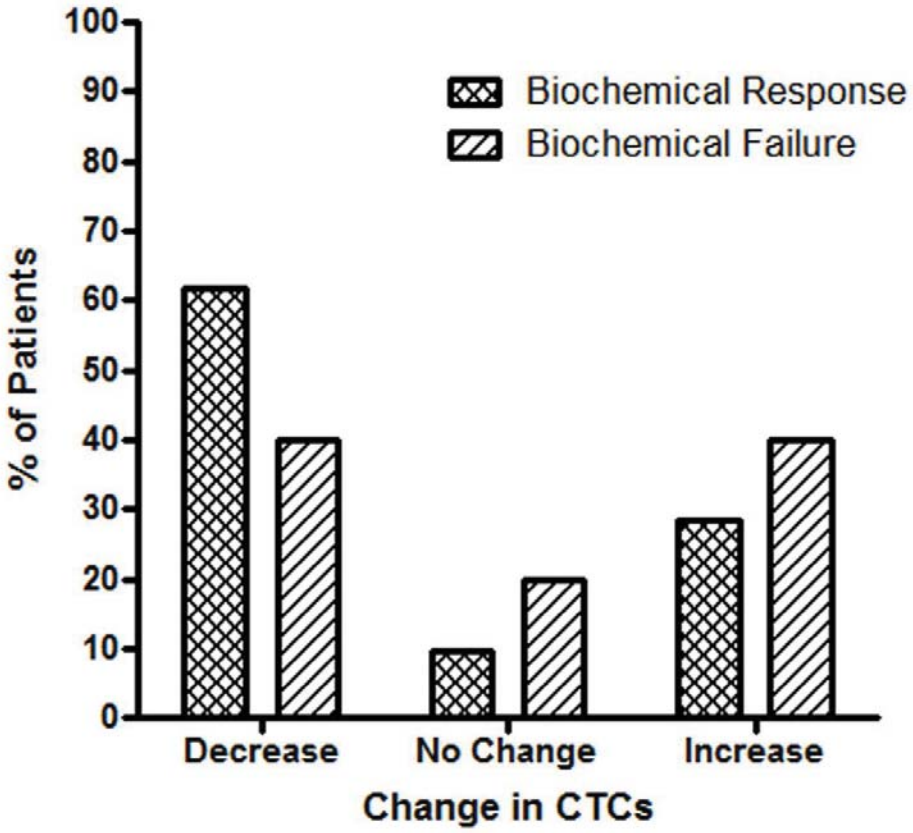

Figure 2.3. Change in CTCs following radiation therapy in relation to treatment response. Comparison of the change in CTCs following RT in patients with biochemical response (decreasing or unchanged PSA following RT; n=21) and biochemical failure (a rising PSA following RT; n=5).

Table 2.5. Characteristics of patients with evidence of biochemical failure

	N (%)
pT Stage:	
T2	2 (40)
T3a	2 (40)
T3b	1 (20)
Gleason Score:	
6 (3+3)	0 (0)
7 (3+4)	3 (60)
7 (4+3)	2 (40)
8 (4+4)	0 (0)
8 (5+3)	0 (0)
9 (4+5)	0 (0)
Extracapsular Extension:	
Negative	3 (60)
Positive	2 (40)
Seminal Vesicle Invasion:	
Negative	4 (80)
Positive	1 (20)
Margins:	
Negative	4 (80)
Positive	1 (20)
PSA Doubling Time:	
≤ 10 Months	4 (80)
> 10 Months	1 (20)
CTC Detection Rate:	
Pre-RT	3 (60)
Post-RT	3 (60)

detect very small numbers of CTCs, is more sensitive than PSA and could conceivably be used as a prognostic tool and/or a clinically meaningful surrogate endpoint in PCa patients with early recurrence or in patients with localized early disease. Tombal et al. (2003) were also able to detect CTCs in a similar patient cohort using an RT-PCR approach to analyze PSA mRNA as a marker of circulating prostate cells, although at a lower frequency (34%) than that observed in our study[12]. This suggests that detection of PSA mRNA may not be as sensitive and/or as accurate as detection with the CSS. Although the CSS is able to detect 1 CTC in 7.5mL of blood, the majority of patients on our study (73%) had 2 or less CTCs. Variability of CTC number between samples increases significantly as the number of CTCs approaches zero, therefore larger patient numbers or sample sizes may be required in order to properly enumerate CTCs in samples with low CTC yields[16]. The presence of CTCs in patients with no clinical or biochemical evidence of disease, as evidenced in our biochemically controlled patients, makes one wonder about the biology of these CTCs and their metastatic potential. It is also important to note that due to the epithelial-to-mesenchymal transition that often occurs in invasive carcinomas[17], it is highly likely that due to a lack of EpCAM expression some tumor cells, potentially those with a more aggressive phenotype, will be missed during CTC analysis using the CSS.

We were also interested in investigating if any associations existed between CTC number and various patient and tumor factors. Unfortunately, we did not observe any significant associations with pre-RT PSA, pT stage, ECE, SVI, margin status, Gleason score or PSADT. However, Tombal et al. (2003) did observe a statistically significant difference in therapy response between patients with and without CTCs prior

to RT using RT-PCR[12]. This discrepancy could be explained by a number of factors in this study including sampling variability, low patient numbers, patient characteristics, and follow-up limited to one time point post-RT. These results however suggest the possibility that with larger patient numbers and continued follow-up, similarly significant results may be observed in our patient population.

Stephenson et al. (2007) described stratification of patients according to PSA level at the time of salvage radiotherapy as well as Gleason score, margin status and PSADT and noted rates of successful salvage radiotherapy ranging from 20-60% depending on these factors[15]. Larger patient cohorts would allow evaluation of the incremental prognostic significance (if any) of CTCs above the clinical factors noted by Stephenson et al. We have undertaken a follow-up study (*Chapter 3*), which includes patients not only from the salvage setting but also from the adjuvant setting. From these patients we have collected serial PSA and CTC samples at baseline, and 6 months, 12 months, 18 months, and 24 months following the completion of RT. CTC values were then correlated with response to RT, and overall survival. This study is aimed at increasing statistical power in order to detect associations between variables.

Primarily the CSS has been utilized for the detection and enumeration of CTCs[8,10,11]. However the system does allow for additional molecular characterization of CTCs based on molecular markers of interest to researchers and physicians, via differential staining. In prostate cancer, molecular markers such as PSA[18], androgen receptor (AR)[19], PTEN deletion[20], and TMPRSS2:ERG[21] gene fusion have been shown to be associated with poor prognosis and metastatic disease. Since CTC analysis represents the opportunity to do a "real time" biopsy using a minimally-invasive blood test,

examination of the molecular characteristics of these markers on prostate CTCs could therefore enable a better understanding of the mechanisms that allow these cells to escape into the circulation, extravasate into distant tissue and form clinically relevant secondary metastases. These studies may also help us determine whether the CTCs being detected in these assays are capable of metastasizing and thus allow for more individualized treatment.

In summary, the novel results presented in this pilot study are the first to suggest the possibility that CTC enumeration using the CSS could be utilized in clinical-decision-making to determine who should receive salvage RT and who would benefit more from palliative hormonal therapy. Validation studies examining the role of CTCs as an independent predictive biomarker among larger cohorts of men with BCF post RP are necessary and seem justified based on our preliminary results.

2.5 References

1 Canadian Cancer Statistics, 2010. Toronto: Canadian Cancer Society 2010. Available at: www.cancer.ca. .

2 Chalasani V, Iansavichene AE, Lock M, Izawa JI. Salvage radiotherapy following radical prostatectomy. *Int J Urol* 2009; **16**: 31–6.

3 Ohori M, Goad JR, Wheeler TM, Eastham JA, Thompson TC, Scardino PT. Can radical prostatectomy alter the progression of poorly differentiated prostate cancer? *J Urol* 1994; **152**: 1843–9.

4 Pound CR, Partin AW, Epstein JI, Walsh PC. Prostate-specific antigen after anatomic radical retropubic prostatectomy. Patterns of recurrence and cancer control. *Urol Clin North Am* 1997; **24**: 395–406.

5 Lee AK, D'Amico A V. Utility of prostate-specific antigen kinetics in addition to clinical factors in the selection of patients for salvage local therapy. *J Clin Oncol* 2005; **23**: 8192–7.

6 Maier J, Forman J, Tekyi-Mensah S, Bolton S, Patel R, Pontes JE. Salvage radiation for a rising PSA following radical prostatectomy. *Urol Oncol*; **22**: 50–6.

7 Pantel K, Brakenhoff RH, Brandt B. Detection, clinical relevance and specific biological properties of disseminating tumour cells. *Nat Rev Cancer* 2008; **8**: 329–40.

8 De Bono JS, Scher HI, Montgomery RB, Parker C, Miller MC, Tissing H *et al.* Circulating tumor cells predict survival benefit from treatment in metastatic castration-resistant prostate cancer. *Clin Cancer Res* 2008; **14**: 6302–9.

9 Mostert B, Sleijfer S, Foekens JA, Gratama JW. Circulating tumor cells (CTCs): detection methods and their clinical relevance in breast cancer. *Cancer Treat Rev* 2009; **35**: 463–74.

10 Cohen SJ, Punt CJ a, Iannotti N, Saidman BH, Sabbath KD, Gabrail NY *et al.* Relationship of circulating tumor cells to tumor response, progression-free survival, and overall survival in patients with metastatic colorectal cancer. *J Clin Oncol* 2008; **26**: 3213–21.

11 Cristofanilli M, Budd GT, Ellis MJ, Stopeck A, Matera J, Miller MC *et al.* Circulating tumor cells, disease progression, and survival in metastatic breast cancer. *N Engl J Med* 2004; **351**: 781–91.

12 Tombal B, Van Cangh PJ, Loric S, Gala J-L. Prognostic value of circulating prostate cells in patients with a rising PSA after radical prostatectomy. *Prostate* 2003; **56**: 163–70.

13 Allard WJ, Matera J, Miller MC, Repollet M, Connelly MC, Rao C *et al.* Tumor cells circulate in the peripheral blood of all major carcinomas but not in healthy subjects or patients with nonmalignant diseases. *Clin Cancer Res* 2004; **10**: 6897–904.

14 Davis JW, Nakanishi H, Kumar VS, Bhadkamkar V a, McCormack R, Fritsche H a *et al.* Circulating tumor cells in peripheral blood samples from patients with increased serum prostate specific antigen: initial results in early prostate cancer. *J Urol* 2008; **179**: 2187–91.

15 Stephenson AJ, Scardino PT, Kattan MW, Pisansky TM, Slawin KM, Klein EA *et al.* Predicting the outcome of salvage radiation therapy for recurrent prostate cancer after radical prostatectomy. *J Clin Oncol* 2007; **25**: 2035–41.
16 Allan AL, Keeney M. Circulating tumor cell analysis: technical and statistical considerations for application to the clinic. *J Oncol* 2010; **2010**: 426218.
17 Thiery JP. Epithelial-mesenchymal transitions in tumour progression. *Nat Rev Cancer* 2002; **2**: 442–54.
18 Lilja H, Ulmert D, Vickers AJ. Prostate-specific antigen and prostate cancer: prediction, detection and monitoring. *Nat Rev Cancer* 2008; **8**: 268–78.
19 Zegarra-Moro OL, Schmidt LJ, Huang H, Tindall DJ. Disruption of androgen receptor function inhibits proliferation of androgen-refractory prostate cancer cells. *Cancer Res* 2002; **62**: 1008–13.
20 Yoshimoto M, Cunha IW, Coudry R a, Fonseca FP, Torres CH, Soares F a *et al.* FISH analysis of 107 prostate cancers shows that PTEN genomic deletion is associated with poor clinical outcome. *Br J Cancer* 2007; **97**: 678–85.
21 Tomlins SA, Mehra R, Rhodes DR, Smith LR, Roulston D, Helgeson BE *et al.* TMPRSS2:ETV4 gene fusions define a third molecular subtype of prostate cancer. *Cancer Res* 2006; **66**: 3396–400.

Chapter 3

The significance of circulating tumor cells in prostate cancer patients undergoing adjuvant or salvage radiation therapy

A version of this chapter has been published:
Lowes LE, Lock M, Rodrigues G, D'Souza D, Bauman G, Ahmad B, Venkatesan V, Allan AL, and Sexton T. In press, *Prostate Cancer and Prostatic Diseases.*

Abstract

Following radical prostatectomy, success of adjuvant and salvage radiation therapy (RT) is dependent on the absence of micrometastatic disease. However, reliable prognostic/predictive factors for determining this are lacking. Therefore, novel biomarkers are needed to assist with clinical decision-making in this setting. Enumeration of circulating tumor cells (CTCs) using the regulatory-approved CellSearch® System (CSS) is prognostic in metastatic prostate cancer (PCa). We hypothesize that CTCs may also be prognostic in the post-prostatectomy setting. Patient blood samples (n=55) were processed on the CSS to enumerate CTCs at 0, 6, 12, and 24 months after completion of RT. CTC values were correlated with predictive/prognostic factors and progression free survival. CTC status (presence/absence) correlated significantly with margin status, and trended toward significance with seminal vesicle invasion (SVI) and extracapsular extension (ECE). CTC positive status at any point appears to be indicative of disseminated disease, and in combination with other risk factors ($margin^{+}$/SVI/ECE) predicts for time to biochemical failure (BCF). Assessment of CTCs during RT may be helpful in clinical decision-making to determine which patients may benefit from RT versus those who may benefit more from systemic treatments.

3.1 Introduction

In the United States in 2014, it is estimated that there will be 233,000 new cases of prostate cancer (PCa) diagnosed and 29,480 deaths from this disease[1]. Upon diagnosis, one commonly recommended treatment option is surgical resection of the prostate via radical prostatectomy (RP)[2]. Following surgical intervention, patients are monitored using prostate-specific antigen (PSA) testing. However, within 10 years of RP, up to 30% of early-stage patients will experience a rise in PSA levels and require additional treatment for residual/recurrent disease[3,4]. Following relapse, evaluation of time to biochemical recurrence, PSA doubling time, and pathological features (Gleason score, margin status, seminal vesicle invasion [SVI], extracapsular extension [ECE]) can assess the risk of PCa-specific mortality. Patients will then be recommended for either surveillance, potentially curative radiation therapy (RT), or palliative hormonal therapy[5]. Although these parameters provide a measure of disease aggressiveness, neither they, nor available imaging technologies, can determine the precise location of recurrent PCa, thereby presenting a unique problem. If recurrent disease is localized to the prostate bed, RT could be curative. However, if the disease has become systemic, local radiation will be insufficient and systemic therapy may be necessary. Therefore, novel biomarkers that could discriminate patients with local recurrence versus those with systemic disease would be of clinical benefit.

The presence of circulating tumor cells (CTCs) in the bloodstream of PCa patients has been correlated with metastatic disease[6]. Additionally, CTC detection in the metastatic setting is prognostic, correlating with significantly reduced progression free- and overall survival[6]. However, given that CTCs are rare and present in a high

background of contaminating blood cells, detection and enumeration of CTCs requires highly sensitive and clinically reproducible assays. Currently, the only CTC analysis platform cleared by the U.S. Food and Drug Administration (FDA) and Health Canada for prognostic use in metastatic breast, prostate and colorectal cancer is the CellSearch® system (CSS) by Janssen Diagnostics[7], thereby making it the current gold standard in CTC technology in the metastatic setting for these disease sites.

Using this platform, the clinical value of CTCs in metastatic PCa has been extensively explored[6,8,9]. Studies demonstrate that patients with ≥5 CTCs/7.5mL of blood have significantly reduced progression free- and overall survival compared to patients with <5 CTCs[6]. In addition, changes in CTC number throughout therapy may be a surrogate endpoint for treatment efficacy in the metastatic setting[8]. However, the clinical value of CTCs in patients with localized PCa is less well described, with the majority of studies focusing on the utility of CTCs in determining biochemical failure (BCF) following RP. However few have explored the utility of CTCs in determining response to intervention to treat residual disease (i.e. RT)[10–12].

Based on these initial reports we hypothesized that the presence of CTCs in the blood of PCa patients undergoing adjuvant or salvage radiation may be an indicator of disseminated disease and may ultimately assist with clinical decision-making in this patient cohort. In this study, we specifically assessed whether the presence of CTCs either before or following completion of RT (measured at baseline and 6, 12, and 24 months post-treatment) is indicative of treatment response. To our knowledge this is the most extensive report in the literature examining the value of CTCs in this uniquely challenging patient population, including serial CTC sampling following treatment

completion and the longest period of follow-up to date (up to 3 years in some patients). Additionally, we are the first to describe the utility of CTCs in adjuvant patients undergoing RT.

3.2 Materials and methods

3.2.1 Patient population

All studies were carried out under protocol #16904E approved by Western University's Health Sciences Research Ethics Board (*Appendix 2*). All patients were enrolled following informed consent. Fifty-five PCa patients who had consented to adjuvant or salvage RT following RP were enrolled. Inclusion criteria for adjuvant patients included presence of any adverse pathological finding such as ECE, positive margins, and/or SVI without the presence of a detectable PSA (<0.1ng/mL). Patients who were enrolled with the intent of adjuvant radiation but who had detectable PSA levels pre-radiation were categorized as adjuvant/salvage and analyzed separately. Inclusion criteria for salvage patients included PSA value of >0.1 ng/mL[13] and a minimum of three PSA values taken one month apart, in order to calculate doubling time. Pre-RT bone scan and CT scan were performed at the discretion of the physician. Blood was drawn before the initiation of RT to determine baseline PSA and CTC levels. Additional baseline characteristics were noted, including Gleason score, pathologic T (pT) stage, margin status, lymph node status, presence of ECE, presence of SVI, months free from relapse, mean PSA, and mean PSA doubling time (PSADT) where appropriate. All patients were treated with radiation to the prostate bed as per Radiation Therapy Oncology Group (RTOG) guidelines with 6600 cGy in 33 fractions using a 5 field intensity modulated

radiation therapy (IMRT) technique[14]. Following completion of RT, PSA levels were determined at 3, 6, 12, 18, 24, 30, and 36 months, while CTC levels were determined at 6, 12, and 24 months post-RT.

3.2.2 PSA determination and biochemical failure

Blood samples for PSA determination were analyzed by the London Health Sciences Centre Endocrinology Laboratory on the AutoDelfia automatic immunoassay system (Perkin Elmer) using a time resolved fluoroimmunoassay. BCF following RT was defined as 3 consecutive rises in PSA during follow-up.

3.2.3 Circulating tumor cell enumeration

All blood samples for CTC analysis were drawn into CellSave tubes (Janssen) and analyzed within 96 hours[15]. CTCs were identified as being selected by anti-EpCAM (epithelial cell adhesion molecule), positive for cytokeratin (CK; 8/18/19) and the DNA stain 4', 6-diamidino-2-phenylindole (DAPI), >4 μm diameter, and with an intact cell membrane. CTCs results were analyzed by 2 independent and blinded observers and enumerated using the criteria described above. A positive CTC result was defined was ≥1 CTCs/7.5mL of blood.

3.2.4 Statistical analysis

Comparisons were made between patients with CTCs at baseline (CTC^{pos}), versus those without CTCs (CTC^{neg}). A two-tailed Fisher's exact test was used to analyze differences between CTC^{pos} and CTC^{neg} groups relative to Gleason score (>7), SVI, margin status, ECE, radiation type (salvage, adjuvant, or adjuvant/salvage), and BCF at 2 years. Unpaired t-tests were used to assess age differences between CTC^{pos} and CTC^{neg} groups. Log-rank tests were utilized to examine time to BCF.

3.3 Results

Fifty-five PCa patients from the adjuvant or salvage settings were enrolled in the study. Of these, 19 (34.5%) were classified as adjuvant, 33 (60%) as salvage, and 3 (5.5%) as adjuvant/salvage. The clinicopathological risk factors (CRFs) of study patients are presented in *Table 3.1*. Mean pre-radiation PSA (and range) was observed to be 0.33 (0.11-1.37) (salvage setting) and 0.42 (0.11-1.0) (adjuvant/salvage setting). Mean PSA doubling time (and range) was 16.4 (2-78) months (only measured in salvage patients). No correlation was observed between PSA levels and CTC status (presence/absence).

To determine the relationship between CTCs at baseline and CRFs, patients were characterized as either CTC^{neg} (0 CTCs; [n=46]) or CTC^{pos} (≥1 CTCs; [n=9]) (*Figure 3.1 and Table 3.2*). No significant differences were observed for patients with a Gleason score of >7 and CTC^{neg} (n=3) versus CTC^{pos} (n=1) status at baseline ($p>0.05$). A statistically significant difference was observed in relation to margin status ($p=0.032$), with 63.0% of CTC^{neg} patients presenting with positive margins (n=29) versus 22.2% of CTC^{pos} patients (n=2).

In addition to CTC status at baseline, analysis was also performed to determine the relationship between detectable CTCs at any time point and CRFs. Patients were characterized as either CTC^{neg} (n=39) at all time points or CTC^{pos} (n=16) at any time point, including at baseline (*Figure 3.2 and Table 3.3*). No significant differences were observed when considering ECE, SVI, or Gleason score of >7 and CTC^{neg} (n=29, 4, and 3, respectively) versus CTC^{pos} (n=9, 4, and 1, respectively) status ($p>0.05$). However, a trend towards statistical significance was observed when considering margin status ($p=0.083$). For CTC^{neg} patients, there was a trend toward the presence of positive

Table 3.1. Comparison of the clinicopathologic factors and CTC status of adjuvant, salvage, and adjuvant/salvage patient populations.

	Adjuvant N (%)	**Salvage** N (%)	**Adjuvant /Salvage** N (%)	**Total** N (%)
Total	19 (34.5)	33 (60)	3 (5.5)	55 (100)
pT Stage:				
T2	2 (11)	15 (45)	0 (0)	17 (31)
T3a	15 (79)	14 (42)	3 (100)	32 (58)
T3b	2 (11)	4 (12)	0 (0)	6 (11)
Gleason Score:				
6	1 (5)	6 (18)	0 (0)	7 (13)
7	17 (89)	25 (76)	2 (67)	44 (80)
8-10	1 (5)	2 (6)	1 (33)	4 (7)
ECE^{pos}:	17 (89)	18 (55)	3 (100)	38 (69)
SVI^{pos}:	2 (11)	5 (15)	1 (33)	8 (15)
$Margins^{pos}$:	12 (63)	17 (52)	2 (67)	31 (56)
CTC^{pos} (Baseline):	3 (16)	4 (12)	2 (67)	9 (16)
CTC^{pos} (Anytime)[1]:	5 (26)	9 (27)	2 (67)	16 (29)

1: The number of CTCs detected in patients within each patient population are as follows, 1 (n=4) and 3 (n=1) [adjuvant]; 1 (n=6), 2 (n=1), 4 (n=1), and 5 (n=1) [salvage, with one patients having CTCs at baseline (4 CTCs) and 12 months (1 CTC)]; 1 (n=1) and 2 (n=1) [adjuvant/salvage].

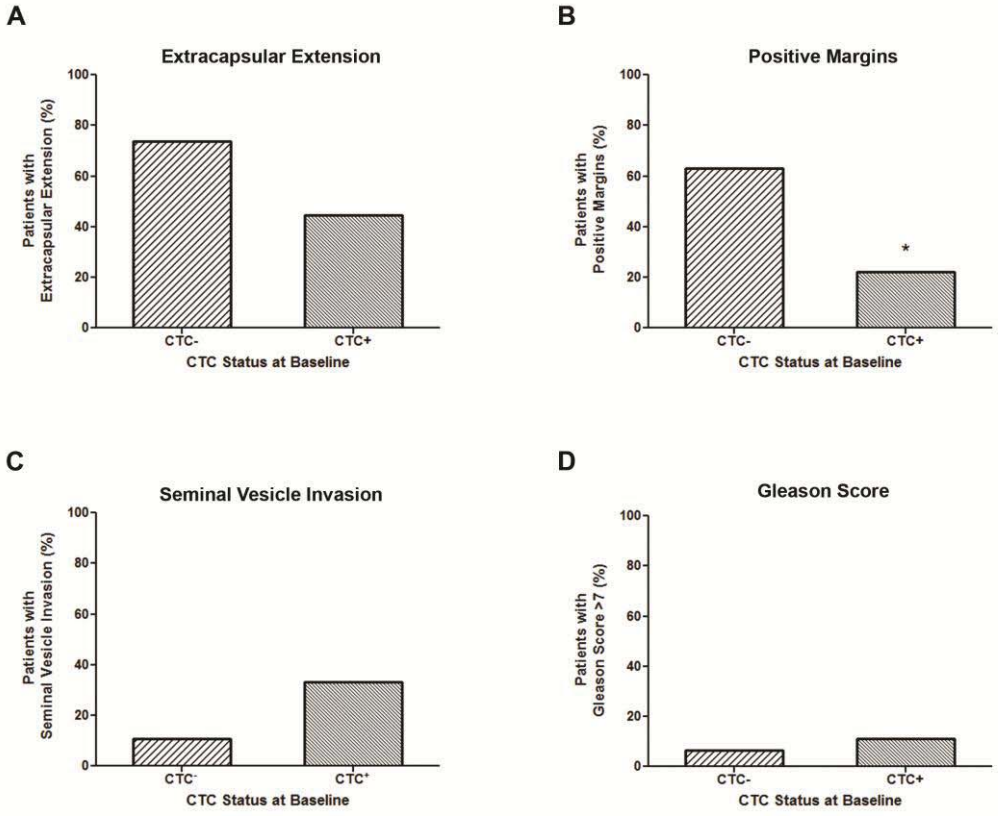

Figure 3.1. CTC status at baseline correlates with previously recognized patterns of disease recurrence of the clinicopathologic risk factors, extracapsular extension, seminal vesicle invasion, and margin status. ***(A)*** Percentage of patients with CTCs absent ($CTC^{neg/-}$; n=34) versus CTCs present ($CTC^{pos/+}$; n=4) at baseline that presented with extracapsular extension. ***(B)*** Percentage of patients with CTC^{neg} (n=29) versus CTC^{pos} (n=2) at baseline that presented with positive margins. ***(C)*** Percentage of patients with CTC^{neg} (n=5) versus CTC^{pos} (n=3) at baseline that presented with seminal vesicle invasion. ***(D)*** Percentage of patients with CTC^{neg} (n=3) versus CTC^{pos} (n=1) at baseline that presented with a Gleason score of greater than 7. * = significantly different ($p \leq 0.05$).

Table 3.2. Relationship of CTCs prior to radiation therapy with known clinicopathologic risk factors and biochemical failure.

	CTC Present		
	No N = 46 N (%)	**Yes N = 9 N (%)**	***p value***
Gleason score >7	3 (6.5)	1 (11.1)	0.522
Seminal Vesicle Invasion	5 (10.8)	3 (33.3)	0.113
Positive Margins	29 (63.0)	2 (22.2)	0.032
Extracapsular Extension	34 (73.9)	4 (44.4)	0.116
Biochemical Failure at 2 yrs	7 (15.6)[1]	3 (33.3)	0.343
Time to Biochemical Failure:			0.176
One year	13.3%	22.2%	
Two years	15.6%	33.3%	
Three years	22.2%	46.7%	

1: n=45; 1 patient was lost to follow-up and BCF could not be assessed at 2 years.

margins, with 64.1% of CTC^{neg} patients presenting with positive margins (n=25) versus 37.5% of CTC^{pos} patients (n=6), similar to that observed for CTC status at baseline.

Ultimately, the usefulness of CTCs in this patient cohort depends on their ability to determine who will experience BCF and who will not. Therefore, patients were divided into those with CTCs absent (n=45) or present (n=9) at baseline and log rank analysis was utilized to assess differences time to BCF in these patient subgroups (*Figure 3.3A*). Although there was a trend toward a decreased time to BCF in baseline CTC^{pos} patients, this trend was not significant (p=0.166). Similar analysis was then performed on patients subdivided as CTC^{neg} at all time points (n=38) versus those who were CTC^{pos} at any time point (n=16). The results demonstrated a significantly decreased time to BCF in CTC^{pos} patients (p=0.043; *Figure 3.3B*). No significant difference was observed in BCF at 2 years in patients with CTC^{neg} versus CTC^{pos} disease at baseline (*Table 3.2*). However, a significant difference was observed in BCF at 2 years when considering patients with CTC^{neg} versus CTC^{pos} disease at any time point (p=0.049; *Table 3.3*). No significant difference was observed in BCF at 2 years or time to BCF between adjuvant and salvage patient groups (*Table 3.4*).

Although CTCs alone at baseline were not an independent predictor of time to BCF, we investigated if combination with one or more of the known CRFs would enhance this ability. This approach demonstrated that patients with the presence of ECE (*Figure 3.4A*) or SVI (*Figure 3.4C*) in combination with a CTC^{pos} status at baseline had a decreased time to BCF (p=0.027 and p=0.043, respectively) versus those with the presence of ECE or SVI alone. However, a significant difference was not observed when comparing patients with the presence of positive margins and a CTC^{pos} status versus

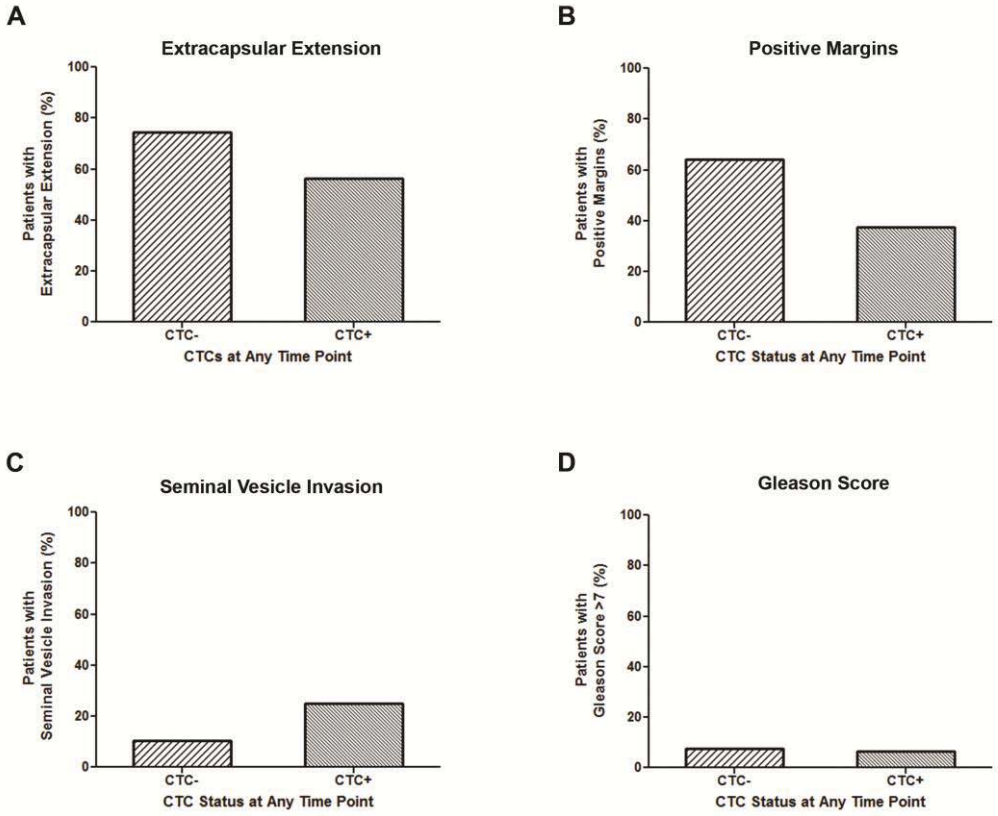

Figure 3.2. CTC status at any time point correlates with previously recognized patterns of disease recurrence of the clinicopathologic risk factor, margin status. ***(A)*** Percentage of patients with CTCs absent ($CTC^{neg/-}$; n=29) at all time points versus CTCs present ($CTC^{pos/+}$; n=9) at any time point that presented with extracapsular extension. ***(B)*** Percentage of patients with CTC^{neg} (n=25) at all time points versus CTC^{pos} (n=6) at any time point that presented with positive margins. ***(C)*** Percentage of patients with CTC^{neg} (n=4) at all time points versus CTC^{pos} (n=4) at any time point that presented with seminal vesicle invasion. ***(D)*** Percentage of patients with CTC^{neg} (n=3) at all time points versus CTC^{pos} (n=1) at any time point that presented with a Gleason score of greater than 7.

Table 3.3. Relationship of CTCs at any time point with known clinicopathologic risk factors and biochemical failure.

	CTC Present		
	No N = 39 N (%)	**Yes N = 16 N (%)**	***p value***
Gleason score >7	3 (7.7)	1 (6.3)	1.000
Seminal Vesicle Invasion	4 (10.3)	4 (25.0)	0.212
Positive Margins	25 (64.1)	6 (37.5)	0.083
Extracapsular Extension	29 (74.3)	9 (56.3)	0.213
Biochemical Failure at 2 yrs	4 (10.5)[1]	6 (37.5)	0.049
Time to Biochemical Failure:			0.043
One year	7.9%	31.3%	
Two years	10.5%	37.5%	
Three years	18.4%	43.8%	

1: n=38; 1 patient was lost to follow-up and BCF could not be assessed at 2 years.

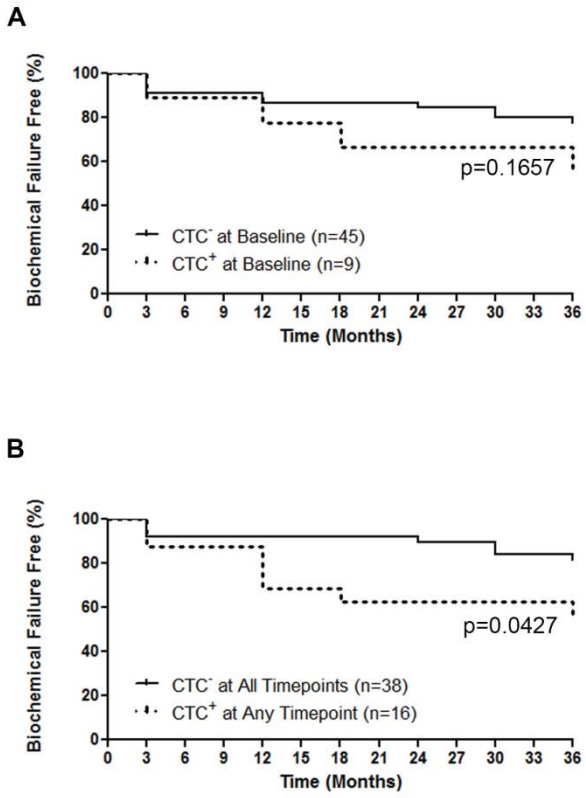

Figure 3.3. CTC^{pos} status at baseline and at any time point correlates with a decrease in time to biochemical failure following adjuvant or salvage radiotherapy. ***(A)*** Percentage of patients with CTCs absent ($CTC^{neg/-}$; n=45) versus CTCs present ($CTC^{pos/+}$; n=9) at baseline that are biochemical failure free over a 36 month period. ***(B)*** Percentage of patients with CTC^{neg} (n=38) at all time points versus CTC^{pos} (n=16) at any time point that are biochemical failure free over a 36 month period.

Table 3.4. Observed differences in biochemical failure at 2 years and time to biochemical failure in adjuvant versus salvage patient populations.

	Disease Setting		
	Adjuvant N = 19 N (%)	**Salvage N = 32 N (%)**	***p value***
Biochemical Failure at 2 yrs	1 (5.3)	7 (21.9)	0.230
Time to Biochemical Failure:			0.213
One year	5.3%	18.8%	
Two years	5.3%	21.9%	
Three years	21.1%	25.0%	

those with the presence of positive margins alone (p=0.250; *Figure 3.4B*). Since the presence of negative margins in this patient population suggests that patient's disease may no longer be confined to the prostate bed, time to BCF analysis was performed to determine if a relationship existed between CTC status at baseline and negative margins. Based on this analysis no significant difference was observed between patients with CTC^{neg} $margin^{neg}$ disease and those with CTC^{pos} $margin^{neg}$ disease (*data not shown*).

Similar analysis was then performed on the ability CTC status at any time point in combination with one or more of the known CRFs to determine time to BCF. Patients that presented with of one or more CRFs were subdivided into those who were either CTC^{pos} versus CTC^{neg} at any time point. This further demonstrated the relationship between the ability of CTCs to determine time to BCF in patients in combination with the presence of ECE (p=0.025; *Figure 3.5A*), although the same was not observed in combination with the presence of SVI (p=0.128; *Figure 3.4C*). However, a significant relationship was observed when comparing patients with the presence of positive margins and CTC^{pos} status at any timepoint versus those with the presence of positive margins alone (p=0.001; *Figure 3.5B*). Additionally, a very strong relationship was observed with the combination of presence of positive margins and ECE and CTC^{pos} status at any time point versus those with the presence of positive margins and ECE alone (p<0.0001; *Figure 3.5D*).

3.4 Discussion

Current imaging technologies cannot differentiate local from systemic failure following RP. Regardless, RT is a common treatment option, as biomarkers that can

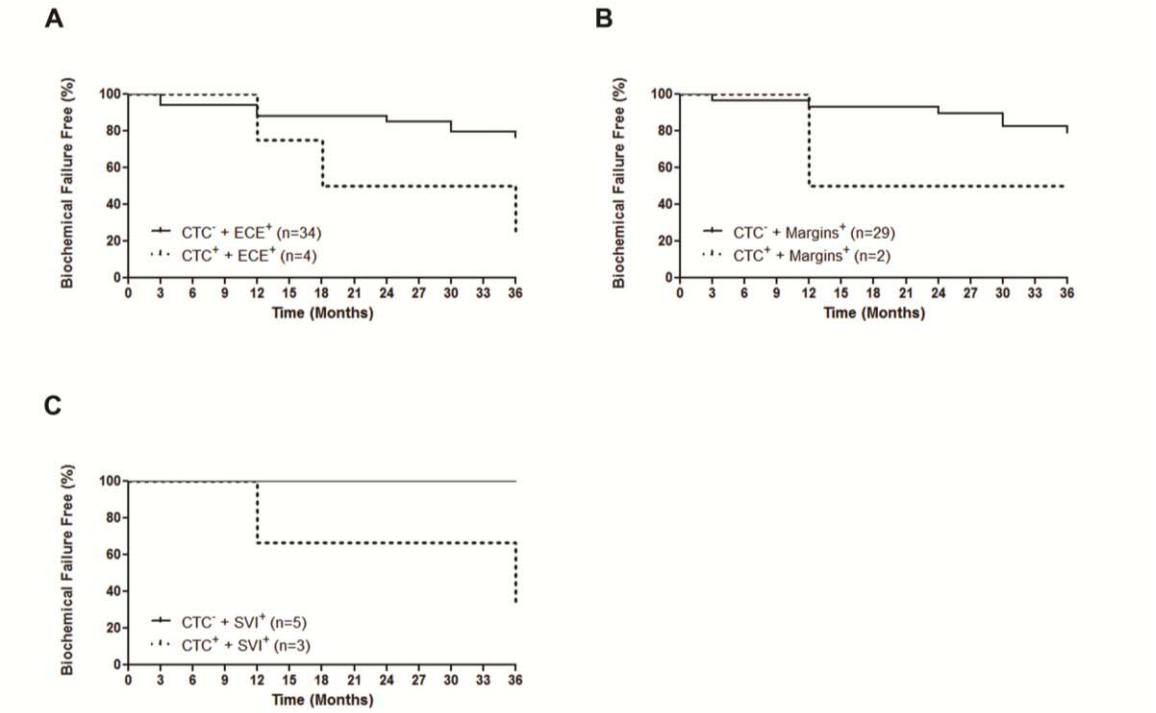

Figure 3.4. Combination of CTC status at baseline and known clinicopathologic risk factors, extracapsular extension or seminal vesicle invasion, can predict for time to biochemical failure following adjuvant or salvage radiotherapy. ***(A)*** Percentage of patients that are biochemical failure free over a 36 month period that presented with extracapsular extension (ECE), but without CTCs ($CTC^{neg/-}$; n=34) versus patients with ECE, but with CTCs ($CTC^{pos/+}$; n=4) at baseline (p=0.027). ***(B)*** Percentage of patients that are biochemical failure free over a 36 month period that presented with positive margins (margins), but CTC^{neg} (n=29) versus patients with positive margins, but CTC^{pos} (n=2) at baseline (p>0.05). ***(C)*** Percentage of patients that are biochemical failure free over a 36 month period that presented with seminal vesicle invasion (SVI), but CTC^{neg} (n=5) versus patients with SVI, but CTC^{pos} (n=3) at baseline (p=0.043).

Figure 3.5. Combination of CTC status at any time point and known clinicopathologic risk factors, extracapsular extension and/or margin status, can predict for time to biochemical failure following adjuvant or salvage radiotherapy. ***(A)*** Percentage of patients that are biochemical failure free over a 36 month period that presented with extracapsular extension (ECE), but without CTCs ($CTC^{neg/-}$; n=29) at all time points versus patients with ECE, but with CTCs ($CTC^{pos/+}$; n=9) at any time point (p=0.025). ***(B)*** Percentage of patients that are biochemical failure free over a 36 month period that presented with positive margins (margins), but CTC^{neg} (n=25) at all time points versus patients with positive margins, but CTC^{pos} (n=6) at any time point (p=0.001). ***(C)*** Percentage of patients that are biochemical failure free over a 36 month period that presented with seminal vesicle invasion (SVI), but CTC^{neg} (n=4) at all time points versus patients with SVI, but CTC^{pos} (n=4) at any time point (p=0.128). ***(D)*** The percentage of patients that are biochemical failure free over a 36 month period that presented with positive margins and ECE, but CTC^{neg} (n=15) at all time points versus patients with positive margins and ECE, but CTC^{pos} (n=2) at any time point ($p<0.0001$).

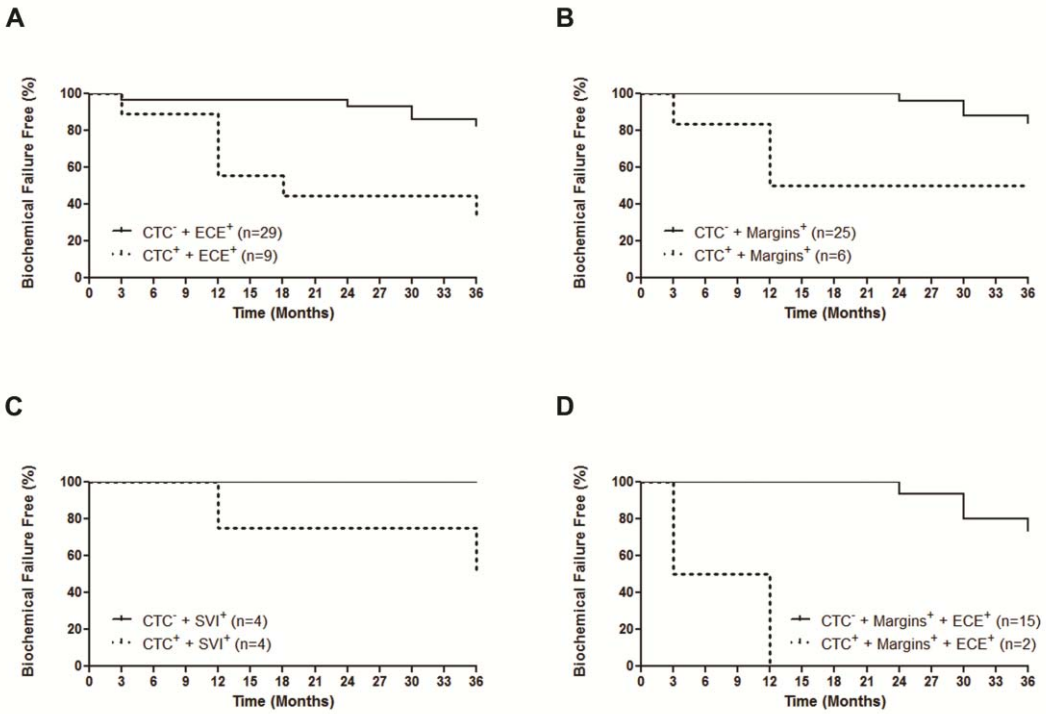
A
Biochemical Failure Free (%)
100
80
60
40
20
0
0 3 6 9 12 15 18 21 24 27 30 33 36
Time (Months)
CTC- + ECE+ (n=29)
CTC+ + ECE+ (n=9)
B
Biochemical Failure Free (%)
100
80
60
40
20
0
0 3 6 9 12 15 18 21 24 27 30 33 36
Time (Months)
CTC- + Margins+ (n=25)
CTC+ + Margins+ (n=6)
C
Biochemical Failure Free (%)
100
80
60
40
20
0
0 3 6 9 12 15 18 21 24 27 30 33 36
Time (Months)
CTC- + SVI+ (n=4)
CTC+ + SVI+ (n=4)
D
Biochemical Failure Free (%)
100
80
60
40
20
0
0 3 6 9 12 15 18 21 24 27 30 33 36
Time (Months)
CTC- + Margins+ + ECE+ (n=15)
CTC+ + Margins+ + ECE+ (n=2)

distinguish those who will benefit from RT versus those who will not are unavailable. Unfortunately, for patients whose cancer has become systemic, RT will not provide benefit, resulting in up to 30% of patients experiencing disease recurrence. Therefore, novel biomarkers that could distinguish these patient groups before initiation of RT are essential. To the best of our knowledge, only two published studies have explored CTCs in this patient population. The first was performed in a small number of patients (n=15) using a non-standardized reverse-transcription polymerase chain reaction (RT-PCR) approach examining the detection of PSA mRNA in the blood[12]. This study suggested that the presence of PSA mRNA following RP was indicative of micrometastatic disease and may predict poor response to salvage RT. The second study, published by our group, was the first to explore the detection and enumeration of CTCs using the U.S. FDA and Health Canada-cleared CSS[15]. This study demonstrated that CTCs were detectable in salvage patients (n=26) using the CSS, and that, similar to metastatic disease, changes in CTC number following RT may be indicative of treatment response. In the current study we sought to determine if detection of CTCs before initiation of RT could be utilized as a surrogate biomarker for disseminated disease and therefore an indicator of treatment failure in this patient cohort.

Despite having only a small number of CTC^{pos} patients prior to RT, strong correlations were observed with regards to CTC status at baseline and known CRFs. Interestingly, CTC^{neg} disease was most highly correlated with CRFs associated with local recurrence, including ECE and positive margins[16]. However, when considering SVI, a CRF associated with systemic relapse[16], a correlation with CTC^{pos} disease was observed. These correlations, although in opposite directions, are consistent with the clinical

observations of local versus systemic relapse associated with these CRFs. Based on the propensity for local relapse in ECE^{+} and $margin^{+}$ patients, we would anticipate that these patients would exhibit a tendency toward non-disseminated and therefore CTC^{neg} disease versus SVI^{+} patients, known to have a propensity for systemic relapse, whom we would anticipate would exhibit a tendency toward disseminated and therefore CTC^{pos} disease. Therefore, CTC status appears to be in agreement with existing CRFs, suggesting that CTCs may relate to disease localization in these patients.

Although these associations suggest a relationship between CTCs and disease spread, the value of CTCs in this patient cohort will depend on their ability to predict RT success. Upon examination of BCF at 2 years and time to BCF, we noted a strong trend toward reduced time to BCF in CTC^{pos} versus CTC^{neg} patients at baseline. However, this trend was statistical significant when considering patients with CTCs at any time point for both measures (BCF at 2 years and time to BCF) . These promising results suggest that the detection of CTCs at any time may be a surrogate biomarker of metastatic disease, and support a recommendation for early initiation of systemic treatment in this patient cohort.

However, this study also aimed to determine if CTCs could predict the outcome of RT *before* treatment initiation, thereby reducing radiation-induced morbidity in patients for which benefit would not be achieved. Therefore CTC status at baseline was examined in combination with known CRFs to determine if this approach could improve our ability to discriminate these patient subsets. We have demonstrated that the presence of ECE or SVI in association with CTC^{pos} status at baseline is predictive of poorer response to RT. However, as this study was not powered appropriately to

determine definitive associations between combinations of CRFs and CTCs, not all significant associations observed at baseline were significant when considering CTC status at any time point and vice versa. Additionally, not all CRF combinations, especially multiple CRFs (e.g., ECE + SVI + CTC), could be effectively examined. However, the results presented here, specifically with regards to ECE and CTC status, demonstrate consistently poorer outcomes following RT, further strengthening the existence of a relationship between the presence of CTCs and disease spread. This suggests that the addition of CTCs to a patient's clinicopathologic "risk profile" (ECE, SVI, and margin status) may further enhance our ability to discriminate patients with localized versus systemic recurrence. Further studies that could elucidate such risk profiles are justified.

The sample size for this study was chosen based on our pilot studies, which demonstrated that over 70% of salvage patients presented with CTCs at baseline using the CSS[15]. Unfortunately, in the current study only 16% of salvage patients and 12% of adjuvant patients presented with CTCs. Interestingly, for patients in the adjuvant/salvage group, 67% had detectable CTCs at baseline and all demonstrated treatment failure within 18 months, suggesting that CTCs may be more readily detectable and particularly valuable in these rapidly progressing patients. However, these results would require confirmation in a larger follow-up study. In agreement with our pilot analysis[15], the majority of patients with detectable CTCs at baseline presented with <2 CTCs (67%), and no patient had >5 CTCs at any point. Although the CSS can detect as few as 1 CTC/7.5mL of blood, variability increases significantly as the number of CTCs approaches 0, and with such low rates of detection the potential for false

negative/positive results cannot be discounted as a confounding factor of this study. Therefore proper enumeration of CTCs in these patients may be difficult and likely contributed to the high number of CTC^{neg} patients at baseline that failed RT (66%). The low number of CTCs observed throughout the course of this study presents a statistical challenge that can be overcome by either increasing sample size, increasing CTC capture by collecting additional blood for analysis (>7.5mL), or utilizing new emerging CTC technologies with increased sensitivity[17]. In doing so analysis of changes in CTC number at baseline compared to a subsequent post-treatment time points may be possible. This measure may also be valuable in determining the origin of disseminating disease (i.e., CTCs). For example, if CTCs number decrease following RT this may indicate that the residual disease was localized to the prostate bed and effectively treated using RT. However, should CTC numbers remain unchanged or increase following RT this may be an indicator of metastatic disease.

In summary, the results presented here are the first to demonstrate that CTC enumeration using the clinical gold standard CTC analysis CSS platform may be valuable in clinical decision-making to determine which patients should receive RT versus those who would benefit more from systemic therapy. Validation studies using larger patient cohorts to examine the clinicopathologic "risk profiles" outlined in this manuscript are necessary and justified based on these novel results.

3.5 References

1 Siegel R, Ma J, Zou Z, Jemal A. Cancer statistics, 2014. *CA Cancer J Clin* 2014; **64**: 9–29.

2 Thompson I, Thrasher JB, Aus G, Burnett AL, Canby-Hagino ED, Cookson MS *et al.* Guideline for the management of clinically localized prostate cancer: 2007 update. *J Urol* 2007; **177**: 2106–31.

3 Ohori M, Goad JR, Wheeler TM, Eastham JA, Thompson TC, Scardino PT. Can radical prostatectomy alter the progression of poorly differentiated prostate cancer? *J Urol* 1994; **152**: 1843–9.

4 Pound CR, Partin AW, Epstein JI, Walsh PC. Prostate-specific antigen after anatomic radical retropubic prostatectomy. Patterns of recurrence and cancer control. *Urol Clin North Am* 1997; **24**: 395–406.

5 Freedland SJ, Humphreys EB, Mangold LA, Eisenberger M, Dorey FJ, Walsh PC *et al.* Risk of prostate cancer-specific mortality following biochemical recurrence after radical prostatectomy. *JAMA* 2005; **294**: 433–9.

6 De Bono JS, Scher HI, Montgomery RB, Parker C, Miller MC, Tissing H *et al.* Circulating tumor cells predict survival benefit from treatment in metastatic castration-resistant prostate cancer. *Clin Cancer Res* 2008; **14**: 6302–9.

7 Lianidou ES, Markou A. Circulating tumor cells in breast cancer: detection systems, molecular characterization, and future challenges. *Clin Chem* 2011; **57**: 1242–55.

8 Olmos D, Arkenau H-T, Ang JE, Ledaki I, Attard G, Carden CP *et al.* Circulating tumour cell (CTC) counts as intermediate end points in castration-resistant prostate cancer (CRPC): a single-centre experience. *Ann Oncol* 2009; **20**: 27–33.

9 Danila DC, Heller G, Gignac G a, Gonzalez-Espinoza R, Anand A, Tanaka E *et al.* Circulating tumor cell number and prognosis in progressive castration-resistant prostate cancer. *Clin Cancer Res* 2007; **13**: 7053–8.

10 Murray NP, Reyes E, Tapia P, Badinez L, Orellana N, Fuentealba C *et al.* Redefining micrometastasis in prostate cancer - a comparison of circulating prostate cells, bone marrow disseminated tumor cells and micrometastasis: Implications in determining local or systemic treatment for biochemical failure after radical prostatecto. *Int J Mol Med* 2012; **30**: 896–904.

11 Murray NP, Reyes E, Orellana N, Fuentealba C, Bádinez L, Olivares R *et al.* Secondary circulating prostate cells predict biochemical failure in prostate cancer patients after radical prostatectomy and without evidence of disease. *ScientificWorldJournal* 2013; **2013**: 762064.

12 Tombal B, Van Cangh PJ, Loric S, Gala J-L. Prognostic value of circulating prostate cells in patients with a rising PSA after radical prostatectomy. *Prostate* 2003; **56**: 163–70.

13 Online: A. http://www.rtog.org/ClinicalTrials/ProtocolTable.aspx (accessed on Mar-10-2015). .

14 Thompson IM, Valicenti RK, Albertsen P, Davis BJ, Goldenberg SL, Hahn C *et al.* Adjuvant and salvage radiotherapy after prostatectomy: AUA/ASTRO Guideline. *J Urol* 2013; **190**: 441–9.

15 Lowes LE, Lock M, Rodrigues G, D'Souza D, Bauman G, Ahmad B *et al.* Circulating tumour cells in prostate cancer patients receiving salvage radiotherapy. *Clin Transl Oncol* 2012; **14**: 150–6.
16 Katz MS, Zelefsky MJ, Venkatraman ES, Fuks Z, Hummer A, Leibel SA. Predictors of biochemical outcome with salvage conformal radiotherapy after radical prostatectomy for prostate cancer. *J Clin Oncol* 2003; **21**: 483–9.
17 Alix-Panabières C, Pantel K. Technologies for detection of circulating tumor cells: facts and vision. *Lab Chip* 2014; **14**: 57–62.

Chapter 4

User-defined protein marker assay development for characterization of circulating tumor cells using the CellSearch® system

A version of this chapter has been published:
Lowes LE, Hedley BD, Keeney M, and Allan AL. *Cytometry A*. 2012;81(11):983-95.

Abstract

The majority of cancer-related deaths result from metastasis, which has been associated with the presence of circulating tumor cells (CTCs). It has been shown that CTC cut-off values exist that predict for poorer overall survival in metastatic breast (≥5), prostate (≥5), and colorectal (≥3) cancer based on assessment of 7.5mL of blood. Development of the CellSearch® system (CSS; Janssen Diagnostics) has allowed for sensitive enumeration of CTCs. In the current study, protocols were developed and optimized for use with the CSS to characterize CTCs with respect to user-defined protein markers of interest in human blood samples, including the cancer stem cell (CSC) marker CD44 and the apoptosis marker M-30. Flow cytometry (FCM) experiments were initially carried out to assess expression of CD44 and M-30 on MDA-MB-468 human tumor cells. Human blood samples were then spiked with MDA-MB-468 cells and processed with the appropriate antibody (CD44/M-30) on the CSS. Detailed optimization of CD44 was carried out on the CSS using various antibody concentrations, exposure times, and cell lines with varying CD44 expression. Troubleshooting experiments were undertaken to explain observed discrepancies between FCM and the CSS results for the M-30 marker. After extensive optimization, the best CD44/M-30 concentrations and exposure times were determined to be 1.5/3.5 μg/mL and 0.2/0.8 s, respectively. The percentage of $CD44^+$ tumor cells was 99.5 ± 0.39% by FCM and 98.8 ± 0.51% by the CSS. The percentage of $M\text{-}30^+$ tumor cells following paclitaxel treatment was 17.6 ± 1.18% by FCM and 10.9 ± 2.41% by the CSS. Proper optimization of the CD44 marker was achieved; however, M-30 does not appear to be a suitable marker for use in this platform. Taken together, the current study provides a detailed description of the process of user-defined protein marker development and optimization using the CSS, and will be an important resource for the future development of protein marker assays by users of this platform.

4.1 Introduction

It has been estimated that 1,658,370 new cases of cancer will be diagnosed in the United States and 589,430 individuals will die from this disease in 2015[1]. The majority of these deaths are as a result of the development of metastases[2]. These deaths are due mainly to the ineffectiveness of current therapies in treating metastatic disease and a general lack of understanding of the metastatic cascade. Metastatic disease has been correlated with the presence of circulating tumor cells (CTCs) in the blood[3]. Detection of very small numbers of these rare cells has been shown to be predictive of overall survival in metastatic breast[4], prostate[5], and colorectal[6] cancer, where patients with ≥5 (breast and prostate) or ≥3 (colorectal) CTCs in 7.5mL of blood have a poorer prognosis then those with fewer or no detectable CTCs.

Several methods have been utilized to enrich and detect CTCs, including density-gradient centrifugation[7,8], immunomagnetic selection[9,10], polymerase chain reaction (PCR)-based assays[11,12], and flow cytometry (FCM)[13,14] techniques. All of these approaches have unique advantages and disadvantages; however, one commonality they all share is a lack of standardization; a necessity for use in the clinical setting. The development of the U.S. Food and Drug Administration (FDA) and Health Canada cleared CellSearch® system (CSS) by Janssen Diagnostics provides a standardized method for the sensitive detection and quantification of these rare CTCs in human blood using fluorescence microscopy and immunology based techniques[4–6]. This system is currently considered the gold standard in CTC enumeration and is the only CTC platform approved for *in vitro* diagnostic (IVD) use in the clinic at the present time. The CSS consists of two components, ***(1)*** the CellTracks™ AutoPrep system, which automates the

blood sample preparation, and ***(2)*** the CellTracks™ Analyzer II, which scans the prepared samples (described in *Chapter 2* and *Figure 2.1*). The CellTracks™ Analyzer II® utilizes a 10X objective lens to scan samples using different filters, each with the exposure time optimized to the appropriate fluorescent particle. The CSS has been primarily utilized for the detection and enumeration of these rare cells. However, this platform does allow for single-cell characterization of CTCs for user-defined markers of interest, using an additional fluorescein isothiocyanate (FITC) fluorescence channel not required for CTC identification and enumeration[15]. However, the detailed process for user-defined protein marker assay development and optimization using this platform is not well-defined.

Tumor profiling of metastatic lesions is not routine practice in the clinic. In fact, this profiling is often impractical or even impossible depending on the location and size of the metastatic tumors. Therefore CTCs could act as a real-time, minimally invasive liquid biopsy, and the characterization of these rare cells could inform clinical decision-making. For example, human epidermal growth factor receptor 2 (HER2) is over-expressed in a subset of breast cancer patients, and has been exploited as a marker for targeted therapy using the HER2 receptor interfering monoclonal-antibody Herceptin®[16]. However, this therapy has only been shown to be effective in patients whose primary tumor expresses sufficient levels of HER2. Fehm et al., demonstrated that approximately one third of breast cancer patients with metastases whose primary tumors were $HER2^-$ had $HER2^+$ CTCs[17,18]. Whether or not these patients with $HER2^+$ CTCs would benefit from treatment with Herceptin® still requires investigation; however, CTCs hold great promise for improving personalized cancer treatment.

Two general categories of protein markers are available for exploration on CTCs; markers that reflect tumor biology (tumor phenotyping) and may act as target molecules for therapy, and those that reflect cellular response to therapy. Currently, Janssen Diagnostics has developed and optimized three tumor phenotyping reagents for assessing well characterized therapeutic targets, and these are commercially available for research use only (RUO) applications on the CSS. Using these reagents, CTCs can be analyzed for expression of either HER2/neu, epidermal growth factor receptor (EGFR), or insulin-like growth factor 1 receptor (IGF-1R). The development and optimization of CSS assays for other user-defined markers of interest on tumor cells could identify new targets for novel therapies and enable a better understanding of the mechanisms that allow these cells to escape into the circulation, extravasate into distant tissue and form clinically relevant macrometastases.

The aim of this study was therefore to develop and optimize protocols for characterization of CTCs on the CCS for two proteins of interest, CD44 and M-30. CD44 has been associated with metastasis and has shown to be expressed by "cancer stem cells" (CSCs), a subpopulation of tumor cells that are believed to be the cells responsible for tumor initiation and metastasis[19]. The ability to characterize and track $CD44^+$ cells would therefore be an important tool for understanding the metastatic cascade. The M-30 CytoDeath antibody recognizes a neoepitope of CK18 that is exposed following caspase cleavage at residue 396 during the early events of apoptosis[20]. This marker could be utilized as a measure of therapy effectiveness, and potentially indicate the necessity for a change in treatment much earlier than standard clinical evaluation techniques such as imaging. For the first time in the literature, the current study provides a detailed

description of the process of user-defined protein marker development and optimization using the CSS, and will be an important resource for the future development of protein marker assays by users of this platform.

4.2 Materials and methods

4.2.1 Cell culture and reagents

The MDA-MB-468 human breast cancer cell line was obtained from Dr. Janet Price (M.D. Anderson Cancer Center, Houston, TX, USA[21]). The 21NT human breast cancer cell line was obtained from Dr. Vimla Band (Dana Farber Cancer Institute, Boston, MA[22]). The LNCaP human prostate cancer cell line was obtained from Dr. John Lewis (London Regional Cancer Program, London, ON, Canada[23]). MDA-MB-468 cells were maintained in αMEM + 10% FBS. 21NT cells were maintained in αMEM + 10% FBS, 3.32µg/mL of HEPES, 1% non-essential amino acids (10mM), 96.02µg/mL of sodium pyruvate, 0.25mg/mL of L-glutamine, 43.63µg/mL of gentamicin, and 0.87µg/mL of insulin (Sigma-Aldrich, St. Louis, MO, USA). LNCaP cells were maintained in RPMI-1640 + 10% FBS. All growth media and supplements were obtained from Invitrogen (Carlsbad, CA, USA). FBS was obtained from Sigma-Aldrich (St. Louis, MO, USA). For induction of apoptosis, MDA-MB-468 human breast cancer cells were grown to ~65% confluency at which time cells were treated with fresh growth media (αMEM + 10% FBS) or 0.1µg/mL of paclitaxel (Biolyse Pharma Corporation, St. Catherines, ON, CAN) in αMEM + 10% FBS. Both the treated and untreated cells were then grown for an additional 48 hours before they were harvested and analyzed as described below.

4.2.2 Flow cytometry sample preparation

For comparison of FITC mean fluorescence intensity (MFI), measured on a 4 decade log scale, MDA-MB-468 cells were spiked into whole blood at a concentration of ~0.01% (equivalent to ~200 MDA-MB-468 cells) of the total white blood cell (WBC) count determined by analysis of whole blood using an LH 780 hematology analyzer (Beckman Coulter, Hialeah, FL, USA). The 0.01% spiked solution was then incubated with fluorescently conjugated antibodies for 20 min at room temperature, including 5µL of anti-CD45-PC5 (clone J33; Beckman Coulter/Immunotech, Marseille, France) and either 150µL of anti-EGFR (epidermal growth factor receptor)-FITC (Janssen Diagnostics, Raritan, NJ, USA) or various amounts (0.05µg – 0.5µg) of anti-CD44-FITC (clone G44-26; BD Biosciences). Following incubation, red blood cells were lysed using 1x ammonium chloride (NH_4Cl) lysing solution (Beckman Coulter/Immunotech) for 10 min at room temperature. Samples were then analyzed using a Beckman Coulter EPICS XL-MCL flow cytometer.

For analysis of differential CD44, EpCAM, and CK expression in the three cell lines, MDA-MB-468, 21NT, and LNCaP tumor cells ($5x10^5$) were resuspended in flow buffer (PBS + 2% FBS), fixed and permeabilized, as necessary (CK), using the IntraPrep™ Fix/Perm kit (Beckman Coulter, Fullerton, CA, USA), and incubated with either 150µL of anti-EGFR-FITC (Veridex; 20 min), 0.5µg of anti-CD44-FITC (clone G44-26; BD Biosciences; 20 min), 0.0075µg of anti-EpCAM-PE (clone EBA-1; BD Biosciences; 20 min), or 25µL of anti-CK-8/18/19-PE (Veridex; 30 min). Following two washes with an excess volume (≥2ml) of flow buffer, samples were analyzed using a Beckman Coulter EPICS XL-MCL flow cytometer. PBS and 5.0µg of FITC-conjugated

mouse $IgG_{2b}\kappa$ (clone MPC-11; BD Biosciences) or 0.0625µg of PE conjugated mouse $IgG_{2b}\kappa$ (clone 27-35; BD Biosciences) were used as negative controls.

For analysis of M-30, paclitaxel-treated and untreated MDA-MB-468 cells ($5x10^5$) diluted in flow buffer were fixed and permeabilized using the IntraPrep™ Fix/Perm kit (Beckman Coulter) and subsequently incubated with 0.1µg of anti-M-30-FITC (Alexis Biochemicals, Lausen, Switzerland; 30 min) and either 0.0075µg of anti-EpCAM-PE (clone EBA-1; BD Biosciences; 20 min), 25µL of anti-CK-8/18/19-FITC (Veridex; 30 min), or 0.07µg of DAPI (Sigma-Aldrich; 15 min). Following 2 washes with an excess volume (≥2ml) of flow buffer, samples were analyzed using either a Beckman Coulter EPICS XL-MCL flow cytometer (EPCAM/CK) or a Beckman Coulter Navios flow cytometer (DAPI).

It is important to note that FCM was used throughout this study as a method to determine the percentage of cells within any given cell population that were positive for our marker of interest (i.e., EGFR, CD44, M-30) and not as a method by which to compare the CSS. Although FCM would seem like an ideal method for CTC characterization based on the results presented in this study, its lower sensitivity for rare-event detection make it less ideal for use in a clinical setting, which further highlights the need to optimize appropriate protocols for CTC characterization on the gold standard CSS.

4.2.3 Flow cytometry analysis and gating strategy

The flow procedures were performed on either a single laser (488nm Argon Laser) four-color Beckman Coulter XL-MCL flow cytometer or a three laser (405 Violet, 488 Argon, 633 Helium-Neon Laser) 10 colour Beckman Coulter Navios flow cytometer.

Alignment and calibration checks were performed daily on both flow cytometers using FlowCheck/FlowSet (for XL-MCL flow cytometer) and FlowCheckPro/FlowSetPro (Beckman Coulter Navios flow cytometer). Fluorochrome emission on the Beckman Coulter XL-MCL was captured for FITC conjugates using a 525/40nm Band Pass (BP) filter and for PE conjugates using 575/25 nm BP filter. Emissions on the Beckman Coulter Navios cytometer for FITC, PE and DAPI were collected using 525/40nm, 575/30nm, and 450/40nm BP filters (respectively). Antibody combinations are detailed elsewhere in the Materials and Methods.

For all assays, forward and side scatter was used for gating to eliminate cellular debris and cell doublets from analysis. A minimum of 10,000 events were acquired for all analyses. For single-colour assays, gates were set based on either FMO (fluorescence minus one) or appropriate IgG controls. For 2 colour assays, an FMO strategy was used to determine compensation coefficients. Gating for blood samples spiked with tumor cells was set up using 10% tumor cell spiked samples (compared to WBC count). Tumor cells were defined as $CK^{+}CD45^{-}$ and/or $EGFR^{+}/CD44^{+}$, whereas WBCs were defined as $CK^{-}CD45^{+}$ and/or $CD44^{-}/EGFR^{-}$. Relative MFI was determined based on IgG isotype or FMO controls (as appropriate) in order to demonstrate changes in expression of the specific marker in question. Populations of interest were observed to be single populations (i.e. similar to what is seen in *Figure 4.1A*), and means were observed to be comparable to medians. Therefore the mean was taken as the value for determining MFI. All data were analyzed offline using the Kaluza™ Beckman Coulter analysis software.

Figure 4.1. Initial validation of the CellSearch® system using EGFR. ***(A)*** FCM analysis of MDA-MB-468 human breast cancer cells incubated with anti-EGFR-FITC (*red*) and an IgG isotype control sample *(blue*). ***(B)*** Representative CellSearch® system gallery images of 7.5ml of healthy donor blood spiked with 1000 MDA-MB-468 human breast cancer cells, incubated with 450µl of anti-EGFR-FITC and standard Veridex CTC reagents (CK-PE, CD45-APC, DAPI), and analyzed at an exposure time of 0.8s as recommended by the manufacturer. Orange squares indicate $EGFR^+$ CTCs, identified as $CK^+/DAPI^+/CD45^-/EGFR^+$. Images acquired at 10x objective magnification. ***(C)*** Percentage recovery of $EGFR^+$ cells as determined by FCM and the CellSearch® system (n=3). Data are presented as the mean ± SEM.

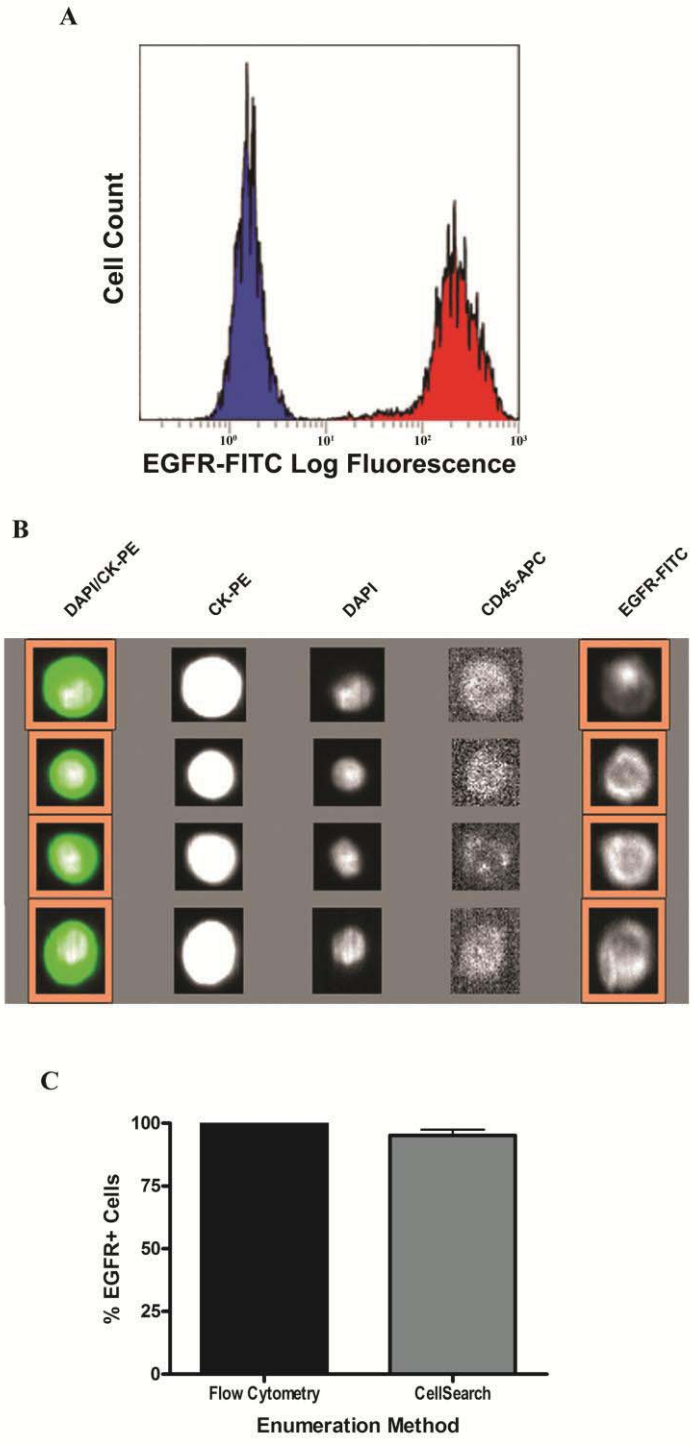
A
Cell Count
EGFR-FITC Log Fluorescence
B
DAPI/CK-PE
CK-PE
DAPI
CD45-APC
EGFR-FITC
C
% EGFR+ Cells
100
75
50
25
0
Flow Cytometry
CellSearch
Enumeration Method

4.2.4 CellSearch analysis

Blood from healthy volunteer donors was drawn into 10ml CellSave preservative tubes (Janssen Diagnostics) containing EDTA (ethylenediaminetetraacetic acid) and a proprietary cellular preservative. Blood in excess of 7.5ml (the standard blood volume for use with the CSS) was removed from each CellSave preservative tube and discarded. One thousand (EGFR/CD44) or 4000 (M-30) cultured human tumor cells from the appropriate cell line, diluted in 100µL of flow buffer, were spiked into each CellSave preservative tube. To avoid sample degradation, spiked blood was processed on the CSS within 96 hours of blood collection as per the manufacturer's guidelines. Following thorough mixture by inversion, 7.5mL of spiked blood was collected from each CellSave preservative tube and mixed with 6.5mL of dilution buffer (Janssen Diagnostics). Spiked blood samples were mixed by inversion 5 times and then centrifuged at 800xg with the brake off for 10 minutes at room temperature. Prepared blood samples were loaded into the CellTracks™ AutoPrep system as per the manufacturer's guidelines and processed using the CellSearch CTC kit as described in the introduction.

Undiluted anti-EGFR-FITC (Janssen Diagnostics) was added to manufacturer-supplied reagent cups in the CellSearch kit cartridge for processing on the CellTracks™ AutoPrep system. Anti-CD44 antibodies conjugated to either FITC (clone G44-26; BD Biosciences) or PE (clone G44-26; BD Biosciences) and FITC-conjugated M-30 CytoDeath antibodies (Alexis Biochemicals) were diluted according to Janssen Diagnostics recommendations[24] in 1X ultrapure PBS (Invitrogen) to obtain the desired working concentration. Ultrapure PBS and PE conjugated mouse $IgG_{2b}\kappa$ (clone 27-35; BD Biosciences) diluted in ultrapure PBS at the corresponding working concentration of

anti-CD44-PE were used as negative controls. For optimization, two variables were altered: the antibody concentration utilized on the CellTracks™ AutoPrep, and the length of time the FITC/PE fluorophore was exposed to the laser (altered using the "Research Protocol" option under the "Set Up" tab, on the CellTracks™ Analyzer II).

4.2.5 Statistical analysis

Statistical analysis was performed using GraphPad Prism© 5.0 (La Jolla, CA, USA). When analyzing two groups of data, the differences between the means was determined using a Student's *t* test. M-30 samples run in parallel were analyzed using a paired Student's *t* test. When analyzing three or more groups of data, two-way ANOVA followed by a Bonferroni post-test was used. In all cases $P<0.05$ was considered to be statistically significant.

4.3 Results

4.3.1 Initial CellSearch® system validation with a commercially available optimized marker

To first determine the sensitivity and specificity of the CSS to detect an optimized marker in the FITC channel, a commercially available marker from Janssen Diagnostics, anti-EGFR-FITC, was processed with blood spiked with MDA-MB-468 human breast cancer cells on the CSS. MDA-MB-468 cells alone were first analyzed by FCM to determine the percentage of the cell population that was $EGFR^+$. These cells were found to be highly $EGFR^+$, with >99.9±0.03% of cells expressing EGFR (*Figure 4.1A,C*). Blood from a healthy volunteer donor was then spiked with MDA-MB-468 cells and processed on the CSS with the commercially available anti-EGFR-FITC antibody. The CSS was able to characterize 95.1±2.34% of spiked cells as $EGFR^+$

(*Figure 4.1B,C*). Comparison of the ability of these two techniques for analyzing the percentage of the cell population that was $EGFR^+$ demonstrated that markers that have been properly optimized for use with the CSS are not significantly different from results obtained by FCM (*Figure 4.1C*).

4.3.2 CD44 protocol development for use with the CellSearch® system

FCM experiments were next performed to determine the optimal concentration of anti-CD44-FITC required for initial testing on the CSS. Blood samples spiked with MDA-MB-468 cells at a concentration equivalent to equivalent to ~0.01% of the WBC count (equivalent to ~200 MDA-MB-468 cells) were incubated with anti-EGFR-FITC and analyzed by FCM. To ensure appropriate gating of tumor cells, 1% (compared to WBC count) spiked samples were utilized. The sample showed a signal-to-noise ratio of 268.5. Several concentrations of anti-CD44-FITC were then analyzed, and based on the FITC MFI values, the anti-CD44-FITC concentration that gave the closest signal-to-noise ratio to that of the anti-EGFR-FITC was 3.5µg/mL, with a signal-to-noise ratio of 257.5 (*Table 4.1 and Figure 4.2*).

Based on these results, anti-CD44-FITC diluted in 1x ultrapure PBS at a working concentration of 3.5µg/mL was chosen as the initial concentration to use with the CSS. As in *Figure 4.1*, MDA-MB-468 cells were first analyzed by FCM to determine the percentage of the cell population that were $CD44^+$. These cells were found to be highly $CD44^+$ with 98.4±0.90% of cells expressing CD44 (*Figure 4.3A,C*). Blood samples spiked with MDA-MB-468 cells were then analyzed using various exposure times and increasing amounts of anti-CD44-FITC on the CSS using the CTC kit. After extensive optimization, the highest percentage of $CD44^+$ cells that could be obtained on

Table 4.1. Optimization of CD44 antibody concentration by flow cytometry.

µg/ml of CD44-FITC	µl of EGFR-FITC	Signal to Noise Ratio
5.0	-	310.5
3.5	-	257.5
2.0	-	211.5
0.5	-	178.5
-	150	268.5

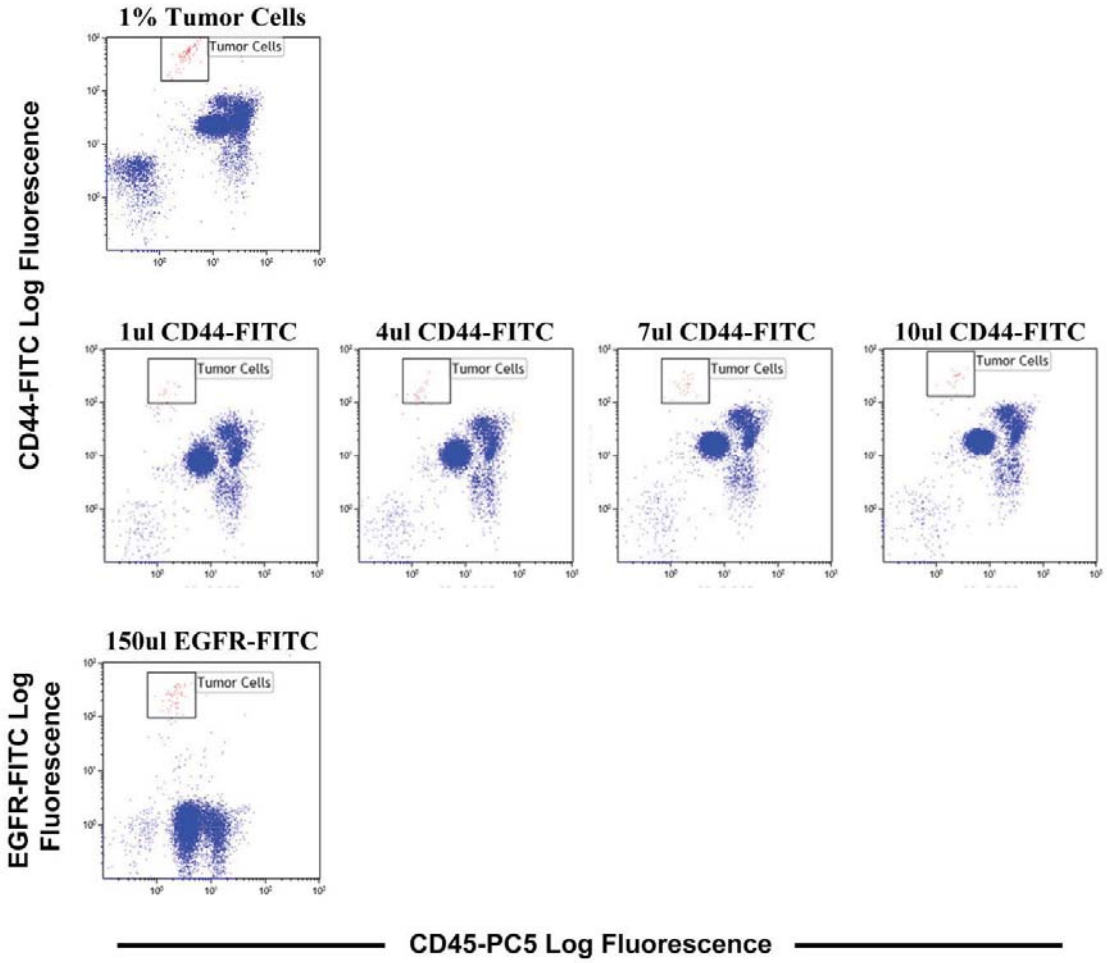

Figure 4.2. Flow cytometry analysis of CD44-FITC titration. MDA-MB-468 tumor cell spiked blood samples (equivalent to 1% of the white blood cell count) were utilized to ensure appropriate tumor cell gating. MDA-MB-468 tumor cells spiked at a concentration equivalent to ~0.01% white blood cells (~200 MDA-MB-468 cells) were then incubated with various CD44-FITC volumes to MDA-MB-468 tumor cells incubated with 150µl of EGFR-FITC to determine the FITC mean fluorescence intensity, measured on a 4 decade log scale, signal-to-noise ratio that best matched that observed when analyzing 150µl of EGFR-FITC. Tumor cells were defined as $CD44^{+}CD45^{-}$ or $EGFR^{+}CD45^{-}$.

Figure 4.3. Protocol development for the CD44 marker using the CellSearch® CTC and CXC kits. ***(A)*** FCM analysis of MDA-MB-468 human breast cancer cells incubated with anti-CD44-FITC (*red*) and an IgG isotype control sample (*blue*). ***(B)*** Representative CellSearch® gallery images of 7.5ml of blood from a healthy volunteer donor, spiked with 1000 MDA-MB-468 human breast cancer cells, incubated with 4.0µg/ml of anti-CD44-FITC and standard Veridex CTC reagents (CK-PE, CD45-APC, DAPI), and analyzed with the CellSearch® CTC kit and an exposure time of 0.5s. Orange squares indicate $CD44^+$ CTCs, identified as $CK^+/DAPI^+/CD45^-/CD44\text{-}FITC^+$. Images acquired at 10x objective magnification. ***(C)*** Percentage recovery of $CD44^+$ cells as determined by FCM and the CellSearch® system using the CTC kit (n=3). Data are presented as the mean ± SEM. *** = significantly different than respective FCM control ($P < 0.0005$). ***(D)*** FCM analysis of MDA-MB-468 human breast cancer cells incubated with anti-CD44-PE *(red*) and an IgG isotype control sample (*blue*). ***(E)*** CellSearch® gallery image of 7.5ml of blood from a healthy volunteer donor, spiked with 1000 MDA-MB-468 human breast cancer cells, incubated with 1.0µg/ml of anti-CD44-PE and standard Veridex CXC reagents (CK-FITC, CD45-APC, DAPI), and analyzed using the CellSearch® CXC kit and an exposure time of 0.6s. Orange squares indicate $CD44^+$ CTCs, identified as $CK^+/DAPI^+/CD45^-/CD44\text{-}PE^+$. Images acquired at 10x objective magnification. ***(F)*** Percentage recovery of $CD44^+$ cells as determined by FCM and the CellSearch® system using the CXC kit (n=3). Data are presented as the mean ± SEM.

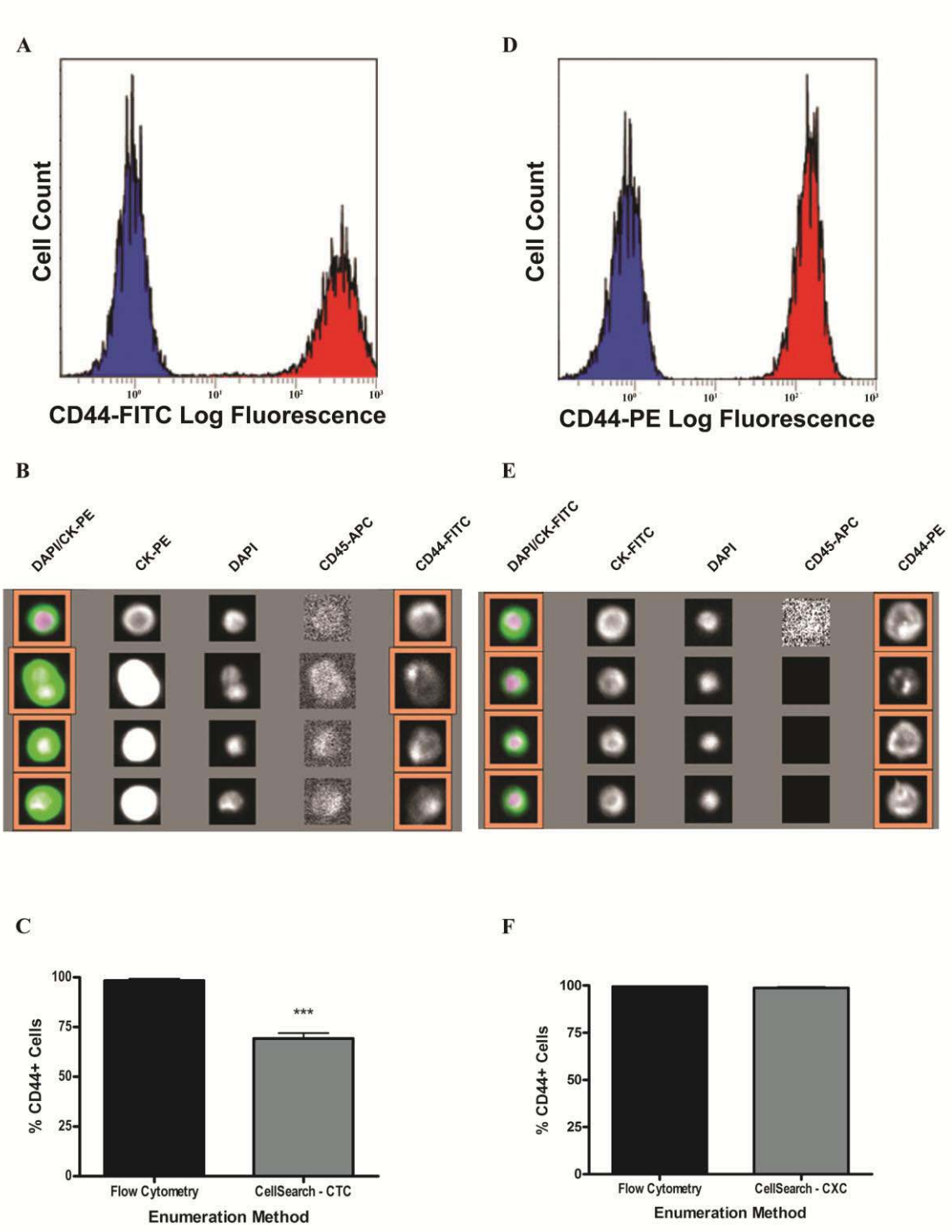
A
Cell Count
CD44-FITC Log Fluorescence
D
Cell Count
CD44-PE Log Fluorescence
B
DAPI/CK-PE
CK-PE
DAPI
CD45-APC
CD44-FITC
E
DAPI/CK-FITC
CK-FITC
DAPI
CD45-APC
CD44-PE
C
% CD44+ Cells
100
75
50
25
0
***
Flow Cytometry
CellSearch - CTC
Enumeration Method
F
% CD44+ Cells
100
75
50
25
0
Flow Cytometry
CellSearch - CXC
Enumeration Method

the CSS was 69.3±2.67% at a concentration of 4.0µg/mL and an exposure time of 0.5s (*Figure 4.3B,C*), and this was still significantly different (p=0.0005) than the CD44 positivity results obtained by FCM (*Figure 4.3C*), and thus were not considered to be suitably optimized. The discrepancy observed between $CD44^+$ cells identified by FCM and the CSS was thought to be a result of either ***(1)*** the FCM assay not taking into account the EpCAM and CK8/18/19 expression of the cells; and/or ***(2)*** the CSS not detecting cells expressing lower levels of CD44. Upon analysis by FCM, lack of EpCAM and/or CK 8/18/19 expression did not appear to contribute to the observed discrepancy, since 99.5±0.47% and 99.0±0.70% of cells were $EpCAM^+$ and $CK8/18/19^+$, respectively (*Figure 4.4A,C and 4.5A,C*). Therefore the CellSearch® CXC kit, optimized for use with lower antigen density markers, was investigated.

4.3.3 CD44 protocol optimization using the CellSearch® CXC kit

The CellSearch® CXC kit differs from the U.S. FDA and Health Canada-cleared CTC kit in that the fluorescence detection of CK8/18/19, normally represented in the PE channel, and the user's marker of interest, normally represented in the FITC channel, are reversed. Therefore the PE channel represents the user's marker of interest and the FITC channel represents CK8/18/19. This change allows for better visualization of lower antigen density markers, ~50,000 antigens/cell on the CXC kit versus ~100,000 antigens/cell using the CTC kit[25]. MDA-MB-468 cells were analyzed by FCM for CD44 positivity using an anti-CD44-PE antibody and were again found to be highly $CD44^+$, with 99.5±0.39% positive for CD44 (*Figure 4.3D,F*). Blood samples spiked with MDA-MB-468 cells were then analyzed using 1.0µg/mL of anti-CD44-PE (equivalent to the volume used for 4.0µg/mL of anti-CD44-FITC) and an exposure time of 0.6s, the

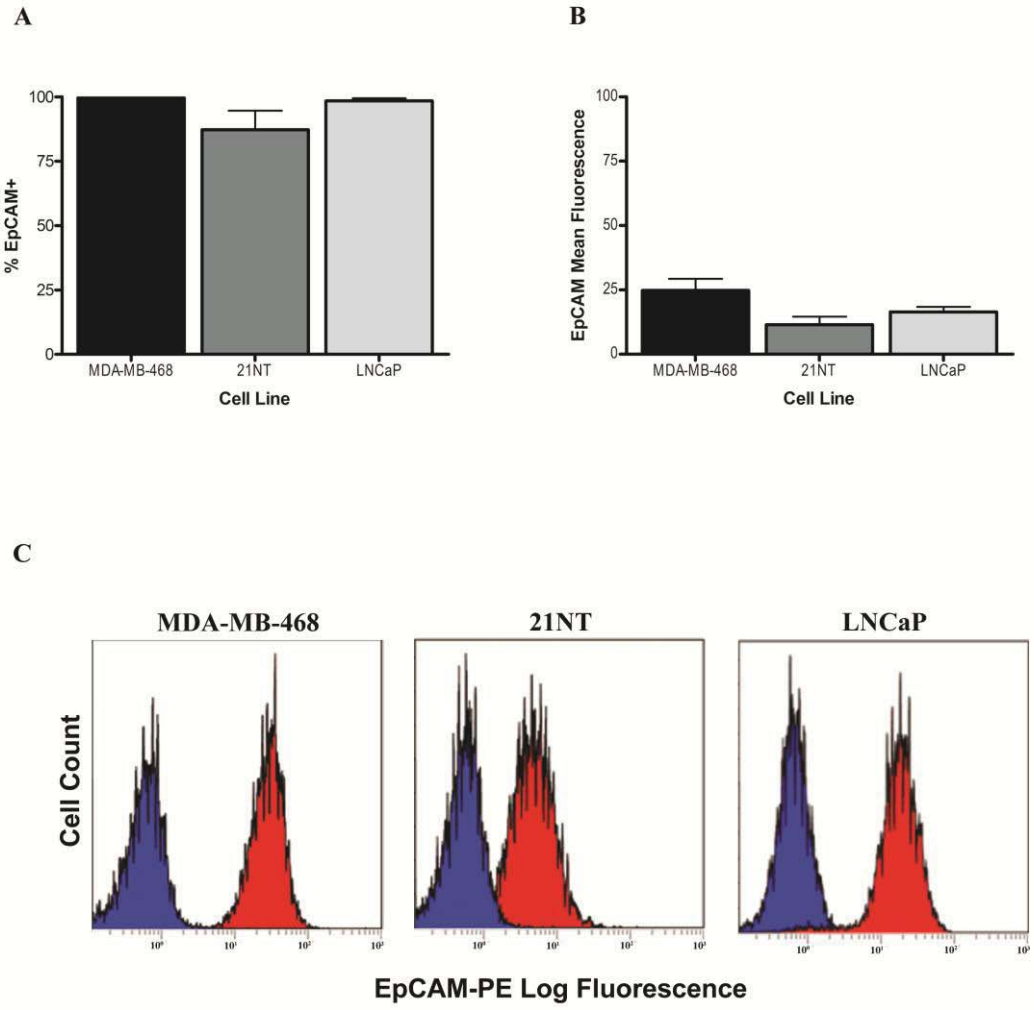

Figure 4.4. Cell line comparison of EpCAM expression by flow cytometry (FCM). ***(A)*** EpCAM expression of the MDA-MB-468, 21NT and LNCaP cell lines (n=3). ***(B)*** PE mean fluorescence intensity (MFI), measure on a 4 decade log scale, as an indicator of EpCAM antigen density, on the MDA-MB-468, 21NT and LNCaP cell lines (n=3). ***(C)*** FCM analysis of MDA-MB-468, 21NT and LNCaP cell lines incubated with anti-EpCAM-PE (red) and an IgG isotype control sample (blue).

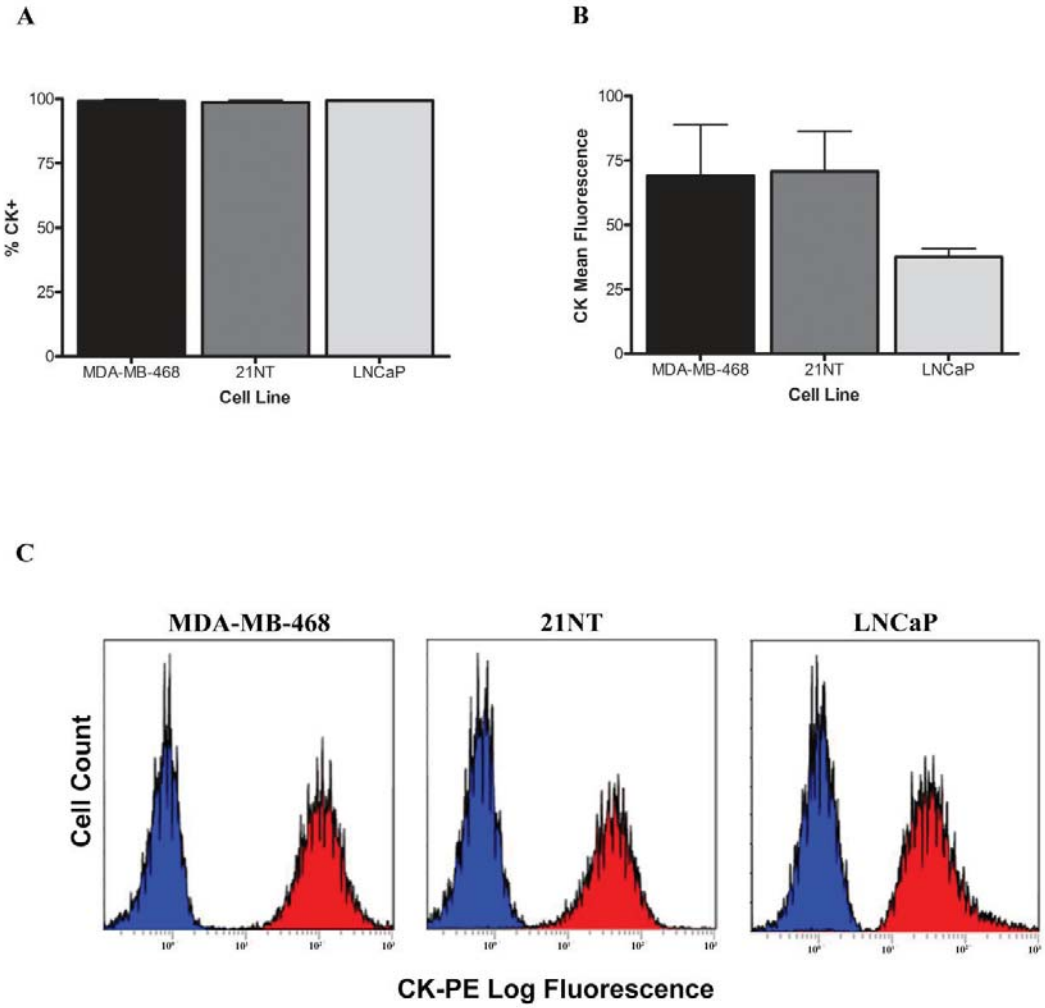

Figure 4.5. Cell line comparison of CK8/18/19 expression by FCM. ***(A)*** CK8/18/19 expression of the MDA-MB-468, 21NT and LNCaP cell lines (n=3). ***(B)*** PE mean fluorescence intensity (MFI), measure on a 4 decade log scale, as an indicator of CK8/18/19 antigen density, on the MDA-MB-468, 21NT and LNCaP cell lines (n=3). ***(C)*** FCM analysis of MDA-MB-468, 21NT and LNCaP cell lines incubated with anti-CK8/18/19-PE (red) and a cells only control sample (blue).

maximum recommended by Janssen Diagnostics for the PE channel, as a starting point. Using these parameters, 98.8±0.51% of cells were observed to be $CD44^+$, a value not significantly different from that obtained by FCM (*Figure 4.3E,F*).

After demonstrating that our developed marker was capable of identifying $CD44^+$ cells to an acceptable degree using the CellSearch® CXC kit, additional optimization was required before the assay could be considered for use in a clinical setting. Three cell lines with varying CD44 expression levels were chosen for this purpose: MDA-MB-468 human breast cancer cells (high expression), 21NT human breast cancer cells (low expression), and LNCaP human prostate cancer cells (no expression) (*Figure 4.6A*). As with the MDA-MB-468 cells, the 21NT cells and LNCaP cells were analyzed for EpCAM and CK8/18/19 positivity to ensure suitable identification by the CSS (*Figure 4.4A,C and 4.5A,C*). All three lines were highly $EpCAM^+$ and $CK8/18/19^+$, 99.5±0.47%/99.0±0.70% (MDA-MB-468), 87.2±7.35%/98.6±0.67% (21NT), and 98.4± 0.97%/99.2±0.20% (LNCaP), respectively, with varying antigen densities represented as EpCAM and CK8/18/19 MFI, measured on a 4 decade log scale, 24.7±4.49/69.0±19.7 (MDA-MB-468), 11.5±3.05/70.7±15.8 (21NT), and 16.4±1.97/37.5±3.22 (LNCaP), respectively *(Figure 4.4B and 4.5B)*. All three cell lines spiked into healthy volunteer blood samples were initially processed using the CellSearch® CXC kit along with 1X ultrapure PBS to determine the level of background noise at various exposure times (0.05–0.6s) and compared to their respective FCM results. At all exposure times tested, no significant differences were observed between the positivity levels obtained on the CSS and those obtained by FCM (*Figure 4.6B-D*). However, background noise does

Figure 4.6. CD44 marker optimization using the CellSearch® CXC kit. ***(A)*** FCM analysis of MDA-MB-468 human breast cancer cells (high CD44-expression), 21NT human breast cancer cells (low CD44-expressing), and LNCaP human prostate cancer cells ($CD44^-$ cell line) incubated with anti-CD44-PE (*red*) and an IgG isotype control sample (*blue*). ***(B-D)*** Comparison of the percentage recovery of $CD44^+$ cells as determined by FCM and the CellSearch® CXC kit incubated with either PBS, IgG-PE, or anti-CD44-PE at stated concentration(s) of the MDA-MB-468 (high CD44-expressing), 21NT (low CD44-expressing), and LNCaP ($CD44^-$ cell line), respectively (n=3). Data are presented as the mean ± SEM. *** = significantly different than respective FCM control ($P<0.05$). Representative CellSearch® gallery images of 7.5ml of blood from a healthy volunteer donor, spiked with 1000 cells from the respective cell line, incubated with 1.5μg/ml of anti-CD44-PE, and analyzed at an exposure time of 0.2s are presented below their respective graph. Orange squares indicate $CD44^+$ CTCs, identified as $CK^+/DAPI^+/CD45^-/CD44\text{-}PE^+$. Images acquired at 10x objective magnification.

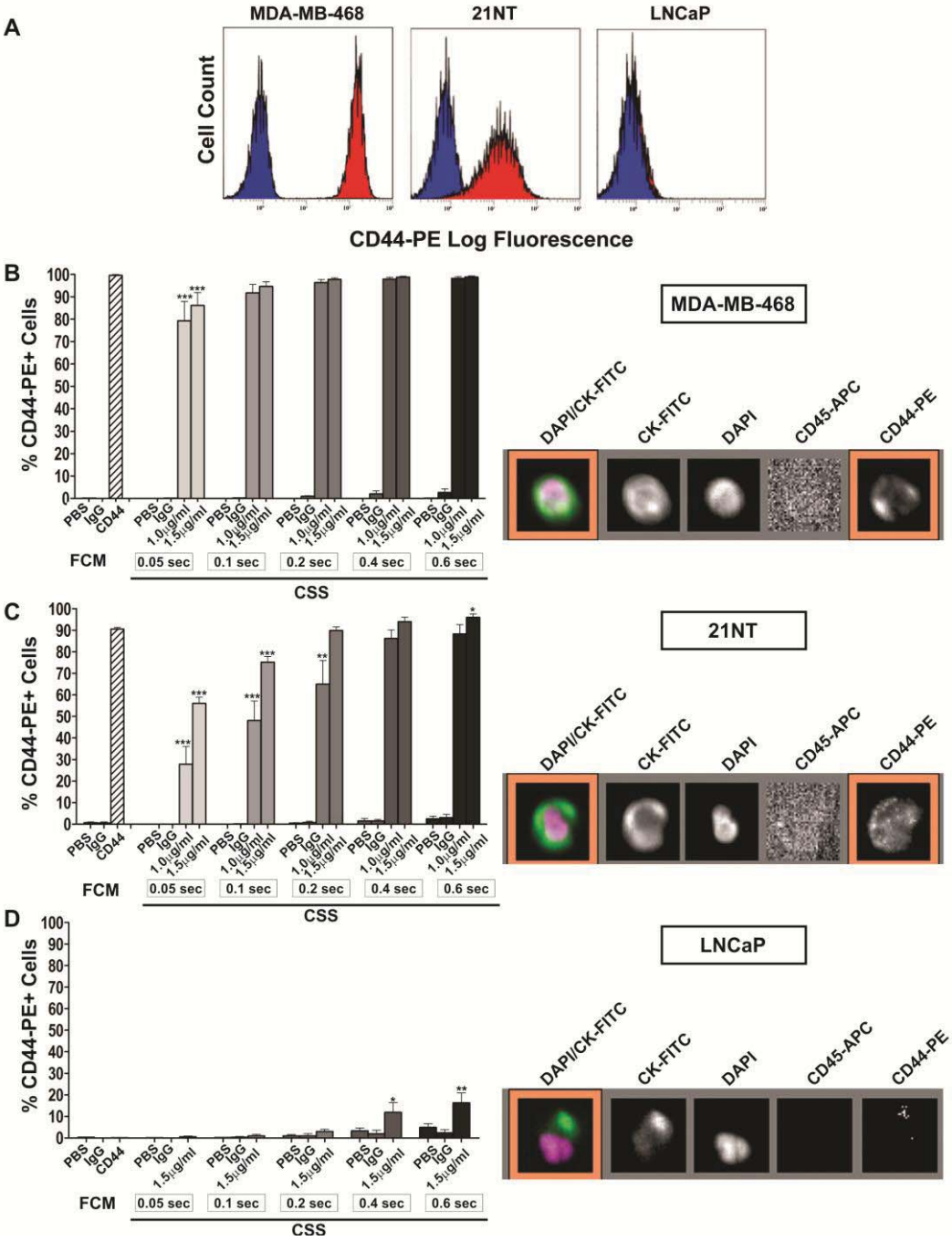
A
MDA-MB-468
21NT
LNCaP
Cell Count
CD44-PE Log Fluorescence
B
% CD44-PE+ Cells
MDA-MB-468
DAPI/CK-FITC
CK-FITC
DAPI
CD45-APC
CD44-PE
PBS
IgG
CD44
1.0μg/ml
1.5μg/ml
FCM
0.05 sec
0.1 sec
0.2 sec
0.4 sec
0.6 sec
CSS
C
% CD44-PE+ Cells
21NT
DAPI/CK-FITC
CK-FITC
DAPI
CD45-APC
CD44-PE
FCM
CSS
D
% CD44-PE+ Cells
LNCaP
DAPI/CK-FITC
CK-FITC
DAPI
CD45-APC
CD44-PE
FCM
CSS

appear to increase, although not significantly, with increasing exposure time, and therefore exposure time should be kept to a minimum.

As demonstrated, MDA-MB-468 cells spiked into blood and processed with 1.0µg/mL of anti-CD44-PE on the CSS (CXC kit) at an exposure time of 0.6s resulted in a similar percentage of $CD44^+$ cell detection to that observed by FCM (*Figure 4.3F*). However, with the goal of keeping exposure times to a minimum, various additional exposure times were investigated. Results demonstrate that 1.0µg/mL of anti-CD44-PE was adequate for identifying CD44 positivity in MDA-MB-468 cells (high CD44-expressing cell line) at all exposure times except 0.05s (*Figure 4.6B*). However, using 1.0µg/mL of anti-CD44-PE in 21NT cells (low CD44-expressing cell line), we observed that only exposure times of 0.4s and 0.6s were adequate for identifying $CD44^+$ cells (*Figure 4.6C*). Therefore, the concentration of anti-CD44-PE was increased to 1.5µg/mL. Upon analysis of both the MDA-MB-468 and 21NT cells on the CSS (CXC kit) at this increased antibody concentration, CD44 positivity of MDA-MB-468 cells was adequate at all exposure times except 0.05s, and CD44 positivity of 21NT cells was now deemed to be adequate at 0.2s and 0.4s (*Figure 4.6B, C*). A higher percentage of cells were detected at 0.6s, however, this was accompanied by an increase in false positive cells in the CD44 negative LNCaP cell line control sample using 1.5µg/mL (*Figure 4.6D*). Based on these results, an antibody concentration of 1.5µg/mL was determined to be optimal for CD44 visualization as it allowed the use of lower exposure times, thereby minimizing background noise and false positive results. Finally, spiked blood samples for all three cell lines were processed with appropriate IgG controls on the CSS and analyzed at various exposure times to ensure antibody specificity (*Figure 4.6B-D*). Based upon these

results, an antibody concentration of 1.5µg/mL and an exposure time of 0.2s were chosen as the optimized parameters for this marker. Additional CellSearch® gallery images for each cell line under optimized conditions can be found in *Figure 4.7*.

4.3.4 M-30 protocol development for use with the CellSearch® system

Next, we chose to investigate M-30, a marker of cellular death. FCM experiments were initially performed to determine the optimal concentration of paclitaxel (0.1µg/mL) to use for apoptosis induction of the MDA-MB-468 cells (*data not shown*). Paclitaxel-treated and untreated cells were then processed in parallel on the flow cytometer and the CSS to control for various confounding factors (i.e., confluency of the cells at time of treatment, slight variations in drug dilution, etc.) that would make direct comparison of the M-30$^+$ cells difficult. It should be noted that, during the development and optimization of the M-30 protocol, images in the FITC channel were observed to be clear, bright, and easily identifiable as M-30$^+$ cells. This was not the case, however, with CD44, where many images showed a faint signal in the FITC channel, but appeared grainy in nature and were therefore not clear and bright enough to be classified as CD44$^+$ Based on these results, the CXC kit was not utilized in the development of the M-30 protocol as the images generated using the CellSearch® CTC kit were of the same quality as those shown using the CellSearch® CXC kit for CD44 and therefore use of this kit would likely not have significantly increased the number of M-30$^+$ CTC. (*Figure 4.8)*.

By FCM, untreated cells showed very low levels of M-30 positivity, with 0.8±0.13% being M-30$^+$, and a small proportion of the paclitaxel treated cells (17.6±1.18%) were classified as apoptotic (M-30$^+$), based on gates set at the outermost limits of an untreated control incubated with equivalent volumes of M-30 antibody

Figure 4.7. Additional representative CellSearch® gallery images of optimized CD44-PE protocol from Figure 3. Representative CellSearch gallery images of 7.5ml of blood from a healthy volunteer donor, spiked with 1000 cells from the respective cell line, incubated with 1.5μg/ml of anti-CD44-PE, standard Veridex CXC reagents (CK-FITC, CD45-APC, DAPI), and analyzed at an exposure time of 0.2s. Orange squares indicate CD44+ CTCs, identified as CK+/DAPI+/CD45–/CD44-PE+.

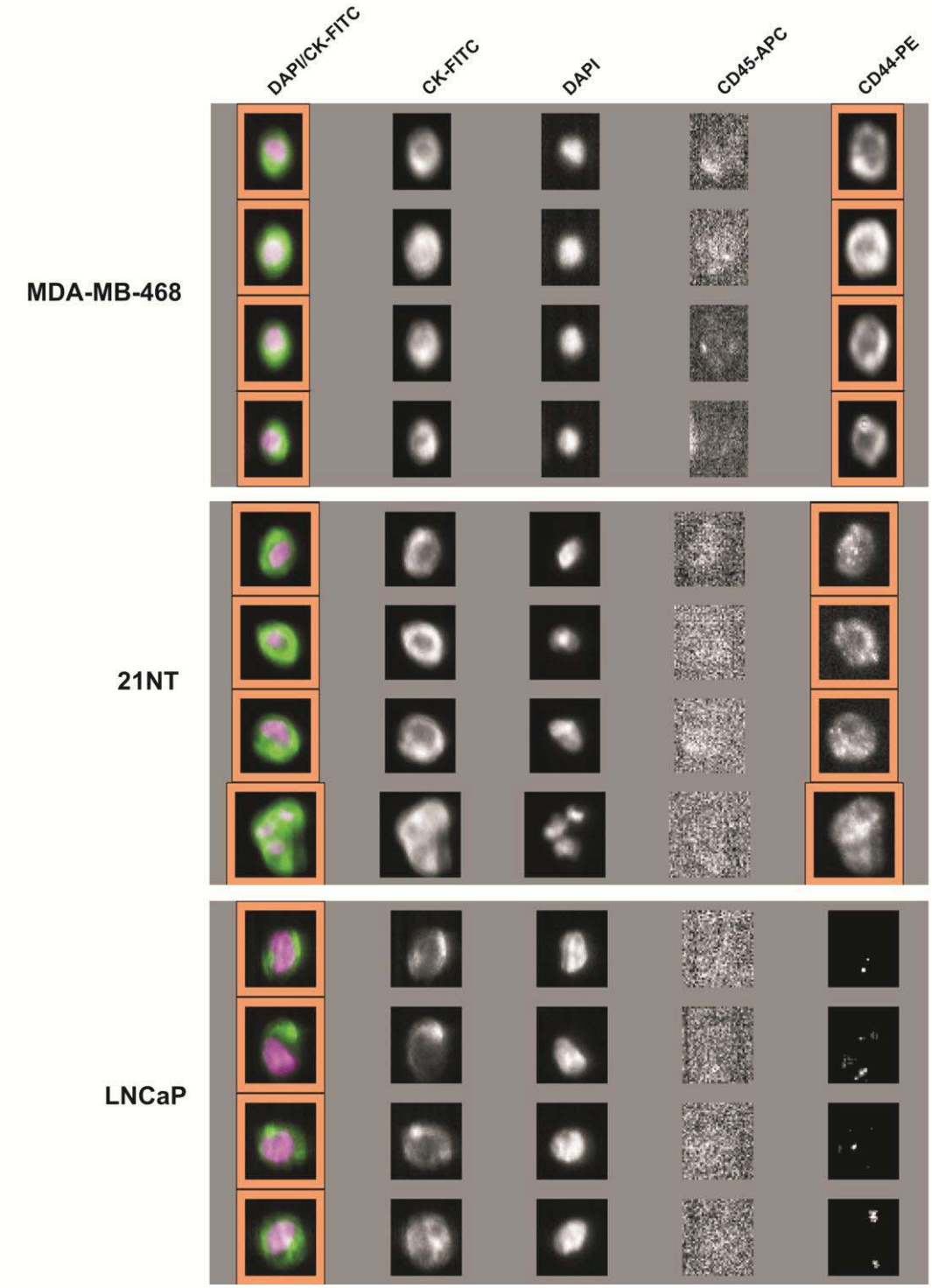
DAPI/CK-FITC
CK-FITC
DAPI
CD45-APC
CD44-PE
MDA-MB-468
21NT
LNCaP

Figure 4.8. Observed staining differences between CD44-FITC and M-30-FITC with the CellSearch® CTC kit. ***(A)*** Representative CellSearch® gallery images of 7.5ml of blood from a healthy volunteer donor, spiked with 4000 MDA-MB-468 human breast cancer cells treated with 0.1μg/ml of paclitaxel and subsequently incubated with 3.5μg/ml of anti-M-30-FITC. Orange squares indicate $M\text{-}30^+$ CTCs, identified as $CK^+/DAPI^+/CD45^-/M\text{-}30^+$. (B) Representative CellSearch gallery images of 7.5ml of blood from a healthy volunteer donor, spiked with 1000 MDA-MB-468 human breast cancer cells, incubated with 4.0μg/ml of anti-CD44-FITC and standard Veridex CTC reagents (CK-PE, CD45-APC, DAPI), and analyzed with the CellSearch CTC kit and an exposure time of 0.5s. Orange squares indicate $CD44^+$ CTCs, identified as $CK^+/DAPI^+/CD45^-/CD44\text{-}FITC^+$ (C) Representative CellSearch gallery images of 7.5ml of blood from a healthy volunteer donor, spiked with 1000 MDA-MB-468 human breast cancer cells, incubated with 1.5μg/ml of anti-CD44-PE and standard Veridex CXC reagents (CK-FITC, CD45-APC, DAPI), and analyzed with the CellSearch CXC kit and an exposure time of 0.2s. Orange squares indicate $CD44^+$ CTCs, identified as $CK^+/DAPI^+/CD45^-/CD44\text{-}PE^+$.

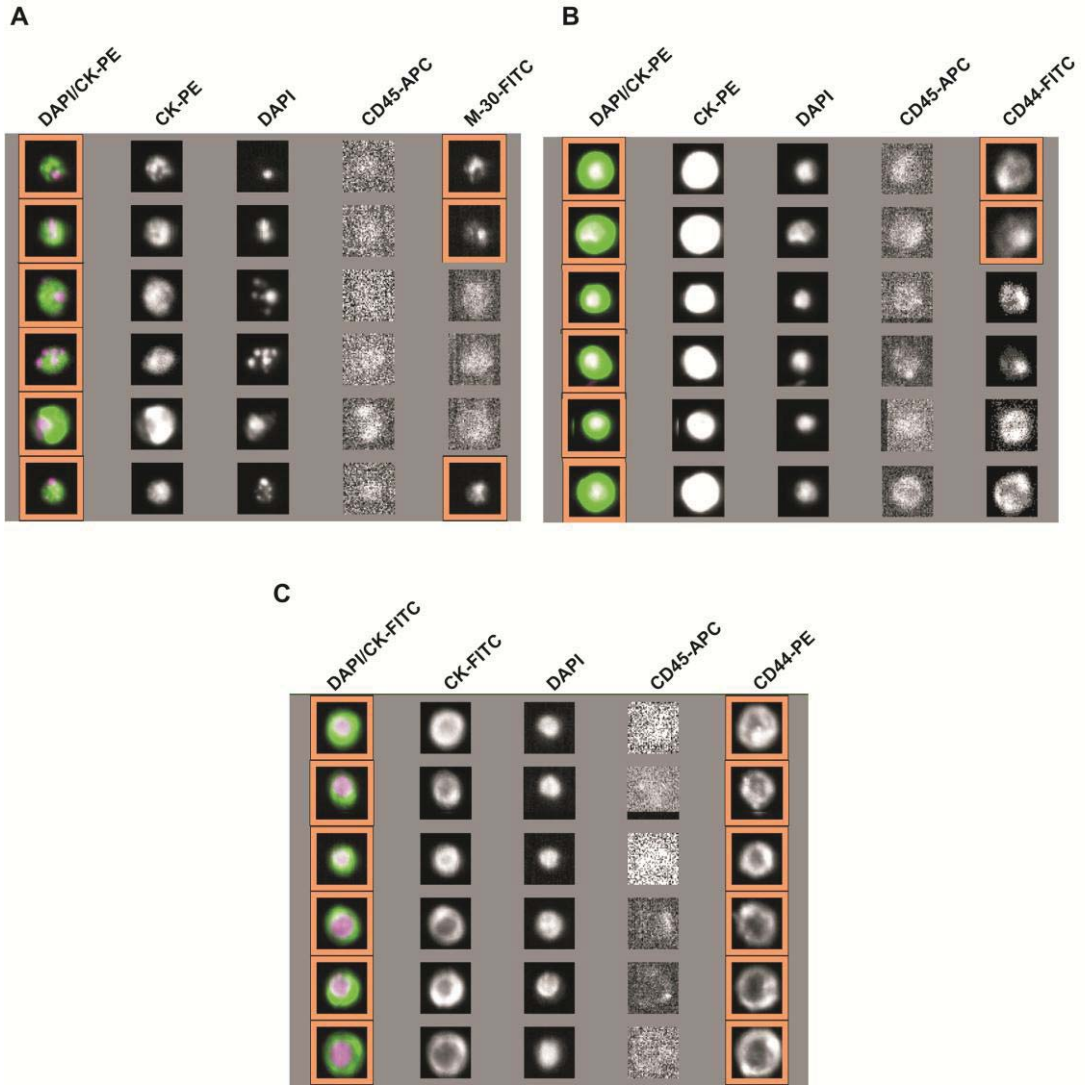
A
DAPI/CK-PE
CK-PE
DAPI
CD45-APC
M-30-FITC
B
DAPI/CK-PE
CK-PE
DAPI
CD45-APC
CD44-FITC
C
DAPI/CK-FITC
CK-FITC
DAPI
CD45-APC
CD44-PE

(*Figure 4.9A,C*). After extensive optimization on the CSS (CTC kit) 3.5µg/mL of anti-M-30-FITC and an exposure time of 0.8s produced the highest percent of M-30$^+$ treated cells, with 10.9±2.42% being M-30$^+$. In addition, this concentration and exposure time when processing blood spiked with untreated cells showed M-30 positivity that was not significantly different from the FCM results (*Figure 4.9B,C*).

In an attempt to explain this observed discrepancy, it was necessary to determine if paclitaxel treatment would affect the ability of the CSS to detect the treated CTCs by decreasing the MFI of EpCAM, CK8/18/19, and/or DAPI. Following 48 hours of treatment with 0.1µg/mL of paclitaxel, treated and untreated cells were incubated with anti-M-30-FITC and either anti-EpCAM-PE, anti-CK8/18/19-PE, or DAPI and analyzed by FCM. Following paclitaxel treatment, there was no significant loss of EpCAM or CK positivity, with 97.5±1.51% and 97.7±0.49% of cells observed to be EpCAM$^+$ and CK$^+$ respectively in untreated samples versus 89.6±5.89% and 91.5±3.88% respectively in paclitaxel-treated samples. In addition, following treatment the vast majority of cells that were apoptotic (M-30$^+$) also appeared to be EpCAM$^+$ (22.7±3.41% [M-30$^+$] versus 19.9±4.62% [M-30$^+$EpCAM$^+$]) and CK$^+$ (24.6±3.13% [M-30$^+$] versus 24.9±2.26% [M-30$^+$CK$^+$]) and therefore a significant population of M-30$^+$/EpCAM$^-$ or M-30$^+$/CK$^-$ cells (that would not be captured by the CSS) was not found (*Figure 4.10A,B*). However, following paclitaxel treatment there was a significant decrease in DAPI MFI relative to untreated cells, 60.4±1.10% versus 96.9±0.46%, respectively, and there was a significant difference between the apoptotic (M-30$^+$) cells and those that were both apoptotic (M-30$^+$) and DAPI$^+$, 17.6±1.18% versus 8.7±0.79%, respectively (*Figure 4.10C*). It is important to note that this decrease in DAPI MFI did not necessarily constitute cells

Figure 4.9. M-30 protocol development for use with the CellSearch® CTC kit. ***(A)*** FCM analysis of M-30 expression in untreated MDA-MB-468 human breast cancer cells (*blue*) and cells treated with 0.1µg/ml of paclitaxel (*green*), and a cells only control sample (*red*). ***(B)*** Representative CellSearch® gallery images of 7.5ml of blood from a healthy volunteer donor, spiked with 4000 MDA-MB-468 human breast cancer cells treated with 0.1µg/ml of paclitaxel and subsequently incubated with 3.5µg/ml of anti-M-30-FITC and standard Veridex CTC reagents (CK-PE, CD45-APC, DAPI). Orange squares indicate $M\text{-}30^+$ CTCs, identified as $CK^+/DAPI^+/CD45^-/M\text{-}30^+$. ***(C)*** Percentage of $M\text{-}30^+$ cells for treated and untreated samples as determined by FCM and the CellSearch® system (n=3). Data are presented as the mean ± SEM. * = significantly different than respective FCM control ($P<0.05$).

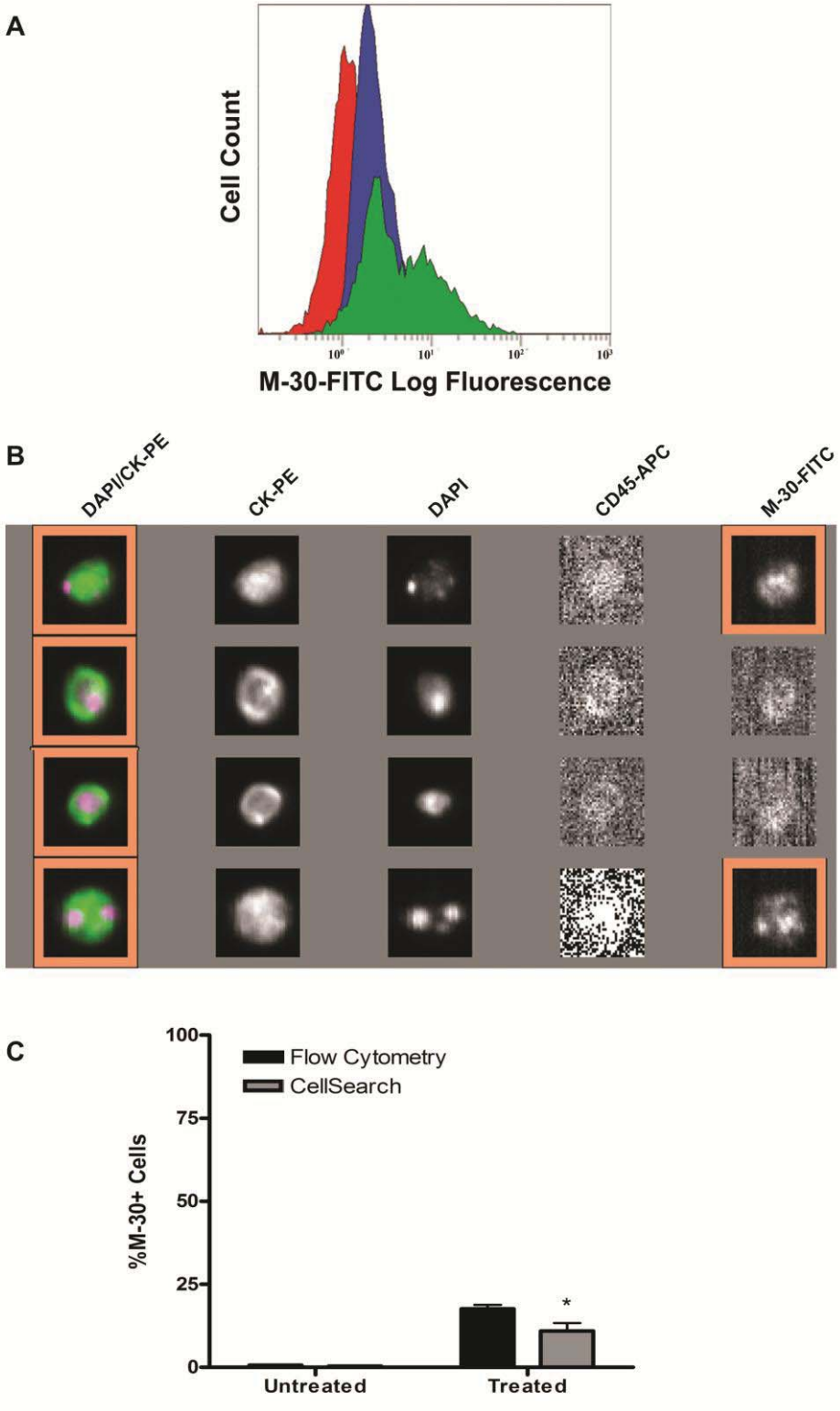
A
Cell Count
M-30-FITC Log Fluorescence
B
DAPI/CK-PE
CK-PE
DAPI
CD45-APC
M-30-FITC
C
Flow Cytometry
CellSearch
%M-30+ Cells
100
75
50
25
0
*
Untreated
Treated

Figure 4.10. Assessment of potential sources of M-30 loss using the CellSearch® system. ***(A)*** Percentage of $EpCAM^+$, $M\text{-}30^+$, and dual stained $M\text{-}30^+/EpCAM^+$ cells in the presence or absence of paclitaxel treatment (0.1 μg/ml for 48 hours; n=3). ***(B)*** Percentage of CK^+, $M\text{-}30^+$, and dual stained $M\text{-}30^+/CK^+$ cells in the presence of absence of paclitaxel treatment (0.1 μg/ml for 48 hours; n=3). ***(C)*** Percentage of $DAPI^+$, $M\text{-}30^+$, and dual stained $M\text{-}30^+/DAPI^+$ cells in the presence or absence of paclitaxel treatment (0.1 μg/ml for 48 hours; n=3). Data are presented as the mean ± SEM. * = significantly different than respective untreated control ($P < 0.05$). a = significantly different than paclitaxel-treated $M\text{-}30^+$ sample.

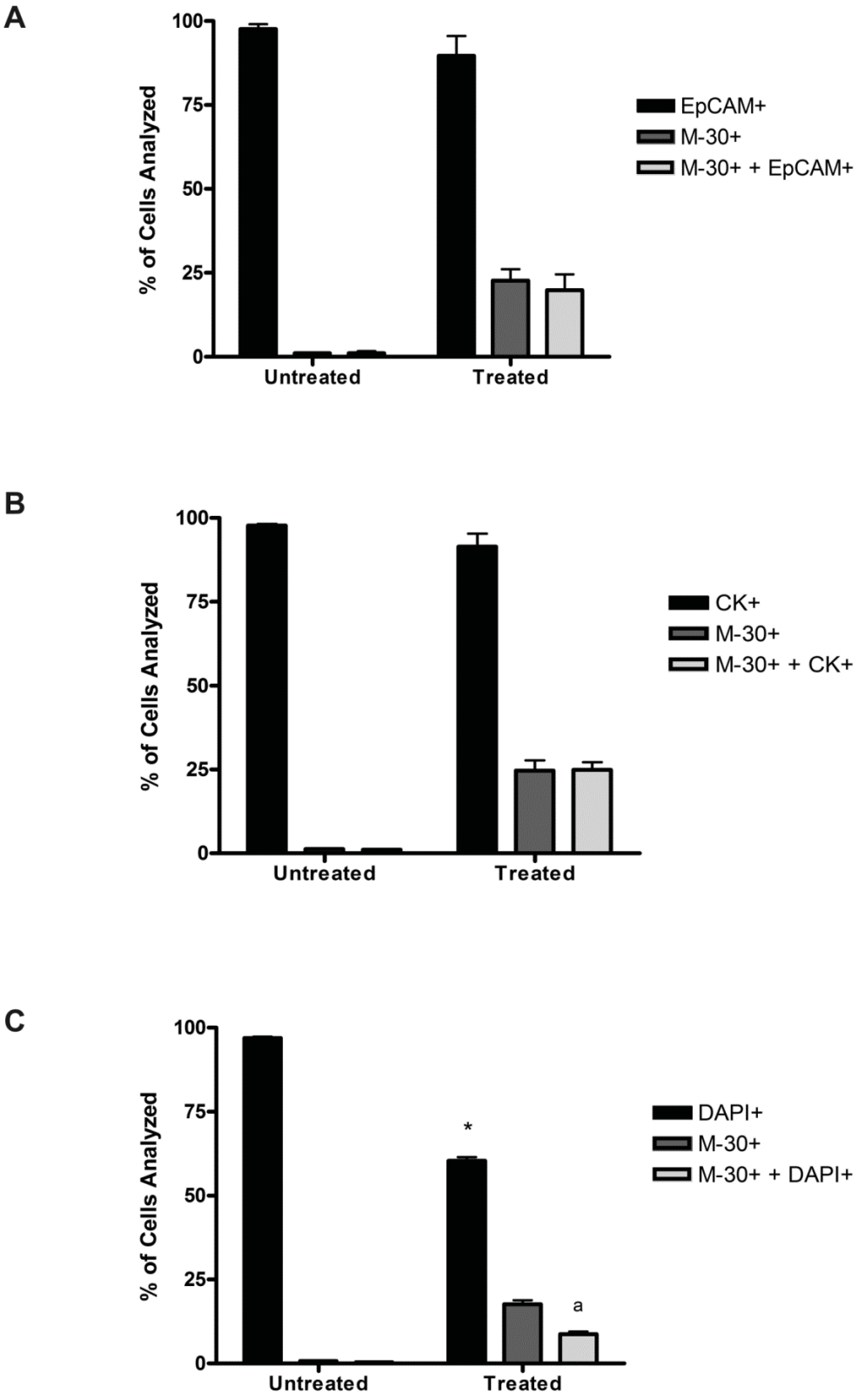
A
100
75
50
25
0
% of Cells Analyzed
Untreated
Treated
EpCAM+
M-30+
M-30+ + EpCAM+
B
100
75
50
25
0
% of Cells Analyzed
Untreated
Treated
CK+
M-30+
M-30+ + CK+
C
100
75
50
25
0
% of Cells Analyzed
*
a
Untreated
Treated
DAPI+
M-30+
M-30+ + DAPI+

becoming $DAPI^-$. Instead cells that demonstrated high levels of DAPI staining ($DAPI^{hi}$ phenotype) prior to treatment appeared to exhibit decreased DAPI staining following treatment ($DAPI^{lo}$ phenotype), which could therefore affect adequate visualization of DAPI positivity on the CSS. This decrease in DAPI MFI lead us to further investigate the percentage of cells that were M-30^+DAPI^{hi} by FCM compared with those that were M-30^+DAPI^+ by the CSS (since DAPI positivity is a requirement to classify an event as a CTC on the CSS). This comparison appeared to rectify the observed difference. However, to validate this observation, reanalysis of the CSS data was necessary, to determine if inclusion of those cells that were not originally classified as a CTC due to poor DAPI staining would increase the number of M-30^+ cells to that originally observed by FCM (17.6±1.18%). However, upon reanalysis the percentage of M-30^+ cells increased only marginally and this increased value was still significantly different (paired t-test) from the M-30^+ data obtained by FCM (*data not shown*).

4.4 Discussion

The majority of cancer-related deaths are due to ineffective treatment of metastatic disease and an incomplete understanding of the biology of metastasis. Advances in the area of CTC detection and enumeration allows for investigation of the early-stages of metastasis that until recently was limited by technological challenges. The characterization of CTCs could be a powerful clinical tool, acting as a real-time, minimally invasive liquid biopsy that would inform clinical decision-making and help direct tailored, individualized therapy. In the present study, our aim was therefore to develop protocols that would allow for the characterization of CTCs using the U.S. FDA

and Health Canada-cleared CSS. To the best of our knowledge, this is the first study in the literature to describe the detailed process of protocol development and optimization using this platform. We have demonstrated the appropriate steps that must be taken for proper optimization of user-defined protein marker assays on this system, including comparison of results with a well validated protein expression technology (FCM); appropriate troubleshooting; and detailed optimization techniques using cell lines with various target marker antigen densities. In addition, we have demonstrated that not all markers are ideal candidates for use with the CSS.

Although previous studies have examined CTCs for the expression of CD44, none of these previous studies have utilized the CSS to do so[25–27]. As this system is still the gold-standard and the only U.S. FDA and Health Canada-cleared instrument for CTC enumeration and clinical decision-making, the ability to characterize CTCs in combination with enumeration using this particular platform is more clinically applicable then the ability to do so using other techniques. Additionally, Rossi et al., 2010, is the only published study (to our knowledge) that has utilized user-defined, non-Janssen optimized protein markers assays (specifically M-30), on the CSS. However, this manuscript fails to provide details of proper optimization of the protocol for the use of this protein marker on the CSS[28]. This highlights the necessity for the current study, which provides a detailed description of the process of protein marker optimization in order for users of this instrument to develop properly optimized protein marker protocols that could be utilized in a clinical setting.

The advantages of utilizing the CSS platform include system standardization; clearance by the U.S. FDA and Health Canada for assessment of prognosis in metastatic

breast, prostate, and colorectal cancer; and the ability to examine CTC heterogeneity at the single cell level. However, the CSS does have a number of disadvantages, including the use of the epithelial marker EpCAM for CTC enrichment. Others have shown that many of the tumor cells found in the circulation are actually mesenchymal in phenotype and are therefore potentially undetectable by this system due to a lack of EpCAM expression[29–32]. In addition, it has been demonstrated that the epithelial-to-mesenchymal transition (EMT), which may produce these undetectable CTCs, is associated with enhanced cancer cell aggressiveness[33,34]. Therefore metastatic cells that may potentially form metastatic lesions and are of great interest for characterization may be missed by the CSS. New CTC platforms are currently under development, and hold great promise for enhanced CTC detection and characterization[35,36]. However, the CSS, although not a perfect detection and characterization platform, is currently the clinical gold standard for CTC analysis, and for this reason we explored the development of additional CTC characterization assays using this system.

We initially began protocol development for the CD44 marker using the CellSearch® CTC kit, with limited success. We hypothesized that the low CD44 positivity results might be due to contamination with leukocytes expressing CD44, thereby simulating a situation in which cells appear to have a lower than expected antigen density. We tested this hypothesis by utilizing the CellSearch® CXC kit, which is optimized for the visualization of lower antigen density markers. Utilization of this kit resolved this observed discrepancy, showing levels of CD44 expression that were not significantly different from those observed by FCM. Three cell lines with various CD44 expression levels were then chosen to optimize this protocol. This was a necessary step in

the optimization process as the CD44 antigen density in patient CTCs is unknown, and likely to be quite variable across patient samples. As demonstrated, the 21NT cell line (low CD44-expressing) was unable to be adequately visualized at a low exposure time using 1.0µg/mL of anti-CD44-PE, and therefore the concentration had to be increased to 1.5µg/mL to ensure adequate sensitivity. In addition, the LNCaP cell line (CD44 negative) was utilized to ensure specificity of the assay protocol.

As with all assays, limitations do exist when utilizing the CSS for the visualization of CD44. CD44 is a marker of cancer stem cells (CSCs)[19], a phenotype that has been associated with EMT[37]. There is always the possibility that CTCs from patient samples may express CD44, but largely by those cells that are undetectable by the CSS, due to a lack of or low level of EpCAM expression. In addition, we have demonstrated that leukocytes can affect adequate CD44 visualization. Therefore this assay could be compromised in patients with exceptionally high levels of contaminating leukocytes. However, we are confident that this assay is appropriately optimized for use in future clinical studies of metastatic cancer patients.

Next we investigated a different type of marker, one that measures cellular death in response to therapy. We attempted to optimize the integration of the early apoptosis marker M-30 with the CSS. However, after extensive experimentation, we have demonstrated that this marker is unlikely to ever capture all early apoptotic cells in patient samples, as these results were unachievable even under highly controlled conditions. The lack of optimal M-30 positivity on the CSS did not appear to be as a result of a decrease in either EpCAM or CK MFI in our paclitaxel-treated cells. However, when nuclear staining using DAPI was investigated by FCM, there did appear to be a

significant decrease in the percentage of overall $DAPI^{hi}$ and $M\text{-}30^{+}DAPI^{hi}$ cells, which could affect adequate visualization of DAPI positivity, and therefore CTC classification, on the CSS. When only the $M\text{-}30^{+}DAPI^{hi}$ FCM results were compared to our $M\text{-}30^{+}DAPI^{+}$ CellSearch® data this appeared to rectify the observed difference. To validate this observation, re-analysis of the CellSearch® data was performed to determine if inclusion of those cells that were not originally classified as a CTC due to poor DAPI staining would increase the number of $M\text{-}30^{+}$ cells to that originally observed by FCM. However, re-analysis only marginally increased the percentage of $M\text{-}30^{+}$ cells on the CSS. This increased value was still significantly different from the $M\text{-}30^{+}$ data obtained by FCM and therefore could not be a plausible explanation for why M-30 positivity using the CSS was lower than that observed by FCM. It is possible that spiking cells that are in the process of cell death could reduce CTC recovery as some of these cells may be damaged during the pre-spiking preparation and others during CellSearch® sample processing. Therefore, experiments would need to be performed to determine $M\text{-}30^{+}$ CTC recovery, using spiked samples with high, medium, and low numbers of $M\text{-}30^{+}$ CTCs, and to demonstrate that these recovery results are reproducible across laboratories before this protocol could be considered for clinical use. However, based on the results obtained in our study and our primary aim of demonstrating proper protocol development and troubleshooting, we will not be moving forward with this marker as we believe that there are other markers that are likely better suited to identifying therapy response.

In previous work by Rossi et al. (2010), attempts were made to utilize the M-30 assay on the CSS[28]. However, direct comparison between M-30 positivity by FCM and the CSS was never performed; instead CellSearch® results were compared to

Annexin V positivity, with somewhat discordant results. The authors attempt to explain this difference as a result of non-classification of some events as CTCs on the CSS; however experimentation was not undertaken to confirm this hypothesis. In addition, optimal M-30 antibody concentration (2μg/mL) and exposure time (0.4s) were chosen based on results from 3 patients with probable M-30^{+} CTCs, not in treated control spiked blood samples, as shown in this study.

The M-30 assay has potential for utilization as a measure of therapy effectiveness and as an early indicator of the necessity for a change in treatment. However, this assay is only able to identify apoptosis, one of many known mechanisms of cellular death (necrosis, autophagy, mitotic catastrophe)[20]. This presents a potential problem when examining CTC death as a marker of therapy effectiveness, as it is likely that not all therapy-induced cellular death will be apoptotic[38–40]. Therefore the discrepancies observed in the visualization of this marker in the present study could be a result of the overall complexity and lack of a complete understanding of cellular death in response to therapy.

Research in this area has led many in the field to believe that there is much overlap in the mechanisms that underlie these cellular death processes[38–40] but that many different pathways exist that may result in cell death (e.g., apoptosis, necrosis, autophagy). Therefore many cells undergoing cellular death may be missed by relying on an assay that only measures apoptosis. Instead, an ideal cellular death marker would measure all types of cell death, however such a marker does not yet exist. The next ideal candidate would measure the most prevalent form of cellular death and be present for the longest detectable period of time. However, even this may be difficult to achieve. Others

have demonstrated that the relative proportion of cells that undergo apoptotic cell death can change quite dramatically based on the stressor applied, stressor intensity (concentration and/or length of application), and the cells induced to undergo apoptosis[38]. Problems therefore arise when examining patient samples as proper timing may be necessary to capture cell death in the appropriate state. Even if ideal conditions were satisfied, highly vascularized versus poorly vascularized/hypoxic tumors may respond differently (i.e., different cellular death pathways) to antitumor agents due to differences in drug concentrations received. The question then becomes whether the identification of *all* early apoptotic CTCs is necessary for prediction of therapeutic efficacy and clinical decision-making. Instead, could the identification of *any* apoptotic cells represent a favourable prognosis for patients? In the study by Rossi et al. (2010)[28], CTC analysis was performed in blood from 8 breast cancer patients using the integrated M-30 assay on the CSS (2μg/mL and exposure time 0.4s). The change in the number of live verses dead (apoptotic) CTCs was determined and found to correlate with radiologic findings of disease status (progressive versus stable disease/partial response), as determined by radiology, with 100% concordance. Obviously larger follow up studies will have to be performed before any meaningful conclusions can be drawn from these data, but the results do appear promising.

In summary, we have demonstrated the detailed process of optimization that is required for the development of a user-defined marker on the CSS. In addition, we have shown that not all markers are suitable candidates for use with this platform and the necessary troubleshooting that must be performed when dealing with markers that might alter CTC identification characteristics. This study will act as an important

troubleshooting guide for the future development of protein marker assays by users of this platform.

4.5 References

1 Siegel RL, Miller KD, Jemal A. Cancer statistics, 2015. *CA Cancer J Clin* 2015. doi:10.3322/caac.21254.

2 Chambers AF, Groom AC, MacDonald IC. Dissemination and growth of cancer cells in metastatic sites. *Nat Rev Cancer* 2002; **2**: 563–72.

3 Pantel K, Brakenhoff RH. Dissecting the metastatic cascade. *Nat Rev Cancer* 2004; **4**: 448–56.

4 Cristofanilli M, Budd GT, Ellis MJ, Stopeck A, Matera J, Miller MC *et al.* Circulating tumor cells, disease progression, and survival in metastatic breast cancer. *N Engl J Med* 2004; **351**: 781–91.

5 De Bono JS, Scher HI, Montgomery RB, Parker C, Miller MC, Tissing H *et al.* Circulating tumor cells predict survival benefit from treatment in metastatic castration-resistant prostate cancer. *Clin Cancer Res* 2008; **14**: 6302–9.

6 Cohen SJ, Punt CJ a, Iannotti N, Saidman BH, Sabbath KD, Gabrail NY *et al.* Relationship of circulating tumor cells to tumor response, progression-free survival, and overall survival in patients with metastatic colorectal cancer. *J Clin Oncol* 2008; **26**: 3213–21.

7 Naume B, Borgen E, Tøssvik S, Pavlak N, Oates D, Nesland JM. Detection of isolated tumor cells in peripheral blood and in BM: evaluation of a new enrichment method. *Cytotherapy* 2004; **6**: 244–52.

8 Rosenberg R, Gertler R, Friederichs J, Fuehrer K, Dahm M, Phelps R *et al.* Comparison of two density gradient centrifugation systems for the enrichment of disseminated tumor cells in blood. *Cytometry* 2002; **49**: 150–8.

9 Yang L, Lang JC, Balasubramanian P, Jatana KR, Schuller D, Agrawal A *et al.* Optimization of an enrichment process for circulating tumor cells from the blood of head and neck cancer patients through depletion of normal cells. *Biotechnol Bioeng* 2009; **102**: 521–34.

10 Wong SCC, Chan CML, Ma BBY, Hui EP, Ng SSM, Lai PBS *et al.* Clinical significance of cytokeratin 20-positive circulating tumor cells detected by a refined immunomagnetic enrichment assay in colorectal cancer patients. *Clin Cancer Res* 2009; **15**: 1005–12.

11 Baker MK, Mikhitarian K, Osta W, Callahan K, Hoda R, Brescia F *et al.* Molecular detection of breast cancer cells in the peripheral blood of advanced-stage breast cancer patients using multimarker real-time reverse transcription-polymerase chain reaction and a novel porous barrier density gradient centrifugation technology. *Clin Cancer Res* 2003; **9**: 4865–71.

12 Hu XC, Chow LW. Detection of circulating breast cancer cells by reverse transcriptase polymerase chain reaction (RT-PCR). *Eur J Surg Oncol* 2000; **26**: 530–5.

13 Beitsch PD, Clifford E. Detection of carcinoma cells in the blood of breast cancer patients. *Am J Surg* 2000; **180**: 446–9.

14 Cruz I, Ciudad J, Cruz JJ, Ramos M, Gómez-Alonso A, Adansa JC *et al.* Evaluation of multiparameter flow cytometry for the detection of breast cancer tumor cells in blood samples. *Am J Clin Pathol* 2005; **123**: 66–74.

15 Lowes LE, Goodale D, Keeney M, Allan AL. Image cytometry analysis of circulating tumor cells. *Methods Cell Biol* 2011; **102**: 261–90.
16 Hudis CA. Trastuzumab--mechanism of action and use in clinical practice. *N Engl J Med* 2007; **357**: 39–51.
17 Fehm T, Müller V, Aktas B, Janni W, Schneeweiss A, Stickeler E *et al.* HER2 status of circulating tumor cells in patients with metastatic breast cancer: a prospective, multicenter trial. *Breast Cancer Res Treat* 2010; **124**: 403–12.
18 Meng S, Tripathy D, Shete S, Ashfaq R, Saboorian H, Haley B *et al.* uPAR and HER-2 gene status in individual breast cancer cells from blood and tissues. *Proc Natl Acad Sci U S A* 2006; **103**: 17361–5.
19 Al-Hajj M, Wicha MS, Benito-Hernandez A, Morrison SJ, Clarke MF. Prospective identification of tumorigenic breast cancer cells. *Proc Natl Acad Sci U S A* 2003; **100**: 3983–8.
20 Leers MPG, Kölgen W, Björklund V, Bergman T, Tribbick G, Persson B *et al.* Immunocytochemical detection and mapping of a cytokeratin 18 neo- epitope exposed during early apoptosis. *J Pathol* 1999; **187**: 567–572.
21 Price JE, Polyzos A, Zhang RD, Daniels LM. Tumorigenicity and metastasis of human breast carcinoma cell lines in nude mice. *Cancer Res* 1990; **50**: 717–721.
22 Band V, Zajchowski D, Swisshelm K, Trask D, Kulesa V, Cohen C *et al.* Tumor progression in four mammary epithelial cell lines derived from the same patient. 1990.
23 Horoszewicz JS, Leong SS, Chu TM, Wajsman ZL, Friedman M, Papsidero L *et al.* The LNCaP cell line--a new model for studies on human prostatic carcinoma. *Prog Clin Biol Res* 1980; **37**: 115–132.
24 Veridex White Pages. Available at: http://www.veridex.com/pdf/CXC_Application_Guideline.PDF. 2008.
25 Wang N, Shi L, Li H, Hu Y, Du W, Liu W *et al.* Detection of circulating tumor cells and tumor stem cells in patients with breast cancer by using flow cytometry : A valuable tool for diagnosis and prognosis evaluation. *Tumour Biol* 2012; **33**: 561–9.
26 Sieuwerts AM, Kraan J, Bolt J, van der Spoel P, Elstrodt F, Schutte M *et al.* Anti-epithelial cell adhesion molecule antibodies and the detection of circulating normal-like breast tumor cells. *J Natl Cancer Inst* 2009; **101**: 61–6.
27 Gradilone A, Iacovelli R, Cortesi E, Raimondi C, Gianni W, Nicolazzo C *et al.* Circulating tumor cells and 'suspicious objects' evaluated through CellSearch® in metastatic renal cell carcinoma. *Anticancer Res* 2011; **31**: 4219–21.
28 Rossi E, Basso U, Celadin R, Zilio F, Pucciarelli S, Aieta M *et al.* M30 neoepitope expression in epithelial cancer: quantification of apoptosis in circulating tumor cells by CellSearch analysis. *Clin Cancer Res* 2010; **16**: 5233–43.
29 Aktas B, Tewes M, Fehm T, Hauch S, Kimmig R, Kasimir-Bauer S. Stem cell and epithelial-mesenchymal transition markers are frequently overexpressed in circulating tumor cells of metastatic breast cancer patients. *Breast Cancer Res* 2009; **11**: R46.

30 Raimondi C, Gradilone A, Naso G, Vincenzi B, Petracca A, Nicolazzo C *et al.* Epithelial-mesenchymal transition and stemness features in circulating tumor cells from breast cancer patients. *Breast Cancer Res Treat* 2011.

31 Armstrong AJ, Marengo MS, Oltean S, Kemeny G, Bitting RL, Turnbull JD *et al.* Circulating tumor cells from patients with advanced prostate and breast cancer display both epithelial and mesenchymal markers. *Mol Cancer Res* 2011; **9**: 997–1007.

32 Mikolajczyk SD, Millar LS, Tsinberg P, Coutts SM, Zomorrodi M, Pham T *et al.* Detection of EpCAM-negative and cytokeratin-negative circulating tumor cells in peripheral blood. *J Oncol* 2011. doi:10.1155/2011/252361.

33 Mego M, Mani S a, Cristofanilli M. Molecular mechanisms of metastasis in breast cancer--clinical applications. *Nat Rev Clin Oncol* 2010; **7**: 693–701.

34 Wells A, Chao YL, Grahovac J, Wu Q, Lauffenburger DA. Epithelial and mesenchymal phenotypic switchings modulate cell motility in metastasis. *Front Biosci* 2011; **16**: 815–837.

35 Sequist L V, Nagrath S, Toner M, Haber DA, Lynch TJ. The CTC-chip: an exciting new tool to detect circulating tumor cells in lung cancer patients. *J Thorac Oncol* 2009; **4**: 281–3.

36 Lin HK, Zheng S, Williams AJ, Balic M, Groshen S, Scher HI *et al.* Portable Filter-Based Microdevice for Detection and Characterization of Circulating Tumor Cells. *Clin Cancer Res* 2010; : 5011–5018.

37 Hollier BG, Evans K, Mani SA. The epithelial-to-mesenchymal transition and cancer stem cells: a coalition against cancer therapies. *J Mammary Gland Biol Neoplasia* 2009; **14**: 29–43.

38 Abend M. Reasons to reconsider the significance of apoptosis for cancer therapy. *Int J Radiat Biol* 2003; **79**: 927–941.

39 Portugal J, Bataller M, Mansilla S. Cell death pathways in response to antitumor therapy. Tumori. 2009; **95**: 409–421.

40 De Bruin EC, Medema JP. Apoptosis and non-apoptotic deaths in cancer development and treatment response. Cancer Treat. Rev. 2008; **34**: 737–749.

Chapter 5

Adaptation of semi-automated circulating tumor cell assays for clinical and pre-clinical research applications

A version of this chapter has been published:
Lowes LE, Hedley BD, Keeney M, and Allan AL. *J. Vis. Exp.*. 2014; (84):e51248.

Abstract

The majority of cancer-related deaths occur subsequent to the development of metastatic disease. This highly lethal disease stage is associated with the presence of circulating tumor cells (CTCs). These rare cells have been demonstrated to be of clinical significance in metastatic breast, prostate, and colorectal cancers. The current gold standard in clinical CTC detection and enumeration is the U.S. Food and Drug Administration (FDA) and Health Canada-cleared CellSearch® system (CSS). This manuscript outlines the standard protocol utilized by this platform as well as 2 additional adapted protocols that describe the detailed process of user-defined marker optimization for protein characterization of patient CTCs and a comparable protocol for CTC capture in very low volumes of blood, using standard CSS reagents, for studying *in vivo* pre-clinical mouse models of metastasis. In addition, differences in CTC quality between healthy donor blood spiked with cells from tissue culture versus patient blood samples are highlighted. Finally, several commonly discrepant items that can lead to CTC misclassification errors are outlined. Taken together, these protocols will provide a useful resource for users of this platform interested in pre-clinical and clinical research pertaining to metastasis and CTCs.

5.1 Introduction

In 2015 it is estimated that 589,430 individuals will die from cancer and that 1,658,370 new cases of this disease will be diagnosed in the United States alone[1]. The majority of these deaths occur subsequent to the development of metastatic disease[2]. The current lack of effective therapies in treating metastasis and a limited understanding of the metastatic cascade makes this stage of disease highly lethal. The presence of circulating tumor cells (CTCs) within the bloodstream has been demonstrated to correlate with metastatic disease[3]. These cells are extremely rare and their detection is indicative of overall survival in metastatic breast[4], prostate[5], and colorectal[6] cancer. In these patients, the presence of $\geq$5 (breast and prostate) or $\geq$3 (colorectal) CTCs in 7.5mL of blood is indicative of poorer prognosis when compared to those patients with fewer or no detectable CTCs in the same blood volume. In addition, the change in CTC number during or after therapeutic intervention has been demonstrated to be useful as a predictor of treatment response, often sooner than currently utilized techniques[7–10].

It has been estimated that, in metastatic cancer patients, CTCs occur at a frequency of approximately 1 CTC per 10^5-10^7 blood mononuclear cells and in patients with localized disease, this frequency may be even lower (~1 in 10^8). The rare nature of these cells can make it difficult to accurately and reliably detect and analyze CTCs[11]. Several methods (reviewed previously[12–14]) have been utilized to enrich and detect these cells by exploiting properties that differentiate them from surrounding blood components. In general, CTC enumeration is a two-part process that requires both an enrichment step and a detection step. Traditionally, enrichment steps rely on differences in physical properties of CTCs (cell size, density, deformability) or on protein marker expression

(i.e., epithelial cell adhesion molecule [EpCAM], cytokeratin [CK]). Following enrichment, CTC detection can be performed in a number of different ways, the most common of which are nucleic acid-based assays and/or cytometric approaches. Each of these strategies are unique, having distinct advantages and disadvantages, however they all lack standardization; a necessity for entrance into the clinical setting. The CellSearch® system (CSS) was therefore developed to provide a standardized method for the detection and enumeration of rare CTCs in human blood using fluorescence microscopy and antibody-based techniques[4–6]. This platform is currently considered the gold standard in CTC enumeration and is the only technique approved by the U.S. Food and Drug Administration (FDA) and Health Canada for use in the clinic[15].

The CSS is a two component platform consisting of, ***(1)*** the CellTracks™ AutoPrep system (hereafter referred to as the preparation instrument), which automates the preparation of human blood samples, and ***(2)*** the CellTracks™ Analyzer II (hereafter referred to as the analysis instrument), which scans these samples following preparation. The CSS is described previously in *Chapter 2* and *Figure 2.1*.

In addition to providing a standardized method for CTC enumeration, the CSS allows for characterization of CTCs for protein markers that are of interest to the user. This interrogation can be performed at the single-cell level, using a fluorescein isothiocyanate (FITC) fluorescence channel not required for CTC identification[16]. Although this platform is capable of user-defined characterization, the detailed process of protocol development and optimization is not well-defined. Three commercially available markers have been developed by the manufacturer for use with the CSS, epidermal growth factor receptor (EGFR), human epidermal growth factor receptor 2 (HER2), and

insulin-like growth factor 1 receptor (IGF-1R). HER2 analysis, in combination with the CSS, has been utilized by several groups to illustrate the potential for CTC characterization to inform clinical decision-making and to potentially change existing treatment guidelines. For example, Fehm et al., demonstrated that approximately one third of breast cancer patients with $HER2^-$ primary tumors had $HER2^+$ CTCs[17]. In addition, Liu et al., recently reported that up to 50% of patients with HER^+ metastatic breast cancer did not have $HER2^+$ CTCs[18]. Herceptin®, a HER2 recepter interfering monoclonal antibody demonstrated to greatly benefit patients whose tumors express sufficient levels of HER2, is a commonly utilized treatment for patients with $HER2^+$ primary tumors[19–21]. However, these studies suggest that Herceptin® may be being sub-optimally utilized and that CTC characterization may aid in predicting treatment response. Ultimately, CTC characterization may have the potential to improve personalized care.

CTC research is unique in that it has largely utilized a bedside-to-benchtop approach. This method, unlike benchtop-to-bedside research, which can often take years to impact patient care, has allowed CTCs quick entry into the clinical setting. However, physicians are hesitant to use results from CTC analysis in patient treatment decision-making due to a lack of understanding of their underlying biology. Therefore appropriate pre-clinical mouse models of metastasis and complementary CTC analysis techniques must be utilized in order to investigate these outstanding questions. In general, there are 2 types of pre-clinical models used to study the metastatic cascade, ***(1)*** spontaneous metastasis models, which allow for the study of all the steps in the metastatic cascade, and ***(2)*** experimental metastasis models, which only allow for the study of later steps in

the metastatic process such as extravasation and secondary tumor formation[22]. Spontaneous metastasis models involve tumor cell injections into appropriate orthotopic locations (i.e. injection of prostate cancer cells into the prostate gland for the study of prostate cancer). Cells are then given time to form primary tumors and spontaneously metastasize to secondary sites such as the bone, lung, and lymph nodes. In contrast, experimental metastasis models involve direct injection of tumor cells into the bloodstream (i.e. via tail vein or intracardiac injection to target cells to specific locations) and therefore skip the initial steps of intravasation and dissemination to secondary organs[22]. Thus far the majority of CTC enumeration in *in vivo* model systems has been performed using either cytometry-based[23] or adapted human-based CTC techniques (i.e., AdnaTest)[24]. Although useful, none of these techniques adequately reflect CTC enumeration using the gold standard CSS. Based on the clinical approval, standardized nature, and widespread usage of the CSS, the development of a CTC capture and detection technique for *in vivo* modeling that utilizes equivalent sample preparation, processing, and identification criteria would be advantageous as results would be comparable to those obtained from patient samples. However, due to the volume requirements of the preparation instrument it is not possible to process small volumes of blood using this automated platform. In addition, previous work by Eliane et al., (2008) has demonstrated that contamination of samples with mouse epithelial cells (which also meet the standard CTC definition [$EpCAM^{+}CK^{+}DAPI^{+}CD45^{-}$]) can lead to misclassification of mouse squamous epithelial cells as CTCs[25]. To address these issues, an adapted technique that allows the utilization of the CSS CTC kit reagents combined with a manual isolation procedure was developed. The addition of a FITC labeled human

leukocyte antigen (HLA) antibody to the assay allows human tumor cells to be distinguished from mouse squamous epithelial cells.

This manuscript describes the standard, commercially developed and optimized CSS protocol for processing patient blood samples and common pitfalls that may be encountered, including discrepant items that can lead to CTC misclassification errors. In addition, customization of the CSS assay to examine user-defined protein characteristics of captured CTCs and a comparable adapted CSS technique that allows for the enrichment and detection of CTCs from small volumes of blood in pre-clinical mouse models of metastasis are described.

5.2 Materials and methods

5.2.1 Standard CTC enumeration from patient blood samples using the CellSearch® system (CSS)

All human studies described in this manuscript were carried out under protocols #15569E and #16904E approved by Western University's Human Research Ethics Board (*Appendices 1 and 2*). Appropriate handling of human blood samples, including both sample collection and preparation, is critical for efficient CTC enumeration using the CSS. Specifically, using standard aseptic phlebotomy techniques, a minimum of 8.0mL of human blood must be collected into a 10mL CellSave tube (Janssen Diagnostics, Raritan, NJ; hereafter referred to as the CTC preservative tube), which contains ethylenediaminetetraacetic acid (EDTA) and a proprietary cellular preservative. This tube is then inverted a minimum of 5 times to prevent blood from clotting. Samples are then processed immediately or stored at room temperature for up to 96 hours. Immediately prior to sample processing, CSS reagents should be removed from

the fridge and allowed to warm to room temperature. Using a disposable 10mL pipette and automated pipettor, 7.5mL of blood is collected from the CTC preservative tube and slowly dispensed into an appropriately labeled preparation instrument processing tube and 6.5mL of dilution buffer is added to each sample. All samples are then mixed by inversion 5 times and centrifuged at 800 x g for 10 min with the brake in the "off" position.

To ensure appropriate instrument operation, a control sample must be run once each day human samples are processed. Control preparation involves an initial gentle vortex of the control vial, followed by inversion 5 times to mix. The cap from the control vial is then carefully removed and an inverted preparation instrument processing tube is placed on top of the uncapped vial. In one swift motion, the control vial is inverted, and the contents of the vial are poured into the processing tube. While inverted, the sides of the control vial are gently flicked to release any remaining contents. The inverted control vial is then carefully removed from the processing tube, ensuring that no liquid is lost. Using a 1,000µL pipette, any remaining contents from the vial and lid are collected and gently deposited into the processing tube. A single control sample (1 per day) and all human blood samples are then loaded onto the preparation instrument by following the on-screen instructions. Samples must be processed within 1 hour of preparation.

Following batch completion, the on-screen instructions on the preparation instrument are used to unload all samples from the system. Each sample, in a separate cartridge, in a magnetic device, must be tapped on the lab bench to release any bubbles that are stuck to the edges of the cartridge. Once all the bubbles have been removed, the

cartridge must be firmly capped, laid flat, and incubated in the dark for at least 20 minutes. Samples must be scanned within 24 hours of preparation.

Sample scanning is performed on the analysis instrument following lamp initialization. Once warmed (~ 15 minutes), quality control measures are performed by selecting the *QC Test* tab, loading the system verification cartridge, and following the on-screen instructions. Selection of the *Patient Test* tab allows for sample scanning. The system will perform a coarse focus and edge detection on the magnetic device cartridge. Edges should be adjusted as necessary using the directional keys. Following acceptance of the described changes the system will perform a fine focus and begin sample scanning. Validation of control samples must be performed using defined criteria for cells spiked at high ($CK^+DAPI^+CD45^-APC^+$) and low ($CK^+DAPI^+CD45^-FITC^+$) concentrations. Captured CTCs from human blood samples must be reviewed and classified using the defined CTC criteria ($CK^+DAPI^+CD45^-$).

5.2.2 CTC characterization for user-defined markers using the CSS

CTC characterization using the CSS requires specific dilution of the antibody of interest. Specifically, the antibody must be diluted using Bond Primary Antibody Diluent (Leica Biosystems, Concord, ON) to the desired concentration in a marker reagent cup using the formula *(stock concentration = ([working concentration x 850µL] / 150µL))*, where the working concentration is the concentration of the antibody after addition to the sample and the stock concentration is the concentration of antibody in the reagent cup. For multiple samples, antibody volumes need to be adjusted as described in *Table 5.1*. Once diluted the reagent cup is placed in position 1 in the reagent cartridge and loaded onto the CSS.

Table 5.1. Total volume requirements for the CSS when processing various numbers of samples with a user-defined marker.

# of Samples with User Defined Marker Added	Total Volume to Add to Reagent Cup (µl)
1	450
2	600
3	750
4	900
5	1050
6	1200
7	1350
8	1500

**This table has been adapted from the Veridex White Paper (available online: http://www.veridex.com/pdf/CXC_Application_Guideline.PDF.)

Once prepared, human blood samples for which characterization is desired are loaded onto the preparation instrument as described above in section 5.2.1. Selection of *User Defined Assay* on the preparation instrument is required to enable custom marker addition to selected samples. Following batch completion, sample scanning is performed as outlined in section 5.2.1. Initialization of the FITC channel (*Setup* tab --> *CellSearch CTC* --> *CTC Research*) is required for visualization of the marker of interest. Exposure times can be edited as necessary. However, it is recommended that an exposure time of 1.0 sec not be exceeded when using the CSS CTC kit as this can increase bleed-through into other fluorescent channels utilized for CTC identification.

5.2.3 Adaptation of the standard CSS protocol for use in pre-clinical mouse models

This protocol has been adapted from the Veridex Mouse/Rat CellCapture Kit (Veridex; no longer commercially available). Blood collection (minimum of 50µL) is performed from mice previously injected with human tumor cells (orthotopic, tail vein, or intracardiac routes) using a 22 gauge needle, pre-coated with ~30µL of 0.5M EDTA. Collected blood from the saphenous vein (for serial CTC analysis) or by cardiac puncture (for terminal CTC analysis) is dispensed, following removal of the needle, into a 1mL EDTA microtainer blood collection tube and mixed by inversion to prevent clotting. Blood may be processed immediately or stored at room temperature for up to 48 hours following the addition of an equal volume of CytoChex cellular preservative (Streck, Omaha, NE).

Immediately prior to processing, the CSS reagents must be removed from the fridge and allowed to warm to room temperature. The equivalent of 50µL of whole blood is then transferred to a 12x75 mm flow cytometry (FCM) tube and 500µL of

dilution buffer (Janssen Diagnostics, CellSearch CTC kit) is added to each sample, washing down any blood that remains on the sides of the tube. If necessary, a short centrifuge spin can be used to collect any remaining blood. Following a gentle vortex, 25µL of anti-EpCAM ferrofluid (Janssen Diagnostics, CellSearch CTC kit) is added to each sample by placing the tip of the pipette directly into the sample. Next, 25µL of Capture Enhancement reagent (Janssen Diagnostics, CellSearch CTC kit) is added to each sample, followed by a gentle vortex to mix. Samples are then incubated at room temperature for 15 min and subsequently placed into a magnet for 10 min. While still in the magnet, residual liquid and unlabelled cells are carefully aspirated, without touching the wall of the tube, using a glass pipette and discarded.

Sample tubes are then removed from the magnet and resuspended in 50µL of Nucleic Acid Dye (Janssen Diagnostics, CellSearch CTC kit), 50µL of Staining Reagent (Janssen Diagnostics, CellSearch CTC kit), 1.5µL of anti-mouse CD45-APC (eBioscience, San Diego, CA), 5.0µL of anti-human HLA-AlexaFluor488 (BioLegend, San Diego, CA) and 100µL of Permeabilization Reagent (Janssen Diagnostics, CellSearch CTC kit). For multiple samples, these reagents may be pre-mixed and 206.5µL of this mixture may be added to each tube. Following a gentle vortex, each sample is incubated for 20 min at room temperature. Dilution buffer (500µL) is then added and the samples are placed into a magnet and incubated for 10 min. While still in the magnet, a glass pipette is used to carefully aspirate the residual liquid and unlabelled cells. Finally, the sample is resuspended in 350µL of dilution buffer and the entire volume is carefully transferred into a cartridge in the magnetic device, starting at the bottom and slowly withdrawing the tip as the sample is dispensed. Once loaded, the

cartridge must be firmly capped as described in section 5.2.1. Bubbles may interfere with sample scanning and therefore should be popped using a sterile 22 gauge needle prior to capping. Samples must be incubated in the dark for at least 10 minutes and scanned within 24 hours of preparation. Prior to sample scanning any existing data on the magnetic device must be cleared using the *Format Sample* button under the *Setup* tab. Sample information must then be input using the *Edit* button on the *Patient Test* tab and samples can be scanned, following initialization of the FITC channel (exposure time set to 1.0 sec), as described in section 5.2.1.

5.3 Results

5.3.1 Standard circulating tumor cell enumeration assay

The sensitivity and specificity of the CSS has been well documented in the literature[26]. However, to validate equivalent CTC recovery, spiked (1,000 LNCaP human prostate cancer cells) and unspiked human blood samples from healthy volunteer donors were processed on the CSS using the standard CSS CTC protocol. As expected, unspiked samples were free of CTCs, 0.00±0.00%, and CTC recovery was demonstrated to be 86.9±4.71% for spiked samples (*Figure 5.1A*). CSS gallery images obtained from spiked samples were of optimal quality and CTCs were easy to distinguish from non-CTCs. However, when processing samples obtained from cancer patients, identification of CTCs is slightly more challenging, with many cells appearing smaller in size and being less easily distinguishable from non-CTCs (*Figure 5.1B*). In addition, when reviewing patient samples 6 categories of events were identified that were commonly discrepant items between reviewers (*Figure 5.1C*). These 6 categories included, ***(1)*** small events that did

Figure 5.1. CTC enumeration and interpretation using the standard CellSearch® system (CSS) protocol. ***(A)*** CTC recovery measured as a percentage of the number of spiked cells. Cells were counted by hemocytometer and ~1,000 LNCaP human prostate cancer cells were spiked into 7.5ml of human blood. Unspiked human blood samples were used as a negative control (n=3). Data are presented as the mean ± SEM. ***(B)*** Representative CSS gallery images of the differences in CTC quality observed in spiked blood samples (i.e., healthy donor blood spiked with tumor cells from culture) versus samples collected from cancer patients. ***(C)*** Representative CSS gallery images of commonly discrepant items that are often misclassified. Orange squares indicate acceptable CTCs, identified as $CK^{+}/DAPI^{+}/CD45^{-}$. Images acquired at 10x objective magnification.

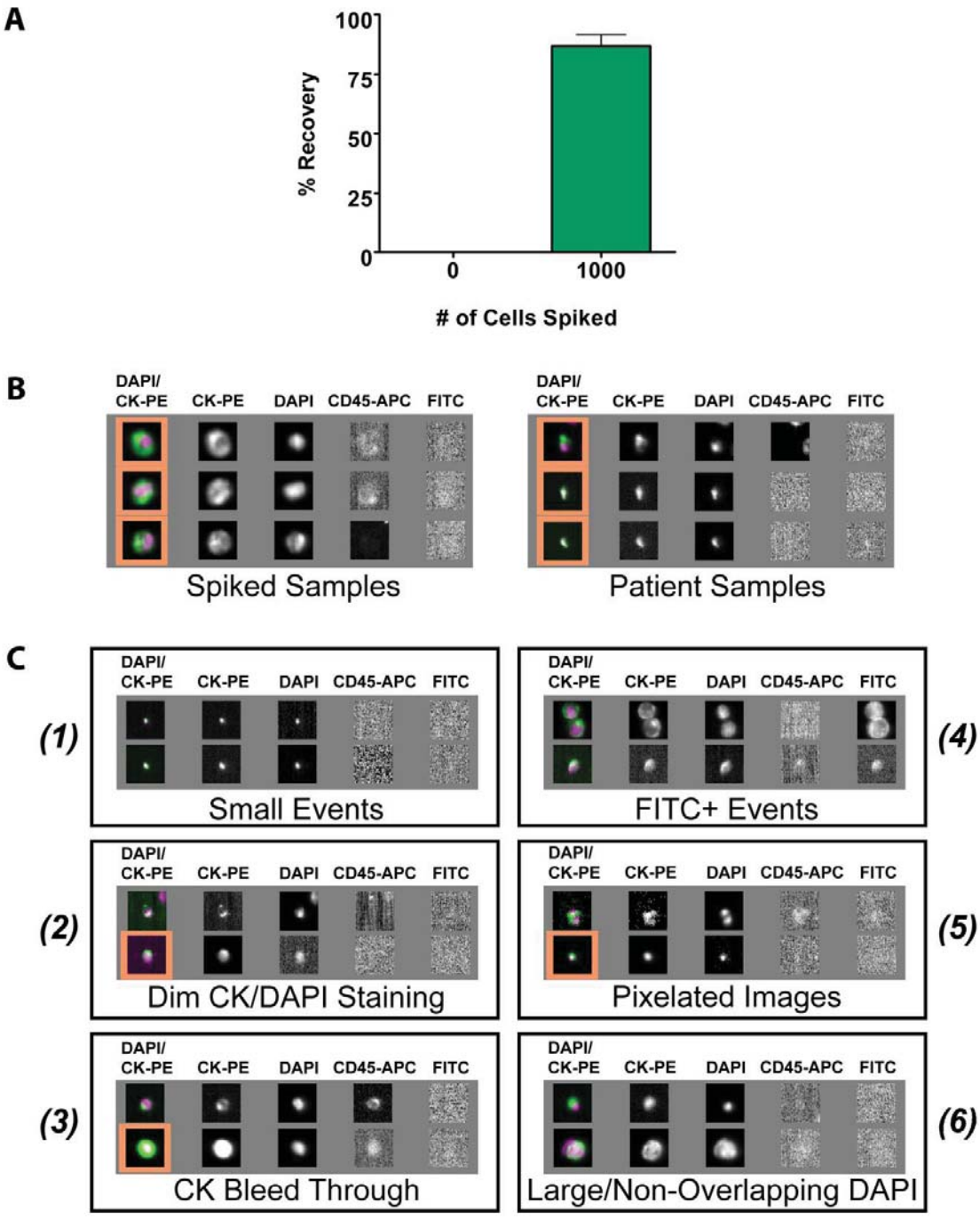
A
100
75
50
25
0
% Recovery
0
1000
# of Cells Spiked
B
DAPI/ CK-PE
CK-PE
DAPI
CD45-APC
FITC
Spiked Samples
Patient Samples
C
(1)
Small Events
(2)
Dim CK/DAPI Staining
(3)
CK Bleed Through
(4)
FITC+ Events
(5)
Pixelated Images
(6)
Large/Non-Overlapping DAPI

not meet the 4 μm size requirement for CTC classification; ***(2)*** items with dim CK and/or DAPI staining; ***(3)*** justified (should be counted as a CTC) versus unjustified (should not be counted as a CTC) bleed through into the CD45-APC channel caused by bright CK-PE staining; ***(4)*** $FITC^+$ events; ***(5)*** pixelated images in the CK and/or DAPI channels; and ***(6)*** events with DAPI staining that is larger than CK images or those with DAPI staining that does not overlap >50% with the CK image. For categories ***(2)*** and ***(5)*** specific criteria exist for CTC classification. For category ***(2)***, items with dim CK/DAPI can be classified as CTCs provided that an intact membrane can be observed in the CK channel and an appropriately sized DAPI image is noted. For category ***(5)***, items with pixelated CK/DAPI cannot be classified as CTCs if *any* pixelation is observed in the CK channel. However, pixelation is acceptable in the DAPI channel provided that it is not too severe (i.e., image is entirely white on a background, no grey areas—described by Janssen Diagnostics as white paint on a black background) or diffuse (must still appear oval in shape and fit within the CK).

5.3.2 User-defined marker assay development

Adaptation of the CSS to characterize CTCs for user-defined markers requires significant work-up with rigorous controls and has been described previously[16]. As a general rule, appropriate optimization of any user-defined marker requires that negative controls be employed to ensure that results are specific. The best results are obtained when spiked samples are processed with both a non-specific IgG control in place of the target antibody and with the antibody diluent alone as described previously. Various target antibody concentrations and exposure times should also be assessed and validated using cell lines with high, low, and absent (negative) antigen densities. Optimal protocol

conditions are achieved when the assay demonstrates both high sensitivity for the target antigen and low background noise from non-specific binding[16].

An example of this work-up using a CSC marker, CD44, is presented here. Initial testing with this marker began using the standard CSS CTC kit (hereafter referred to as the traditional CTC kit), which utilizes the FITC channel for user-defined marker development. Using the traditional CTC kit, it was demonstrated that, after significant optimization, the maximum number of CTCs that could be classified as $CD44^+$ was 69.3±2.67% using samples spiked with 1,000 MDA-MB-468 human breast cancer cells, known to demonstrate high CD44 expression with the majority of cells (98.4±0.90%; as determined by FCM expressing this protein (*Figure 5.2A*). Based upon these findings it was hypothesized that the commercially available CSS CXC kit might produce improved results. This kit allows for improved visualization of markers with a lower antigen density (~50,000 antigens/cell) compared with the traditional CTC kit (optimized for markers with a density of ~100,000 antigens/cell) by reversing the fluorescence channel in which the CK8/18/19 (traditionally represented in the PE channel) and the user's marker of interest (traditionally represented in the FITC channel) are represented (therefore hereafter the CXC kit will be referred to as the low antigen density CTC kit)[27]. After significant optimization, it was demonstrated that this change allowed for improved CD44 staining, with 98.8±0.51% of CTCs classified as $CD44^+$ using CD44-PE at a concentration of 1.0µg/mL and an exposure time of 0.6s (*Figure 5.2A*)**.** Appropriate optimization of any user-defined marker also requires validation using high antigen density (MDA-MB-468), low antigen density (21NT), and negative (LNCaPs) cell lines for the marker of interest (*Figure 5.2B*).

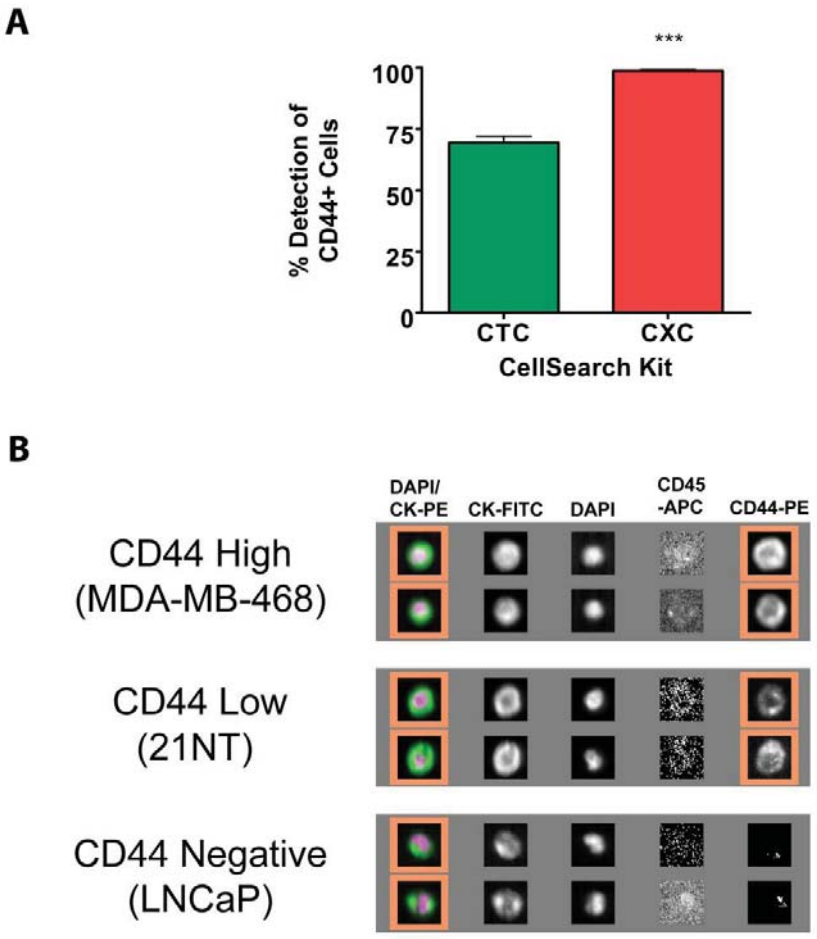

Figure 5.2. Characterization of CTCs for user-defined markers using the CSS. **(A)** Percentage of cells classified as CD44+ using the CTC and CXC kits on the CSS (n=3). Data are presented as the mean ± SEM. *** = significantly different ($P < 0.0005$). **(B)** Representative CSS gallery images of blood from a healthy volunteer donor (7.5ml), spiked with ~1,000 cells from the identified cell line, incubated with 1.5µg/ml of anti-CD44-PE, and scanned at an exposure time of 0.2s. Orange squares indicate $CD44^+$ CTCs, identified as $CK^+/DAPI^+/CD45^-/CD44\text{-}PE^+$.

5.3.3 Circulating tumor cell analysis in pre-clinical mouse models

To determine the sensitivity and specificity of the adapted mouse CSS protocol, spiked (1,000 LNCaP human prostate cancer cells) and unspiked mouse blood samples were processed manually and scanned on the analysis instrument and compared to results obtained using the same cell line processed using the standard automated CSS protocol on the preparation instrument (*Figure 5.3A*). As expected, unspiked samples were free of CTCs using both assays, 0.00±0.00% and CTC recovery using the adapted mouse kit (90.8±5.18%) was not significantly different from results obtained using the standard automated system (86.9±4.71%; $p > 0.05$). Images obtained using the manual mouse adapted protocol did not differ from those observed using the standard automated technique, with the exception of the addition of the HLA-FITC marker. In addition, mouse squamous epithelial cells do not stain positively for HLA-FITC (*Figure 5.3B*). To confirm that this technique was as sensitive as the standard CSS protocol for the isolation of low number of CTCs, serial dilutions were performed with spiked blood samples and the correlation of expected number of cells versus recovered number of cells was assessed (*Figure 5.3C*). Results demonstrate that CTCs could effectively be recovered down to a sensitivity of 5 cells per 50µL of whole blood using this assay. These values correlated with expected results with an $r^2 = 0.99$.

5.4 Discussion

Despite the development of many new CTC technologies since the introduction of the CSS in 2004, this technique is still the only clinically approved technology on the market today and therefore it is considered the current gold standard for CTC detection

Figure 5.3. Adaptation of the CSS procedure for use in pre-clinical mouse models of metastasis. ***(A)*** CTC recovery using the adapted mouse CSS protocol measured as a percentage of the number of spiked cells and compared to results obtained using the standard human CSS protocol. Cells were counted by hemocytometer and ~1,000 LNCaP human prostate cancer cells were spiked into 7.5ml of human blood. Unspiked human blood samples were used as a negative control (n=3). Data are presented as the mean ± SEM. ns = not significant. ***(B)*** Representative CSS gallery images of CTCs captured the adapted mouse CSS protocol demonstrating that HLA-AF488 is able to distinguish human from mouse cells. ***(C)*** Analysis of correlation and linear regression of the expected versus recovered number of spiked tumor cells at various concentrations. LNCaP human prostate cancer cells were initially counted by hemocytometer and subsequently spiked into mouse blood at a concentration of ~1,000 tumor cells/50µl of blood. Spiked mouse blood was then serially diluted to a concentration of 5 tumor cells/50µl and processed using the mouse adapted CSS protocol (n=3).

A

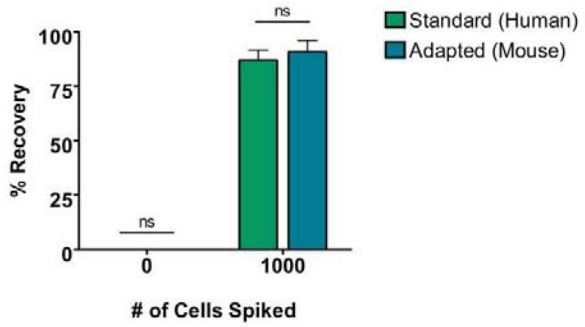
ns
Standard (Human)
Adapted (Mouse)
100
75
50
25
0
% Recovery
ns
0
1000
# of Cells Spiked

B

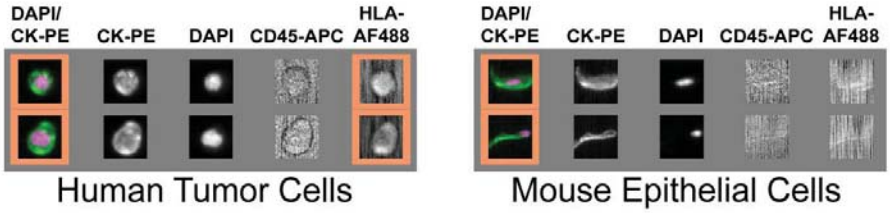
DAPI/ CK-PE
CK-PE
DAPI
CD45-APC
HLA- AF488
Human Tumor Cells
DAPI/ CK-PE
CK-PE
DAPI
CD45-APC
HLA- AF488
Mouse Epithelial Cells

C

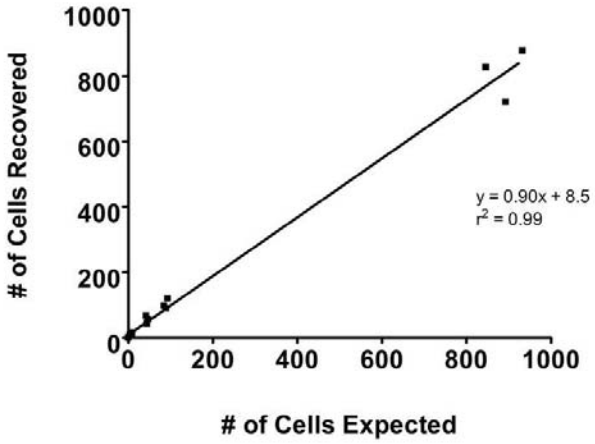
1000
800
600
400
200
0
# of Cells Recovered
y = 0.90x + 8.5
r2 = 0.99
0
200
400
600
800
1000
# of Cells Expected

and enumeration. This manuscript has demonstrated that although the CSS has rigorous quality control standards it can be subject to interpretation bias and that CTC identification in patient samples is much different from identification in spiked samples. Six categories of commonly discrepant items were identified that can cause CTC misclassifications to occur. These discrepant items highlight the need for multiple reviewers on each patient sample processed on this instrument. In addition, the differences observed in spiked versus patient obtained CTCs demonstrates that there is a necessity for any new CTC technologies to be validated in both spiked and patient samples. In addition, these new technologies must be compared to the gold standard CSS using split sample testing of both spiked and patient samples, as efficient CTC capture from spiked samples only does not necessarily reflect CTC capture efficiency in patient samples.

Although the CSS has the capability to perform characterization of captured CTCs, it is quite restricted with regards to highly customizable optimization. In general, the only parameters that can be changed on this instrument for optimization of user-defined markers are the antibody concentration and the length of time that the fluorophore is exposed to the mercury lamp. This limited capacity for optimization can present problems when working-up user-defined markers on the CSS. One solution proposed in this manuscript (described in detail previously[16]) is the use of the low antigen density CTC kit which switches the FITC and PE fluorescent channels allowing for better visualization of markers with a low antigen density. Regardless of which kit is utilized (traditional- or low antigen density CTC kit) there are several necessary steps that must be undertaken to ensure appropriate marker sensitivity, specificity, and optimization.

First, assay sensitivity must be assessed in comparison to a well validated method, such as FCM, that will allow determination of the expected detection level (i.e., the % of cells in the cell population that express the marker of interest) of the user-defined marker[16]. Secondly, the assay must be assessed for its ability to detect the marker of interest in cell lines with various levels of expression (i.e., high and low antigen densities) and its specificity must be validated in a cell line that is negative for the marker of interest. In all cases, all cell lines must be tested using a cells only control (no antibody added), the appropriate IgG control, and the antibody of interest at various concentrations and exposure times to determine the most appropriate settings that will ensure optimization of the user-defined marker. However, it should be noted that although characterization of CTCs is possible on the CSS, currently only one user-defined marker of interest can be explored in each sample, and that the system is very limited with regards to downstream applications due to the harsh processing of the samples.

The unique bedside-to-benchtop approach utilized in CTC research has allowed for quick entry of this useful assay into the clinical setting. However, it has resulted in an inadequate understanding of the basic biology of these rare cells. Therefore the development and optimization of assays that allow for assessment of CTCs in pre-clinical *in vivo* mouse models of cancer are needed. This manuscript describes an adapted CSS protocol that allows for CTCs to be assessed in 50μL volumes of mouse blood, ideally suited for serial CTC collection experimentation. This manuscript demonstrates that CTC enumeration using this protocol is comparable to results obtained using the CSS in combination with the traditional CTC kit, with no significant differences in CTC capture efficiency between the automated and manual separation techniques. In addition,

during the development of this assay it was recognized, as previously described in the literature[25], that mouse squamous epithelial cell contamination can make accurate identification of CTCs more difficult and sometimes impossible. Therefore to combat this issue a user-defined HLA-AlexaFluor488 was added to this protocol to ensure that only human cells ($CK^{+}DAPI^{+}CD45^{-}$HLA-$AlexaFluor488^{+}$) are being appropriately assigned as CTCs. It is important to note that the LNCaP cell line used in this manuscript is HLA^{low} and therefore HLA-AlexaFluor488 may need to be titrated for cell lines with varying HLA expression. Although we have added an HLA-AlexaFluor 488 to our protocol to ensure accurate identification of CTCs, it is noteworthy that the vast majority of mouse squamous epithelial cells were easily identifiable by morphology and were limited in cell number. Higher cell numbers were only observed when blood collection, via cardiac puncture, proved difficult and repeated attempts were necessary. Therefore we propose that if desired, on-system characterization of CTCs could be accomplished by omitting this marker. In addition, although not described here, we anticipate that downstream characterization could be easily achieved as demonstrated previously[28,29].

Although the CSS has been utilized clinically to effectively detect CTCs in the blood of metastatic breast, prostate and colorectal cancer patients[4,30,10], it does have several limitations. In up to 35% of patients with various metastatic cancers, CTCs are undetectable despite the presence of widespread systemic disease[26]. This lack of detection has been proposed to be as a result of the epithelial-to-mesenchymal transition (EMT), a well-documented process known to enhance cancer invasion, metastasis, and overall aggressiveness[31]. This transition has been associated with a significant reduction in epithelial markers, such as EpCAM, and a corresponding increase in mesenchymal

markers[32]. Several studies have recently demonstrated that the presence of these mesenchymal markers in CTCs are predictive of poorer prognosis and that many of these cells lack expression of epithelial markers that would be necessary for their detection using the CSS[24,33–38]. This suggests that the standard CSS definition may be missing some of the most aggressive CTCs.

Despite these limitations, it is anticipated the protocols described in this manuscript will be important tools for improved CTC analysis using the CSS, development of novel CTC technologies, optimization of user-defined markers, and improved understanding of CTC biology using *in vivo* pre-clinical mouse models. Taken together, these protocols will provide a useful resource for users of this platform interested in pre-clinical and clinical research pertaining to metastasis and CTCs.

5.5 References

1 Siegel RL, Miller KD, Jemal A. Cancer statistics, 2015. *CA Cancer J Clin* 2015. doi:10.3322/caac.21254.

2 Chambers AF, Groom AC, MacDonald IC. Dissemination and growth of cancer cells in metastatic sites. *Nat Rev Cancer* 2002; **2**: 563–72.

3 Pantel K, Brakenhoff RH. Dissecting the metastatic cascade. *Nat Rev Cancer* 2004; **4**: 448–56.

4 Cristofanilli M, Budd GT, Ellis MJ, Stopeck A, Matera J, Miller MC *et al.* Circulating tumor cells, disease progression, and survival in metastatic breast cancer. *N Engl J Med* 2004; **351**: 781–91.

5 De Bono JS, Scher HI, Montgomery RB, Parker C, Miller MC, Tissing H *et al.* Circulating tumor cells predict survival benefit from treatment in metastatic castration-resistant prostate cancer. *Clin Cancer Res* 2008; **14**: 6302–9.

6 Cohen SJ, Punt CJ a, Iannotti N, Saidman BH, Sabbath KD, Gabrail NY *et al.* Prognostic significance of circulating tumor cells in patients with metastatic colorectal cancer. *Ann Oncol* 2009; **20**: 1223–9.

7 Hayes DF, Cristofanilli M, Budd GT, Ellis MJ, Stopeck A, Miller MC *et al.* Circulating tumor cells at each follow-up time point during therapy of metastatic breast cancer patients predict progression-free and overall survival. *Clin Cancer Res* 2006; **12**: 4218–24.

8 Budd GT, Cristofanilli M, Ellis MJ, Stopeck A, Borden E, Miller MC *et al.* Circulating tumor cells versus imaging--predicting overall survival in metastatic breast cancer. *Clin Cancer Res* 2006; **12**: 6403–9.

9 Olmos D, Arkenau H-T, Ang JE, Ledaki I, Attard G, Carden CP *et al.* Circulating tumour cell (CTC) counts as intermediate end points in castration-resistant prostate cancer (CRPC): a single-centre experience. *Ann Oncol* 2009; **20**: 27–33.

10 De Bono JS, Scher HI, Montgomery RB, Parker C, Miller MC, Tissing H *et al.* Circulating tumor cells predict survival benefit from treatment in metastatic castration-resistant prostate cancer. *Clin Cancer Res* 2008; **14**: 6302–9.

11 Allan AL, Keeney M. Circulating tumor cell analysis: technical and statistical considerations for application to the clinic. *J Oncol* 2010; **2010**: 426218.

12 Lowes LE, Goodale D, Keeney M, Allan AL. Image cytometry analysis of circulating tumor cells. *Methods Cell Biol* 2011; **102**: 261–90.

13 Alix-Panabières C, Pantel K. Circulating tumor cells: liquid biopsy of cancer. *Clin Chem* 2013; **59**: 110–8.

14 Lianidou ES, Markou A. Circulating tumor cells in breast cancer: detection systems, molecular characterization, and future challenges. *Clin Chem* 2011; **57**: 1242–55.

15 Parkinson DR, Dracopoli N, Petty BG, Compton C, Cristofanilli M, Deisseroth A *et al.* Considerations in the development of circulating tumor cell technology for clinical use. *J Transl Med* 2012; **10**: 138.

16 Lowes LE, Hedley BD, Keeney M, Allan AL. User-defined protein marker assay development for characterization of circulating tumor cells using the CellSearch® system. *Cytometry A* 2012; **81**: 983–95.

17 Fehm T, Müller V, Aktas B, Janni W, Schneeweiss A, Stickeler E *et al.* HER2 status of circulating tumor cells in patients with metastatic breast cancer: a prospective, multicenter trial. *Breast Cancer Res Treat* 2010; **124**: 403–12.
18 Liu Y, Liu Q, Wang T, Bian L, Zhang S, Hu H *et al.* Circulating tumor cells in HER2-positive metastatic breast cancer patients: a valuable prognostic and predictive biomarker. *BMC Cancer* 2013; **13**: 202.
19 Slamon DJ, Leyland-Jones B, Shak S, Fuchs H, Paton V, Bajamonde A *et al.* Use of chemotherapy plus a monoclonal antibody against HER2 for metastatic breast cancer that overexpresses HER2. *N Engl J Med* 2001; **344**: 783–92.
20 Marty M, Cognetti F, Maraninchi D, Snyder R, Mauriac L, Tubiana-Hulin M *et al.* Randomized phase II trial of the efficacy and safety of trastuzumab combined with docetaxel in patients with human epidermal growth factor receptor 2-positive metastatic breast cancer administered as first-line treatment: the M77001 study group. *J Clin Oncol* 2005; **23**: 4265–74.
21 Slamon D, Eiermann W, Robert N, Pienkowski T, Martin M, Press M *et al.* Adjuvant trastuzumab in HER2-positive breast cancer. *N Engl J Med* 2011; **365**: 1273–83.
22 Welch DR. Technical considerations for studying cancer metastasis in vivo. *Clin Exp Metastasis* 1997; **15**: 272–306.
23 Goodale D, Phay C, Postenka CO, Keeney M, Allan AL. Characterization of tumor cell dissemination patterns in preclinical models of cancer metastasis using flow cytometry and laser scanning cytometry. *Cytometry A* 2009; **75**: 344–55.
24 Gorges TM, Tinhofer I, Drosch M, Röse L, Zollner TM, Krahn T *et al.* Circulating tumour cells escape from EpCAM-based detection due to epithelial-to-mesenchymal transition. *BMC Cancer* 2012; **12**: 178.
25 Eliane J-P, Repollet M, Luker KE, Brown M, Rae JM, Dontu G *et al.* Monitoring serial changes in circulating human breast cancer cells in murine xenograft models. *Cancer Res* 2008; **68**: 5529–32.
26 Allard WJ, Matera J, Miller MC, Repollet M, Connelly MC, Rao C *et al.* Tumor cells circulate in the peripheral blood of all major carcinomas but not in healthy subjects or patients with nonmalignant diseases. *Clin Cancer Res* 2004; **10**: 6897–904.
27 Veridex White Pages. Available at: http://www.veridex.com/pdf/CXC_Application_Guideline.PDF. 2008.
28 Flores LM, Kindelberger DW, Ligon a H, Capelletti M, Fiorentino M, Loda M *et al.* Improving the yield of circulating tumour cells facilitates molecular characterisation and recognition of discordant HER2 amplification in breast cancer. *Br J Cancer* 2010; **102**: 1495–502.
29 Sieuwerts AM, Kraan J, Bolt-de Vries J, van der Spoel P, Mostert B, Martens JWM *et al.* Molecular characterization of circulating tumor cells in large quantities of contaminating leukocytes by a multiplex real-time PCR. *Breast Cancer Res Treat* 2009; **118**: 455–68.
30 Cohen SJ, Punt CJ a, Iannotti N, Saidman BH, Sabbath KD, Gabrail NY *et al.* Relationship of circulating tumor cells to tumor response, progression-free

survival, and overall survival in patients with metastatic colorectal cancer. *J Clin Oncol* 2008; **26**: 3213–21.

31 Thiery JP, Acloque H, Huang RYJ, Nieto MA. Epithelial-mesenchymal transitions in development and disease. *Cell* 2009; **139**: 871–90.

32 Yang J, Weinberg R a. Epithelial-mesenchymal transition: at the crossroads of development and tumor metastasis. *Dev Cell* 2008; **14**: 818–29.

33 Gradilone A, Raimondi C, Nicolazzo C, Petracca A, Gandini O, Vincenzi B *et al.* Circulating tumour cells lacking cytokeratin in breast cancer: the importance of being mesenchymal. *J Cell Mol Med* 2011; **15**: 1066–70.

34 Königsberg R, Obermayr E, Bises G, Pfeiler G, Gneist M, Wrba F *et al.* Detection of EpCAM positive and negative circulating tumor cells in metastatic breast cancer patients. *Acta Oncol* 2011; **Epub**: Epub.

35 Kasimir-Bauer S, Hoffmann O, Wallwiener D, Kimmig R, Fehm T. Expression of stem cell and epithelial-mesenchymal transition markers in primary breast cancer patients with circulating tumor cells. *Breast Cancer Res* 2012; **14**: R15.

36 Mego M, Mani SA, Lee B-N, Li C, Evans KW, Cohen EN *et al.* Expression of epithelial-mesenchymal transition-inducing transcription factors in primary breast cancer: The effect of neoadjuvant therapy. *Int J Cancer* 2011; **Epub**: Epub.

37 Yu M, Bardia A, Wittner BS, Stott SL, Smas ME, Ting DT *et al.* Circulating breast tumor cells exhibit dynamic changes in epithelial and mesenchymal composition. *Science* 2013; **339**: 580–4.

38 Armstrong AJ, Marengo MS, Oltean S, Kemeny G, Bitting RL, Turnbull JD *et al.* Circulating tumor cells from patients with advanced prostate and breast cancer display both epithelial and mesenchymal markers. *Mol Cancer Res* 2011; **9**: 997–1007.

Chapter 6

Role of epithelial-to-mesechymal transition on circulating tumor cell generation and metastasis in prostate cancer

This chapter has been prepared for peer review:
Lowes LE, Goodale, D., Xia, Y., Postenka, C., Piaseczny, M., Paczkowski, F., and Allan AL. In preparation for *Clinical Cancer Research*.

Abstract

Metastatic disease is responsible for the majority of prostate cancer (PCa) deaths and is associated with the presence of circulating tumor cells (CTCs). Detection of ≥5 CTCs/7.5mL of blood predicts for poor prognosis in metastatic PCa. The U.S. Food and Drug Administration (FDA) and Health Canada-cleared CellSearch® system (CSS) is the current gold standard for CTC enumeration. However, using the CSS ~35% of metastatic PCa patients have undetectable CTCs, which may result from the epithelial-to-mesenchymal transition (EMT) and subsequent loss of necessary CTC detection markers. Although valuable clinically, little is known about the biology of CTCs, due in large part to a lack of appropriate CTC analysis tools in pre-clinical models of metastasis. In the current study, we have developed two pre-clinical assays for assessing human CTCs in xenograft mouse models of metastasis; one that is comparable to the EpCAM-based CSS (dependent on EMT status) and one that detects CTCs semi-independent of EMT status based on capture with EpCAM and HLA (human leukocyte antigen). Using mouse blood spiked with PCa cell lines with varying epithelial (LNCaP and LNCaP C4-2B) and mesenchymal (PC-3 and PC-3M) phenotypes, we demonstrate that the EpCAM-based assay (comparable to the CSS) is unable to detect a significant number (~40-50%) of mensechymal CTCs. *In vivo* analysis demonstrates that cell lines with an increasingly mesenchymal phenotype shed a greater number of CTCs, and that these cells are shed more quickly and have a greater metastatic capacity than cell lines with an epithelial phenotype. Interestingly, the EpCAM-based CSS appears to capture the majority of CTCs shed during the early-stages of disease, and it is only after the establishment of metastases that a significant number of undetectable CTCs are shed into the circulation. Overall these results provide a better understanding of the role of the EMT in CTC generation and metastasis. In addition, this study also highlights that the pursuit of novel technologies aimed at capturing CTCs that are currently presumed to be undetectable may only be useful in the metastatic setting.

6.1 Introduction

Prostate cancer (PCa) is the most commonly diagnosed cancer and third most common cause of cancer death in Canadian men[1]. The majority of PCa deaths result from the development of metastatic disease, due to a lack of effective treatment options for patients with metastases. During the metastatic cascade, tumor cells disseminate from the primary site (i.e., prostate) to distant locations throughout the body via the bloodstream[2]. The presence of circulating tumor cells (CTCs) in the blood correlates with metastatic disease and the enumeration of these rare cells has been demonstrated to be an indicator of overall survival[3–6]. In metastatic PCa patients, the detection of ≥5 CTCs/7.5ml of blood is indicative of poorer progression-free and overall survival compared to patients with <5 CTCs in the same blood volume[6]. In addition, changes in CTC number throughout the course of treatment have been demonstrated to be indicative of treatment success[7].

Due to the rare nature of CTCs (~1 CTC per 10^5-10^7 blood mononuclear cells in a metastatic patient) extremely sensitive technologies are required in order to accurately and reliably detect these cells[8]. Several techniques have been utilized to detect CTCs, including polymerase chain reaction (PCR)-based assays[9,10], density-gradient centrifugation[11,12], and flow cytometry (FCM)[13–15] techniques. All of these techniques have unique advantages and disadvantages, however all of these techniques lack standardization, a necessity for use in the clinical setting. The development of the CellSearch® system (CSS) by Janssen Diagnostics provides a standardized method for the sensitive detection and quantification of these rare CTCs in human blood using fluorescence microscopy and immunology based techniques[4,6,5]. The CSS is also the only

CTC technology currently approved by the U.S.FDA (Food and Drug Administration) and Health Canada for clinical management of metastatic PCa (as well as metastatic breast and colorectal cancers) and therefore it is considered the current gold standard in CTC technology.

The CSS distinguishes CTCs from contaminating leukocytes by first selecting for cells with an $EpCAM^+$ (epithelial cell adhesion molecule) phenotype and subsequently performing differential fluorescent staining with cytokeratins (CK) 8/18/19 (CK), CD45 (leukocyte marker), and DAPI. CTCs identified by this assay are thus defined as cells with an $EpCAM^+/CK^+/DAPI^+/CD45^-$ phenotype. Therefore CTC detection using the CSS is not based on the expression of tumor-specific markers, but instead on the expression of epithelial-specific markers (EpCAM and CK), thereby only allowing it to capture CTCs from tumors of epithelial origin (i.e., carcinomas).

Although the CSS has been utilized clinically to effectively detect CTCs in the blood of metastatic PCa patients[6], in up to 35% of patients CTCs are undetectable despite the presence of widespread systemic disease[16]. This suggests one of two things, either *(1)* CTCs are truly not present in ~1/3 of patients with metastatic disease or *(2)* CTCs are present but are undetectable by the CSS as they do not meet the standard definition of CTCs ($EpCAM^+/CK^+/DAPI^+/CD45^-$). This lack of detection has been proposed to be as a result of the epithelial-to-mesenchymal transition (EMT), a process first described in the setting of embryogenesis that is now being explored for its contribution to the metastatic spread of various cancers of epithelial origin[17–19]. EMT has been demonstrated to result in a significant reduction in various epithelial markers (EpCAM and E-cadherin), some of which are necessary for CTC capture and enumeration[17,20,21]. In addition to a reduction in

epithelial marker expression, EMT also results in a corresponding increase in mesenchymal marker expression (N-cadherin and vimentin), and in doing so, has been well documented for its role in enhancing cancer invasion, metastasis, and overall disease aggressiveness[17,18]. This therefore suggests that the standard CSS definition of CTCs may be missing some of the most invasive and highly metastatic cells in the bloodstream and that the capture and subsequent characterization of these CTCs with an increasingly mesenchymal phenotype may be more informative then those with a purely epithelial phenotype. In fact, several studies have recently demonstrated that CTCs with a purely mesenchymal phenotype are undetectable by the CSS, but that the presence of mesenchymal marker expression on CTCs with a hybrid phenotype is predictive of poorer prognosis[20,22–27]. This suggests that current technology may be limiting our ability to capitalize on the full potential of CTCs and that a greater understanding of CTC biology is necessary in guiding future research.

The unique bedside-to-bench approach utilized in the field of CTC research has allowed for quick entry of this technology into the clinic. However, outstanding questions regarding the biology of these rare cells has resulted in a hesitance in utilizing this information to direct patient care. Unfortunately appropriate tools needed to address these outstanding questions are lacking and therefore appropriate mouse models and complementary CTC analysis techniques are necessary in order to move this field of study forward. Previous work on CTC biology in our laboratory has shown that CTC dissemination appears to occur at relatively early time points in the metastatic cascade and that CTCs may also be generated by metastases in an orthotopic mouse model of

breast cancer metastasis[28,29]. However, very little is currently known about the role of EMT in CTC dissemination patterns and metastasis.

In the current study, we have developed two pre-clinical assays for assessing human CTCs in xenograft mouse models of metastasis; one that is comparable to the EpCAM-based CSS (dependent on EMT status) and one that detects CTCs semi-independent of EMT status based on capture with EpCAM and HLA (human leukocyte antigen). Using these assays, differences in CTC capture efficiency and kinetics *in vivo* was assessed using 4 prostate cancer cell lines (LNCaP, LNCaP C4-2B, PC-3, and PC-3M) with varying EMT phenotypes. Additionally, primary tumor formation and metastatic dissemination was compared for each investigated cell line. The novel results presented here provide a better understanding of CTC biology and may shed light on which CTCs are the most important to study and characterize, thereby guiding strategies on how to utilize CTCs most effectively in a clinical setting.

6.2 Materials and methods

6.2.1 Cell culture and reagents

LNCaP[30] (ATCC, Manassas, VA) and PC-3M[31] (a kind gift from Dr. Paula Foster, Western University, London, ON) human prostate cancer cell lines were maintained in RPMI-1640 + 10% fetal bovine serum (FBS). LNCaP C4-2B[32] human prostate cancer cells (a kind gift from Dr. Katherine Stemke Hale, M.D. Anderson Cancer Center, Houston, TX) were maintained in T-media + 10% heat-inactivated FBS. PC-3[33] human prostate cancer cells (ATCC, Manassas, VA) were maintained in F12K media + 10% FBS. MDA-MB-468[34] human breast cancer cells (a kind gift from Dr. Janet Price,

M.D. Anderson Cancer Center, Houston, TX) were maintained in αMEM + 10% FBS. HeLa[35] human cervical cancer cells (a kind gift from Dr. Jim Koropatnick, Western University, London, ON) were maintained in DMEM + 10% FBS. Upon reaching 80% confluency, cells were passaged using 0.25% trypsin/EDTA (ethylenediaminetetraacetic acid). Media and 0.25% trypsin/EDTA was obtained from Life Technologies (Carlsbad, CA). FBS was obtained from Sigma (St. Louis, MO).

6.2.2 RNA extraction, cDNA synthesis, and real-time PCR

Total RNA was isolated from the appropriate prostate cancer (LNCaP, LNCaP C4-2B, PC-3, and PC-3M) and control (MDA-MB-468 and HeLa) cell lines using TRIzol reagent (Life Technologies) following the manufacturer's instructions and quantified using a Nanodrop ND-1000 (Thermo Scientific, Waltham, MA). Following quantification, for each reaction 1.0 μg of total RNA was reverse transcribed into complementary DNA (cDNA) by Superscript III reverse transcriptase and oligo$(dT)_{20}$ primers (Life Technologies). Quantitative reverse-transcription polymerase chain reactions (qRT-PCR) were performed in triplicate using Brilliant II SYBR Green qPCR Master Mix (Agilent Technologies, Santa Clara, CA) on a Stratagene Mx3000P qPCR system (Life Technologies). Sequence specific primers for E-cadherin, N-cadherin, vimentin, EpCAM, α-catenin, and GAPDH were designed based on gene sequence information from the National Center for Biotechnology Information (NCBI; Bethesda, MD), and are presented in *Table 6.1*. The thermal cycling profile used for all genes was 40 cycles of 94°C for 1 min, 60°C for 1 min, and 72°C for 2 min. To account for differences in GAPDH expression between cell lines, samples were normalized using a

Table 6.1. Forward and reverse primers used for qPCR analysis of prostate cancer cell lines.

Target Gene	Forward Primer (5' → 3')	Reverse Primer (5' → 3')
E-cadherin	TGCTGATGCCCCCAATACCCCA	GTGATTTCCTGGCCCACGCCAA
N-cadherin	TGACTCCAACGGGGACTGCACA	AGCTCAAGGACCCAGCAGTGGA
EpCAM	CGACTTTTGCCGCAGCTCAGGA	GGGCCCCTTCAGGTTTTGCTCT
Vimentin	AACCAACGACAAAGCCCGCGTC	TTCCGGTTGGCAGCCTCAGAGA
α-catenin	CCACGTTTTACTGAGCAAGT	AGTCAGAGTCATCCAACTCC
GAPDH	TCCATGGCACCGTCAAGGCTGA	GCCAGCATCGCCCCACTTGATT

standard curve generated using pooled qPCR human reference total RNA (Agilent Technologies)[36].

6.2.3 Immunoblotting

Human prostate cancer (LNCaP, LNCaP C4-2B, PC-3, and PC-3M) and control (MDA-MB-468 and HeLa) cell lines were harvested from tissue culture using either cell scraping (E-cadherin and N-cadherin analysis) or trypsinization (vimentin, EpCAM, and α-catenin analysis). Cell lysates were collected from harvested cells using 1% NP-40 lysis buffer and samples were quantified using the DC Protein Assay (Biorad, Hercules, CA). Protein (10µg) was subjected to sodium dodecyl sulfate polyacrylamide gel electrophoresis (SDS-PAGE) and transferred onto polyvinylidene difluoride membranes (PVDF; Millipore, Billerica, MA). Membranes were blocked using 5% skim milk in Tris-buffered saline + 0.1% Tween-20 (TBS-T; Sigma). Anti-human primary antibodies, diluted in 5% skim milk in TBS-T, were used as described in *Table 6.2*. Goat anti-mouse IgG and goat anti-rabbit IgG secondary antibodies (Calbiochem, Billerica, MA) conjugated to horseradish peroxidase, diluted in 5% skim milk in TBS-T, were utilized at a 1:2,000 dilution for all proteins except E-cadherin (1:10,000). Protein expression was visualized using Amersham ECL Prime Western Blotting Detection Reagent (GE Healthcare, Wauwatosa, WI), and normalized using total protein based on amido black (Sigma) staining on the transfer membrane. MDA-MB-468 and HeLa cell lines were utilized as positive controls for E-cadherin/EpCAM and N-cadherin/vimentin/α-catenin expression, respectively.

Table 6.2. Details of the anti-human antibodies utilized for western blot analysis of prostate cancer cell lines.

Target Protein	Clone	Commercial Source	1° Host	kDa	1° Conditions
N-Cadherin	EPR1791-4	Abcam	Rabbit	100	1:1,000 (1 hr @ RT)
E-Cadherin	36/E-cadherin	BD Biosciences	Mouse	120	1:20,000 (1 hr @ RT)
Vimentin	V9	Millipore	Mouse	60	1:1,000 (1 hr @ RT)
EpCAM	E144	Abcam	Rabbit	39	1:1,000 (1 hr @ RT)
α-catenin	EP1793Y	Abcam	Rabbit	100	1:50,000 (1 hr @ RT)
β-Actin	Polyclonal	Sigma	Rabbit	42	1:5,000 (1 hr @ RT)

6.2.4 Flow cytometry

Human prostate cancer (LNCaP, LNCaP C4-2B, PC-3, and PC-3M) and control (MDA-MB-468 and HeLa) control cells were harvested from tissue culture using either 1mM EDTA or 0.25% trypsin/EDTA, as necessary, and resuspended in flow buffer (PBS + 2% FBS). For each cell line, 5 x 10^5 tumor cells were fixed and permeabilized using the IntraPrep™ Fix/Perm kit (Beckman Coulter, Fullerton, CA, USA), and incubated with blocking buffer (PBS + 5% BSA [bovine serum albumin]) for 15 min. Cells were then washed with 1mL of flow buffer and incubated with either 0.80 μg of anti-E-cadherin (36/E-cadherin; BD Biosciences, San Jose, CA), 0.15 μg of anti-EpCAM (E144; Abcam, Cambridge, MA), 100μL of anti-CK 8/18/19-PE (Veridex, Raritan, NJ), 0.40 μg of anti-N-cadherin (EPR1791-4; Abcam), 0.80 μg of anti-vimentin (V9; Millipore), and/or 0.35 μg of anti-α-catenin (EP1793Y; Abcam). Following 3 washes with 1mL of flow buffer, samples were incubated with 1.0 μg of either AlexaFluor488 conjugated goat-anti-mouse IgG or AlexaFluor488 conjugated goat-anti-rabbit IgG secondary antibodies (Life Technologies). Following 3 washes with 1mL of flow buffer, samples were resuspended in 500μL of flow buffer and analyzed using either a Beckman Coulter EPICS XL-MCL or Cytomics FC 500 flow cytometer. Flow buffer alone (cells only), mouse IgG (BD Biosciences), mouse $IgG2_{a,\kappa}$ (Abcam), rabbit IgG (Abcam), and 10μL of PE conjugated mouse IgG (BD Biosciences) were used as negative controls at corresponding assay-specific concentrations. MDA-MB-468 and HeLa cell lines were utilized as positive controls for E-cadherin/EpCAM/CK and N-cadherin/vimentin/α-catenin expression, respectively.

6.2.5 Immunofluorescence

LNCaP, LNCaP C4-2B, PC-3, and PC-3M prostate cancer cell lines were seeded at cell line specific concentrations into Lab Tek 8-well glass chamber slides (Thermo Scientific) pre-coated with 5 μg/mL of fibronectin (LNCaP and LNCaP C4-2B cells; Santa Cruz Biotechnologies, Dallas, TX) and grown until confluent. Cells were then fixed using freshly prepared 2% paraformaldehyde for 10 min and washed with PBS (3 x 5 min). Following fixation, cells were permeabilized using 0.1% Triton X-100 (Sigma) for 5 min and washed with PBS (3 x 5 min). Cells were then blocked using PBS + 1% BSA for 1 hour and subsequently incubated with anti-E-cadherin and/or anti-α-catenin primary antibodies diluted (1:50) in PBS + 1% BSA for 1 hour. Following 3 washes with PBS, cells were fluorescently labelled using AlexaFluor488 conjugated goat-anti-mouse IgG and/or AlexaFluor594 conjugated goat-anti-rabbit IgG (Life Technologies) diluted (1:300) in PBS + 1% BSA for 1 hour. Finally, cells were washed (3 x 5 min) using PBS and mounted using 20μL of VectaShield mounting media with DAPI (Vector Laboratories, Burlingame, CA), coverslipped, and stored at 4°C until analyzed and imaged at 60x magnification using an Olympus Provis AX70 microscope (Olympus, Richmond Hill, ON).

6.2.6 Blood sample collection

A minimum of 100μL of whole blood was collected from 6-8 week old male athymic nude (*nu/nu*) mice (Harlan Sprague-Dawley, Indianapolis, IN) via terminal cardiac puncture of the right ventricle. Cardiac puncture was performed using a 22-G needle, pre-coated with sterile 0.5M EDTA, attached to a 1mL syringe. Following collection, the needle was removed, and whole blood was dispensed into a 1mL EDTA

microtainer blood collection tube (BD Microtainer, Franklin Lakes, NJ) and mixed by inversion to prevent clotting. Blood was either processed immediately or stored for up to 48 hours after the addition of an equal volume of CytoChex cellular preservative (Streck, Omaha, NE). For EMT-dependent and semi-independent assay development, 50µL of whole blood was "spiked" with either 1000 LNCaP, LNCaP C4-2B, PC-3, or PC-3M tumor cells. To assess assay recovery of low numbers of spiked cells (100, 50, 10, 5) serial dilutions were performed using whole blood (*data not shown*).

6.2.7 EMT dependent circulating tumor cell assay

This assay was adapted from the Veridex mouse/rat CellCapture kit (no longer commercially available) and has been described in detail previously[37]. Briefly, following blood collection, the equivalent of 50µL of whole blood was incubated with 25µL of anti-EpCAM ferrofluid (Janssen Diagnostics; CellSearch CTC kit) and 25µL of Capture Enhancement Reagent (Janssen Diagnostics; CellSearch CTC kit) for 15 min. Samples were then incubated in a magnet for 10 min and unlabelled cells were aspirated using a glass pipette. Fluorescent labelling of the remaining cells was performed using 50µL of Nucleic Acid Dye (Janssen Diagnostics; CellSearch CTC kit), 50µL of Staining Reagent (Janssen Diagnostics; CellSearch CTC kit), 0.30 µg of anti-mouse CD45-APC (30-F11; eBioscience, San Diego, CA), 1.5 µg of anti-human HLA-AlexaFluor488 (W6/32; BioLegend, San Diego, CA) and 100µL of Permeabilization Reagent (Janssen Diagnostics; CellSearch CTC kit) for 20 min. Dilution buffer (500µL; Veridex; CellSearch CTC kit) was added and samples were incubated in a magnet for 10 min. Unlabelled cells were aspirated using a glass pipette and the remaining sample was resuspended in 350µL of dilution buffer and transferred to a MagNest™ device for

analysis using the CellSearch analyzer (Janssen Diagnostics). Events with an $EpCAM^{+}/CK^{+}/DAPI^{+}/CD45^{-}/HLA^{+}$ phenotype and a round/oval morphology were classified as CTCs.

6.2.8 EMT semi-independent circulating tumor cell assay

Following blood collection, the equivalent of 50µL of whole blood was transferred to a 5mL flow tube and red blood cells (RBC) were lysed using 2mL of 1x NH_4Cl for 10 min. Following RBC lysis, samples were washed with 2mL of dilution buffer and centrifuged to collect cells. Cells were then fluorescently labelled using 0.2 µg of anti-human HLA-PE (W6/32; BioLegend), 0.0075 µg of anti-human EpCAM-PE (EBA-1; BD Bioscience), and 0.30 µg of anti-mouse CD45-APC and incubated for 20 min. Samples were washed with 1mL of dilution buffer and immunomagnetically enriched using the EasySep APC Positive Selection kit (StemCell Technologies, Vancouver, BC) as per the manufacturer's instructions. Following enrichment, the fraction containing the tumor cells (supernatant) was centrifuged and the cell pellet was resuspended in 100µL of Permeabilization Reagent and 50µL of Nucleic Acid Dye and incubated for 20 min. Samples were then washed with 1mL of dilution buffer and cells bound by PE-conjugated antibodies (HLA and/or EpCAM) were immunomagnetically labelled using the EasySep PE Positive Selection kit (StemCell Technologies) as per the manufacturer's instructions. Samples were washed, resuspended in 350µL of dilution buffer, and transferred to a MagNest™ device for analysis using the CellSearch analyzer. Events with an $EpCAM/HLA^{+}/DAPI^{+}/CD45^{-}$ phenotype and a round/oval morphology were classified as CTCs.

6.2.9 *In vivo* metastasis assays

All animal experiments were conducted under protocol #2012-031 approved by Western University's animal care and use committee *(Appendix 3*). LNCaP, LNCaP C4-2B, PC-3, and PC-3M cancer cells were prepared in sterile Hank's buffered saline solution (HBSS; Life Technologies) and injected ($1x10^6$ cells/40µL per mouse) orthotopically into 6-8 week old male athymic nude (*nu/nu*) mice (Harlan Sprague-Dawley) via the right dorsolateral lobe of the prostate as described previously[38,39]. At various time points post-injection (2, 4, 8, 12, and 16 weeks) mice were sacrificed, necropsies performed to assess for gross metastases, and tissues collected for pathohistological analysis. Blood (100µL) was also collected and processed using both the EMT dependent and EMT semi-independent assays (50µL/assay), described above, to assess differences in CTC presence in the bloodstream. Whenever possible, CTC sub-cell lines were generated using excess blood not required for CTC analysis using the EMT-dependent or EMT semi-independent assays. Specifically, any unused blood was lysed using 1x NH_4Cl (Beckman Coulter), washed with PBS, and plated (in 6 well dishes) for tissue culture in the complete growth media utilized for the parental cell line. The cells were grown for ~1-2 weeks, with regular media changes every 1-2 days to remove contaminating blood cells until a sufficient number of cells were available for freezing.

6.2.10 Histology and immunohistochemistry

At necropsy, tissue (prostate, lymph nodes, liver, lungs, and bone) was collected and fixed using 10% neutral-buffered formalin before processing. Tissue was subsequently paraffin-embedded, sectioned (4 µm) and stained using standard hematoxylin and eosin (H&E) staining. Slides were imaged at 400x magnification using

an Aperio ScanScope microscope (Aperio Technologies,Vista, CA) and assessed for tumor incidence and histological characteristics. Slides containing serial sections were deparaffinised using xylene and rehydrated using a graded series of alcohols (100%, 95%, 80%, 75%) prior to tissue staining. Antigen retrieval was then performed via immersion in 10 mM sodium citrate buffer + 0.05% Tween-20 at 100°C for 20 min, followed by cooling for 20 min at room temperature, and washing with PBS + 0.05% Tween-20 (3 x 2 min). Slides were incubated in BLOXALL Endogenous Peroxidase and Alkaline Phosphatase Blocking Solution (Vector Laboratories) for 10 min, washed with PBS + 0.05% Tween-20 for 5 min, and rinsed with running water (2 x 1 min). Tissue staining for E-cadherin (1:100) and N-cadherin (1:750) was performed using the Polink DS-MR-Hu kit (GBI Labs, Bothell, WA). Slides were stored at room temperature until imaged at 40x magnification using an Aperio ScanScope microscope.

6.2.11 Statistical analysis

Statistical analysis was performed using GraphPad Prism 5.0 (San Diego, CA). Analysis of CTC recovery using the EMT dependent and semi-independent assays was performed using 1-way ANOVA with Tukey's post-test for multiple comparisons. To assess differences in the mean number of CTCs between cell lines at a given time point using either the EMT dependent assay, EMT semi-independent assay, or differences between each assay within individual mice, a Mann-Whitney test was performed. Comparison of differences between each assay in matched data sets within cell lines at a given time point was performed using a Wilcoxon matched-pairs signed rank test. Primary tumor weights and mean metastatic burden were compared using 1-way ANOVA with Bonferroni's post-test for multiple comparisons. Differences in the

incidence of primary tumors, lymph node metastasis, and distant metastasis were assessed using Fisher's Exact Test. Differences in the mean number of CTCs in mice with no metastasis versus those with metastatic disease were compared using a Student's T-test. Changes in EMT gene expression in isolated CTC sub-cell lines were compared to the parental cell line using 1-way AVONA with Dunnett's post-test for multiple comparisons. Linear regression and Spearman analysis was utilized to examine the relationship between mean number of CTCs and primary tumor weight. Unless otherwise stated, data are presented as the mean ± SEM. In all cases, p values of ≤ 0.05 were considered statistically significant.

6.3 Results

6.3.1 Human prostate cancer cell lines display differences in EMT phenotype

Four human prostate cancer cell lines (LNCaP, LNCaP C4-2B, PC-3, and PC-3M) previously reported to have progressively increasing metastatic capacity[40–43] were characterized for epithelial (E-cadherin, EpCAM, and/or CK 8/18/19) and mesenchymal (N-cadherin and vimentin) markers using qRT-PCR (*Figure 6.1*), western blot (*Figure 6.2*), and FCM (*Figure 6.3*). Results of this analysis demonstrated that the LNCaP and LNCaP C4-2B cell lines had consistently higher expression of the epithelial-associated markers E-cadherin and CK 8/18/19 (investigated by FCM only), while the PC-3 and PC-3M cell lines had consistently higher expression of the mesenchymal-associated markers N-cadherin and vimentin across all 3 assays. Although EpCAM levels appeared similar between cell lines at the mRNA level (*Figure 6.1*), relative differences in EpCAM expression were evident at the protein level, with the LNCaP and LNCaP C4-2B cell

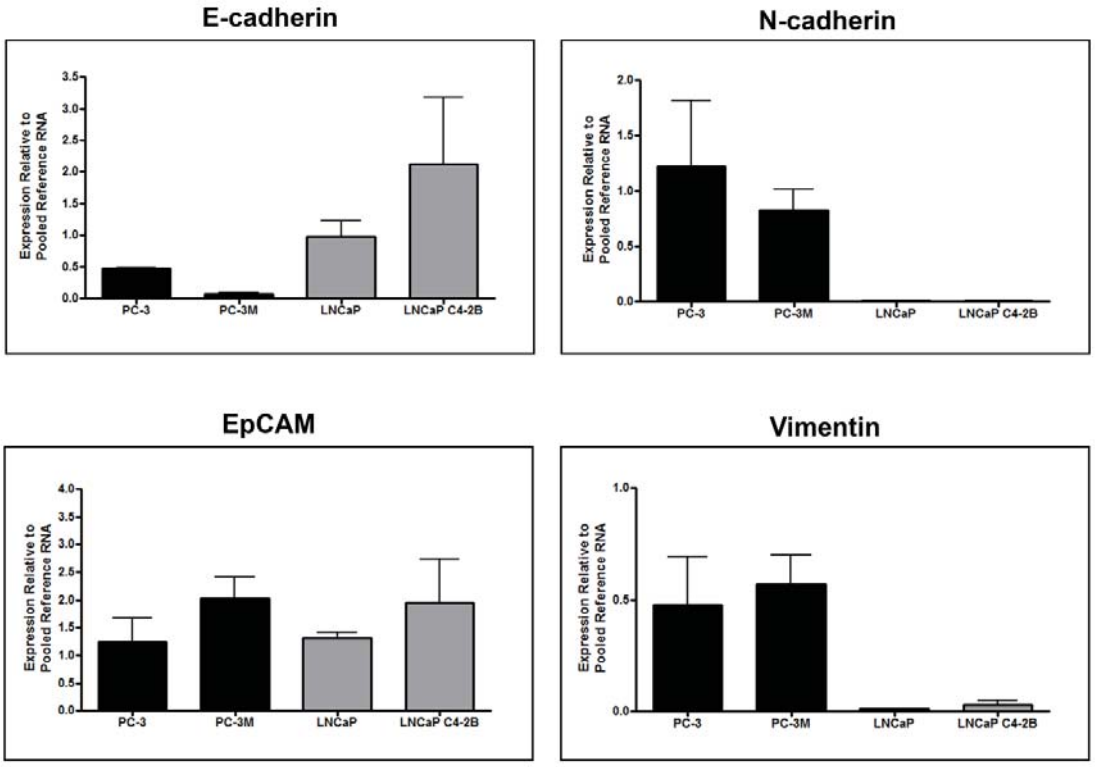

Figure 6.1. Human prostate cancer cell lines display differences in epithelial-to-mesenchymal transition (EMT) phenotype at the RNA level. The expression of epithelial-associated (grey bars) and mesenchymal-associated genes (black bars) correlates with previously reported cell aggressiveness and *in vivo* metastatic capacity. Results of real time quantitative PCR mRNA expression analysis for the epithelial-associated markers E-cadherin and EpCAM and mesenchymal-associated markers N-cadherin and vimentin are presented as relative expression compared to pooled reference RNA (n=3).

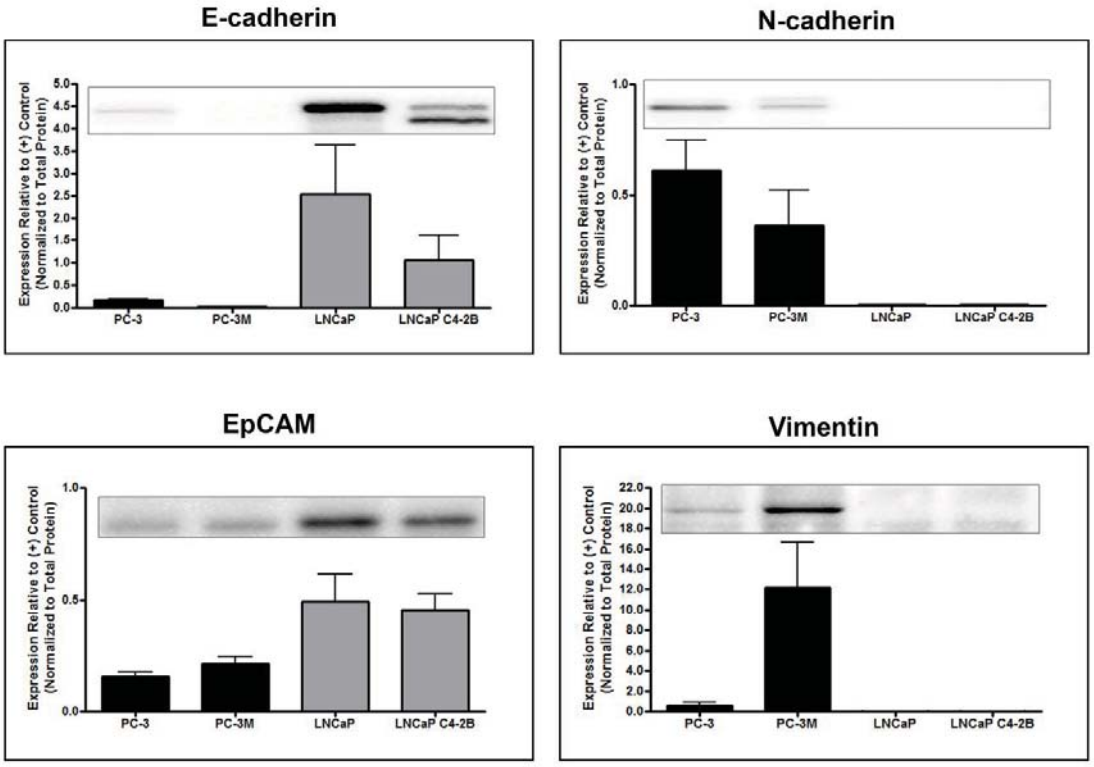

Figure 6.2. Human prostate cancer cell lines display differences in EMT phenotype at the protein level as assessed by immunoblotting. The expression of epithelial-associated (grey bars) and mesenchymal-associated proteins (black bars) correlates with previously reported cell aggressiveness and *in vivo* metastatic capacity. Results of western blot protein expression analysis for the epithelial-associated markers E-cadherin and EpCAM and the mesenchymal-associated markers N-cadherin and vimentin are presented as quantitative densitometric data relative to appropriate positive control cell lines and normalized to total protein loaded as assessed by amido black staining, and as representative western blots shown as cropped gel images (n=3).

Figure 6.3. Human prostate cancer cell lines display differences in EMT phenotype at the protein level as assessed by flow cytometry. The expression of epithelial-associated (grey bars) and mesenchymal-associated proteins (black bars) correlates with previously reported cell aggressiveness and *in vivo* metastatic capacity. Results of protein expression analysis by flow cytometry for the epithelial-associated markers E-cadherin and EpCAM and the mesenchymal-associated markers N-cadherin and vimentin are presented as relative fluorescence intensity (expression) compared to appropriate positive control cell lines (n=3).

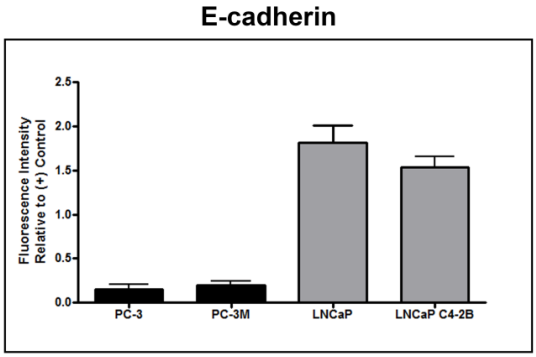
E-cadherin
Fluorescence Intensity
Relative to (+) Control
2.5
2.0
1.5
1.0
0.5
0.0
PC-3
PC-3M
LNCaP
LNCaP C4-2B

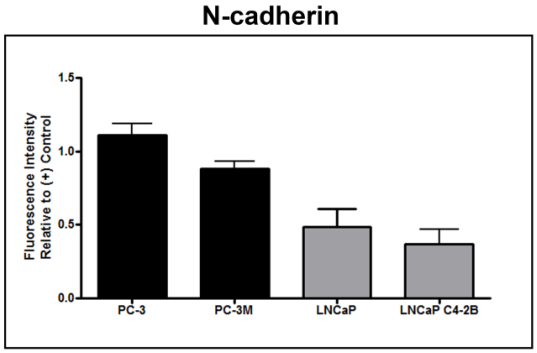
N-cadherin
Fluorescence Intensity
Relative to (+) Control
1.5
1.0
0.5
0.0
PC-3
PC-3M
LNCaP
LNCaP C4-2B

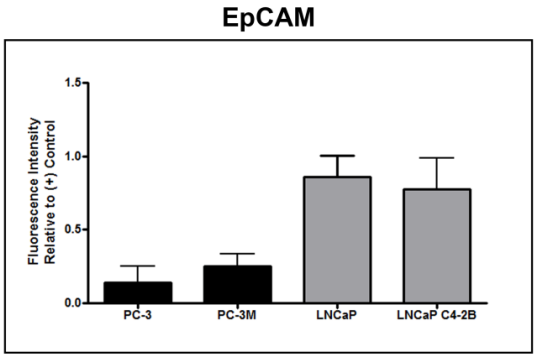
EpCAM
Fluorescence Intensity
Relative to (+) Control
1.5
1.0
0.5
0.0
PC-3
PC-3M
LNCaP
LNCaP C4-2B

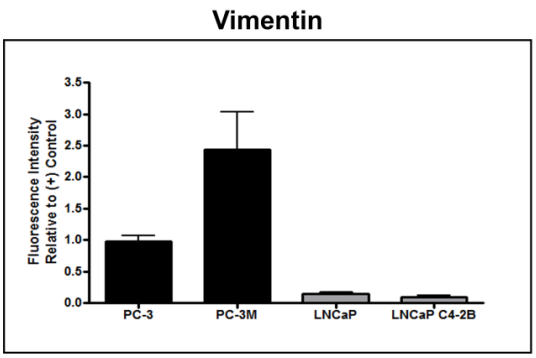
Vimentin
Fluorescence Intensity
Relative to (+) Control
3.5
3.0
2.5
2.0
1.5
1.0
0.5
0.0
PC-3
PC-3M
LNCaP
LNCaP C4-2B

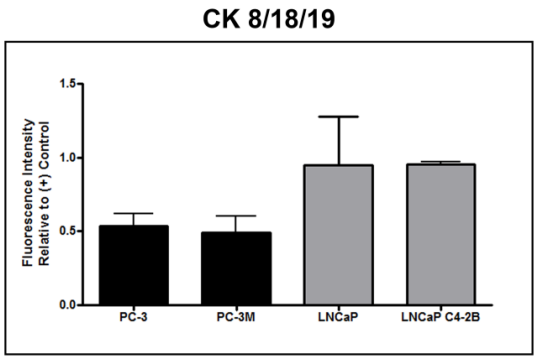
CK 8/18/19
Fluorescence Intensity
Relative to (+) Control
1.5
1.0
0.5
0.0
PC-3
PC-3M
LNCaP
LNCaP C4-2B

lines demonstrating higher levels of expression compared to the PC-3 and PC-3M cell lines (*Figure 6.2 and 6.3*).

To further investigate the potential capacity for capture of these cells by the EpCAM and CK 8/18/19 reliant CSS, differences in the co-expression of these proteins on individual cells was assessed using FCM in order to determine relative differences in co-expression of these proteins within each cell line (*Figure 6.4*). This analysis further confirmed the differential EpCAM expression between these 4 cell lines, but interestingly demonstrated a similar distribution of CK 8/18/19 expression. This suggested that any differences in CTC capture between these 4 cell lines would likely be as a result of differences in EpCAM expression and would be less impacted by differences in CK 8/18/19.

Finally, the ability of E-cadherin to maintain the epithelial phenotype of cells is due, in part, to its localization on the cell membrane. In fact, this localization has been reported to be a requirement for normal adhesive functions of epithelial cells[44,45]. Therefore localization studies using immunofluorescence were performed on the 4 investigated cell lines. These studies demonstrated that although E-cadherin expression could be detected in the PC-3 cell line via western blot, the protein was aberrantly localized to the cytoplasm in these cells, most likely due to a lack of α-catenin expression, a protein necessary for appropriate E-cadherin membrane localization[46]. In contrast, we observed that LNCaP and LNCaP C4-2B cell lines strongly expressed E-cadherin with appropriate membrane localization (*Figure 6.5*). Validation of the loss of α-catenin expression in the PC-3 and PC-3M cell lines was further confirmed using qRT-PCR, western blot, and FCM (*Figure 6.6*).

Figure 6.4. Human prostate cancer cell lines express similar levels of CK 8/18/19 but variable levels of EpCAM as assessed by flow cytometry. ***(A)*** Representative flow cytometry dot plots of the differential expression of EpCAM (AF488) and CK 8/18/19 (PE) in investigated prostate cancer cell lines. ***(B)*** Results of flow cytometry protein expression analysis for epithelial-associated markers, EpCAM and CK 8/18/19, presented as the mean (± SEM) fluorescence intensity of the investigated proteins for each cell line (n=3).

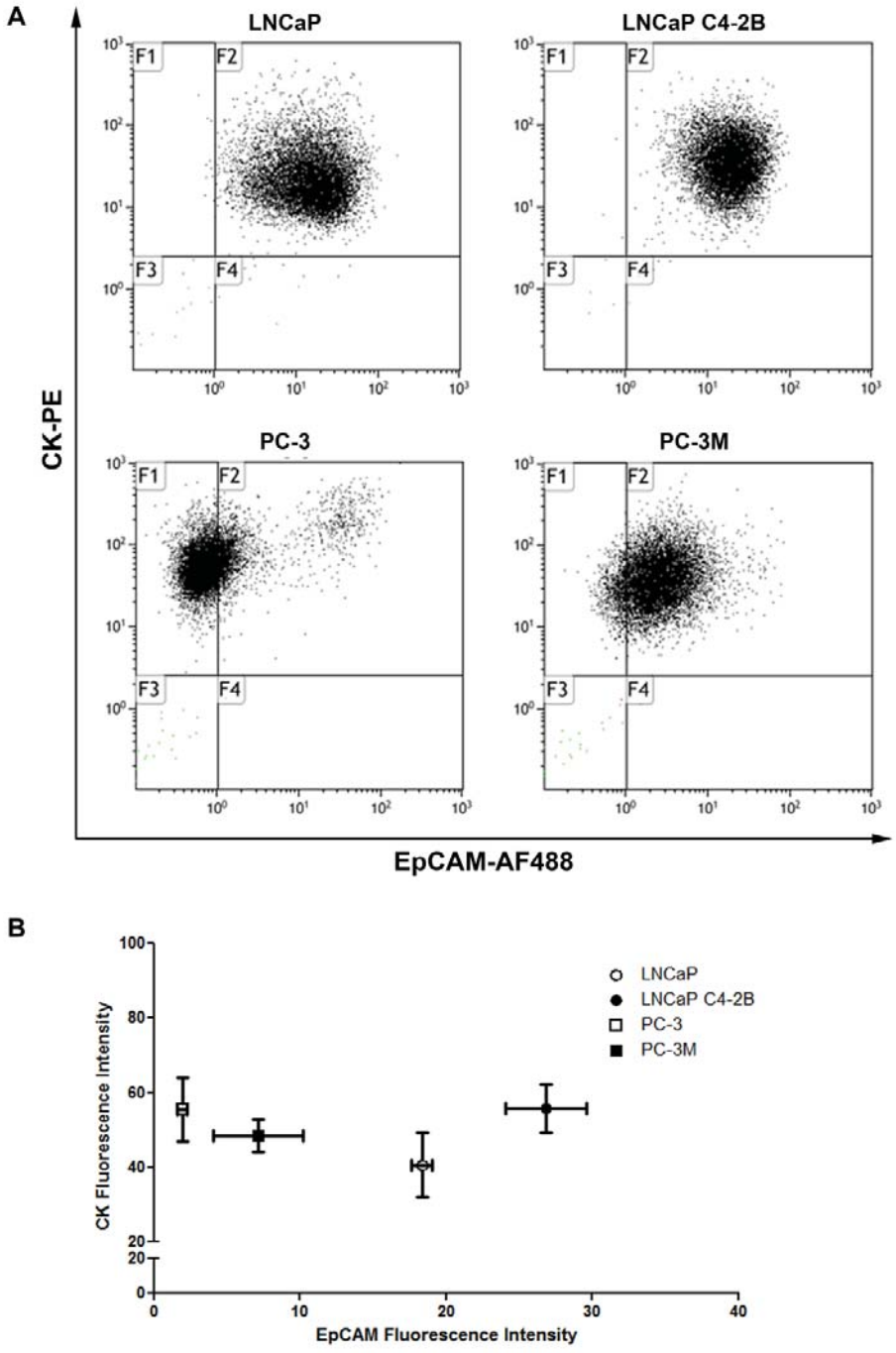
A
LNCaP
LNCaP C4-2B
PC-3
PC-3M
F1
F2
F3
F4
CK-PE
EpCAM-AF488
B
LNCaP
LNCaP C4-2B
PC-3
PC-3M
CK Fluorescence Intensity
EpCAM Fluorescence Intensity

Figure 6.5. E-cadherin cell membrane localization is aberrant in human prostate cancer cell lines that do not express α-catenin. ***(A)*** Representative immunofluorescent images of E-cadherin (green) and DAPI (blue) stained PC-3, PC-3M, LNCaP, and LNCaP C4-2B cell lines cultured on glass chamber slides. ***(B)*** Representative immunofluorescent images of co-localization (yellow) of E-cadherin (green) and α-catenin (red) in PC-3, PC-3M, LNCaP, and LNCaP C4-2B cell lines cultured on glass chamber slides (DAPI [blue]). Images were obtained at 60x magnification, scale bars = 15 μm (n=3).

A

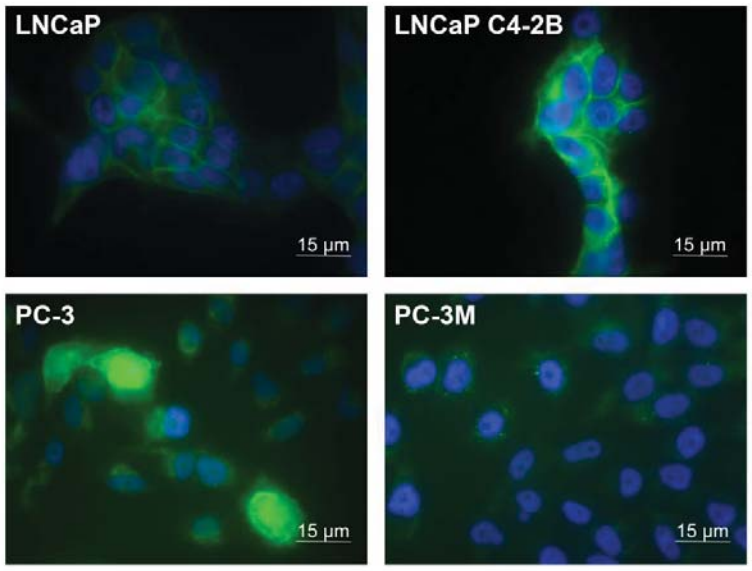
LNCaP
15 µm
LNCaP C4-2B
15 µm
PC-3
15 µm
PC-3M
15 µm

B

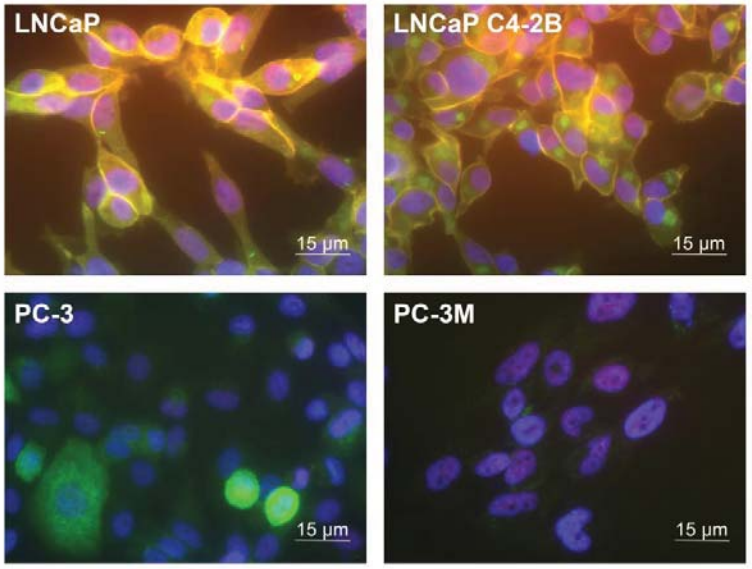
LNCaP
15 µm
LNCaP C4-2B
15 µm
PC-3
15 µm
PC-3M
15 µm

Figure 6.6. α-catenin mRNA and protein are aberrantly expressed in PC-3 and PC-3M human prostate cancer cell lines. ***(A)*** Results of real time quantitative PCR mRNA expression analysis for α-catenin in the investigated cell lines (PC-3M, PC-3, LNCaP C4-2B, and LNCaP) are presented as relative expression compared to pooled reference RNA (n=3). ***(B)*** Results of western blot protein expression analysis for α-catenin in the investigated cell lines are presented in quantitative densitometric form relative to an appropriate positive control cell line and as a representative western blot, shown as a cropped gel image (n=3). ***(C)*** Results of flow cytometry expression analysis for α-catenin in the investigated cell lines are presented as relative fluorescence intensity (expression) compared to an appropriate positive control cell line (n=3).

A

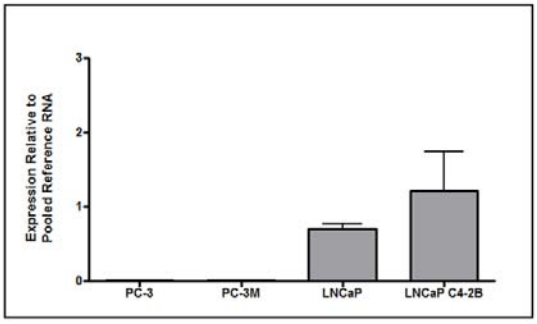
Expression Relative to Pooled Reference RNA
3
2
1
0
PC-3
PC-3M
LNCaP
LNCaP C4-2B

B

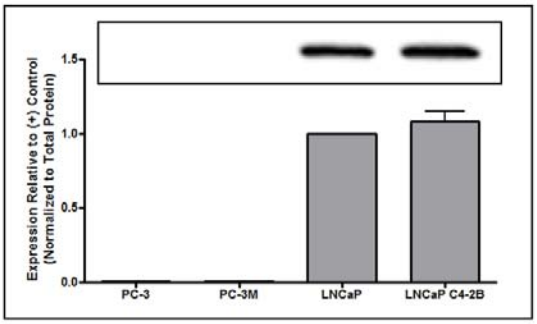
Expression Relative to (+) Control (Normalized to Total Protein)
1.5
1.0
0.5
0.0
PC-3
PC-3M
LNCaP
LNCaP C4-2B

C

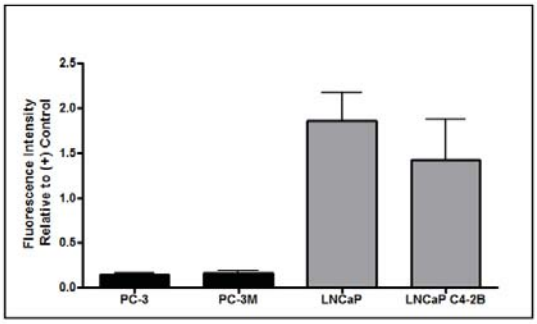
Fluorescence Intensity Relative to (+) Control
2.5
2.0
1.5
1.0
0.5
0.0
PC-3
PC-3M
LNCaP
LNCaP C4-2B

6.3.2 Circulating tumor cell recovery using the CellSearch® system is lower for prostate cancer cells with a mesenchymal phenotype

As the current gold standard CTC detection technology, the CSS relies solely on the expression of the epithelial-associated marker EpCAM for CTC capture. However, this marker has been shown to be downregulated in cells with an invasive phenotype[47], suggesting that EpCAM-based CTC detection techniques such as the CSS may be missing at least a portion of the CTCs that enter the bloodstream. In order to assess this, we developed 2 novel CTC assays for use with pre-clinical models of cancer metastasis; one that would recapitulate the EpCAM-based CTC capture of the CSS in a mouse model ("EMT dependent assay"), and one that would capture all the CTCs shed into the circulation regardless of EMT status ("EMT semi-independent assay"). Following development, all 4 prostate cancer cell lines were spiked into mouse blood at a known concentration (1000 tumor cells/50μL blood) and were assessed using both assays to determine differences in CTC recovery relative to the EMT phenotype of the cells (*Figure 6.7*). Use of the EMT dependent assay resulted in significantly reduced recovery of CTCs with a mesenchymal phenotype (PC-3 and PC-3M) when compared to CTCs with an epithelial phenotype (LNCaP and LNCaP C4-2B; $p \leq 0.05$) (*Figure 6.7A*). However, when the EMT semi-independent assay was utilized, although overall the CTC recovery was lower than that demonstrated using the EMT dependent assay, the percent recovery was not significantly different across all 4 cell lines regardless of EMT status (*Figure 6.7B*). The reasons underlying the reduced recovery of the EMT semi-independent assay was further investigated by incorporating the additional sample handling steps required for the EMT semi-independent assay (i.e. red blood cell lysis and

Figure 6.7. CTC recovery using the CellSearch® system (CSS) is lower in human prostate cancer cells with a mesenchymal phenotype. Prostate cancer cells were counted by hemocytometer and spiked at a concentration of 1,000 tumour cells/50µl of whole mouse blood. 50µl of mouse blood was subsequently processed using a 1 of 2 mouse-adapted protocols and CTC recovery was measured as a percentage recovery of the number of spiked cells. ***(A)*** CTC recovery using the EMT dependent assay is significantly lower in cells with a more mesenchymal and metastatic phenotype. ***(B)*** CTC recovery using the EMT semi-independent assay is lower relative to the EMT dependent assay. However, equivalent recovery is observed across all 4 cell lines regardless of EMT phenotype. ***(C)*** Reduced recovery observed when using the EMT semi-independent assay was further investigated and determined to be as a result of extra processing steps required in this protocol. Data are presented as the mean ± SEM (n=3; * = significantly different [$p \leq 0.05$]).

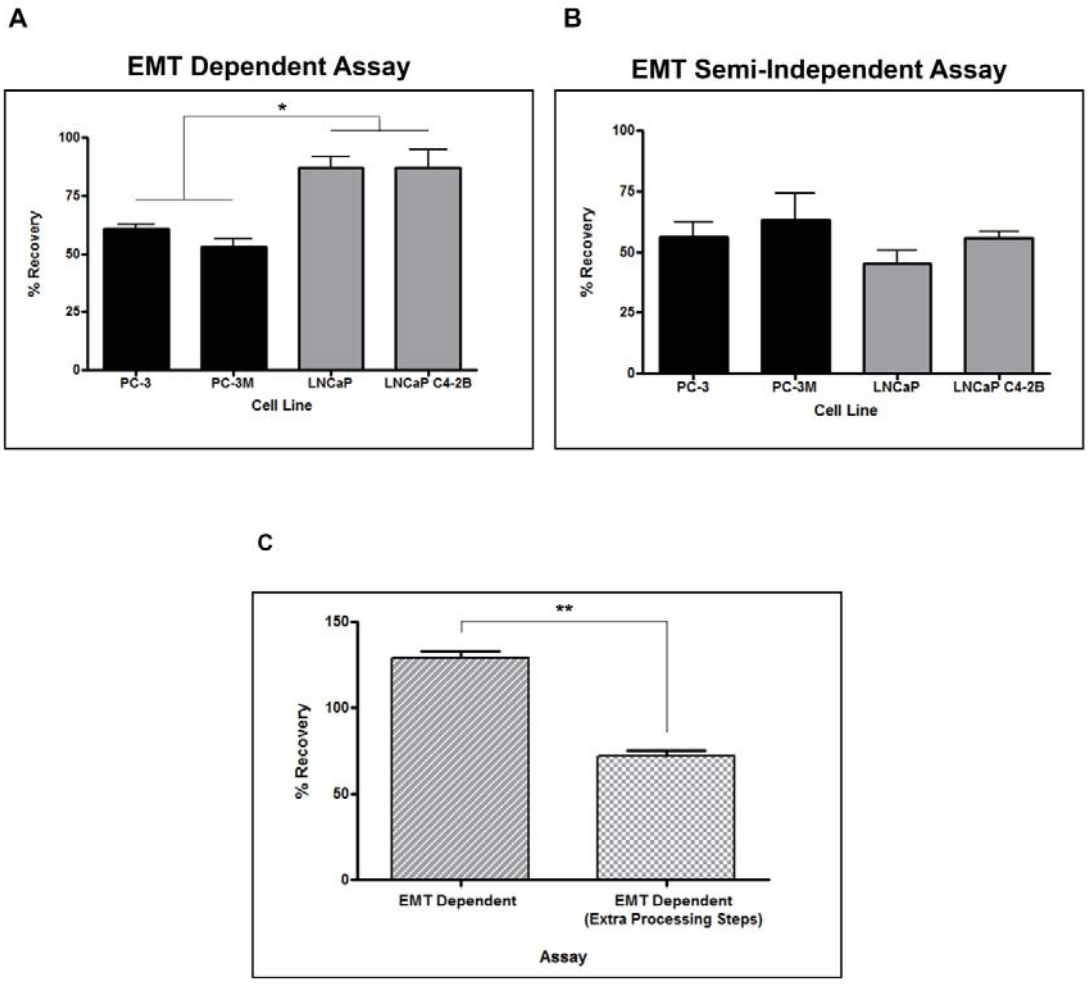
A
EMT Dependent Assay
*
100
75
50
25
0
% Recovery
PC-3
PC-3M
LNCaP
LNCaP C4-2B
Cell Line
B
EMT Semi-Independent Assay
100
75
50
25
0
% Recovery
PC-3
PC-3M
LNCaP
LNCaP C4-2B
Cell Line
C
**
150
100
50
0
% Recovery
EMT Dependent
EMT Dependent
(Extra Processing Steps)
Assay

additional washes) into the EMT dependent assay. The results demonstrated that when using the same reagents and a highly epithelial cell line (LNCaP C4-2B), addition of the extra processing steps resulted in additional sample loss between matched samples as previously seen when comparing both assays (*Figure 6.7C*).

6.3.3 Tumors generated from prostate cancer cell lines with an increasingly mesenchymal phenotype have an enhanced capacity for circulating tumor cell shedding *in vivo* and may produce circulating tumor cells that are undetectable by the CellSearch® system

LNCaP, LNCaP C4-2B, PC-3, and PC-3M prostate cancer cells were injected into 6-8 week old male nude mice via the right dorsolateral lobe of the prostate ($1x10^6$ cells/mouse) to assess spontaneous metastasis. At several time points post-injection (2, 4, 8, 12, and 16 weeks) mice were sacrificed and blood (100µL) was collected and processed using both the EMT dependent and EMT semi-independent assays (50µL/assay) and CTC numbers were normalized to the assay-specific cell line recovery determined in *Figure 6.7*. Throughout the study mice were occasionally sacrificed at modified time points (±1-2 weeks), either due to morbidity or other technical issues. However, to ensure an adequate number of animals were included for the final statistical analysis, mice were categorized based on time of sacrifice (1-3, 4-6, 8-10, 11-13, and 14-16 weeks). For simplicity, the data will be presented at the initially defined time points (2, 4, 8, 12, and 16 weeks). Unfortunately, due to the rapid progression of the PC-3M cell line, CTC analysis in this group of mice could only be assessed at 2 and 4 weeks. We observed that, using the EMT dependent assay, the highly mesenchymal PC-3M cell line shed CTCs very quickly post-injection and the number of CTCs shed was significantly greater than all other cell lines at both time points investigated (2 and 4 weeks; $p \leq 0.05$)

(*Figure 6.8A*). Additionally, the mesenchymal-like PC-3 cell line shed a similar number of CTCs as the epithelial LNCaP and LNCaP C4-2B cell lines until week 12, at which time the number of CTCs increased significantly compared to the LNCaP C4-2B cell line ($p \leq 0.05$). Although this trend appeared to continue at 16 weeks post-injection, it was not significantly different from the LNCaP and LNCaP C4-2B cell lines. Similarly, using the EMT semi-independent assay the PC-3M cell line shed a significantly greater number of CTCs then all other cell lines at 2 weeks, and greater than the LNCaP and LNCaP C4-2B cell lines at 4 weeks ($p \leq 0.05$) (*Figure 6.8B*). When considering the PC-3 cell line, unlike with the EMT dependent assay, no significant differences were observed between any of the cell lines at 12 weeks. However, significant differences between the PC-3 and LNCaP C4-2B cell lines were observed at 16 weeks ($p \leq 0.05$).

To quantify differences in CTC recovery based on EMT status, normalized CTC values obtained using both assays from each time point were compared. The results demonstrated there were no significant differences observed in CTC recovery between the EMT dependent and EMT semi-independent assays at any time point examined, except for the C4-2B cell line at 8 weeks (*data not shown*). To assess if the lack of statistical significance observed was due to a truly non-significant result or due to a high level of variability with regards to CTC number in individual mice within each time point further investigation was undertaken to assess the difference in CTCs recovered using the EMT dependent and EMT semi-independent assays within *individual* animals. To assess this, the normalized number of CTCs identified using the EMT dependent assay were subtracted from the normalized number of CTCs identified using the EMT semi-independent assay and presented as the mean for each time point (*Figure 6.8C*). In this

Figure 6.8. Human prostate cancer cell lines with an increasingly mesenchymal phenotype have an enhanced *in vivo* capacity for shedding CTCs that are undetectable by the CSS. PC-3M, PC-3, LNCaP C4-2B, and LNCaP prostate cancer cells were orthotopically injected into 6-8 week old male nude mice via the right dorsolateral lobe of the prostate ($1x10^6$ cells/mouse) to assess spontaneous metastasis. At several time points post injection (2, 4, 8, 12, and 16 weeks) mice were sacrificed and blood (100 µl) was collected and processed using both the ***(A)*** EMT dependent and ***(B)*** EMT semi-independent assays (50 µl/assay) to assess differences in CTC recovery. Data are presented as the mean ± SEM (n=5-12 mice/group). ***(C)*** Comparison of the observed difference in the number of CTCs detected using the EMT dependent and EMT semi-independent assays in matched samples. Data are presented as the mean (± SEM) difference in the number of observed CTCs between both assays (# captured by EpCAM/HLA assay - # captured by EpCAM assay) at a given time point (n=5-12 mice/group). Negative values represent groups in which more CTCs were detected with the EMT dependent assay. Positive values represent groups in which more CTCs were detected with the EMT semi-independent assay. * = significantly increased relative to the PC-3 cell line; α = significantly increased relative to the LNCaP C4-2B cell line; δ = significantly increased relative to the LNCaP cell line ($p \leq 0.05$).

A

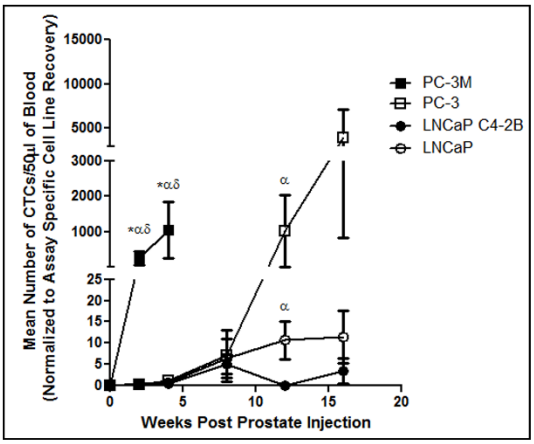
Mean Number of CTCs/5Qμl of Blood
(Normalized to Assay Specific Cell Line Recovery)
15000
10000
5000
3000
2000
1000
25
20
15
10
5
0
0
5
10
15
20
Weeks Post Prostate Injection
*α,δ
*α,δ
α
α
PC-3M
PC-3
LNCaP C4-2B
LNCaP

B

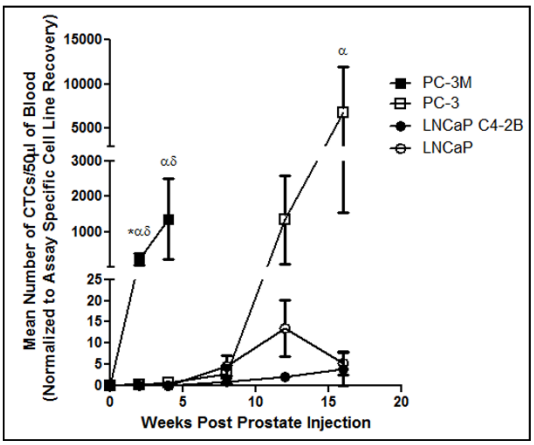
Mean Number of CTCs/5Qμl of Blood
(Normalized to Assay Specific Cell Line Recovery)
15000
10000
5000
3000
2000
1000
25
20
15
10
5
0
0
5
10
15
20
Weeks Post Prostate Injection
*α,δ
α,δ
α
PC-3M
PC-3
LNCaP C4-2B
LNCaP

C

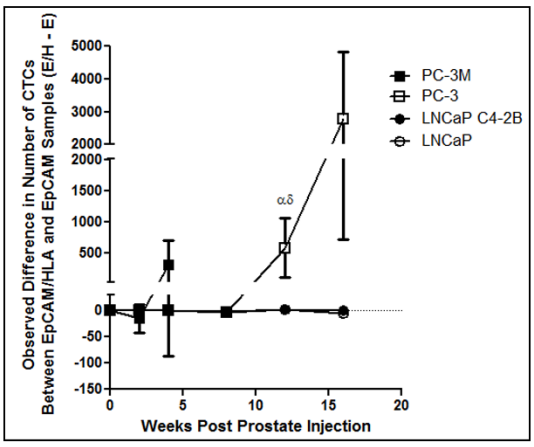
Observed Difference in Number of CTCs
Between EpCAM/HLA and EpCAM Samples (E/H - E)
5000
4000
3000
2000
2000
1500
1000
500
0
-50
-100
-150
0
5
10
15
20
Weeks Post Prostate Injection
α,δ
PC-3M
PC-3
LNCaP C4-2B
LNCaP

way, negative values represent time points in which more CTCs were detected with the EMT dependent assay and positive values represent groups in which more CTCs were detected with the EMT semi-independent assay. Based on this analysis it was demonstrated that the epithelial cell lines LNCaP and LNCaP C4-2B had similar CTC recovery numbers across both assays at all time points investigated. However, the mesenchymal cell lines PC-3 and PC-3M showed increased numbers of CTCs recovered using the EMT semi-independent assay at later time points, with significant differences observed when comparing the PC-3s to the LNCaP C4-2Bs and the PC-3s to the LNCaPs at 12 weeks post-injection ($p \leq 0.05$).

6.3.4 Prostate cancer cell lines with an increasingly mesenchymal phenotype have an enhanced capacity for primary tumor formation and metastasis

In addition to differences in CTC kinetics, comparison of the metastatic capacity of these 4 prostate cancer cell lines and the relationship between CTC dissemination and metastasis, has not yet been established in the literature. Therefore, at each time point, mice were sacrificed and tissue (all major organs and bone) was collected and assessed for the presence of primary and metastatic lesions based on both gross observations at necropsy (all organs) and microscopic (prostate, lymph nodes, liver, lung, and bone) analysis following standard H&E staining. In addition, the prostate and bladder were weighed as a surrogate of primary tumor volume, as caliper measurements of primary tumors in the prostate gland were not possible in live animals.

Incidence of primary tumor formation and tumor weight was significantly increased in the highly mesenchymal PC-3M cell line compared to all other cell lines investigated ($p \leq 0.05$), except when considering tumor weight of the PC-3s at 2 weeks

post-injection (*Figure 6.9A, B*). All other cell lines showed comparable primary tumor incidence and weight at all of the investigated time points. Additionally, when considering primary tumor weight and CTC number (using the EMT-semi-independent assay), for all cell lines there was a positive correlation between the weight of the primary tumor and the number of CTCs shed into the circulation (*Figure 6.9C*), with larger primary tumors shedding a greater number of CTCs.

Additional differences between the mesenchymal and epithelial cell lines were observed when considering the incidence of metastasis and metastatic burden to the lymph nodes. Microscopic histology analysis revealed that the PC-3M cell line had a significantly increased incidence of lymph node metastases compared to all other investigated cell lines at 4 weeks ($p \leq 0.05$), while the PC-3 cell line had a significantly increased incidence at weeks 8 and 12 compared to the LNCaP C4-2B cell line ($p \leq 0.05$). Interestingly, the incidence of metastases to the lymph node did not differ significantly between the PC-3 and LNCaP cell lines (*Figure 6.10A*). However, when metastatic burden to the lymph node was assessed, the PC-3 cell line demonstrated significantly increased metastatic burden compared to both the LNCaP C4-2Bs and the LNCaPs at 12 weeks post-injection ($p \leq 0.05$) (*Figure 6.10B*). Therefore, it appears that although these cell lines have a similar capacity to disseminate to the lymph nodes, they do not have the same capacity for subsequent growth in this organ. Finally, differences in metastases to distant sites were also investigated, based on both gross assessment at necropsy, and microscopic assessment following H&E staining. We observed that both the PC-3M and PC-3 cell lines were able to disseminate to and establish gross macrometastases in a number of distant organs. In fact, no visible macrometastases were

Figure 6.9. The highly mesenchymal PC-3M cell line exhibits a greater incidence of primary tumour formation and mean tumour weight compared to other investigated cell lines and all cell lines show a positive correlation of CTC number with primary tumour weight. ***(A)*** Incidence of primary tumour formation of PC-3M, PC-3, LNCaP C4-2B, and LNCaP prostate cancer cell lines based on microscopic histological examination of formalin fixed, H&E stained tissue following orthotopic injection. Data are presented as the percentage of mice per cell line per time point with detectable primary tumours (n=6-39 mice/group). ***(B)*** Mean combined weight of prostate and bladder at time of sacrifice following orthotopic injection of prostate cancer cell lines. Data are presented as the mean ± SEM (n=6-39 mice/group). ***(C)*** Mean normalized number of CTCs/50 µl of blood (assessed using the EMT semi-independent assay) positively correlates with the primary tumour weight in all of the investigated cell lines. * = significantly different ($p \leq 0.05$).

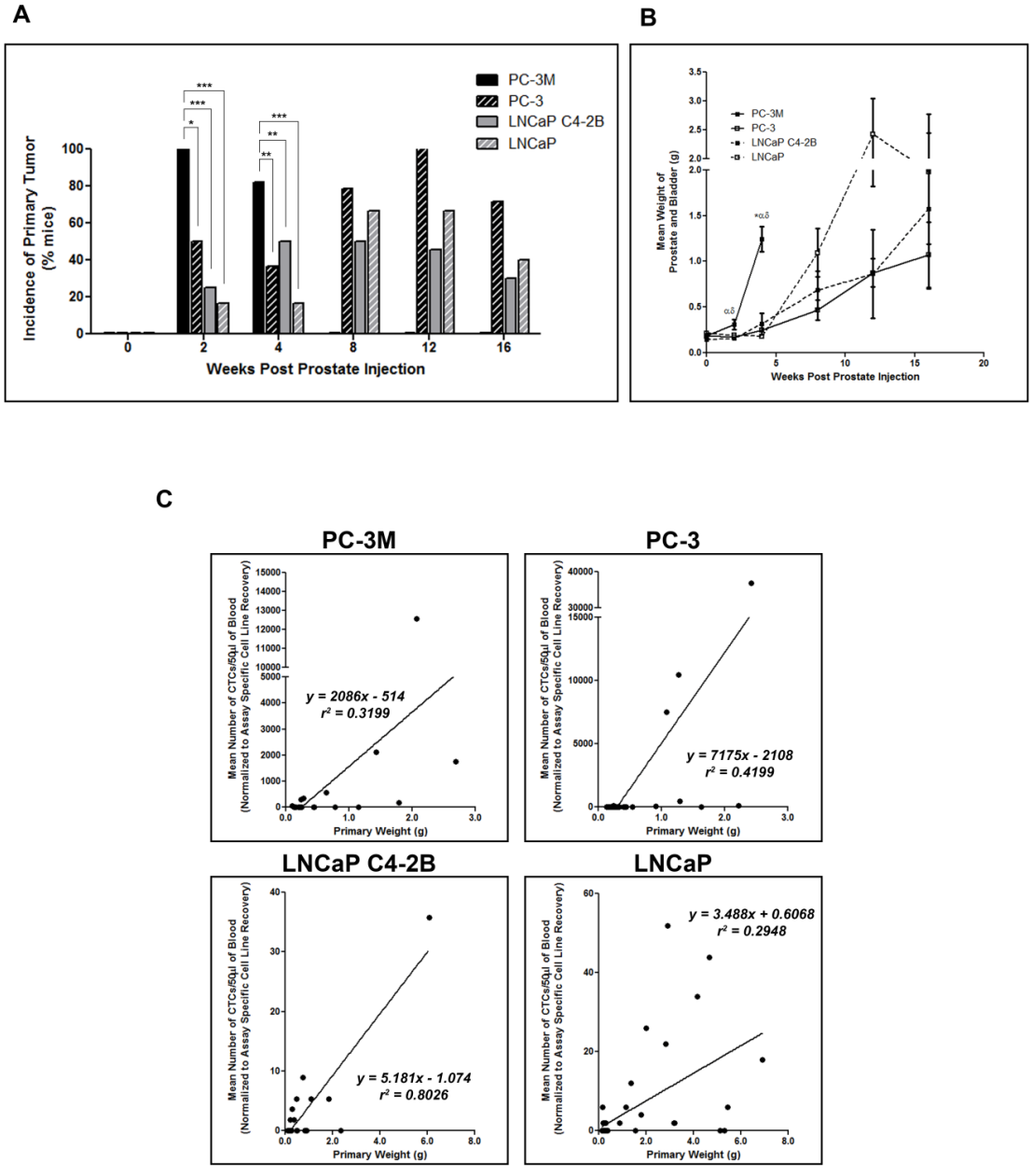
A
B
C
PC-3M
PC-3
LNCaP C4-2B
LNCaP
Incidence of Primary Tumor (% mice)
Weeks Post Prostate Injection
Mean Weight of Prostate and Bladder (g)
Mean Number of CTCs/5µl of Blood (Normalized to Assay Specific Cell Line Recovery)
Primary Weight (g)
y = 2086x - 514
r² = 0.3199
y = 7175x - 2108
r² = 0.4199
y = 5.181x - 1.074
r² = 0.8026
y = 3.488x + 0.6068
r² = 0.2948

Figure 6.10. The mesenchymal PC-3M and PC-3 cell lines exhibit a greater incidence of lymph node metastases and mean lymph node metastatic burden. ***(A)*** Incidence of lymph node metastasis of PC-3M, PC-3, LNCaP C4-2B, and LNCaP prostate cancer cell lines based on microscopic histological examination of formalin fixed, H&E stained tissue following orthotopic injection. Data are presented as the percentage of mice per cell line per time point with detectable lymph node metastases (n=7-39 mice/group). ***(B)*** Quantitative analysis of tumour burden (mean % of lymph nodes occupied by tumour) following orthotopic injection of prostate cancer cell lines. Data are presented as the mean ± SEM (n=7-39 mice/group). * = significantly different ($p \leq 0.05$).

A

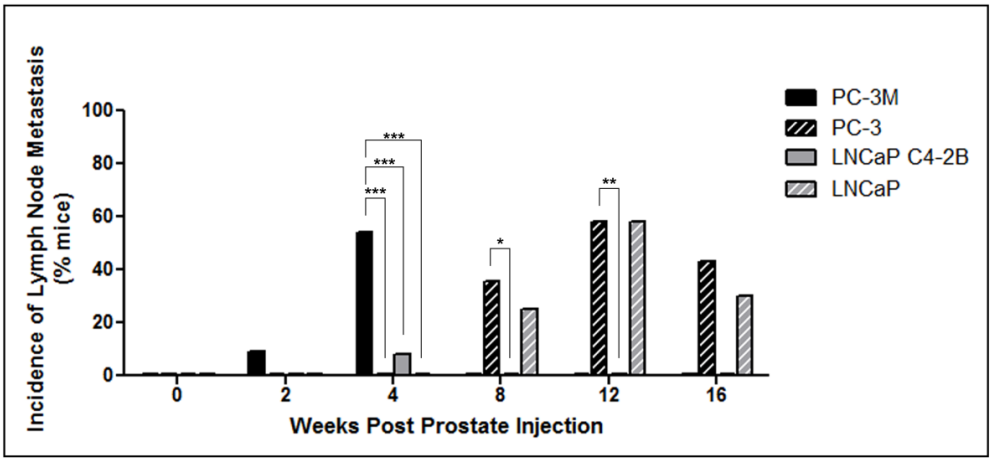
Incidence of Lymph Node Metastasis
(% mice)
100
80
60
40
20
0
0
2
4
8
12
16
Weeks Post Prostate Injection
***
***
***
*
**
PC-3M
PC-3
LNCaP C4-2B
LNCaP

B

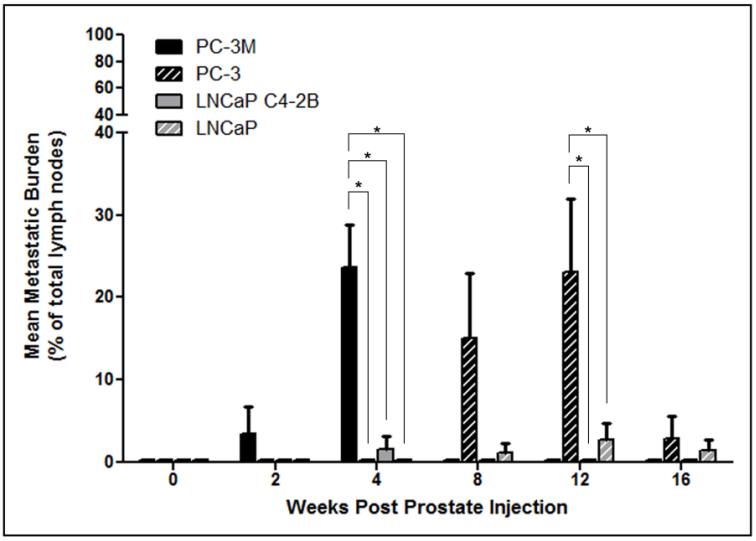
Mean Metastatic Burden
(% of total lymph nodes)
100
80
60
40
40
30
20
10
0
0
2
4
8
12
16
Weeks Post Prostate Injection
*
*
*
*
*
*
PC-3M
PC-3
LNCaP C4-2B
LNCaP

observed in mice injected with either the LNCaP and LNCaP C4-2B cell lines at necropsy (*Figure 6.11*). However, microscopic histology analysis of the lung and liver revealed distant metastases to these organs for all of the investigated cell lines. Analysis of the overall metastatic capacity of the investigated cell lines, based on the incidence of gross distant metastases to any of described organs, demonstrated that the more mesenchymal PC-3M and PC-3 cell lines had a significantly increased metastatic capacity compared to the more epithelial LNCaP and LNCaP C4-2B cell lines ($p \leq 0.05$). Specifically, the PC-3M cell line had an increased incidence of distant metastases compared to the LNCaP and LNCaP C4-2B cell lines at both 2 and 4 weeks post-injection ($p \leq 0.05$), and to the PC-3s at 4 weeks post-injection ($p \leq 0.05$). Similarly, at later time points the PC-3s had an increased incidence of distant metastases compared to the LNCaP C4-2Bs (16 weeks) and the LNCaPs (12 and 16 weeks; $p \leq 0.05$) (*Figure 6.12A*).

Finally, we wanted to determine the relationship between CTCs and metastatic spread. CTC numbers were compared in mice that had the presence of metastasis to the lymph node or any distant organ (based on gross or microscopic analysis) to those without metastasis (*Figure 6.12B*). This data clearly demonstrates that the number of CTCs was significantly higher, across all 4 cell lines, in mice with metastatic disease, compared to those without, validating the relationship between CTC dissemination and metastasis, and that the mean CTC numbers were higher in those cell lines with the greatest metastatic capacity.

Figure 6.11. Human prostate cancer cell lines with an increasingly mesenchymal phenotype have an enhanced *in vivo* capacity for metastasis to distant organs. Incidence of metastasis to distant organs of PC-3M, PC-3, LNCaP C4-2B, and LNCaP prostate cancer cell lines based on gross observations at necropsy (left panel) and microscopic histological examination (right panel) of tissue following orthotopic injection. Data are presented as the percentage of mice per cell line per time point with detectable distant metastases to the lung, liver diaphragm, intestines, kidney, and/or spleen/pancreas (n=7-39 mice/group).

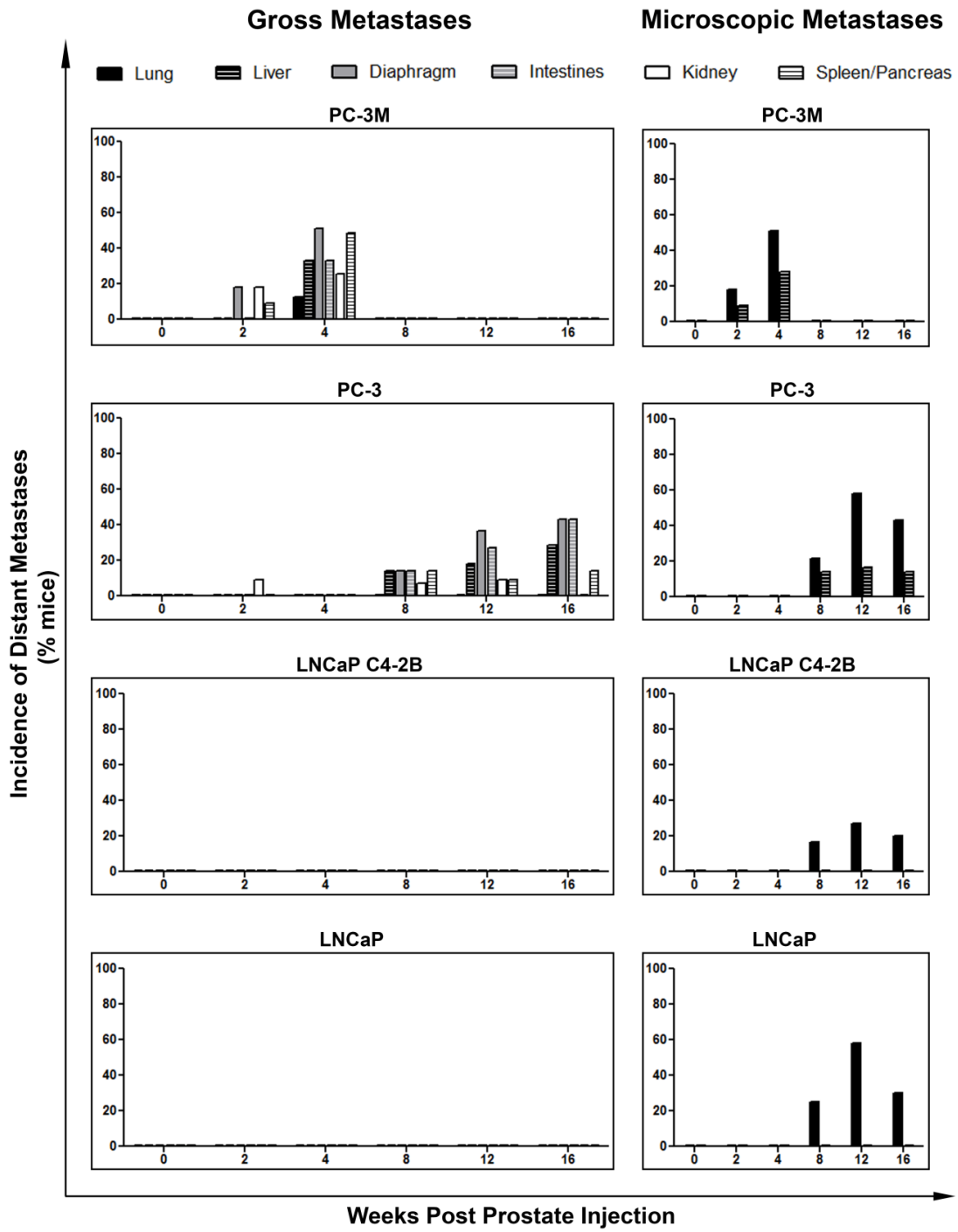
Gross Metastases
Microscopic Metastases
Lung
Liver
Diaphragm
Intestines
Kidney
Spleen/Pancreas
PC-3M
PC-3M
PC-3
PC-3
LNCaP C4-2B
LNCaP C4-2B
LNCaP
LNCaP
Incidence of Distant Metastases (% mice)
Weeks Post Prostate Injection

Figure 6.12. The mesenchymal PC-3M and PC-3 human prostate cancer cell lines exhibit a greater capacity for metastasis and this correlates with CTC dissemination. ***(A)*** Incidence of metastasis to distant organs of PC-3M, PC-3, LNCaP C4-2B, and LNCaP prostate cancer cell lines based on gross observations at necropsy following orthotopic injection. Data are presented as the percentage of mice per cell line per time point with detectable distant metastases (n=7-39 mice/group). ***(B)*** The mean number of CTCs/50 µl of blood, assessed using the EMT semi-independent assay, are presented for mice with either metastasis to the lymph nodes or any distant organ (based on gross and/or microscopic analysis) or mice with no evidence of metastasis at any time point (n=6-47 mice/group). * = significantly different ($p \leq 0.05$).

A

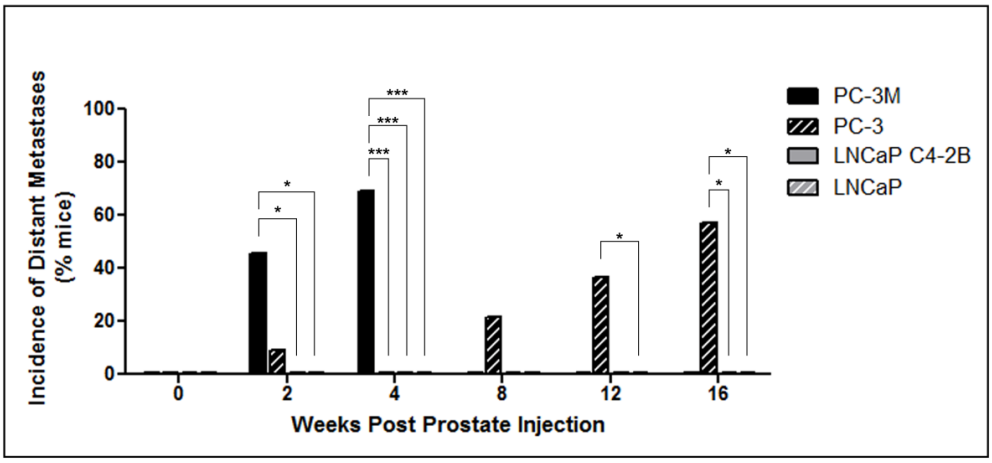
Incidence of Distant Metastases (% mice)
100
80
60
40
20
0
0
2
4
8
12
16
Weeks Post Prostate Injection
PC-3M
PC-3
LNCaP C4-2B
LNCaP
*
***

B

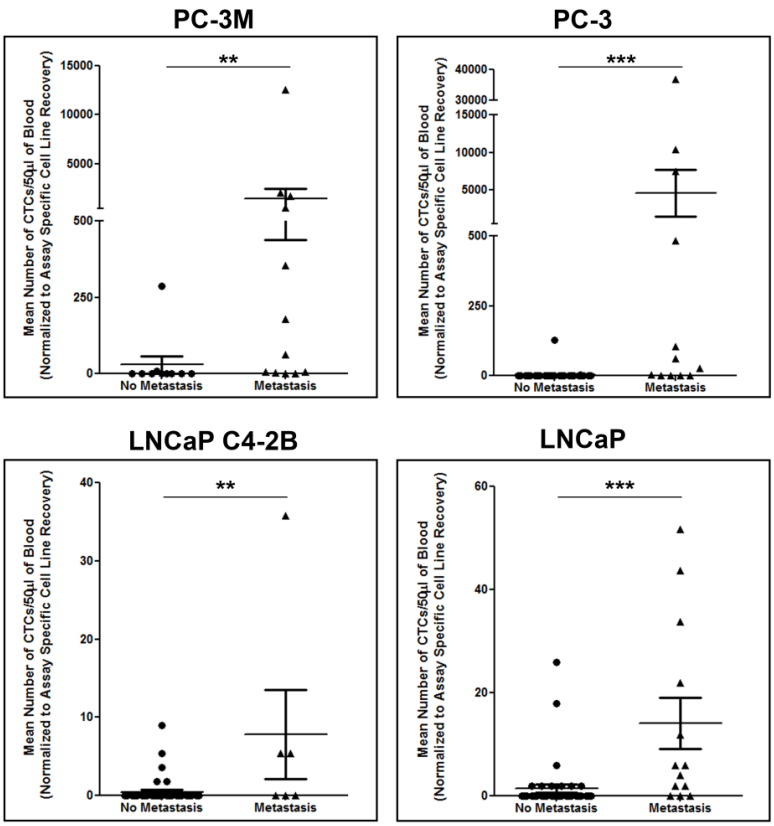
PC-3M
PC-3
LNCaP C4-2B
LNCaP
Mean Number of CTCs/5Qul of Blood (Normalized to Assay Specific Cell Line Recovery)
No Metastasis
Metastasis
**
***

6.3.5 Prostate cancer cell lines maintain their established EMT phenotypes *in vivo*

Although it appeared that cell lines with an increasingly mesenchymal phenotype had a higher capacity for CTC shedding and metastatic capacity, we wanted to confirm that the investigated cell lines demonstrated comparable epithelial and mesenchymal phenotypes *in vitro* and *in vivo*. Therefore immunohistochemistry was performed on tissue collected at necropsy for E-cadherin and N-cadherin expression (*Figure 6.13 and 6.14*). As expected, following orthotopic injection, primary tumors from all investigated cell lines displayed E-cadherin and N-cadherin expression in patterns similar to that seen using *in vitro* analysis techniques (western blot and FCM; *Figure 6.13*). However, interestingly, it did appear that the PC-3M cell line expressed a low level of E-cadherin *in vivo*, versus nearly absent expression *in vitro* (*Figure 6.2 and 6.3*). Additionally, immunohistochemistry performed on metastases from each cell line to the lymph nodes and lung showed similar expression for these markers in the mesenchymal cell lines, however slight increases in N-cadherin expression were noted in the lymph nodes and lungs for the LNCaP and LNCaP C4-2B cell lines respectively (*Figure 6.14*). However, further assessment of this trend will need to be explored in all mice positive for metastases to the lymph nodes and/or lungs to confirm this result.

6.3.6 Circulating tumor cells acquire a more mesenchymal phenotype during disease progression

To further investigate the EMT profile of CTCs shed into the circulation, blood that was not utilized for CTC analysis using the EMT dependent and EMT semi-independent assays was used to generate CTC sublines representing different timepoints along the metastatic cascade. Unfortunately due to the low number of CTCs collected

Figure 6.13. Prostate cancer cell lines maintain their established EMT phenotypes when forming primary tumors *in vivo*. PC-3M, PC-3, LNCaP C4-2B, and LNCaP prostate cancer cells were orthotopically injected into 6-8 week old male nude mice via the right dorsolateral lobe of the prostate ($1x10^6$ cells/mouse). At 2 weeks post injection mice were sacrificed and prostate tissue was collected, formalin fixed, and assessed for tumour cells using standard H&E staining, as well as immunohistochemistry for E-cadherin (red) and N-**cadherin** (brown) expression on selected animals. Sections stained with hematoxylin alone (cells only) and appropriate secondary antibodies (secondary only) are presented as negative controls. Histological sections are presented at 40x magnification. Scale bars = 50 µm.

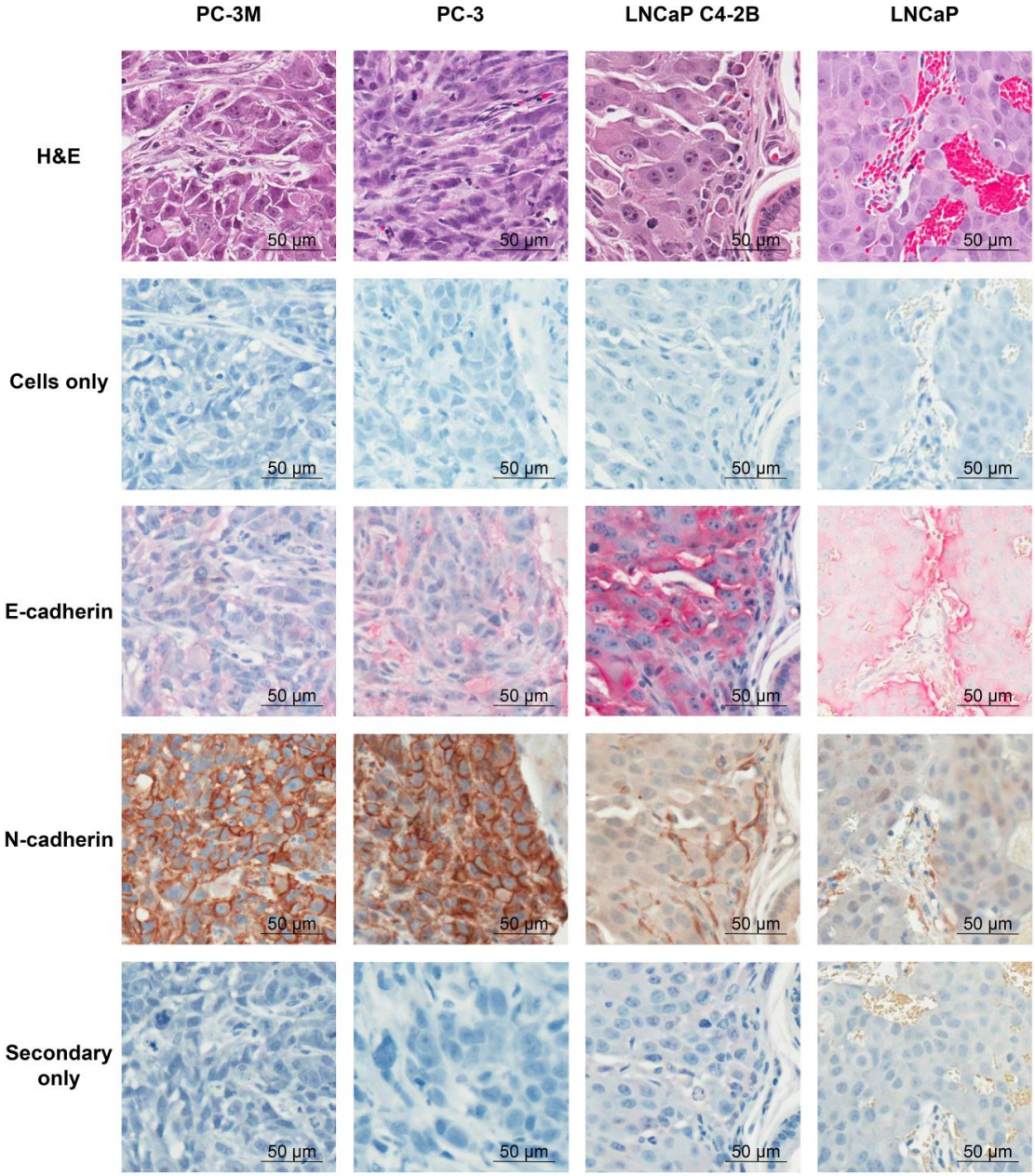
PC-3M
PC-3
LNCaP C4-2B
LNCaP
H&E
Cells only
E-cadherin
N-cadherin
Secondary only
50 µm

Figure 6.14. EMT phenotype may change between primary tumors and metastases *in vivo*. PC-3M, PC-3, LNCaP C4-2B, and LNCaP prostate cancer cells were orthotopically injected into 6-8 week old male nude mice via the right dorsolateral lobe of the prostate ($1x10^6$ cells/mouse). At various time points post injection mice were sacrificed and ***(A)*** lymph nodes and ***(B)*** lung were collected, formalin fixed, and assessed for tumour cells using standard H&E staining, as well as immunohistochemistry for E-cadherin (red) and N-cadherin (brown) expression. PC-3M and PC-3 cell lines demonstrate a similar EMT phenotype following metastatic dissemination to the lymph nodes and lung as that demonstrated using *in vitro* assays. However, some differences are observed in N-cadherin expression of the epithelial cell lines (LNCaP and LNCaP C4-2B) following dissemination. Histological sections are presented at 40x magnification. Arrowheads on H&E images indicate regions of tumour within the given tissue. Scale bars = 50 µm.

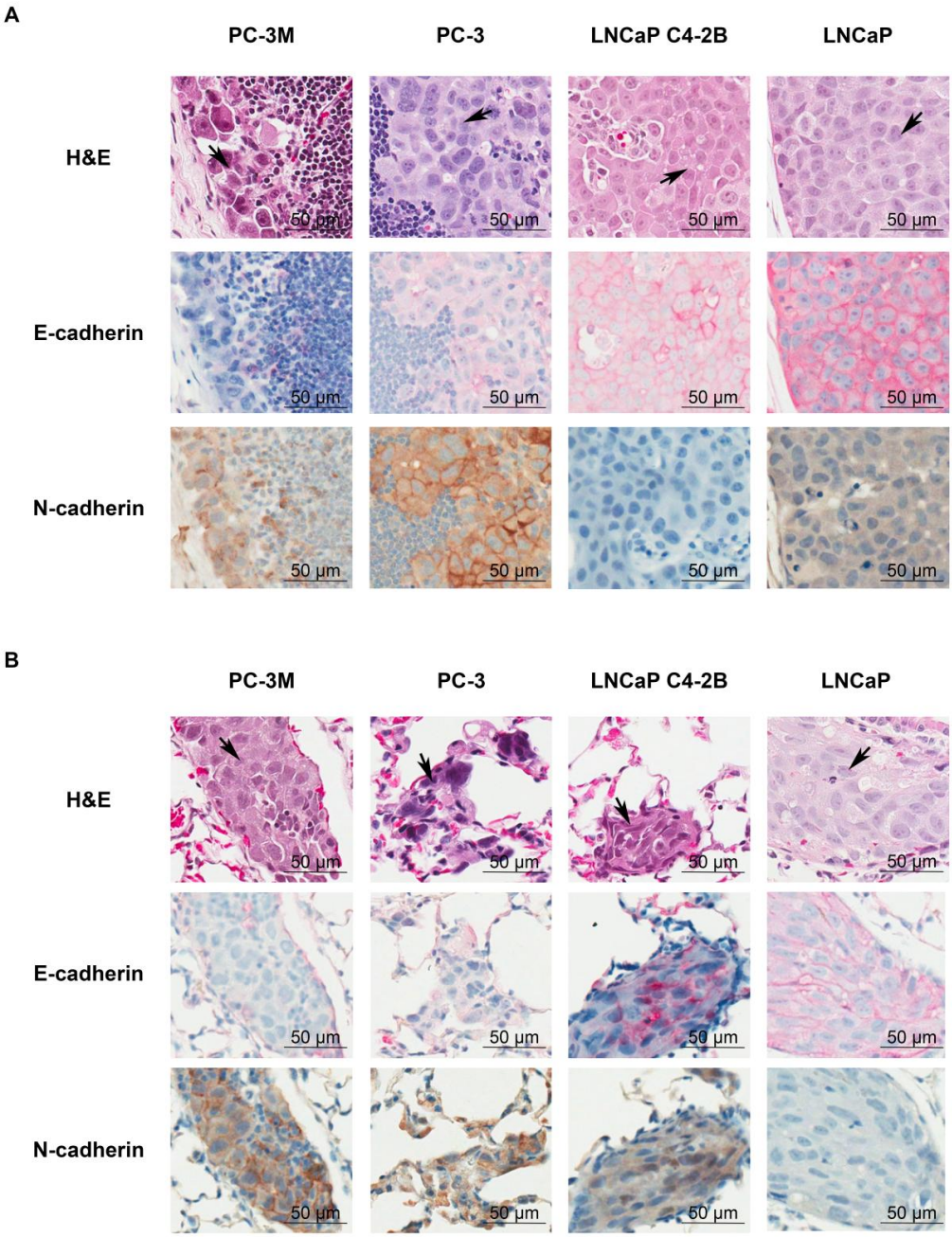
A
PC-3M
PC-3
LNCaP C4-2B
LNCaP
H&E
E-cadherin
N-cadherin
50 µm
B
PC-3M
PC-3
LNCaP C4-2B
LNCaP
H&E
E-cadherin
N-cadherin
50 µm

from the LNCaP and LNCaP C4-2B cell lines, CTC growth following plating did not occur. However several cell lines were created for both the PC-3 and PC-3M cell lines. To explore differences in EMT expression in CTCs, the PC-3 parental cell line (initially expressing a mesenchymal-like phenotype), as well as 3 sub lines collected at 8, 12, and 16 weeks, were assessed via western blot for expression of various EMT markers, including E-cadherin, N-cadherin, EpCAM, and vimentin. Based on this analysis, it was demonstrated that there is a significant reduction in E-cadherin expression in CTCs collected at all time points compared to the parental cell line ($p \leq 0.05$) (*Figure 6.15*). Additionally, there was an increase in N-cadherin expression at all timepoints, however this difference was only significantly different from the parental cell line at 12 and 16 weeks ($p \leq 0.05$). Although there was a trend toward a reduction in EpCAM and an increase in vimentin expression at all the timepoints investigated, the expression was not statistically different from the parental cell line. This data suggest that CTCs may become more mesenchymal as disease progresses, however additional analysis of the remaining CTC sublines will need to be conducted to validate these results.

6.4 Discussion

Although CTCs are now being utilized for prognostication in the clinical settings of metastastic breast, prostate and colorectal cancer, their underlying biology remains poorly understood. This lack of information stems from both the unique bedside-to-bench approach that has been employed in the CTC field, as well as the lack of appropriate tools for studying CTCs *in vivo* in pre-clinical models of metastasis. Inadequate knowledge in the area of CTC biology has ultimately led to confusion with

Figure 6.15. Circulating tumour cells acquire a more mesenchymal phenotype during disease progression. Following orthotopic injection of PC-3 prostate cancer cells into the right dorsolateral lobe of the prostate (1×10^6 cells/mouse) blood collected at 8 weeks, 12 weeks, and 16 weeks post-injection was lysed with sterile 1x NH_4Cl, washed with PBS, and plated for tissue culture. Following 1-2 weeks of growth, with regular media changes to remove contaminating blood cells, the remaining CTCs were assessed using western blot for the expression of the epithelial-associated markers E-cadherin and EpCAM and the mesenchymal-associated markers N-cadherin and vimentin. Results are presented in quantitative densitometric form normalized to β-actin and as representative western blots, shown as cropped gel images (n=3).

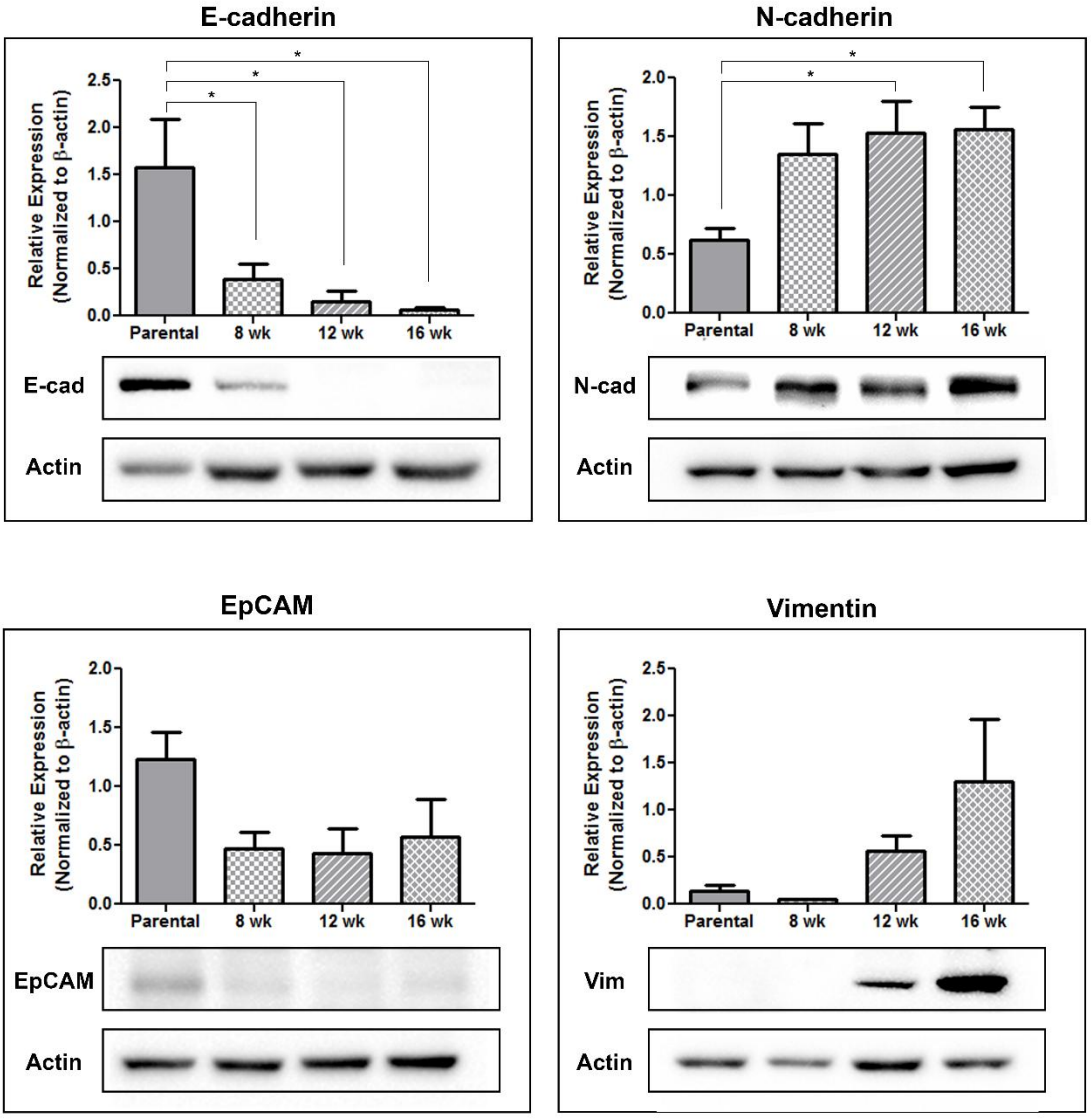
E-cadherin
Relative Expression (Normalized to β-actin)
2.5
2.0
1.5
1.0
0.5
0.0
*
*
*
Parental
8 wk
12 wk
16 wk
E-cad
Actin
N-cadherin
Relative Expression (Normalized to β-actin)
2.0
1.5
1.0
0.5
0.0
*
*
Parental
8 wk
12 wk
16 wk
N-cad
Actin
EpCAM
Relative Expression (Normalized to β-actin)
2.0
1.5
1.0
0.5
0.0
Parental
8 wk
12 wk
16 wk
EpCAM
Actin
Vimentin
Relative Expression (Normalized to β-actin)
2.5
2.0
1.5
1.0
0.5
0.0
Parental
8 wk
12 wk
16 wk
Vim
Actin

regards to which CTCs are the most valuable to capture, and which will serve as the best tools for personalized cancer treatment based on CTC molecular characterization. We believe that improved understanding of the biology of CTCs and how these cells relate to the dynamic processes of EMT and metastasis will provide important translational information that will help inform the use of CTCs as valuable biomarkers of cancer progression in the clinic.

In the current study we have utilized 2 CTC enumeration assays to assess the differences in CTC capture using the epithelial-based CSS (EMT-dependent) and a human versus mouse based (EMT semi-independent) capture technique to assess the generation of mesenchymal CTCs that would be missed by current technologies. Additionally, we performed a comprehensive assessment of the EMT phenotype in 4 of the most commonly utilized prostate cancer cell lines and compared the potential of these cell lines for CTC generation and metastasis.

Significant effort is currently being focused on the development of CTC capture techniques capable of recovering not only CTCs expressing epithelial markers (i.e., EpCAM and CK), but also those with a highly mesenchymal phenotype. This pursuit is largely based on the current understanding of EMT, specifically regarding phenotypes imparted by this process on the primary tumor (i.e., enhanced invasiveness, increased metastatic capacity, reduced apoptosis, improved therapy resistance, and the generation of stem cell-like properties). However, the results of the current study demonstrate that although prostate cancer cell lines with an increasingly mesenchymal phenotype shed more CTCs early in disease compared to epithelial cell lines, the majority of CTCs shed from these mesenchymal cells are captured, at least before the

establishment of metastatic disease, by the CSS. This thereby suggests that CTCs shed early in disease have a hybrid EMT phenotype and still express sufficient levels of EpCAM and CK 8/18/19 for detection using epithelial-based techniques. While the observation that cell lines with an increasingly mesenchymal phenotype are more invasive and metastatic is not surprising[17], it appears that CTCs with a hybrid phenotype may be those that are most important for establishing metastasis and therefore the most interesting to characterize, at least in early-stage patients. In fact, some have suggested that CTCs with a hybrid phenotype may be of particular importance based on their plasticity for EMT and MET related phenotypic changes[27].

Based upon our data, however, it appears that following the establishment of distant metastases there is a significant increase in the number of mesenchymal CTCs that are undetectable by the CSS. This increase in the mesenchymal characteristics of CTCs in later stage disease has also been demonstrated in clinical samples with a number of studies reporting an increase in CTCs (captured by epithelial methods) expressing mesenchymal markers in metastatic versus primary breast cancer patients[48,49]. Therefore further studies are needed to determine if and how these undetectable CTCs are contributing to disease progression and metastasis.

Despite widespread speculation, there is very little evidence in the literature to support the hypothesis that CTCs with a highly mesenchymal phenotype have any additional prognostic value compared to CTCs with a hybrid epithelial-mesenchymal phenotype or even a purely epithelial phenotype in patient samples. However, we must consider that technological limitations with regards to mesenchymal CTC capture may significantly hinder the ability to test this hypothesis in the clinic. In addition, we cannot

rule out the possibility that highly mesenchymal CTCs are present in early-stage disease but not in high enough number to significantly contribute to differences between the 2 assays presented here. In fact, the cancer stem cell (CSC) hypothesis posits that only a small number of cells that make up the bulk primary tumor efficiently complete the metastatic process[50]. Based upon this theory it is possible that the dramatic increase in mesenchymal CTCs following the development of metastases is due to a selective outgrowth of highly mesenchymal CSCs. Therefore, although this study provides many valuable insights into the role of EMT in CTC dissemination and kinetics, many questions remain, for which the assays developed here will be very useful in answering.

In addition to the contributions this manuscript makes towards understanding CTC biology and its relationship to EMT, to our knowledge it is also the first comprehensive head-to-head comparison and EMT characterization of the *in vivo* behavior of 4 of the most commonly utilized cell lines in prostate cancer research. Specifically, this manuscript describes the EMT phenotype of the PC-3M, PC-3, LNCaP C4-2B, and LNCaP cell lines at both the mRNA and protein level. It also details differences in primary tumor incidence, CTC dissemination and kinetics, and metastatic capacity to multiple organs. This will therefore serve as an incredibly valuable tool for future research in the field of prostate cancer.

Overall the results presented here highlight that how CTC characterization is utilized in a clinical setting may greatly depend on disease stage. Specifically, in early-stage patients, it has been suggested by our group and others that the use of novel CTC technologies capable of capturing highly mesenchymal CTCs could result in an increase in the overall number of detectable CTCs and thereby increase the potential prognostic

power of CTCs in these patients. However, our data suggest that the application of these novel technologies may not lead to a dramatic increase in CTC enumeration in these patients and that instead the detection of an increased number of CTCs will require the processing of additional blood (>7.5mL) on traditional epithelial-based CTC detection technologies such as the CSS. In addition, the data also suggest, as has been previously reported[17], that primary tumors with an increasingly mesenchymal phenotype may have an enhanced metastatic capacity and therefore the detection of CTCs with a hybrid phenotype may be of prognostic importance in these patients. In contrast, when considering metastatic patients, we have demonstrated a significant increase in undetectable highly mesenchymal CTCs. Therefore further research in this patient cohort will need to examine the functional role of these CTCs versus those with an epithelial or hybrid phenotype in disease progression and, importantly, in therapy resistance. Ultimately a better understanding of the biology of CTCs will aid in the identification of those cells that would be most valuable for determining individualized treatment.

6.5 References

1 Canadian Cancer Statistics, 2015. Toronto: Canadian Cancer Society 2015. Available at: www.cancer.ca. .

2 Chambers AF, Groom AC, MacDonald IC. Dissemination and growth of cancer cells in metastatic sites. *Nat Rev Cancer* 2002; **2**: 563–72.

3 Pantel K, Brakenhoff RH, Brandt B. Detection, clinical relevance and specific biological properties of disseminating tumour cells. *Nat Rev Cancer* 2008; **8**: 329–40.

4 Cristofanilli M, Budd GT, Ellis MJ, Stopeck A, Matera J, Miller MC *et al.* Circulating tumor cells, disease progression, and survival in metastatic breast cancer. *N Engl J Med* 2004; **351**: 781–91.

5 Cohen SJ, Punt CJ a, Iannotti N, Saidman BH, Sabbath KD, Gabrail NY *et al.* Prognostic significance of circulating tumor cells in patients with metastatic colorectal cancer. *Ann Oncol* 2009; **20**: 1223–9.

6 De Bono JS, Scher HI, Montgomery RB, Parker C, Miller MC, Tissing H *et al.* Circulating tumor cells predict survival benefit from treatment in metastatic castration-resistant prostate cancer. *Clin Cancer Res* 2008; **14**: 6302–9.

7 Olmos D, Arkenau H-T, Ang JE, Ledaki I, Attard G, Carden CP *et al.* Circulating tumour cell (CTC) counts as intermediate end points in castration-resistant prostate cancer (CRPC): a single-centre experience. *Ann Oncol* 2009; **20**: 27–33.

8 Allan AL, Keeney M. Circulating tumor cell analysis: technical and statistical considerations for application to the clinic. *J Oncol* 2010; **2010**: 426218.

9 Hu XC, Chow LW. Detection of circulating breast cancer cells by reverse transcriptase polymerase chain reaction (RT-PCR). *Eur J Surg Oncol* 2000; **26**: 530–5.

10 Baker MK, Mikhitarian K, Osta W, Callahan K, Hoda R, Brescia F *et al.* Molecular detection of breast cancer cells in the peripheral blood of advanced-stage breast cancer patients using multimarker real-time reverse transcription-polymerase chain reaction and a novel porous barrier density gradient centrifugation technology. *Clin Cancer Res* 2003; **9**: 4865–71.

11 Ntouroupi TG, Ashraf SQ, McGregor SB, Turney BW, Seppo A, Kim Y *et al.* Detection of circulating tumour cells in peripheral blood with an automated scanning fluorescence microscope. *Br J Cancer* 2008; **99**: 789–795.

12 Rosenberg R, Gertler R, Friederichs J, Fuehrer K, Dahm M, Phelps R *et al.* Comparison of two density gradient centrifugation systems for the enrichment of disseminated tumor cells in blood. *Cytometry* 2002; **49**: 150–8.

13 Beitsch PD, Clifford E. Detection of carcinoma cells in the blood of breast cancer patients. *Am J Surg* 2000; **180**: 446–9.

14 Cruz I, Ciudad J, Cruz JJ, Ramos M, Gómez-Alonso A, Adansa JC *et al.* Evaluation of multiparameter flow cytometry for the detection of breast cancer tumor cells in blood samples. *Am J Clin Pathol* 2005; **123**: 66–74.

15 Wu LY, Liu T, Grimm AL, Davis WC, Berkman CE. Flow cytometric detection of prostate tumor cells using chemoaffinity labels. *Prostate* 2010.

16 Allard WJ, Matera J, Miller MC, Repollet M, Connelly MC, Rao C *et al.* Tumor cells circulate in the peripheral blood of all major carcinomas but not in healthy

subjects or patients with nonmalignant diseases. *Clin Cancer Res* 2004; **10**: 6897–904.

17 Thiery JP, Acloque H, Huang RYJ, Nieto MA. Epithelial-mesenchymal transitions in development and disease. *Cell* 2009; **139**: 871–90.

18 Yang J, Weinberg R a. Epithelial-mesenchymal transition: at the crossroads of development and tumor metastasis. *Dev Cell* 2008; **14**: 818–29.

19 Joosse SA, Gorges TM, Pantel K. Biology, detection, and clinical implications of circulating tumor cells. *EMBO Mol Med* 2015; **7**: 1–11.

20 Gorges TM, Tinhofer I, Drosch M, Röse L, Zollner TM, Krahn T *et al.* Circulating tumour cells escape from EpCAM-based detection due to epithelial-to-mesenchymal transition. *BMC Cancer* 2012; **12**: 178.

21 Santisteban M, Reiman JM, Asiedu MK, Behrens MD, Nassar A, Kalli KR *et al.* Immune-induced epithelial to mesenchymal transition in vivo generates breast cancer stem cells. *Cancer Res* 2009; **69**: 2887–2895.

22 Gradilone A, Raimondi C, Nicolazzo C, Petracca A, Gandini O, Vincenzi B *et al.* Circulating tumour cells lacking cytokeratin in breast cancer: the importance of being mesenchymal. *J Cell Mol Med* 2011; **15**: 1066–70.

23 Königsberg R, Obermayr E, Bises G, Pfeiler G, Gneist M, Wrba F *et al.* Detection of EpCAM positive and negative circulating tumor cells in metastatic breast cancer patients. *Acta Oncol* 2011; **Epub**: Epub.

24 Kasimir-Bauer S, Hoffmann O, Wallwiener D, Kimmig R, Fehm T. Expression of stem cell and epithelial-mesenchymal transition markers in primary breast cancer patients with circulating tumor cells. *Breast Cancer Res* 2012; **14**: R15.

25 Mego M, Mani SA, Lee B-N, Li C, Evans KW, Cohen EN *et al.* Expression of epithelial-mesenchymal transition-inducing transcription factors in primary breast cancer: The effect of neoadjuvant therapy. *Int J Cancer* 2011. doi:10.1002/ijc.26037.

26 Yu M, Bardia A, Wittner BS, Stott SL, Smas ME, Ting DT *et al.* Circulating breast tumor cells exhibit dynamic changes in epithelial and mesenchymal composition. *Science* 2013; **339**: 580–4.

27 Armstrong AJ, Marengo MS, Oltean S, Kemeny G, Bitting RL, Turnbull JD *et al.* Circulating tumor cells from patients with advanced prostate and breast cancer display both epithelial and mesenchymal markers. *Mol Cancer Res* 2011; **9**: 997–1007.

28 Goodale D, Phay C, Postenka CO, Keeney M, Allan AL. Characterization of tumor cell dissemination patterns in preclinical models of cancer metastasis using flow cytometry and laser scanning cytometry. *Cytometry A* 2009; **75**: 344–55.

29 Allan AL, Vantyghem S a, Tuck AB, Chambers AF, Chin-Yee IH, Keeney M. Detection and quantification of circulating tumor cells in mouse models of human breast cancer using immunomagnetic enrichment and multiparameter flow cytometry. *Cytometry A* 2005; **65**: 4–14.

30 Horoszewicz JS, Leong SS, Chu TM, Wajsman ZL, Friedman M, Papsidero L *et al.* The LNCaP cell line--a new model for studies on human prostatic carcinoma. *Prog Clin Biol Res* 1980; **37**: 115–132.

31 Kozlowski JM, Fidler IJ, Campbell D, Xu ZL, Kaighn ME, Hart IR. Metastatic behavior of human tumor cell lines grown in the nude mouse. *Cancer Res* 1984; **44**: 3522–3529.
32 Thalmann GN, Anezinis PE, Chang SM, Zhau HE, Kim EE, Hopwood VL *et al.* Androgen-independent cancer progression and bone metastasis in the LNCaP model of human prostate cancer. *Cancer Res* 1994; **54**: 2577–2581.
33 Kaighn ME, Narayan KS, Ohnuki Y, Lechner JF, Jones LW. Establishment and characterization of a human prostatic carcinoma cell line (PC-3). *Invest Urol* 1979; **17**: 16–23.
34 Price JE, Polyzos A, Zhang RD, Daniels LM. Tumorigenicity and metastasis of human breast carcinoma cell lines in nude mice. *Cancer Res* 1990; **50**: 717–721.
35 Scherer WF, Syverton JT, Gey GO. Studies on the propagation in vitro of poliomyelitis viruses. IV. Viral multiplication in a stable strain of human malignant epithelial cells (strain HeLa) derived from an epidermoid carcinoma of the cervix. *J Exp Med* 1953; **97**: 695–710.
36 Pfaffl M. Quantification strategies in real-time PCR Michael W . Pfaffl. In: Bustin SA (ed). *A-Z of quantitative PCR*. International University Line (IUL): La Jolia, 2004, pp 87–112.
37 Lowes LE, Hedley BD, Keeney M, Allan AL. Adaptation of semiautomated circulating tumor cell (CTC) assays for clinical and preclinical research applications. *J Vis Exp* 2014; : e51248.
38 Thalmann GN, Sikes RA, Wu TT, Degeorges A, Chang SM, Ozen M *et al.* LNCaP progression model of human prostate cancer: Androgen-independence and osseous metastasis. *Prostate* 2000; **44**: 91–103.
39 Valta MP, Tuomela J, Vuorikoski H, Loponen N, Väänänen RM, Pettersson K *et al.* FGF-8b induces growth and rich vascularization in an orthotopic PC-3 model of prostate cancer. *J Cell Biochem* 2009; **107**: 769–784.
40 Stephenson RA, Dinney CP, Gohji K, Ordóñez NG, Killion JJ, Fidler IJ. Metastatic model for human prostate cancer using orthotopic implantation in nude mice. *J Natl Cancer Inst* 1992; **84**: 951–957.
41 Shah G V., Thomas S, Muralidharan A, Liu Y, Hermonat PL, Williams J *et al.* Calcitonin promotes in vivo metastasis of prostate cancer cells by altering cell signaling, adhesion, and inflammatory pathways. *Endocr Relat Cancer* 2008; **15**: 953–964.
42 Fu Z, Smith PC, Zhang L, Rubin MA, Dunn RL, Yao Z *et al.* Effects of raf kinase inhibitor protein expression on suppression of prostate cancer metastasis. *J Natl Cancer Inst* 2003; **95**: 878–889.
43 Pettaway CA, Pathak S, Greene G, Ramirez E, Wilson MR, Killion JJ *et al.* Selection of Highly Metastatic Variants of Different Human Prostatic Carcinomas Using Orthotopic Implantation in Nude Mice. *Clin Cancer Res* 1996; **2**: 1627–1636.
44 Nagafuchi A, Takeichi M. Cell binding function of E-cadherin is regulated by the cytoplasmic domain. *EMBO J* 1988; **7**: 3679–3684.
45 Ozawa M, Ringwald M, Kemler R. Uvomorulin-catenin complex formation is regulated by a specific domain in the cytoplasmic region of the cell adhesion molecule. *Proc Natl Acad Sci U S A* 1990; **87**: 4246–4250.

46 Morton RA, Ewing CM, Nagafuchi A, Tsukita S, Isaacs WB. Reduction of E-cadherin levels and deletion of the alpha-catenin gene in human prostate cancer cells. *Cancer Res* 1993; **53**: 3585–3590.

47 Gosens MJEM, van Kempen LCL, van de Velde CJH, van Krieken JHJM, Nagtegaal ID. Loss of membranous Ep-CAM in budding colorectal carcinoma cells. *Mod Pathol* 2007; **20**: 221–232.

48 Papadaki MA, Kallergi G, Zafeiriou Z, Manouras L, Theodoropoulos PA, Mavroudis D *et al*. Co-expression of putative stemness and epithelial-to-mesenchymal transition markers on single circulating tumour cells from patients with early and metastatic breast cancer. *BMC Cancer* 2014; **14**: 1–10.

49 Kallergi G, Papadaki MA, Politaki E, Mavroudis D, Georgoulias V, Agelaki S. Epithelial to mesenchymal transition markers expressed in circulating tumour cells of early and metastatic breast cancer patients. Breast Cancer Res. 2011; **13**: R59.

50 Nguyen DX, Bos PD, Massagué J. Metastasis: from dissemination to organ-specific colonization. *Nat Rev Cancer* 2009; **9**: 274–284.

Chapter 7
Overall Discussion

Prostate cancer (PCa) is a leading cause of death in men and the majority of these deaths result from metastatic spread[1,2]. The presence of circulating tumor cells (CTCs) is associated with metastatic disease and has been demonstrated to be prognostic in metastatic prostate cancer patients, predicting for progression-free and overall survival[3]. Prior to the initiation of this work, CTCs were utilized almost exclusively in the metastatic setting with little known about their role in early-stage PCa[3,4]. Additionally, significant focus had been placed on the characterization of CTCs and their potential for optimizing patient treatment with limited understanding of the underlying biology of these cells[5–7]. This lack of exploration of CTC biology was due, in large part, to inadequate tools for studying CTCs in experimental mouse models of metastasis. Therefore this thesis aimed to investigate the role of CTCs in early-stage prostate cancer and assess their potential for determining prognosis as has been demonstrated for metastatic patients[3,8]. Additionally, we sought to provide detailed protocols that would allow users of the regulatory-approved CellSearch® system (CSS) to capitalize on its potential for CTC molecular characterization and to develop novel tools that would allow for detailed investigation of the biology of CTCs.

7.1 Summary of key experimental findings

1. CTCs are detectable in early-stage PCa patients post-prostatectomy undergoing treatment with adjuvant or salvage radiation therapy (RT) for recurrent or residual disease.
2. The CTC status (presence/absence) of PCa patients in the adjuvant and salvage settings correlates with the clinical observations of local versus systemic relapse associated with previously described clinicopathologic risk factors (margin status, extracapsular extension [ECE], and seminal vesicle invasion [SVI]), suggesting that CTCs may relate to disease localization in these patients.
3. The presence of either ECE or SVI in combination with CTC^{pos} disease prior to RT in adjuvant and salvage PCa patients predicts for poorer response to localized treatment compared to CTC^{neg} patients with the same clinicopathologic risk factors. In addition, CTC^{pos} status at any point throughout treatment correlated significantly with time to biochemical failure (BCF) and incidence of BCF at 2 years. This suggests that the addition of CTCs to a patient's clinicopathologic "risk profile" (ECE, SVI, and margin status) may further enhance our ability to discriminate patients with localized versus systemic recurrence.
4. Although promising in theory, the detailed process of optimization required for the development of user-defined markers on the CSS requires significant work-up with rigorous controls. In addition, not all markers may be suitable

candidates for use with this platform and therefore marker selection should be carefully considered.

5. Prostate cancer cell lines display differences in EMT status at both the RNA and protein level. Cell lines with an increasingly mesenchymal phenotype (PC-3M and PC-3) demonstrate an enhanced capacity for CTC generation and metastasis when compared to cell lines with a more epithelial phenotype.

6. CTCs with a highly mesenchymal phenotype may be undetectable by epithelial-based detection systems. However, these undetectable CTCs only appear in significant number following the establishment of metastatic disease.

7.2 Implications of experimental findings

7.2.1 Circulating tumor cells are detectable in early-stage prostate cancer patients and may be useful in guiding clinical decision-making

When this work was first initiated, CTC enumeration and characterization was being utilized almost exclusively in the setting of metastatic disease and very little research was exploring the prognostic value of these rare cells in patients with early-stage disease[3,4,8–11]. Current research has begun to focus on the clinical value of CTCs in early-stage patients, however the majority of this research has been performed in non-standardized systems that do not have FDA or Health Canada approval for use in the clinic[4,12–16]. Our group was the first to describe the detection and enumeration of CTCs in early-stage PCa patients undergoing salvage or adjuvant radiation therapy using the only regulatory-approved CTC technology, the CSS[17]. In addition, we also demonstrated that CTCs may contribute to a patient's clinicopathologic risk profile and that the detection of

CTCs prior to or following localized treatment with radiation therapy may be an indicator of residual/recurrent disease and ultimately treatment failure.

This data suggests that the detection of CTCs at any disease stage may be a sign of the potential for metastatic spread, regardless of the clinical confirmation of macrometastatic disease. CTCs, especially those detected early, may alert clinicians of aggressive disease sooner than currently used techniques thereby suggesting that more aggressive treatment options should be considered for these patients and/or that these patients may be spared unnecessary localized treatments[8,9,11,18]. Additionally, these results provide clinical support that CTCs shed early aid in the establishment of micrometastatic disease and these CTCs may be of particular value for CTC characterization.

Unfortunately based on the low number of CTCs detected in these patient cohorts, characterization would require either additional blood (>7.5ml) to be processed if using the CSS or for novel CTC technologies with greater sensitivity to be utilized in this regard. However, CTC characterization in these patient populations may provide valuable clinical information regarding which CTCs have the greatest capacity for metastatic dissemination. In fact, characterizing CTCs in early-stage patients may be of particular value as the disease will have had less opportunity for significant mutation, as compared to patients with metastatic disease, and may better represent the phenotype of the cells that are capable of metastasis. Additionally, identifying the CTCs with the greatest metastatic capacity may be easier in early-stage patients as there will be fewer "contaminating" CTCs with phenotypes that do not necessarily represent the phenotype of metastasis-initiating CTCs. Currently, there is a need for novel biomarkers that could

be utilized for prognosis in clinically challenging early-stage patients. Our data suggests that CTCs may serve as a valuable tool for clinical decision-making in early-stage PCa.

7.2.2 Novel tools developed throughout this thesis will be important for future work in the area of CTC biology and in clinical samples

The field of CTC research is exceedingly reliant on appropriate technology development. The rarity of CTCs in the bloodstream presents significant challenges for the detection, enumeration, and characterization of these cells. Additionally, the overwhelming number of technologies developed in recent years has made the field extremely complicated and made choosing an appropriate technology for both clinical and research uses difficult[19–21]. However, thus far the only CTC platform approved for use in the clinic is the CSS, thereby making it the current gold standard in CTC technology[3,10,11]. It is for this reason that throughout the course of this thesis we have provided a detailed description of common discrepancies encountered during CTC enumeration from clinical samples and a guide to CTC molecular characterization using the CSS that will aid users of this platform in the development of user-defined protein markers[22,23]. In addition, we have also provided novel techniques that can be utilized to study CTCs in pre-clinical mouse models of metastasis[22]. These tools hold particular value as they not only allow for the study of CTC biology based on CTCs that would be captured by the gold standard technology, but also allow for the study of CTCs that would be missed using this system. Although CTC enumeration has previously been performed in *in vivo* model systems, due to the capture methods utilized, these results do not necessarily represent the results that would be obtained using the CSS[24,25]. Particularly in this field, where CTCs are extremely rare, there can be dramatic

differences in the sensitivity and specificity of given assays and these results are not necessarily able to be generalized to all other platforms[26–29]. Ultimately these tools will allow users of the CSS to capitalize on its limited potential for CTC characterization and also to investigate important biological questions regarding the CTCs which are both captured and missed by the standard clinical assay used on this platform.

7.2.3 Prostate tumors displaying a mesenchymal phenotype may predict for an enhanced capacity for CTC shedding and metastatic spread of disease.

While the observation that the epithelial-to-mesenchymal transition (EMT) imparts cells with an enhanced capacity for invasion and migration[30], very little is known about the influence EMT has on CTC generation and the timing of metastasis. The data presented in this thesis indicates that primary prostate tumors that possess an increasingly mesenchymal phenotype will have an enhanced capacity for CTC generation and metastasis. Ultimately this suggests that further investigation of the EMT status of primary tumor specimens and their impact on patient prognosis may be warranted. In fact, a number of studies have performed such investigations and demonstrated a correlation between EMT status and patient outcomes[31–33]. Additionally, not only did we demonstrate that mesenchymal primary tumors may shed more CTCs than those with an epithelial phenotype, but also that these CTCs may be shed earlier in disease. From a clinical perspective, this therefore suggests that patients with mesenchymal primary tumors may already have undetectable micrometastatic disease at the time of diagnosis and therefore are at greater risk for metastatic dissemination and subsequent relapse following localized first-line treatments. Therefore incorporating analysis of EMT status of primary tumors into a patient's clinicopathologic risk profile may improve the ability

to discriminate patients with aggressive versus indolent disease and ultimately improve our ability to choose appropriate treatment options for PCa patients.

7.2.4 Technologies aimed at capturing mesenchymal CTCs may fail to enhance the prognostic value of CTCs in the setting of early disease

One interesting observation that was made using our *in vivo* model of PCa metastasis was that highly mesenchymal CTCs that are undetectable by the standard CSS assay are not shed in significant numbers until the establishment of metastatic disease. This result suggests that CTCs with a purely epithelial and/or hybrid EMT phenotype are those capable of establishing initial metastases and that novel technologies aimed at capturing these cells will not enhance the prognostic value of CTCs in the setting of early disease. Alternatively (or additionally), highly mesenchymal CTCs capable of metastasis are very rare at the early stages of metastatic dissemination and present only in very low numbers, thereby making them difficult to visualize using these assays and only noticeable after metastatic dissemination and selective outgrowth of these aggressive clones. Either way, this suggests that the clinical value of CTC molecular characterization may be greatly affected by the patient population chosen for proof-of-principle studies. Until the importance of these highly mesenchymal, undetectable CTCs are understood from a biological perspective, careful consideration must be made when choosing these patient cohorts for clinical trials and assay validation.

This data may also have a significant impact on how we view EMT and cellular plasticity. Currently much focus is being placed on finding highly mesenchymal CTCs as they are viewed as the most aggressive and valuable to characterize[34–42]. However this may not be the case and CTCs with a hybrid phenotype, allowing for quick

phenotypic switching may be more important, as has been previously suggested[43,44]. This data also suggests that the mixed results seen in clinical trials examining the utilization of CTC molecular characterization for individualized cancer treatments may be due to a lack of understanding of the biology of these cells, resulting in inappropriate trial design, and not due to lack of appropriate technologies for capturing CTCs that are highly mesenchymal[45–49].

7.3 Possible limitations of the thesis work

The data presented throughout this thesis has described novel findings in the areas of CTC biology, clinical uses, and technology development. Although these results represent significant contributions to the field of CTC research and PCa metastasis, as with all research, there are limitations that exist. These limitations are discussed below.

7.3.1 Clinical studies

In Chapter 2, we performed a pilot study in 26 early-stage PCa patients consented to undergo salvage RT. From this small patient cohort we found that CTCs were detectable in ~70% of these patients. In this study, we also demonstrated that changes in CTC number (increased, decreased, or unchanged) before initiation and following completion of salvage RT correlated with BCF[17]. However, these results were only correlative, and no significant differences were observed. Regardless, we anticipated that significant results would be possible by increasing the number of accrued patients and therefore we sought to recruit 55 patients for a follow-up study. In addition, based on the high CTC detection rate demonstrated in the first study (~70%) we also decided to include patients in the adjuvant setting, thus reducing the number of salvage patients

accrued. Unfortunately in the follow-up study presented in Chapter 3, the number of patients with detectable CTCs dropped significantly to ~15% and therefore limited the statistical power of our follow-up study. The choice to include patients from both the adjuvant and salvage settings may have limited our analysis of results from both cohorts and the selection to study either salvage or adjuvant patients may have led to more conclusive data.

Additionally, analysis of the results from Chapters 2 and 3 were also limited due to the low number of CTCs detected in individual patients, with the vast majority having CTC counts of ≤ 2 and only 1 patient having 5 CTCs (the number that predicts for poor outcomes in metastatic PCa[3]). If financially feasible, it may have been beneficial to increase the amount of blood collected and processed at each time point from individual patients (>7.5mL). The detection of additional CTCs would reduce the potential for false negative and positive results and likely increase the number of patients in the CTC^{pos} group, thereby enhancing the statistical power of this study. The detection of more CTCs in the follow-up study would have allowed for comparison of pre- and post-treatment numbers (increased, decreased, or unchanged), as was performed in the pilot study[17] and utilized for patients in the metastatic setting[8], which may be more informative then the presence or absence of CTCs alone.

Finally, during the analysis of the follow-up study a small group of patients (n=3) initially presenting in the adjuvant setting shortly thereafter were found to have a detectable PSA and were instead considered salvage patients by the time of RT initiation. These patients in particular appeared to be more likely to have CTC^{pos} disease (66%) compared to the patients with less aggressive disease. Therefore we anticipate that more

conclusive results may have been possible if stricter inclusion criteria were set that selected for patients with intermediate or high-risk disease. However, it is also important to consider that these stricter criteria would likely have significantly slowed patient accrual as there may have been fewer patients presenting in this setting and fewer may have been recommended for RT.

7.3.2 Technology development studies

Although the protocol described in Chapter 4 outlined the proper development of user-defined protein markers for on-system CTC molecular characterization, the optimization of these assays requires the use of cell lines with known protein expression and relative antigen density comparisons. For example, when optimizing the CD44 marker for use with the CSS, a panel of cell lines were chosen to represent high (MDA-MB-468), low (21NT), and negative (LNCaP) expression of this marker. However, in doing so, assumptions are being made regarding the expression levels of this protein in patient samples, which could be much higher (leading to significant bleed-through and misclassification of CTCs) or much lower (leading to false negatives) than anticipated. Therefore, comparison and validation of user-defined protein markers in patient samples should be considered as the final optimization step. Unfortunately this was not performed here. In addition, we have demonstrated that not all user-defined protein markers can be properly optimized for use with the CellSearch CTC kit and instead for low antigen density markers the CellSearch CXC kit must be utilized. However, FDA and Health Canada approval have only been given for the traditional CTC kit and not the CXC kit as it has been shown to have reduced CTC recovery due to the switching of PE and FITC fluorophores for CK 8/18/19 detection[50]. Therefore, when utilizing the CXC kit, the

unique advantage imparted on the CSS over other enumeration and characterization technologies (i.e., the ability to perform CTC enumeration and characterization in individual cells on a regulatory-approved platform) is lost.

7.3.3 *In vivo* prostate xenograft studies

The time points (2, 4, 8, 12, and 16 weeks) and number of mice per group (n=12) utilized for the *in vivo* studies performed in Chapter 6 were chosen based on previously reported data regarding each cell line[51–57]. However, this was our laboratory's first experience with these cell lines *in vivo* and our first experience with orthotopic injection into the prostate gland. Therefore there was uncertainty with regards to the number of mice utilized and the time points chosen that would allow for comparison of the various steps in the metastatic cascade across all 4 of the investigated PCa cell lines. Although the chosen time points appeared reasonable, the PC-3M cell line was highly aggressive and the longest surviving animal was sacrificed at 6 weeks post-injection, with the majority being sacrificed earlier than anticipated, at 4-5 weeks post-injection. Additionally, the 16 week time point may have been too long, as the early sacrifice of mice originally allocated to this time point, due to significant morbidity, led to an enrichment of this group specifically with healthy animals (with no evidence of primary tumors) compared to the other groups. Ideally it would have been advantageous to exclude these healthy animals from the subsequent analysis, however due to the modest number (n=12) of mice chosen for each group this would have reduced our ability to do appropriate statistical analysis and therefore these mice had to be included.

Regardless of the challenges in mouse number, the results obtained in Chapter 6 demonstrated that some CTCs may be missed by the EMT dependent assay

(representative of CSS based capture) due to its reliance on EpCAM expression. However, it is important to remember that the EMT semi-independent assay also has some reliance on EpCAM expression as it selects cells based on expression of both EpCAM and HLA. Therefore if HLA and/or EpCAM are significantly down-regulated in the circulation this assay may not work as expected *in vivo*. The downregulation of HLA has previously been described to occur as a method of immune evasion and demonstrated to enhance tumorigenicity in immunocompromised mice[58]. Ideally, a simple assessment would be to compare HLA and EpCAM expression on CTCs to that of the primary tumor following orthotopic injection. However, unfortunately, as these antigens are used for CTC capture, cells with significant EpCAM and/or HLA downregulation may not be able to be captured and subsequently assessed for expression.

Finally, as with all xenograft models there are always concerns with regards to the use of human cell lines in an immunocompromised mouse background and how accurately this represents human disease. To reduce as many confounding variables as possible we performed orthotopic injections directly into the dorsolateral lobe of the mouse prostate instead of subcutaneously or into the renal capsule (other common sites utilized for xenograft models of PCa)[59]. Despite the technical difficulty of the surgery itself and the limitations with regards to the volume of sample that can be delivered to this site, we felt it was most appropriate, compared to other sites, as it best mimics the microenvironment and vasculature of human PCa[59]. However, we must also consider that the mouse prostate is quite dissimilar from the human prostate. Specifically the mouse prostate is a multi-lobular structure composed of 4 lobes, the anterior, ventral, dorsal, and lateral lobes versus the human prostate, composed of a single "lobe" divided into 3 zones,

the peripheral, transitional, and central[60]. The majority of human prostate cancers develop in the peripheral zone and the dorsal and lateral lobes of the mouse prostate (often referred to as the dorsolateral lobe) has been described as being the most similar to this zone, hence why it was chosen for these studies[61]. However, there is no histological evidence that a relationship exists between any one lobe of the mouse prostate and a particular zone of the human prostate gland[62]. In addition to the observed structural differences, the use of immunocompromised mice may also have an impact on the metastatic capacity of the investigated cell lines. The immune system plays a large role in PCa and cannot be discounted as a confounding factor of this study[63–66]. Finally, the use of human prostate cancer cell lines is always a point of contention when investigating xenograft models as the majority of cancer cell lines are isolated from patients with highly aggressive disease and are often not collected from the primary site, but instead from a metastatic lesion, as are all the cell lines described in this thesis[67–70]. Ideally these experiments would be repeated with human primary cells isolated from isolated primary tumors. However, such attempts have proven difficult and based on the number of mice utilized in this study this would likely not be feasible[59,71,72].

7.4 Future directions

The work presented here will have a significant impact on guiding future CTC research. In addition, the results obtained from both pre-clinical and clinical studies have raised a number of new questions to be addressed in future studies.

From our clinical studies we have demonstrated that consideration should be given to using CTCs as biomarkers in early-stage patients and not solely in the metastatic

setting. Inclusion of CTC analysis in these patients specifically, may aid in the stratification of patients into low and high risk groups, and ultimately result in improved progression-free survival and overall survival in patients with poor prognosis, and in improved quality of life (due to less aggressive treatment options) in patients with good prognosis. However, the added benefit of inclusion of CTCs into a patient's clinicopathologic risk profile in determining prognosis will need to be validated in larger patient cohorts in the future. Based on the work presented here we suggest that this validation could occur by using the gold standard CSS alone or in combination with newer emerging technologies, but that larger blood volumes would likely need to be utilized to allow for an increase in the number of CTCs captured and ultimately allowing for more rigorous statistical analysis to be performed. The capture of additional CTCs would also allow for comparison of CTCs pre- and post-treatment, which may have greater prognostic value. Finally, the results presented here highlight the need for appropriate patient selection in the development of these future validation studies.

Potentially the greatest area in need of future work is in understanding the underlying biology of CTCs. The results of this work suggest that the search for highly mesenchymal CTCs that are missed by EpCAM-based technologies may not lead to the added prognostic value that has been proposed. Our results suggest that CTCs with a hybrid phenotype may be the most important in initially establishing metastatic disease and that those CTCs with a highly mesenchymal phenotype only appear in significant number after metastasis has occurred. Therefore future research needs to address the role that both these highly mesenchymal and hybrid CTCs play in disease progression across

all stages of disease. The tools developed throughout the course of this thesis will aid in answering these questions.

Additionally, many outstanding questions remain regarding the impact of EMT on the various steps of the metastatic cascade. Specifically, how phenotypic switching of EMT to MET phenotypes or vice versa at different stages of disease progression would impact CTC generation and metastasis is an important area for future investigation. Unfortunately the timeline of this thesis did not allow for such investigation. However future work in this area will be important in better understanding EMT and its contribution to metastatic spread.

Finally, although careful consideration was given when selecting both the PCa cell lines and site of injection utilized in our xenograft models in order to best represent disease conditions in the clinic, we did not have time to investigate the implications of therapy related interventions (i.e., surgical removal of the prostate and/or localized versus systemic therapies) on the results presented here. It would be interesting to investigate differences in CTC generation and/or metastasis in response to these typical clinical intervention strategies. Additionally, it has been suggested that androgen deprivation may be important in the generation of EMT phenotypes[73], and as it is known that eventually PCa will progress to an androgen-independent state[74]. Therefore it may be beneficial to further explore the role of androgen deprivation on CTCs and metastasis *in vivo*.

7.5 Final conclusions

Throughout this project, we have demonstrated that CTCs may be valuable biomarkers in the setting of early-stage PCa, and that their inclusion in a patient's

clinicopathologic risk profile may change clinical decision-making. In addition, several detailed guides have been presented enable users of the CSS to capitalize on its full potential for both CTC enumeration and molecular characterization. Finally, we have reported on the role of EMT in CTC generation and metastasis and the capacity for mesenchymal CTC capture using the current clinical gold standard CTC technology.

Overall, the knowledge gained in these studies is important from several different perspectives, including; ***(1)*** *the therapeutic perspective*, defining the relationship between therapy response and CTC detection in the setting of early stage prostate cancer and salvage/adjuvant radiation; ***(2)*** *the technical perspective*, identifying the limitations of existing CTC methodologies and aiding in the development/optimization of novel CTC enumeration/characterization techniques; and ***(3)*** *the biological perspective*, providing a more detailed understanding of the metastatic process in prostate cancer, its mechanism(s) and the molecular characteristics of the cells involved.

7.6 References

1 Prostate Cancer, Malignant Tumours. June 10 2015. Toronto: Canadian Cancer Society 2015. Available at: www.cancer.ca. .

2 Pantel K, Brakenhoff RH. Dissecting the metastatic cascade. *Nat Rev Cancer* 2004; **4**: 448–56.

3 De Bono JS, Scher HI, Montgomery RB, Parker C, Miller MC, Tissing H *et al.* Circulating tumor cells predict survival benefit from treatment in metastatic castration-resistant prostate cancer. *Clin Cancer Res* 2008; **14**: 6302–9.

4 Tombal B, Van Cangh PJ, Loric S, Gala J-L. Prognostic value of circulating prostate cells in patients with a rising PSA after radical prostatectomy. *Prostate* 2003; **56**: 163–70.

5 Stojadinovic A, Mittendorf E a, Holmes JP, Amin A, Hueman MT, Ponniah S *et al.* Quantification and phenotypic characterization of circulating tumor cells for monitoring response to a preventive HER2/neu vaccine-based immunotherapy for breast cancer: a pilot study. *Ann Surg Oncol* 2007; **14**: 3359–68.

6 Sieuwerts AM, Kraan J, Bolt-de Vries J, van der Spoel P, Mostert B, Martens JWM *et al.* Molecular characterization of circulating tumor cells in large quantities of contaminating leukocytes by a multiplex real-time PCR. *Breast Cancer Res Treat* 2009; **118**: 455–68.

7 Attard G, Swennenhuis JF, Olmos D, Reid AHM, Vickers E, A'Hern R *et al.* Characterization of ERG, AR and PTEN gene status in circulating tumor cells from patients with castration-resistant prostate cancer. *Cancer Res* 2009; **69**: 2912–8.

8 Olmos D, Arkenau H-T, Ang JE, Ledaki I, Attard G, Carden CP *et al.* Circulating tumour cell (CTC) counts as intermediate end points in castration-resistant prostate cancer (CRPC): a single-centre experience. *Ann Oncol* 2009; **20**: 27–33.

9 Budd GT, Cristofanilli M, Ellis MJ, Stopeck A, Borden E, Miller MC *et al.* Circulating tumor cells versus imaging--predicting overall survival in metastatic breast cancer. *Clin Cancer Res* 2006; **12**: 6403–9.

10 Cristofanilli M, Budd GT, Ellis MJ, Stopeck A, Matera J, Miller MC *et al.* Circulating tumor cells, disease progression, and survival in metastatic breast cancer. *N Engl J Med* 2004; **351**: 781–91.

11 Cohen SJ, Punt CJ a, Iannotti N, Saidman BH, Sabbath KD, Gabrail NY *et al.* Relationship of circulating tumor cells to tumor response, progression-free survival, and overall survival in patients with metastatic colorectal cancer. *J Clin Oncol* 2008; **26**: 3213–21.

12 Pal SK, He M, Wilson T, Liu X, Zhang K, Carmichael C *et al.* Detection and Phenotyping of Circulating Tumor Cells in High-Risk Localized Prostate Cancer. *Clin Genitourin Cancer* 2014; : 1–7.

13 Kolostova K, Broul M, Schraml J, Cegan M, Matkowski R, Fiutowski M *et al.* Circulating tumor cells in localized prostate cancer: isolation, cultivation in vitro and relationship to T-stage and Gleason score. *Anticancer Res* 2014; **34**: 3641–6.

14 Helo P, Cronin AM, Danila DC, Wenske S, Gonzalez-Espinoza R, Anand A *et al.* Circulating prostate tumor cells detected by Reverse transcription-PCR in men with localized or castration-refractory prostate cancer: Concordance with

CellSearch assay and association with bone metastases and with survival. *Clin Chem* 2009; **55**: 765–773.

15 Murray NP, Reyes E, Orellana N, Fuentealba C, Bádinez L, Olivares R *et al.* Secondary circulating prostate cells predict biochemical failure in prostate cancer patients after radical prostatectomy and without evidence of disease. *ScientificWorldJournal* 2013; **2013**: 762064.

16 Murray NP, Reyes E, Tapia P, Badinez L, Orellana N, Fuentealba C *et al.* Redefining micrometastasis in prostate cancer - a comparison of circulating prostate cells, bone marrow disseminated tumor cells and micrometastasis: Implications in determining local or systemic treatment for biochemical failure after radical prostatecto. *Int J Mol Med* 2012; **30**: 896–904.

17 Lowes LE, Lock M, Rodrigues G, D'Souza D, Bauman G, Ahmad B *et al.* Circulating tumour cells in prostate cancer patients receiving salvage radiotherapy. *Clin Transl Oncol* 2012; **14**: 150–6.

18 Hayes DF, Cristofanilli M, Budd GT, Ellis MJ, Stopeck A, Miller MC *et al.* Circulating tumor cells at each follow-up time point during therapy of metastatic breast cancer patients predict progression-free and overall survival. *Clin Cancer Res* 2006; **12**: 4218–24.

19 Joosse SA, Gorges TM, Pantel K. Biology, detection, and clinical implications of circulating tumor cells. *EMBO Mol Med* 2015; **7**: 1–11.

20 Alix-Panabières C, Pantel K. Technologies for detection of circulating tumor cells: facts and vision. *Lab Chip* 2014; **14**: 57–62.

21 Lianidou ES, Markou A. Circulating tumor cells in breast cancer: detection systems, molecular characterization, and future challenges. *Clin Chem* 2011; **57**: 1242–55.

22 Lowes LE, Hedley BD, Keeney M, Allan AL. Adaptation of semiautomated circulating tumor cell (CTC) assays for clinical and preclinical research applications. *J Vis Exp* 2014; : e51248.

23 Lowes LE, Hedley BD, Keeney M, Allan AL. User-defined protein marker assay development for characterization of circulating tumor cells using the CellSearch® system. *Cytometry A* 2012; **81**: 983–95.

24 Bonnomet a, Syne L, Brysse a, Feyereisen E, Thompson EW, Noël a *et al.* A dynamic in vivo model of epithelial-to-mesenchymal transitions in circulating tumor cells and metastases of breast cancer. *Oncogene* 2011; : 1–13.

25 Gorges TM, Tinhofer I, Drosch M, Röse L, Zollner TM, Krahn T *et al.* Circulating tumour cells escape from EpCAM-based detection due to epithelial-to-mesenchymal transition. *BMC Cancer* 2012; **12**: 178.

26 Andreopoulou E, Yang L-Y, Rangel KM, Reuben JM, Hsu L, Krishnamurthy S *et al.* Comparison of assay methods for detection of circulating tumor cells (CTCs) in metastatic breast cancer (MBC): AdnaGen AdnaTest BreastCancer Select/Detect™ versus Veridex CellSearch™ system. *Int J Cancer* 2011; **Epub**: Epub.

27 Van Der Auwera I, Peeters D, Benoy IH, Elst HJ, Van Laere SJ, Prové A *et al.* Circulating tumour cell detection: a direct comparison between the CellSearch System, the AdnaTest and CK-19/mammaglobin RT-PCR in patients with metastatic breast cancer. *Br J Cancer* 2010; **102**: 276–84.

28 Balic M, Dandachi N, Hofmann G, Samonigg H, Loibner H, Obwaller A *et al.* Comparison of two methods for enumerating circulating tumor cells in carcinoma patients. *Cytometry B Clin Cytom* 2005; **68**: 25–30.
29 Rosenberg R, Gertler R, Friederichs J, Fuehrer K, Dahm M, Phelps R *et al.* Comparison of two density gradient centrifugation systems for the enrichment of disseminated tumor cells in blood. *Cytometry* 2002; **49**: 150–8.
30 Thiery JP, Acloque H, Huang RYJ, Nieto MA. Epithelial-mesenchymal transitions in development and disease. *Cell* 2009; **139**: 871–90.
31 Umbas R, Isaacs WB, Bringuier PP, Schaafsma HE, Karthaus HFM, Oosterhof GON *et al.* Decreased E-cadherin expression is associated with poor prognosis in patients with prostate cancer. *Cancer Res* 1994; **54**: 3929–3933.
32 Zhang Q, Helfand BT, Jang TL, Zhu LJ, Chen L, Yang XJ *et al.* Nuclear factor-kappaB-mediated transforming growth factor-beta-induced expression of vimentin is an independent predictor of biochemical recurrence after radical prostatectomy. *Clin Cancer Res* 2009; **15**: 3557–3567.
33 Lang SH, Hyde C, Reid IN, Hitchcock IS, Hart CA, Bryden AAG *et al.* Enhanced expression of vimentin in motile prostate cell lines and in poorly differentiated and metastatic prostate carcinoma. *Prostate* 2002; **52**: 253–263.
34 Raimondi C, Gradilone A, Naso G, Vincenzi B, Petracca A, Nicolazzo C *et al.* Epithelial-mesenchymal transition and stemness features in circulating tumor cells from breast cancer patients. *Breast Cancer Res Treat* 2011.
35 Papadaki MA, Kallergi G, Zafeiriou Z, Manouras L, Theodoropoulos PA, Mavroudis D *et al.* Co-expression of putative stemness and epithelial-to-mesenchymal transition markers on single circulating tumour cells from patients with early and metastatic breast cancer. *BMC Cancer* 2014; **14**: 1–10.
36 Barriere G, Riouallon A, Renaudie J, Tartary M, Michel P rigaud. Mesenchymal and stemness circulating tumor cells in early breast cancer diagnosis. BMC Cancer. 2012; **12**: 114.
37 Kasimir-Bauer S, Hoffmann O, Wallwiener D, Kimmig R, Fehm T. Expression of stem cell and epithelial-mesenchymal transition markers in primary breast cancer patients with circulating tumor cells. *Breast Cancer Res* 2012; **14**: R15.
38 Mego M, Mani S a, Lee B-N, Li C, Evans KW, Cohen EN *et al.* Expression of epithelial-mesenchymal transition-inducing transcription factors in primary breast cancer: The effect of neoadjuvant therapy. *Int J Cancer* 2012; **130**: 808–16.
39 Kallergi G, Papadaki MA, Politaki E, Mavroudis D, Georgoulias V, Agelaki S. Epithelial to mesenchymal transition markers expressed in circulating tumour cells of early and metastatic breast cancer patients. Breast Cancer Res. 2011; **13**: R59.
40 Giordano A, Gao H, Anfossi S, Cohen E, Mego M, Lee B-N *et al.* Epithelial-mesenchymal transition and stem cell markers in patients with HER2-positive metastatic breast cancer. *Mol Cancer Ther* 2012; **11**: 2526–34.
41 Chen CL, Mahalingam D, Osmulski P, Jadhav RR, Wang CM, Leach RJ *et al.* Single-cell analysis of circulating tumor cells identifies cumulative expression patterns of EMT-related genes in metastatic prostate cancer. *Prostate* 2013; **73**: 813–826.

42 Yu M, Bardia A, Wittner BS, Stott SL, Smas ME, Ting DT *et al.* Circulating breast tumor cells exhibit dynamic changes in epithelial and mesenchymal composition. *Science* 2013; **339**: 580–4.
43 Armstrong AJ, Marengo MS, Oltean S, Kemeny G, Bitting RL, Turnbull JD *et al.* Circulating tumor cells from patients with advanced prostate and breast cancer display both epithelial and mesenchymal markers. *Mol Cancer Res* 2011; **9**: 997–1007.
44 Bitting RL, Schaeffer D, Somarelli J a., Garcia-Blanco M a., Armstrong AJ. The role of epithelial plasticity in prostate cancer dissemination and treatment resistance. *Cancer Metastasis Rev* 2014; **33**: 441–468.
45 Meng S, Tripathy D, Shete S, Ashfaq R, Haley B, Perkins S *et al.* HER-2 gene amplification can be acquired as breast cancer progresses. *Proc Natl Acad Sci U S A* 2004; **101**: 9393–8.
46 Hayashi N, Nakamura S, Tokuda Y, Shimoda Y, Yagata H, Yoshida A *et al.* Prognostic value of HER2-positive circulating tumor cells in patients with metastatic breast cancer. *Int J Clin Oncol* 2012; **17**: 96–104.
47 Pestrin M, Bessi S, Puglisi F, Minisini AM, Masci G, Battelli N *et al.* Final results of a multicenter phase II clinical trial evaluating the activity of single-agent lapatinib in patients with HER2-negative metastatic breast cancer and HER2-positive circulating tumor cells. A proof-of-concept study. *Breast Cancer Res Treat* 2012; **134**: 283–9.
48 Riethdorf S, Müller V, Zhang L, Rau T, Loibl S, Komor M *et al.* Detection and HER2 expression of circulating tumor cells: prospective monitoring in breast cancer patients treated in the neoadjuvant GeparQuattro trial. *Clin Cancer Res* 2010; **16**: 2634–45.
49 Georgoulias V, Bozionelou V, Agelaki S, Perraki M, Apostolaki S, Kallergi G *et al.* Trastuzumab decreases the incidence of clinical relapses in patients with early breast cancer presenting chemotherapy-resistant CK-19mRNA-positive circulating tumor cells: Results of a randomized phase II study. *Ann Oncol* 2012; **23**: 1744–1750.
50 Veridex White Pages. Available at: http://www.veridex.com/pdf/CXC_Application_Guideline.PDF. 2008.
51 Mallett CL, Lim H, Thind K, Chen Y, Ribot EJ, Martinez F *et al.* Longitudinal anatomical and metabolic MRI characterization of orthotopic xenograft prostate tumors in nude mice. J. Magn. Reson. Imaging. 2013. doi:10.1002/jmri.24433.
52 Valta MP, Tuomela J, Vuorikoski H, Loponen N, Väänänen RM, Pettersson K *et al.* FGF-8b induces growth and rich vascularization in an orthotopic PC-3 model of prostate cancer. *J Cell Biochem* 2009; **107**: 769–784.
53 Koshida K, Konaka H, Imao T, Egawa M, Mizokami A, Namiki M. Comparison of two in vivo models for prostate cancer: Orthotopic and intratesticular inoculation of LNCaP or PC-3 cells. *Int J Urol* 2004; **11**: 1114–1121.
54 Shah G V., Thomas S, Muralidharan A, Liu Y, Hermonat PL, Williams J *et al.* Calcitonin promotes in vivo metastasis of prostate cancer cells by altering cell signaling, adhesion, and inflammatory pathways. *Endocr Relat Cancer* 2008; **15**: 953–964.

55 Yamamichi F, Matsuoka T, Shigemura K, Kawabata M, Shirakawa T, Fujisawa M. Potential establishment of lung metastatic xenograft model of androgen receptor-positive and androgen-independent prostate cancer (C4-2B). *Urology* 2012; **80**. doi:10.1016/j.urology.2012.06.023.

56 Pfitzenmaier J, Quinn JE, Odman AM, Zhang J, Keller ET, Vessella RL *et al.* Characterization of C4-2 prostate cancer bone metastases and their response to castration. *J Bone Miner Res* 2003; **18**: 1882–1888.

57 Pettaway CA, Pathak S, Greene G, Ramirez E, Wilson MR, Killion JJ *et al.* Selection of Highly Metastatic Variants of Different Human Prostatic Carcinomas Using Orthotopic Implantation in Nude Mice. *Clin Cancer Res* 1996; **2**: 1627–1636.

58 Garrido C, Algarra I, Maleno I, Stefanski J, Collado A, Garrido F *et al.* Alterations of HLA class i expression in human melanoma xenografts in immunodeficient mice occur frequently and are associated with higher tumorigenicity. *Cancer Immunol Immunother* 2010; **59**: 13–26.

59 Toivanen R, Taylor R a, Pook DW, Ellem SJ, Risbridger GP. Breaking through a roadblock in prostate cancer research: an update on human model systems. *J Steroid Biochem Mol Biol* 2012; **131**: 122–31.

60 Valkenburg KC, Williams BO. Mouse Models of Prostate Cancer. Prostate Cancer. 2011; **2011**: 1–22.

61 Powell WC, Cardiff RD, Cohen MB, Miller GJ, Roy-Burman P. Mouse strains for prostate tumorigenesis based on genes altered in human prostate cancer. *Curr Drug Targets* 2003; **4**: 263–279.

62 Shappell SB, Thomas G V., Roberts RL, Herbert R, Ittmann MM, Rubin MA *et al.* Prostate Pathology of Genetically Engineered Mice: Definitions and Classification. The Consensus Report from the Bar Harbor Meeting of the Mouse Models of Human Cancer Consortium Prostate Pathology Committee. In: *Cancer Research*. 2004, pp 2270–2305.

63 De Nunzio C, Kramer G, Marberger M, Montironi R, Nelson W, Schröder F *et al.* The controversial relationship between benign prostatic hyperplasia and prostate cancer: The role of inflammation. Eur. Urol. 2011; **60**: 106–117.

64 Penna G, Fibbi B, Amuchastegui S, Cossetti C, Aquilano F, Laverny G *et al.* Human benign prostatic hyperplasia stromal cells as inducers and targets of chronic immuno-mediated inflammation. *J Immunol* 2009; **182**: 4056–4064.

65 Steiner GE, Stix U, Handisurya A, Willheim M, Haitel A, Reithmayr F *et al.* Cytokine expression pattern in benign prostatic hyperplasia infiltrating T cells and impact of lymphocytic infiltration on cytokine mRNA profile in prostatic tissue. *Lab Invest* 2003; **83**: 1131–1146.

66 De Marzo AM, Platz EA, Sutcliffe S, Xu J, Grönberg H, Drake CG *et al.* Inflammation in prostate carcinogenesis. *Nat Rev Cancer* 2007; **7**: 256–269.

67 Horoszewicz JS, Leong SS, Chu TM, Wajsman ZL, Friedman M, Papsidero L *et al.* The LNCaP cell line--a new model for studies on human prostatic carcinoma. *Prog Clin Biol Res* 1980; **37**: 115–132.

68 Thalmann GN, Anezinis PE, Chang SM, Zhau HE, Kim EE, Hopwood VL *et al.* Androgen-independent cancer progression and bone metastasis in the LNCaP model of human prostate cancer. *Cancer Res* 1994; **54**: 2577–2581.

69 Kaighn ME, Narayan KS, Ohnuki Y, Lechner JF, Jones LW. Establishment and characterization of a human prostatic carcinoma cell line (PC-3). *Invest Urol* 1979; **17**: 16–23.

70 Kozlowski JM, Fidler IJ, Campbell D, Xu ZL, Kaighn ME, Hart IR. Metastatic behavior of human tumor cell lines grown in the nude mouse. *Cancer Res* 1984; **44**: 3522–3529.

71 Lopez-Barcons LA. Human prostate cancer heterotransplants: a review on this experimental model. *Asian J Androl* 2010; **12**: 509–518.

72 Wang Y, Revelo MP, Sudilovsky D, Cao M, Chen WG, Goetz L *et al.* Development and characterization of efficient xenograft models for benign and malignant human prostate tissue. *Prostate* 2005; **64**: 149–159.

73 Sun Y, Wang BE, Leong KG, Yue P, Li L, Jhunjhunwala S *et al.* Androgen deprivation causes epithelial-mesenchymal transition in the prostate: Implications for androgen- deprivation therapy. *Cancer Res* 2012; **72**: 527–536.

74 Chen CD, Welsbie DS, Tran C, Baek SH, Chen R, Vessella R *et al.* Molecular determinants of resistance to antiandrogen therapy. *Nat Med* 2004; **10**: 33–39.

Appendices

Appendix 1. Human Ethics Approval for Chapter 2

Office of Research Ethics

The University of Western Ontario
Room 4180 Support Services Building, London, ON, Canada N6A 5C1
Telephone: (519) 661-3036 Fax: (519) 850-2466 Email: ethics@uwo.ca
Website: www.uwo.ca/research/ethics

Use of Human Subjects - Ethics Approval Notice

Principal Investigator: Dr. T. Sexton
Review Number: **15569E** **Review Level:** Expedited
Review Date: October 22, 2008
Protocol Title: Detection of circulating tumour cells in prostate cancer patients with rising PSA post-prostatectomy
Department and Institution: Oncology, London Health Sciences Centre
Sponsor:
Ethics Approval Date: January 07, 2009 **Expiry Date:** September 30, 2009
Documents Reviewed and Approved: UWO Protocol, Letter of Information and Consent.
Documents Received for Information:

This is to notify you that The University of Western Ontario Research Ethics Board for Health Sciences Research Involving Human Subjects (HSREB) which is organized and operates according to the Tri-Council Policy Statement: Ethical Conduct of Research Involving Humans and the Health Canada/ICH Good Clinical Practice Practices: Consolidated Guidelines; and the applicable laws and regulations of Ontario has reviewed and granted approval to the above referenced study on the approval date noted above. The membership of this REB also complies with the membership requirements for REB's as defined in Division 5 of the Food and Drug Regulations.

The ethics approval for this study shall remain valid until the expiry date noted above assuming timely and acceptable responses to the HSREB's periodic requests for surveillance and monitoring information. If you require an updated approval notice prior to that time you must request it using the UWO Updated Approval Request Form.

During the course of the research, no deviations from, or changes to, the protocol or consent form may be initiated without prior written approval from the HSREB except when necessary to eliminate immediate hazards to the subject or when the change(s) involve only logistical or administrative aspects of the study (e.g. change of monitor, telephone number). Expedited review of minor change(s) in ongoing studies will be considered. Subjects must receive a copy of the signed information/consent documentation.

Investigators must promptly also report to the HSREB:

a) changes increasing the risk to the participant(s) and/or affecting significantly the conduct of the study;
b) all adverse and unexpected experiences or events that are both serious and unexpected;
c) new information that may adversely affect the safety of the subjects or the conduct of the study.

If these changes/adverse events require a change to the information/consent documentation, and/or recruitment advertisement, the newly revised information/consent documentation, and/or advertisement, must be submitted to this office for approval.

Members of the HSREB who are named as investigators in research studies, or declare a conflict of interest, do not participate in discussion related to, nor vote on, such studies when they are presented to the HSREB.

Appendix 2. Human Ethics Approval for Chapter 3

Office of Research Ethics

The University of Western Ontario
Room 4180 Support Services Building, London, ON, Canada N6A 5C1
Telephone: (519) 661-3036 Fax: (519) 850-2466 Email: ethics@uwo.ca
Website: www.uwo.ca/research/ethics

Use of Human Subjects - Ethics Approval Notice

Principal Investigator: Dr. T. Sexton
Review Number: 16904E **Review Level:** Expedited
Review Date: February 24, 2010 **Approved Local # of Participants:** 100
Protocol Title: Significance of circulating tumor cells in prostate cancer patients receiving adjuvant or salvage radiotherapy
Department and Institution: Oncology, London Regional Cancer Program
Sponsor:
Ethics Approval Date: March 24, 2010 **Expiry Date:** January 31, 2012
Documents Reviewed and Approved: UWO Protocol, Letter of Information and Consent, Letter of Information and Consent (Female).
Documents Received for Information:

This is to notify you that The University of Western Ontario Research Ethics Board for Health Sciences Research Involving Human Subjects (HSREB) which is organized and operates according to the Tri-Council Policy Statement: Ethical Conduct of Research Involving Humans and the Health Canada/ICH Good Clinical Practice Practices: Consolidated Guidelines; and the applicable laws and regulations of Ontario has reviewed and granted approval to the above referenced study on the approval date noted above. The membership of this REB also complies with the membership requirements for REB's as defined in Division 5 of the Food and Drug Regulations.

The ethics approval for this study shall remain valid until the expiry date noted above assuming timely and acceptable responses to the HSREB's periodic requests for surveillance and monitoring information. If you require an updated approval notice prior to that time you must request it using the UWO Updated Approval Request Form.

During the course of the research, no deviations from, or changes to, the protocol or consent form may be initiated without prior written approval from the HSREB except when necessary to eliminate immediate hazards to the subject or when the change(s) involve only logistical or administrative aspects of the study (e.g. change of monitor, telephone number). Expedited review of minor change(s) in ongoing studies will be considered. Subjects must receive a copy of the signed information/consent documentation.

Investigators must promptly also report to the HSREB:

a) changes increasing the risk to the participant(s) and/or affecting significantly the conduct of the study;
b) all adverse and unexpected experiences or events that are both serious and unexpected;
c) new information that may adversely affect the safety of the subjects or the conduct of the study.

If these changes/adverse events require a change to the information/consent documentation, and/or recruitment advertisement, the newly revised information/consent documentation, and/or advertisement, must be submitted to this office for approval.

Members of the HSREB who are named as investigators in research studies, or declare a conflict of interest, do not participate in discussion related to, nor vote on, such studies when they are presented to the HSREB.

Appendix 3. Animal Protocol Approval for Chapter 6

Western

2012-031::2:

AUP Number: 2012-031
AUP Title: Circulating tumor cells (CTCs) in prostate cancer
Yearly Renewal Date: 12/01/2014

The YEARLY RENEWAL to Animal Use Protocol (AUP) 2012-031 has been approved, and will be approved for one year following the above review date.

This AUP number must be indicated when ordering animals for this project.
Animals for other projects may not be ordered under this AUP number.
Purchases of animals other than through this system must be cleared through the ACVS office.
Health certificates will be required.

REQUIREMENTS/COMMENTS
Please ensure that individual(s) performing procedures on live animals, as described in this protocol, are familiar with the contents of this document.

The holder of this Animal Use Protocol is responsible to ensure that all associated safety components (biosafety, radiation safety, general laboratory safety) comply with institutional safety standards and have received all necessary approvals. Please consult directly with your institutional safety officers.

Submitted by: Kinchlea, Will D
on behalf of the Animal Use Subcommittee

Curriculum Vitae

Post-Secondary Education and Degrees

- PhD Candidate: The University of Western Ontario, London, ON, 2009-Present
  Department: Anatomy & Cell Biology
  Supervisors: Dr. Alison Allan & Dr. Tracy Sexton

- Bachelor of Medical Sciences: The University of Western Ontario, London, ON, 2004-2009
  Program: Honors Specialization in Microbiology and Immunology

Honours and Awards

1. Senior Women's Academic Administrators of Canada (SWAAC) Award of Merit ($3,000), 2015.
2. CIHR Doctoral Award ($35,000/year), 2012 – 2015.
3. Ontario Graduate Scholarship ($15,000/year), 2011 – 2012, 2012 – 2013 (declined for CIHR).
4. Schulich Graduate Scholarship ($7,400/year), 2009 – 2014.
5. CIHR Strategic Training Program in Cancer Research and Technology Transfer (CaRTT) Studentship ($8,200 – $25,700/year), 2009 – 2012.
6. CIHR Master's Award ($17,500/year), 2010 – 2011.
7. Poster Presentation Award, 11th Annual Oncology Research and Education Day ($100), June 2014.
8. Morris Kroll Memorial Scholarship in Cancer Research ($500), June 2013.
9. Centre for Translational Cancer Research Award, 10th Annual Oncology Research and Education Day ($100), June 2013.
10. Poster Presentation Award, 10th Annual Oncology Research and Education Day ($100), June 2013.
11. UWO Division of Experimental Oncology Graduate Student Travel Award ($1,500), 2011, 2012.
12. Poster Presentation Award, 8th Annual Oncology Research and Education Day ($100), June 2011.
13. Canadian Cancer Society-Ontario Trainee Travel Award, 2011.
14. Leadership Award Nominee, Lawson Research Day, March 2011.
15. Graduate Thesis Research Award ($437), 2010.
16. CIHR Institute for Cancer Research Travel Award ($1,000) for Joint Metastasis Research Society – American Association of Cancer Research Annual Meeting, Philadelphia, PA. September 2010.
17. Poster Presentation Award, 7th Annual Oncology Research and Education Day ($100), June 2010.

Publications

Referred Papers

1. **Lowes, L.E.**, Lock, M., Rodrigues, G., D'Souza, D., Bauman, G., Ahmad, B., Venkatesan, V., Allan, A.L., and Sexton, T. The significance of circulating tumor cells in prostate cancer patients undergoing adjuvant or salvage radiation therapy. *Prostate Cancer and Prostatic Diseases.* 2015; In press.
2. **Lowes, L.E.,** and Allan, A.L. Recent advances in the molecular characterization of circulating tumor cells. *Cancers (Basel).* 2014; 6(1):595-624. PMID: 24633084
3. **Lowes, L.E.**, Hedley, B.D., Keeney, M., and Allan, A.L. Adaptation of semi-automated circulating tumor cell (CTC) assays for clinical and pre-clinical research applications. *J. Vis. Exp.* 2014; (84):e51248. PMID: 24637923
4. Mohamadi, R.M., Besant, J.D., Mepham, A., Green, B., Mahmoudian, L., Gibbs, T., Ivanov, I., Malvea, A., Stojcic, J., Allan, A.L., **Lowes, L.E.,** Sargent, E.H., Nam, R.K., and Kelley, S.O. Nanoparticle-Mediated Binning and Profiling of Heterogeneous Circulating Tumor Cell Subpopulations. *Angew. Chem. Int. Ed. Engl.* 2014; Epub. PMID: 25377874
5. **Lowes, L.E.**, Hedley, B.D., Keeney, M., and Allan, A.L. Molecular marker development for characterizing CD44 and M-30 on circulating tumor cells in metastatic cancer using the CellSearch system. *Cytometry A.* 2012; 81(11):983-95. PMID: 22899576. *This manuscript was a featured paper in the "In This Issue" alert for the November 2012 issue of *Cytometry A*.
6. **Lowes, L.E.**, Lock, M., Rodrigues, G., D'Souza, D., Bauman, G., Venkatesan, V., Allan, A.L., and Sexton, T. Circulating tumor cell analysis in prostate cancer patients receiving salvage radiotherapy. *Clin. Transl. Oncol*. 2012; 14(2):150-6. PMID: 22301405
7. Nichols A.C., **Lowes, L.E.**, Szeto, C.C.T., Basmaji, J., Dhaliwal, S., Chapeskie, C., Todorov, B., Read, N., Venkatesan, V., Hammond, A., Palma, D.A., Winquist, E., Ernst, S., Fung, K., Franklin, J.H., Yoo, J., Koropatnick, J., Mymryk, J.S., Barrett, J.W., and Allan, A.L. Detection of circulating tumor cells in advanced head and neck cancer using the CellSearch system. *Head Neck.* 2012; 34(10):1440-4 PMID: 22076949
8. **Lowes, L.E.**, Goodale, D., Keeney, M., and Allan, A.L. Image cytometry analysis of circulating tumor cells. *Methods Cell Biol.* 2011; 102:261-90. PMID: 21704842

Presentations as an Invited Guest Speaker

Invited Oral Research Presentations

1. **Lowes, L.E.**, and Allan, A.L. Circulating tumor cells in prostate cancer: clinical and experimental studies. Circulate: Non Invasive Cancer Diagnostics, Berlin, DE. March 2015.
2. **Lowes, L.E.**, and Allan, A.L. Role of epithelial-to-mesenchymal (EMT) transition on circulating tumor cell (CTC) generation and metastasis in prostate cancer. 2nd

International Symposium on Advances in Circulating Tumor Cells, Crete, GR. October 2014.
3. **Lowes, L.E.**, Allan, A.L., and Sexton, T. Significance of circulating tumor cells (CTCs) in prostate cancer patients undergoing adjuvant or salvage radiation therapy. Canadian Association of Radiation Oncology, St. John's, NL. August 2014.
4. **Lowes, L.E.**, and Allan, A.L. Role of epithelial-to-mesenchymal (EMT) transition on circulating tumor cell (CTC) generation and metastasis in prostate cancer. Canadian Cancer Research Conference, Toronto, ON. November 2013.
5. **Lowes, L.E.** Circulating tumor cell analysis in prostate cancer patients receiving salvage radiotherapy. 17th Annual Anatomy and Cell Biology Research Day, London, ON. October 2010.

Abstracts

National/International Conferences

1. **Lowes, L.E.**, Hedley, B.D., Keeney, M., and Allan, A.L. Role of epithelial-to-mesenchymal (EMT) transition on circulating tumor cell generation and metastasis in prostate cancer. The Canadian Cancer Research Conference 2013, Toronto, ON. [accepted for poster presentation, L. Lowes].
2. **Lowes, L.E.**, Bazov, J., Good, J., Squire, J., Chi, K., Eisenhauer, E., Hotte, S., Datar, R., and Allan, A.L. Circulating tumor cell (CTC) analysis and characterization using novel microfiltration technology: A correlative biology companion study to the NCIC CTG Phase II clinical trial IND.205. Ontario Institute for Cancer Research Scientific Meeting 2013, Toronto, ON. March 2013 [poster presentation, L. Lowes].
3. **Lowes, L.E.**, Lock, M., Rodrigues, G., D'Souza, D., Bauman, G., Ahmad, B., Venkatesan, V., Allan, A.L., and Sexton, T. Circulating tumor cell analysis in prostate cancer patients receiving salvage radiotherapy. High Impact Clinical Trials Meeting 2011, Toronto, ON. February 2012 [poster presentation, L. Lowes].
4. **Lowes, L.E.**, Lock, M., Rodrigues, G., D'Souza, D., Bauman, G., Ahmad, B., Venkatesan, V., Allan, A.L., and Sexton, T. Circulating tumor cell analysis in prostate cancer patients receiving salvage radiotherapy. The Canadian Cancer Research Conference 2011, Toronto, ON. November 2011 [poster presentation, L. Lowes].
5. **Lowes, L.E.**, Lock, M., Rodrigues, G., D'Souza, D., Bauman, G., Ahmad, B., Venkatesan, V., Allan, A.L., and Sexton, T. Circulating tumor cell analysis in prostate cancer patients receiving salvage radiotherapy. 8th International Symposium on Minimal Residual Cancer Meeting 2011, Osaka, Japan. September 2011 [poster presentation, L. Lowes].
6. **Lowes, L.E.**, Hedley, B.D., Keeney, M., and Allan, A.L. Molecular marker development for characterizing CD44, M-30, and prostate-specific antigen on circulating tumor cells in metastatic cancer. Joint Metastasis Research Society-American Association of Cancer Research Annual Meeting 2010, Philadelphia, PA. September 2010 [poster presentation, L. Lowes].
7. Sexton, T., Allan, A., **Lowes, L.**, Lock, M., Rodrigues, G., D'Souza, D., Bauman, G., and Venkatesan, V. Significance of circulating tumor cells in prostate cancer patients

receiving salvage radiation. Canadian Association of Radiation Oncologists Annual Meeting 2010, Vancouver, BC. September 2010 [oral presentation, T. Sexton].

8. **Lowes, L.E.**, Hedley, B.D., Keeney, M., and Allan, A.L. Molecular marker development for characterization of circulating tumour cells in breast and prostate cancer. 7th International Symposium on Minimal Residual Cancer, Athens, Greece. September 2009 [poster presentation, B. Hedley].
9. Sexton, T., Allan, A.L., Hedley, B.D., **Lowes, L.**, Venkatesan, V., Rodrigues, G., and Ahmad, B. Detection of circulating tumor cells in prostate cancer patients with rising PSA post-prostatectomy. Canadian Association of Radiation Oncologists Annual Meeting 2009, Quebec City, QC. September 2009 [oral presentation, T. Sexton].

Local Meetings

1. **Lowes, L.E.**, Goodale, D., Postenka, C., Xia, Y., Piaseczny, M., and Allan, A.L. Role of epithelial-to-mesenchymal (EMT) transition on circulating tumor cell generation and metastasis in prostate cancer. Oncology Research and Education Day, London, ON. June 2015 [poster presentation, L. Lowes].
2. **Lowes, L.E.**, Goodale, D., Postenka, C., and Allan, A.L. Role of epithelial-to-mesenchymal (EMT) transition on circulating tumor cell generation and metastasis in prostate cancer. London Health Research Day, London, ON. March 2015 [poster presentation, L. Lowes].
3. **Lowes, L.E.**, and Allan, A.L. Role of epithelial-to-mesenchymal (EMT) transition on circulating tumor cell generation and metastasis in prostate cancer. 11th Annual Oncology Research and Education Day, London, ON. June 2014 [poster presentation, L. Lowes].
4. **Lowes, L.E.**, and Allan, A.L. Role of epithelial-to-mesenchymal (EMT) transition on circulating tumor cell generation and metastasis in prostate cancer. London Health Research Day, London, ON. March 2014 [poster presentation, L. Lowes].
5. **Lowes, L.E.**, Bazov, J., Good, J., Squire, J., Chi, K., Eisenhauer, E., Hotte, S., Datar, R., and Allan, A.L. Circulating tumor cell (CTC) analysis and characterization using novel microfiltration technology: A correlative biology companion study to the NCIC CTG Phase II clinical trial IND.205. 10th Annual Oncology Research and Education Day, London, ON. June 2013 [poster presentation, L. Lowes].
6. **Lowes, L.E.**, Bazov, J., Good, J., Squire, J., Chi, K., Eisenhauer, E., Hotte, S., Datar, R., and Allan, A.L. Circulating tumor cell (CTC) analysis and characterization using novel microfiltration technology: A correlative biology companion study to the NCIC CTG Phase II clinical trial IND.205. London Health Research Day, London, ON. March 2013 [poster presentation, L. Lowes].
7. **Lowes, L.E.**, Bazov, J., Good, J., Squire, J., Chi, K., Eisenhauer, E., Hotte, S., Datar, R., and Allan, A.L. A novel microfiltration approach to circulating tumor cell (CTC) enumeration and characterization: A companion study to the NCIC CTG Phase II clinical trial IND.205. 19th Annual Anatomy and Cell Biology Research Day, London, ON. October 2012 [poster presentation, L. Lowes].
8. **Lowes, L.E.**, Bazov, J., Good, J., Squire, J., Chi, K., Eisenhauer, E., Hotte, S., Datar, R., and Allan, A.L. A novel microfiltration approach to circulating tumor cell (CTC) enumeration and characterization: A companion study to the NCIC CTG Phase II

clinical trial IND.205. 9th Annual Oncology Research and Education Day, London, ON. June 2012 [poster presentation, L. Lowes].

9. **Lowes, L.E.**, Lock, M., Rodrigues, G., D'Souza, D., Bauman, G., Ahmad, B., Venkatesan, V., Allan, A.L., and Sexton, T. Circulating tumor cell analysis in prostate cancer patients receiving salvage radiotherapy. 18th Annual Anatomy and Cell Biology Research Day, London, ON. October 2011 [poster presentation, L. Lowes].
10. **Lowes, L.E.**, Hedley, B.D., Keeney, M., and Allan, A.L. Molecular marker development for characterizing CD44 and M-30 on circulating tumor cells in metastatic cancer. 8th Annual Oncology Research and Education Day, London, ON. June 2011 [poster presentation, L. Lowes].
11. **Lowes, L.E.**, Lock, M., Rodrigues, G., D'Souza, D., Bauman, G., Venkatesan, V., Allan, A.L., and Sexton, T. The prognostic significance of circulating tumor cells in prostate cancer patients with a rising PSA post-prostatectomy. Lawson Research Day 2011, London, ON. March 2011 [poster presentation, L. Lowes].
12. **Lowes, L.E.**, Hedley, B.D., Keeney, M., and Allan, A.L. Molecular marker development for characterizing CD44, M-30, and prostate-specific antigen on circulating tumor cells in metastatic cancer. 17th Annual Anatomy and Cell Biology Research Day, London, ON. October 2010 [poster presentation, L. Lowes].
13. **Lowes, L.E.,** Hedley, B.D., Keeney, M., Allan, A.L. and Sexton, T. The prognostic significance of circulating tumor cells in prostate cancer patients with a rising prostate-specific antigen post-prostatectomy. 7th Annual Oncology Research and Education Day, London, ON. June 2010 [poster presentation, L. Lowes].
14. **Lowes, L.E.,** Hedley, B.D., Keeney, M., and Allan, A.L. Molecular marker development for characterization of circulating tumour cells in breast and prostate cancer. Lawson Research Day 2010, London, ON. March 2010 [poster presentation, L. Lowes].
15. **Lowes, L.E.**, Hedley, B.D., Keeney, M., and Allan, A.L. Molecular marker development for characterization of circulating tumour cells in breast and prostate cancer. 16th Annual Anatomy and Cell Biology Research Day, London, ON. October 2009 [poster presentation, L. Lowes].
16. **Lowes, L.E.**, Hedley, B.D., and Allan, A.L. Molecular characterization of circulating tumour cells in metastatic breast cancer. 6th Annual Oncology Research and Education Day, London, ON. June 2009 [poster presentation, L. Lowes].
17. Sexton, T., Allan, A., Hedley, B., **Lowes, L.**, Venkatesan, V., Rodrigues, G., and Ahmad, B. Detection of circulating tumor cells in prostate cancer patients with rising PSA post-prostatectomy. 6th Annual Oncology Research and Education Day, London, ON. June 2009 [poster presentation, T. Sexton].

Knowledge Translation

1. **Featured Scientist, Lowes L.E.** Prostate of the art. International Innovation: Healthcare, March 2014 (Research Media, UK, pp 12-14), ISSN 2054-6254 [international scientific publication]
2. **Featured Scientist, Lowes L.E.** Exploiting circulating tumor cells in the battle against prostate cancer. Research Information Outreach Team (RIOT), June 2014 (The Londoner, ON, pp 19) [lay scientific article]

Leadership Roles

1. Circulating Tumor Cell (CTC) Clinical Research Coordinator, Sept 2009-Present
2. Let's Talk Science – Senior Coordinator, May 2012-July 2015
3. Graduate Teaching Assistant – Medical Sciences 4900, Western University, 2011-May 2015
4. CIHR Strategic Training Program – Seminar Selection Committee Member, Sept 2010-Aug 2013
5. Lawson Health Research Day - Planning Committee Member, May 2011-Mar 2012
6. Partners in Experiential Learning (PEL) Co-Op Mentorship, Jan 2011-June 2011
7. Let's Talk Science – Teacher Partnership Coordinator, May 2010-Apr 2012

Community and Youth Outreach

1. Let's Talk Science Volunteer, Sept 2009-Present
2. Virtual Researchers on Call (VROC) Career Interview, June 2011
3. London Health Sciences Foundation (LHSF) Donor Presentation, May 2011
4. Rose in My Book, 2010-2011
5. CIBC Run For The Cure, 2009-2011
6. ONERUN, 2010-2011
7. Graduate Student Open House & Recruitment Weekend, 2010, 2012, 2014

Other Contributions

1. Completion of Clinical Research Standard Operating Procedures Training Program, Lawson Health Research Institutes), 2013
2. Completion of CellSearch Circulating Tumor Cell Operation and Clinical Interpretation Training, Janssen Diagnostics, 2013
3. Attendance and participation at weekly disease site team meetings and weekly seminar series focused on cancer research, 2009 – Present
4. Teaching Assistant Training Program (TATP), Western University, June 2011